FUNCTIONAL AND STRUCTURAL INTERACTIONS WITHIN PANCREATIC ATP-SENSITIVE POTASSIUM CHANNELS

by

Emily Brook Pratt

A DISSERTATION

Presented to the Neuroscience Graduate Program
and the Oregon Health & Science University
School of Medicine
in partial fulfillment of
the requirements for the degree of

Doctor of Philosophy

November 2010

School of Medicine
Oregon Health & Science University

CERTIFICATE OF APPROVAL

This is to certify that the Ph.D. dissertation of
EMILY PRATT
has been approved

Advisor, Show-Ling Shyng, PhD

Member and Chair, Peter Gillespie, PhD

Member, John Adelman, PhD

Member, William Skach, PhD

Member, Beth Habecker, PhD

Dedication

To all the Ryans, Isaacs, Isabellas, Heathers, Christas, Angelas, Kimberlys, Maragarets, Isaiahs, Lesemenes and Felicias in my world.

Table of Contents

List of Figures and Tables

CHAPTER 1

CHAPTER 2

CHAPTER 3

CHAPTER 4

CHAPTER 5

APPENDIX

Abbreviations Used

ABC	ATP-binding cassette
ATP	Adenosine-5'-triphosphate
BSA	bovine serum albumin
CFTR	cystic fibrosis transmembrane conductance regulator
CHI	congenital hyperinsulinism
DEND	developmental delay, epilepsy, neonatal diabetes mellitus syndrome
DM	diabetes mellitus
DTT	dithiothreitol
EDTA	ethylenediaminetetraacetic acid
ELISA	enzyme-linked immunosorbent assay
ER	endoplasmic reticulum
H_2O_2	hydrogen peroxide
HBSS	Hanks' balanced salt solution
HEPES	4-(2-hydroxyethyl)-1-piperazineethanesulfonic acid
HRP	horseradish peroxidase
IC_{50}	half maximal inhibitory concentration
K_{ATP}	ATP-sensitive potassium channel
KCO	potassium channel opener
Kint	intracellular potassium solution
Kir	inward rectifier potassium channel
L0	loop zero
NBD	nucleotide binding domain
NBF	nucleotide binding fold
PBS	phosphate-buffered saline
PHHI	persistent hyperinsulinism and hypoglycemia of infancy
PIP_2	phosphatidylinositol 4,5-bisphosphate
PNDM	permanent neonatal diabetes mellitus
P_o	open probability
RMP	resting membrane potential
SEM	standard error of the mean
SU	sulfonylurea
SUR	sulfonylurea receptor
TM	tramsmembrane
TMD	transmembrane domain
VGCC	voltage-gated calcium channel
WT	wild type

Acknowledgments

No (wo)man is an Island, entire of itself; every man is a piece of the Continent, a part of the main; if a clod be washed away by the sea, Europe is the less, as well as if a promontory were, as well as if a manor of thy friends or of thine own were; any man's death diminishes me, because I am involved in Mankind; and therefore never send to know for whom the bell tolls; it tolls for thee.

John Donne, *Meditation XVII*

Thank you, Show-Ling Shyng. Over the last six years you have led by example. Every day you show what commitment looks like and what success in science requires. You have championed me and trusted me. You encouraged me when I needed it and were patient when I asked you to be. I admire your courage tempered with pragmatism. Without doubt, the lessons I am meant to learn from my time in your lab will continue to emerge for years to come. Your positive influence on me is indelible.

Thank you, members of the Shyng lab, for your humor and camaraderie. You helped transform what could have been a solitary and exhausting journey into one infused with laughter and friendship. The collective knowledge I have been surrounded by on a daily basis is impressive but would have been nearly useless if not for your generosity…I am awed by you all.

Thank you, Dr. Bill Skach and members of your lab, for your mad skills at the bench and interpreting data. Without fail, Dr. Skach, your optimism buoyed my spirits. Eric Carlson and Yoshihiro Matsumoto, you have my gratitude for your help on many occasions working out protocols and sharing your knowledge.

Thank you, Luis ‘Rudy’ Martinez, Jill Wentzell, Maria Nash, Jennifer Pederson, Malini Kochhar, Cheng Fang, Jennifer Trayner, Ashley Hart, Nicole Kearney and Gabriel Andeen. How lucky am I to have crossed your paths?!

Thank you, Marilyn and Terence Carey. You believe in me no matter what, you’re there whenever I need help and are a boundless source of warmth. Thank you for being loving and supportive parents.

Dissertation Abstract

The ATP-sensitive potassium channel (K_{ATP}) is central to the translation of metabolic status into cellular electrical excitability. In no place is this more evident than pancreatic β-cells where K_{ATP} functions to translate blood glucose concentrations into insulin secretion. K_{ATP} dysfunction leads to a spectrum of life-threatening insulin secretion disorders usually presenting within the first days to weeks of life. Great strides have been made in understanding the molecular determinants of K_{ATP} function through the study of disease-causing mutations in the two proteins that make up its structure: the inward rectifier channel 6.2 (Kir6.2) and the sulfonylurea receptor1 (SUR1). Presented in this dissertation is the extensive analysis of two mutations in SUR1 (R74W and E128K) through mutagenesis screening that has led to numerous insights into K_{ATP} function. Both residues are vital to the maintenance of SUR1-Kir6.2 inter-connectivity, which up till now has proven to be enigmatic. By studying both full-length and minimal channel constructs harboring mutations at R74 and E128, it has become clear that these residues are important for functional coupling between SUR1 and the pore-forming Kir6.2 subunit. However, they are required for very different processes. R74 is necessary for proper folding of SUR1's N-terminal transmembrane domain (TMD0), the region positioned most closely to Kir6.2. E128K alters SUR1 TMD0 conformation in some as yet undefined manner that leads to a phenotype of dramatic and consequential functional uncoupling. E128 modulates K_{ATP} interactions with membrane phosphatidylinositol 4,5-bisphosphate (PIP_2), the most abundant poly-phosphoinositide in the plasma membrane. This finding presents a new paradigm in which to understand the nuanced effects SUR1 contributes to Kir6.2 gating. While attempting to define the structural targets in Kir6.2 that E128K might be neglecting, a wholly separate SUR1-Kir6.2 interface was discovered – SUR1 E203: Kir6.2 Q52. Results from experiments on this pair suggest they are involved in fine-tuning the inhibitory nucleotide binding pocket in Kir6.2 and augmenting affinity for ATP. Interestingly, the conformational defect brought about by E128K is able to dissociate E203 from Q52. E203 lies adjacent to a proposed amphipathic "sliding helix" in SUR1 that has been hypothesized to interact with Kir6.2 in a way that can adjudicate SUR1 influence on Kir6.2. The proximity of the E203 to this helix in addition to positive results from a sizeable mutagenesis screen carried out in SUR1 lends weight to the idea that the sliding helix is also involved in SUR1-Kir6.2 interactions. The work presented in this dissertation characterizes multiple new interactions between SUR1 and Kir6.2.

CHAPTER 1: INTRODUCTION

K_{ATP}: A Brief History and Overview

The history of K_{ATP} channels really begins with the serendipitous discovery of sulfonylurea drugs—the target of which are K_{ATP} channels. In 1942 France, Marcel Janbon observed that three of his human test subjects died after being treated with a potential new antibiotic for typhoid fever (called 2254RP) (Duhault and Lavielle, 1991; Henquin, 1992). The drug effectively and rapidly caused hypoglycemia, the acute cause of death in his subjects (Janbon, 1942). He shared the compound with a colleague, Auguste Loubatières, who went on to test and in 1946 hypothesize the cause of hypoglycemia: a direct action on pancreatic islet cells to stimulate secretion of insulin. It took 50 years before the actual molecular target of this sulfonamide compound was determined, but this did not stop it from being developed into some of the most successful clinical pharmaceuticals in the history of modern medicine. Sulfonylurea (SU) drugs are still considered a viable first-line therapy for newly diagnosed type II diabetes mellitus and, as discussed below, a relatively new treatment option for some genotypes of congenital forms of diabetes.

Identifying the target of SU drugs, however, was a long road with some mis-steps along the way. The first report of ATP-sensitive potassium (K_{ATP}) currents came from cardiomyocytes (Noma, 1983). From the beginning their role in coupling metabolic status to membrane excitability was appreciated, however the extent of K_{ATP} current's influence has been a work in progress since. For instance, when a similar ATP-sensitive potassium current was identified in pancreatic β-cells, the missing link between how extracellular blood glucose could control membrane excitability and insulin secretion was made (Rorsman and Trube, 1985). Soon after, SU compounds were found to have an effect on the pancreatic K_{ATP} current, but it was not clear whether the SU receptor was one-and-the-same as the K_{ATP} channel or merely affecting its

activity from a distance (Sturgess et al., 1985). This question remained unanswered until the age of molecular cloning eased the identification of the K_{ATP} channel.

We now know that K_{ATP} channels are composed of two dissimilar subunits: Kir6.X and SURX (Figure 1). The inwardly rectifying potassium channel subunit Kir6.1 (originally called uKATP-1 because it was ubiquitously expressed) was the first K_{ATP} subunit to be cloned in March of 1995 (Inagaki et al., 1995c) using ^{32}P-labeled cDNA probes based on a different Kir subfamily member (Kir3.1) to screen a pancreatic β-cell cDNA library for the unidentified channel. The mystery of the K_{ATP} current was not solved, however, because uKATP-1 showed small currents and incomplete pharmacological properties when it was exogenously expressed. The first sulfonylurea receptor (SUR1) was cloned shortly after in April of 1995 using high affinity ^{125}I-labeled SU compound as a tracer to isolate the protein for sequencing (Aguilar-Bryan et al., 1995) but SUR1's fundamental role in K_{ATP} channel structure was still undetermined. The first reports of reconstituted K_{ATP} channel activity were published seven months later with co-expression of Kir6.1 or (newly cloned) Kir6.2 with SUR1 (Inagaki et al., 1995a; Sakura et al., 1995). Fifty-three years after Janbon's trial participants died, the K_{ATP} channel was identified. Two more isoforms of SUR were subsequently cloned, SUR2A and SUR2B, which are splice variants of each other differing in the last 42 amino acids (Inagaki et al., 1996; Isomoto et al., 1996). Interestingly, the genes encoding SUR1 (ABCC8) and Kir6.2 (KCNJ11) lie in series on chromosome 11 (11p15.1); similarly SUR2 (ABCC9) and Kir6.1 (KCNJ8) genes are located together on chromosome 12 (12p12.1) (Inagaki et al., 1995b; Thomas et al., 1995; Ayyagari et al., 1996; Chutkow et al., 1996). As one would expect, Kir6.X and SURX subunit isoform varies with tissue distribution and contribute differential channel properties (Table 1) [reviews: (Lawson and Dunne, 2001; Bryan et al., 2004), (Beech et al., 1993; Isomoto et al., 1996; Gribble et al., 1998; Matsuo et al., 2000)]. The pancreatic isoform of K_{ATP} is the focus of this dissertation and is made up of Kir6.2 and SUR1.

Introduction to K_{ATP} Structure and Regulation

Since its cloning and reconstitution, much work has gone into studying the structure and regulation of K_{ATP} channels. Kir6.2 has two transmembrane (TM) segments with cytoplasmic N- and C-termini, whereas SUR1 is a massive 17 TM segment protein with three TM domains (TMD0, 1 and 2) that also has extensive cytoplasmic architecture (Figure 1, and discussed in greater detail below). We know K_{ATP} is a hetero-octameric structure made up of four pore-forming Kir6.X subunits surrounded by four accessory SUR subunits (Clement et al., 1997; Inagaki et al., 1997; Shyng and Nichols, 1997). Like channel activity, contributions to K_{ATP} assembly, stability and trafficking are made by both subunits [reviewed in (Neagoe and Schwappach, 2005)]. For instance, SURX and Kir6.X subunits both contain a three amino acid ER-retention motif (RKR) that becomes shielded upon attaining proper tertiary structure (Zerangue et al., 1999). A detailed definition of that tertiary structure, however, is far from complete.

Intact K_{ATP} channels have yet to be crystallized for high resolution 3-D structure determination. One low resolution electron microscopy single-particle structure of an SUR1-Kir6.2 fusion construct has been published (Figure 1B) (Mikhailov et al., 2005). This model is consistent with the body of functional data placing the N-terminal transmembrane-domain zero (TMD0) of SUR1 close to Kir6.2; unfortunately, at 18 Å resolution, this structure does not facilitate hypothesis-building in the search for specific interactions within or between subunits. High resolution homology models do exist for most of Kir6.2 and isolated cytoplasmic regions of SUR1 (and these have contributed predictive power to design structure-function experiments as well as support for models based on functional and biochemical data) but these models exist as homomeric structures and in the absence of each other. **Therefore, precise interfaces between SUR1 and Kir6.2, and therefore transduction mechanisms, are entirely unspecified by current crystallographic data.**

K_{ATP} channel activity is regulated by a host of different molecules. Classes of regulatory molecules discussed in this thesis include: intracellular nucleotides, phosphoinositides, sulfonylureas (SU) and K-channel openers (KCOs). In addition, long-chain acyl coenzyme As (CoAs) (Branstrom et al., 1998; Branstrom et al., 2004), G proteins (Sanchez et al., 1998), phosphorylation by several kinases (Beguin et al., 1999; Chang et al., 2009; Orie et al., 2009) and zinc (which is co-secreted with insulin and may play a role in negative feedback of β-cell activation) (Bloc et al., 2000; Fu et al., 2009) have all been shown to directly modulate K_{ATP} channels, though the extent of their physiologic importance is unknown at this time.

Introduction to K_{ATP} in Physiology and Disease

Because pancreatic β-cells constitutively express the low-affinity, high-capacity glucose transporter, GLUT2, blood and intracellular β-cell glucose concentrations rise in parallel. Glucose is converted to ATP through classic glycolytic pathways, leading to a rise in the intracellular [ATP/ADP] ratio. K_{ATP} is the main resting membrane conductance of β-cells, so as [ATP/ADP] rises and the channels close the membrane potential depolarizes significantly. This leads to activation of voltage-gated calcium channels (VGCCs) and an influx of Ca^{2+} ions that, in turn, stimulate exocytosis of insulin granules (Figure 2).

Genetic mutations in SUR1 and Kir6.2 are well established causes of insulin secretion disorders that present in the first days to weeks of life. A spectrum of disease phenotypes exist such that K_{ATP} over-activity causes too little insulin secretion [Permanent Neonatal Diabetes Mellitus (PNDM)] and channel under-activity causes too much insulin secretion [Congenital Hyperinsulinism (CHI)] (Figure 2). The molecular mechanisms by which K_{ATP} subunit mutations can lead to channel over- or under-activity are numerous and represent properties of ligand binding, signal transduction and channel biogenesis, and sometimes multiple effects combined.

As such, investigating the mechanisms of action by disease causing variants has led to significant advancements in our understanding of basic principles of K_{ATP} channel function.

Inward Rectifier Potassium Channel 6.2

Kir6.2 Structure

Kir6.X subunits are homologous in sequence and structure to the six other subfamilies and at least 13 other Kir genes that constitute all mammalian inwardly rectifying potassium channels. The Kir6 subfamily is unique among the Kir proteins, however, because they do not express or assemble into channels at the plasma membrane in the absence of a second non-Kir protein, SUR (Hibino et al., 2010). Four Kir6.2 subunits comprise the conduction pore of K_{ATP} and instill it with certain intrinsic properties including ATP and PIP_2 sensitivity.

Several potassium channels have been crystallized and high resolution structures attained. Nobel prize-worthy bacterial KcsA was the first; it is a two-TM channel whose general structural elements have proven to be well conserved among all subsequent structures (Doyle et al., 1998). KcsA structure includes an outer helix (M1), extracellular turret protrusion, pore helix, selectivity filter and inner helix (M2) (Figure 3A). Cytoplasmic regions of this channel were either removed or disordered and therefore not resolved. Subsequently, several inward rectifier potassium channel structures from mammalian and bacterial sources were solved that included substantial portions of the cytoplasmic N- and C-termini [**Kir3.1** (Nishida and MacKinnon, 2002), **KirBac1.1** (Kuo et al., 2003), **Kir2.1 and Kir3.1** (Pegan et al., 2005), **Kir3.2 cytoplasmic region** (Inanobe et al., 2007), **Kir3.1-KirBac1.3 chimera** (Nishida et al., 2007), **KirBac1.1 and KirBac3.1** (Clarke et al., 2010)]. An important addition to the KcsA model has been the inclusion of an amphipathic helix positioned parallel to the intracellular aspect of the plasma membrane just prior to TM1, the so called ‘slide helix’ (residues R54 – L66 in Kir6.2, see

also Figure 7A). Models of Kir6.2 can and have been developed based on these Kir structures (Lin et al., 2003; Antcliff et al., 2005; Haider et al., 2007).

Francis Ashcroft's group found that by truncating the C-terminus of Kir6.2 (Kir6.2ΔC) functional homotetrameric channels can be expressed in the absence of SUR (Tucker et al., 1997). It turns out that Kir6.2 can also be expressed in the absence of SUR1 by mutating an ER-retention/retrieval sequence located on the C-terminal (which is absent in the Kir6.2ΔC channels) from RKR to AAA (schematic in Figure 4A) (Zerangue et al., 1999). By employing these molecular tricks, many research teams have characterized properties of the K_{ATP} channel that are due to Kir6.2 in the absence of SUR1.

In this dissertation, reference to K_{ATP} implies channels composed of full-length Kir6.2 and SUR1 subunits, in contrast to Kir6.2ΔC channels. Additionally, channels composed of Kir6.2ΔC and the TMD0 portion of SUR1 only (see Figure 4A) are referred to as mini-K_{ATP} and are one tool available to study the contributions of this SUR domain to K_{ATP} properties.

Kir6.2 Gating

Kir6.2ΔC channels exhibit different single channel properties than K_{ATP}. The single channel open probability (P_o) is a calculation of how much time an individual channel spends in the open/conducting conformation and ranges from 0 to 1; a P_o of 1 means the channel is always open. Kir6.2ΔC channels have much lower P_o than K_{ATP} (~0.1 versus 0.6, respectively) (Tucker et al., 1997; Pratt et al., 2009). The pattern of activity between the channel types is also visibly different (Figure 4 B versus C). Kir6.2ΔC channels have very brief channel openings separated by relatively long closures (Figure 4C, top). K_{ATP} [and channels made up of full-length SUR1 plus Kir6.2ΔC (Chan et al., 2003)] display 'bursts' of activity where the channel flickers open and closed rapidly separated by longer periods of closure (Figure 4B). In terms of kinetic analysis,

K_{ATP} exhibits a singly exponential open life-time and multi-exponential closed lifetimes which means, simply, it displays only one type of open state (i.e., within bursts in K_{ATP} or brief non-bursts in Kir6.2ΔC) and at least two closed states [i.e, 'fast' (within bursts) and 'slow' (between bursts)]. Kinetic models of open- and closed-states have been developed based on these properties [review: (Enkvetchakul and Nichols, 2003)]. Contributions of the different parts of SUR1 to these bursting properties are discussed in greater detail below, including the fact that TMD0 of SUR1 is necessary and sufficient to change Kir6.2ΔC single channel kinetics to include fast bursting (Babenko and Bryan, 2003; Chan et al., 2003).

Identification of the structural changes within Kir channels that are associated with gating is an active (and controversial) field of study. Gating of ion channels refers to the processes by which the conduction pathway transitions from open to closed. Crystal structures of other Kir channels in what appear to be open (Nishida et al., 2007; Clarke et al., 2010) and closed states (Doyle et al., 1998; Kuo et al., 2003; Nishida et al., 2007; Clarke et al., 2010) direct how we think about Kir gating in general and K_{ATP} (Kir6.2) in particular. For instance, the fact that Kir6.2 shows two kinds of channel closures, 'slow' and 'fast', suggest there are at least two different gates to ion flow. The selectivity filter within the transmembrane section of the pore is thought to regulate fast gating (Proks et al., 2001; Enkvetchakul and Nichols, 2003). The gate mediating slow, long-lasting closures is more mysterious, but may involve motions in the cytoplasmic section of the pore that constrict ion flow (more on this below).

Kir6.2 and ATP

There are four identical ATP binding sites in K_{ATP}, thought to be composed primarily, if not exclusively, of residues in the Kir6.2 subunit. Although Kir6.2ΔC channels retain ATP-sensitive inhibition, ATP is more effective in the presence of SUR1. Thus, SUR1 is said to provide a hypersensitizing effect on ATP-sensitivity (referred to as SUR1 hypersensitization in this

dissertation). Kir6.2ΔC channels have a half-maximal inhibitory concentration (IC_{50}) for ATP of ~100-350 μM, whereas full-length K_{ATP} channels have an IC_{50} nearer 10-20μM (Figure 4D) (Tucker et al., 1997; Pratt et al., 2009).

Identification of the ATP-binding site in Kir6.2 was achieved using functional and biochemical approaches, utilizing disease-causing and exogenously introduced mutations as well as structural models based on homologous Kir proteins. It took several years to determine the ATP-binding residues in part because the primary sequence of Kir6.X does not contain any classical nucleotide binding motifs; this originally surprising finding can be explained by the fact that N- and C-termini from adjacent Kir6.X subunits contribute to each ATP-binding site.

Electrophysiological experiments have contributed greatly to the identification of residues involved in ATP-binding. Generally, mutations that change ligand-sensitivity can fall in to three broad categories: 1) **direct effects at the ligand biding site** which will decrease binding affinity for the ligand; 2) **allosteric effects** in which a structural change somewhere outside the binding site leads to an indirect structural change at that binding site and decreased ligand binding; 3) **transduction effects** such that ligand binding remains intact but the ability of bound ligand to modify activity is hindered. If a mutation decreases ATP-sensitivity without altering intrinsic channel properties, i.e., spontaneous activity in the absence of nucleotide, it is considered to be a good candidate for potential involvement in ATP binding. In contrast, a mutation that decreases ATP-sensitivity but also alters intrinsic properties is said to change the “apparent” ATP sensitivity and likely effect transduction of ATP-induced closure rather than binding. Multiple mutations in Kir6.2 have been described that decrease ATP-inhibition without affecting intrinsic P_o of K_{ATP} or mini-K_{ATP} channels: R50, I182, K185, R201, F333 and G334 (Drain et al., 1998; Koster et al., 1999; Li et al., 2000; Proks et al., 2004; Tammaro et al., 2005; Shimomura et al., 2006; Masia et al., 2007). Further, by considering how mono-, di- and tri-phosphate

nucleotide inhibition is affected, relationships between the adenosine and three phosphates of ATP and Kir6.2 residues has been described. For instance, R50 is thought to interact with ATP's γ-phosphate and K185 with the β-phosphate (Trapp et al., 2003).

Complementary approaches to determine the ATP-binding site support the functional data. Homology models of Kir6.2 based on crystal structures of related Kir channels include a pocket for ATP made up of N- and C-terminal residues (Antcliff et al., 2005; Haider et al., 2007). Additionally, photo-affinity labeling of Kir6.2 subunits with R50G or K185Q mutations by ATP (8-azido-[γ-^{32}P] is reduced, as would be expected for binding-site mutations (Tanabe et al., 1999).

Based in part on best fits of single-channel data to multi-state kinetics models and on data collected from K_{ATP} channels containing Kir6.2 subunits incapable of binding ATP, a single ATP molecule is thought to be sufficient to close K_{ATP} (Qin et al., 1989; Nichols et al., 1991; Enkvetchakul et al., 2000; Markworth et al., 2000). The extent of conformational change throughout K_{ATP} that results from a single binding event is not known.

Kir6.2 and PIP_2

Kir6.2, like all other mammalian Kir channels, is activated by interactions with phospholipids, including phosphatidylinositol 4,5-bisphosphate (PIP_2) (Fan and Makielski, 1997; Baukrowitz et al., 1998; Shyng and Nichols, 1998; Logothetis et al., 2007a). Importantly, Wang et al. showed direct interaction of PIP_2 with purified Kir6.2 (Wang et al., 2002). Mapping out the residues that are involved in PIP_2 binding has also taken advantage of mutagenesis and structural data. Like the ATP-binding site, putative PIP_2-binding residues reside in both N- and C- termini. Kir6.2 sites that have been identified as candidates for PIP_2 interaction by mutagenesis and electrophysiologic studies include: R54, K67, R176, R177, R206, R301 (Fan and Makielski, 1997; Shyng et al., 2000; Cukras et al., 2002a, b; Schulze et al., 2003). Note these are all

positively charged residues, in harmony with the idea they would be interacting with the negatively charged phosphoinositol headgroup of PIP_2. Mapping these residues onto a Kir6.2 homology model indicates they are clustered near the top of the cytoplasmic domain adjacent to the plasma membrane; of course, proximity of the PIP_2 binding residues to the source of membrane lipids is what one would predict (Haider et al., 2007; Stansfeld et al., 2009). Additional PIP_2 interacting residues identified by molecular modeling include K39 and N41, though functional data to support their role is lacking (Haider et al., 2007).

Some mutations that affect PIP_2 response lie away from the plasma membrane, and often map to sites within the interface between two Kir6.2 subunits (e.g., R192, E229, R314). Rather than directly mediating PIP_2-binding, these residues are probably involved in maintaining channel stability. For instance, E229 and R314 form an ion-pair between adjacent Kir6.2 subunits. When either is mutated to alanine (extinguishing their electrostatic interaction) the channels cannot maintain steady-state current under nucleotide-free conditions and are said to inactive (Figure 5) (Lin et al., 2003). It is thought that the loss of E229:R324 interaction leads to an architectural weak point and the open state becomes unstable. Interestingly, exposure of the inactivating channels to high concentrations of ATP can briefly re-set them such that they can open again upon removal of inhibitory nucleotide (Figure 5A). ATP binding (between adjacent N- and C-termini) likely draws back together Kir6.2 subunits. Additionally PIP_2 slows or reverses the inactivation (Figure 5B), implying phosopholipids grip Kir6.2 cytosolic regions to the plasma membrane, delaying the structural breakdown of the open state. The E229:R314 interaction was shown to be between adjacent subunits by testing multiple different K_{ATP} channels composed of mutant Kir6.2 dimers (Figure 5C). This work shows that conformational stability of Kir6.2 cytosolic regions contribute to PIP_2-responsiveness.

The mechanism by which PIP_2 binding causes K_{ATP} channels to open remains an unanswered question. One model supported by mutagenesis and cysteine-modification data involves significant conformational changes in the cytoplasmic domains of Kir6.2 brought about by PIP_2 exerting tangential forces on Kir6.2 N- and C-termini. In this model, the N-terminus slide helix and PIP_2-binding residues of the C-terminus get pulled away from the central axis of the channel which, in turn, apply forces on gates in permeation pathway (Figure 6) (Enkvetchakul et al., 2007; Logothetis et al., 2007a). There are several putative gates described within the TM and cytosolic permeation pathway of Kir6.2 and determining which is/are affected by PIP_2 stimulation is a research target of great interest. Toward this end, it would be helpful to know in detail how PIP_2 changes single channel kinetic properties of K_{ATP}. Kinetic analysis has been performed on cardiac K_{ATP} (SUR2 + Kir6.2) and PIP_2 reportedly increases P_o in part by lengthening the duration of bursts and by shortening long (between burst) closed times. The length of open times does not significantly change, implying an effect at some gate other than the selectivity filter which governs K_{ATP} fast gating (Fan and Makielski, 1999). An energetics consideration also supports a mechanism by which PIP_2 induces conformational changes near the site of initiation (i.e., at a gate within the cytosolic pore region) because structural changes at more-distant sites (selectivity filter) would be thermodynamically less favorable.

Activation of K_{ATP} channels by PIP_2 causes a concomitant decrease in ATP sensitivity (Baukrowitz et al., 1998; Shyng and Nichols, 1998). Although the binding sites for both ligands are predicted to be composed of N- and C- termini, adjacent Kir6.2 subunits and to be near one another in homology models, current agreement in the field is that ATP and PIP_2 are not competitive ligands. The binding of PIP_2 is hypothesized to tether cytoplasmic domains of Kir6.2 to the plasma membrane, physically drawing out and stabilizing an open conformation (Figure 6) (Enkvetchakul et al., 2007). This stabilized open state is thought to either cause a transduction effect such that the energy barrier of bound ATP to drive the channel into the

closed state increases (Enkvetchakul et al., 2000) or cause an allosteric effect such that the PIP_2-bound channel has a decreased probability to take on a conformational state competent to bind ATP (MacGregor et al., 2002; Wang et al., 2002; Haider et al., 2007), or both. Identification of two residues by molecular simulations that appear to contribute to both the ATP- and PIP_2-binding sites, K39 (Haider et al., 2007) and R50 (Stansfeld et al., 2009) accentuates their intimacy. However, a subtle distinction of how K39 contributes to both supports that the two sites are distinct: backbone atoms interact with ATP and side-chain atoms with PIP_2.

Kir6.2 and Pharmaceuticals

In general, Kir6.X is not considered a pharmacologic target for exogenous K_{ATP} inhibitors (SU, glinides, etc.) or potassium channel openers (KCOs, diazoxide, pinacidil, nicorandil, etc). Rather, SUR1 acts as the pharmacologic target. At high doses, however, Kir6.2ΔC channels can be inhibited by SU drugs (Gribble et al., 1997b). Also the dose-response curve of K_{ATP} channels for SU compounds has three inflection points, indicating high- (SUR1 binding) and low- (Kir6.2 binding) affinity inhibition. Finally, photo-sensitive SU compounds have been used to label Kir6.2 in the presence of SUR1 (Nelson et al., 1992; Schwanstecher et al., 1994a; Clement et al., 1997; Gros et al., 1999).

Sulfonylurea Receptor 1

SUR1 Structure

SUR1 plays a critical role in modulating the gating of Kir6.2 pore-subunits, conferring altered nucleotide and lipid sensitivities as well as drug sensitivities (Table 1). The presence of SUR1 changes intrinsic properties of the channel, including P_o and the kinetics of pore opening and closure. SUR1 also helps to define the biogenesis, degradation and trafficking of K_{ATP} channels.

SUR1 is a member of the ATP-binding cassette (ABC) transporter subfamily, whose members also include multi-drug resistance protein and cystic fibrosis transmembrane conductance regulator (Dean and Allikmets, 2001). SUR is composed of the core ABC transporter structure: two six-spanning transmembrane domains (TMD1 and TMD2) and two large cytoplasmic ABC domains [also called nucleotide binding domains (NBD) or nucleotide binding folds (NBF)]. Further, SUR1 is rare among members of the ABC transporter subfamily in that it has an additional five-spanning N-terminal domain (TMD0) and inter-connecting cytoplasmic loop (L0) (Figure 1) (Conti et al., 2001). SUR1 shares 67% sequence identity with SUR2; SUR2A and SUR2B share 98% sequence identity. With regard to TMD0 (aa1-198) or TMD0-L0 (aa1-295), SUR1 and SUR2 share 72% and 70% sequence identity, respectively.

SUR1 TMD0-L0

In contrast to Kir6.2, a dearth of crystallographic structures exists for SUR1 on which it can be modeled. High resolution structures of some ABC transporter family members' core domains do exists, but these structures only involve regions of low sequence and/or topological conservation with SUR (Rees et al., 2009). In contrast, NBDs are highly conserved among ABC transporter proteins, and have been isolated, crystallized and used as the basis for predictions about SUR's NBD structure and function (Masia and Nichols, 2008). As no homologous structures exist for TMD0-L0 domains of SUR, structural predictions are based on sequence and biochemical data. TMD0 was predicted and then shown to have a five-TM structure (Tusnady et al., 1997; Raab-Graham et al., 1999; Conti et al., 2001). An amphipathic helix predicted to exist within L0 (residues ~K205–F217) is termed the 'sliding helix,' akin to the 'slide helix' in Kir6.2 (Figure 7A). A second amphipathic helix is predicted near-by (residues ~Y230–K242) and is conserved and functionally important among other ABC transporter proteins that also include the TMD0-L0 domain (Bakos et al., 2000).

TMD0 and L0 are critically important for proper SUR1-Kir6.2 coupling. Single channel recordings of K_{ATP}-mini channels composed of Kir6.2ΔC plus TMD0 indicate TMD0 (aa1-196) is sufficient to cause bursting and increase P_o to near full-length K_{ATP} values (Figure 4C, bottom) (Babenko and Bryan, 2003; Chan et al., 2003). Within K_{ATP}, one structural model has TMD0-L0 juxtaposed against the Kir6.2 N-terminal where it can manipulate Kir6.2 gating (Figure 7B). In this model, L0's sliding helix is proposed to lie adjacent to and determine positioning of Kir6.2's slide-helix by supplying a pulling force, which in turn leads to repositioning of pore-lining TM segments and increased P_o. More distal sections of L0, in contrast, counteract this force and even push back on the Kir6.2 N-terminus to decrease P_o (Babenko and Bryan, 2003; Babenko, 2005). Evidence to support this model includes: 1) extension of TMD0 to include varying lengths of L0 affects K_{ATP}-mini channel P_o in the following way: inclusion of the sliding helix (aa1–232) leads to near maximal P_o (0.91) but lengthening L0 further (aa1–256 and aa1–288) attenuates P_o (0.31 and 0.23, respectively); 2) exposure of K_{ATP} to purified Kir6.2 N-terminal fragments (aa2–33) increases the P_o to near maximal (0.92); 3) co-expression of SUR1 with Kir6.2 N-terminal truncations of between 32 and 44 residues [i.e., Kir6.2ΔN32(or 44)] also increase P_o to near maximal (0.92) (Babenko et al., 1999b; Koster et al., 1999; Babenko and Bryan, 2002). **Clarifying TMD0-L0 structural and functional interactions is of utmost importance because this segment of SUR1 is so clearly involved in Kir6.2 modulation.**

SUR1 and ATP

There are at least two ways in which SUR1 contributes to K_{ATP}'s net response to intracellular nucleotide. First, the presence of SUR1 enhances ATP sensitivity and inhibition by the Kir6.2 binding sites (discussed above), termed SUR1 hypersensitization (Shyng et al., 1997b; Tucker et al., 1997). Second, SUR1 confers Mg·ATP-sensitive stimulation to ATP-inhibited K_{ATP} channels. Besides the obvious sign reversal, ATP-stimulation via SUR1 differs from ATP-inhibition via Kir6.2 in at least two respects—it is Mg^{2+} and hydrolysis dependent. The net

activity of the Kir6.2 pore, therefore, is influenced by inhibitory (through Kir6.2 binding sites) and stimulatory (through SUR1 binding sites) effects of intracellular nucleotides. The necessary hydrolysis of Mg·ATP can be bypassed using Mg·ADP, but it is still Mg^{2+}-dependent. Interestingly, estimates of β-cell intracellular ATP concentrations are in the millimolar range, well above the IC_{50} for ATP-inhibition, so prior to our knowledge of Mg·ATP-stimulation by SUR1 it was not clear how K_{ATP} channels could ever open even under the most hypoglycemic of conditions (Cook and Hales, 1984). By responding to [ATP/Mg·ADP] rather than [ATP] only, the physiologic range of metabolic statuses over which K_{ATP} can respond is maximized.

SUR's two cytoplasmic NBDs are homologous to and presumably behave similar to other members of the ABC transporter subfamily. Catalytic ATPase activity has been shown for SUR2, such that Mg-bound ATP gets hydrolyzed to Mg·ADP (Matsuo et al., 1999; Bienengraeber et al., 2000). The hypothetical mechanism of action for hydrolysis is that NBD1 and NBD2 form a dimer creating two nucleotide binding sites at their interface and enabling hydrolysis of ATP to ADP (Masia and Nichols, 2008). The energy from this reaction is converted into (unknown) conformational changes within SUR and ultimately to the Kir pore. Hydrolysis is not necessary to induce K_{ATP} activity, however, as addition of Mg·ADP is also an effective stimulatory ligand. Select mutations within the NBDs can completely block Mg·nucleotide stimulation (Shyng et al., 1997b). It is not known which or how conformational changes within SUR1 are transduced into achievement/stabilization of a Kir6.2 open state.

SUR1 and Sulfonylureas

Sulfonylurea drug effects on SUR have been extensively studied. The dose-response relationship for SU drugs (including glibenclamide and tolbutamide) is biphasic (Figure 8A) because K_{ATP} channels have high-affinity binding sites on SUR1 and low-affinity binding sites on Kir6.2, both of which are located intracellularly (Schwanstecher et al., 1994b; Gribble et al.,

1997b). A bipartite binding pocket was predicted based on differential responses and chemical structures of SU compounds long before the molecular biology revolution enabled its identification (Bryan et al., 2005). For example, the low affinity SU tolbutamide has only a short-chain sulfonylurea moiety versus the high affinity glibenclamide which includes two chemical moieties: a sulfonylurea structure and an amide moiety. Indeed, the binding pocket for SU compounds is now modeled as having 'A' (for the SU moiety) and 'B' (for the non-SU benzamido moiety) sites (Figure 8B). Residues that disrupt these sites have been identified (Figure 8C) [A site: In TMD2, S1237Y (Ashfield et al., 1999; Hambrock et al., 2001); B site: In L0, Y230A (Bryan et al., 2004)]. Further, based on photo-affinity labeling, it appears that in addition to L0, the N-terminal portion of Kir may directly contribute to the B-site (Vila-Carriles et al., 2007). Whether a given compound interacts with one or both sites is correlated to certain drug properties. For instance, glibenclamide binds at both sites and has lower IC_{50} and binds irreversibly compared to tolbutamide, which has higher IC_{50} and binds reversibly.

In addition to their channel inhibitory action, SU compounds can function as chemical chaperones of K_{ATP} trafficking (Yan et al., 2004). Numerous mutations located in Kir6.2 or SUR1 that diminish K_{ATP} surface expression can be 'rescued' by treatment with SU. Concentrations necessary for the chemical chaperone effect are greater than needed for channel inhibition (~100-1000 fold). Contrary to photo-labeling experiments that show SU interaction with SUR1 expressed alone (Crane and Aguilar-Bryan, 2004; Vila-Carriles et al., 2007), Kir6.2 must be present for the chaperone effect to occur on SUR1 mutant channel (Yan et al., 2006). In addition, the presence of the SU binding sites appear to be necessary for the chaperone effect as mini-K_{ATP} channels are unaffected by SU treatment, and mutations within either the 'A' or 'B' bipartite SU binding site greatly diminish the SU chaperone effect (Yan et al., 2006). Together these findings lend strong support to the idea that SU are acting directly on the K_{ATP} channel

complex. Interestingly, to date, only SUR1 mutations that lie within the TMD0 domain are sensitive to SU rescue (Yan et al., 2007).

SUR1 and Potassium Channel Openers

Potassium channel openers (KCOs) bind to SUR in an isoform specific manner (Table 1). Details of their binding sites are generally less refined than for SUs, but several studies using SUR1-SUR2 chimeras have identified regions and residues that may be important in conferring KCO sensitivities (Uhde et al., 1999; Moreau et al., 2000). Concerning KCOs' ability to act as chemical chaperones, this is debated. At least one report using diazoxide is in the affirmative, but this result could not be recapitulated by our lab (Partridge et al., 2001; Yan et al., 2004).

SUR1 and PIP_2

All Kir channels, and a growing number of other ion channels and transporters, require PIP_2 to function [review: (Suh and Hille, 2008)]. The majority of what we know about modulation of K_{ATP} activity by PIP_2 is based on structure-function analysis of the Kir6.2 subunit and comparisons to homologous sites in other members of the Kir family (Baukrowitz et al., 1998; Haider et al., 2007), which neglects almost entirely the contributions SUR1 make to this fundamental property. Application of PIP_2 increases K_{ATP} P_o, thus augmenting channel current. Interactions between membrane-bound PIP_2 and the cytoplasmic domains of Kir6.2 are important for this response, but certainly SUR1 is also involved. In the absence of SUR1, for instance, Kir6.2ΔC channels are relatively insensitive to PIP_2 stimulation (Baukrowitz et al., 1998; Shyng and Nichols, 1998). Suggestively, Kir6.2ΔC channels have very low P_o (~0.1) that increases substantially with the addition of minimal portions (~0.6-0.9) of or full-length SUR1 (~0.6) in part by introducing bursts of activity (see Figure 4). As discussed above, PIP_2 lengthens the duration of bursts in the cardiac isoform of K_{ATP} (SUR2 + Kir6.2) (Fan and Makielski, 1999). Is it possible, therefore, that SUR and PIP_2 act on Kir6.2 by converging mechanisms – that the transduction of

signals from SUR1 to Kir6.2 requires PIP_2? Studies in other classes of Kir channels have shown that PIP_2-Kir interactions are stabilized by a myriad of channel modulators (Logothetis et al., 2007b; Xie et al., 2007). Perhaps SUR1 is analogous to a 'channel modulator' in this context. PIP_2 affinity for K_{ATP} has not been directly measured and experiments that assess PIP_2 binding to the K_{ATP} complex [as has been done for Kir6.2ΔC (Wang et al., 2002)] could help to clarify this issue. Considerable more work is necessary to illuminate the molecular interactions and adjustments within and between SUR1 and Kir6.2 that define PIP_2's effects.

Generally, K_{ATP} channels display low specificity to activation by different phosphoinositides but this does not seem to be SUR-dependent (i.e., Kir6.2ΔC channels also show low specificity) (Rohacs et al., 2003). However, differential responses to PIP_2 (and other phospholipids) do exist between K_{ATP} channels composed of different SUR isoforms, and this difference is mediated by the first 6 TM segments (including TMD0 and L0) of the SUR isoforms (Song and Ashcroft, 2001).

K_{ATP} in Disease

Monogenic Hyperinsulinemic Disorders

Genetic mutations in K_{ATP} that cause under-activity short-circuit its ability to act as a biosensor, and persistent activation of VGCCs and insulin granule release ensue leading to CHI [also known as Persistent Hyperinsulinemic Hypoglycemia of Infancy (PHHI)] (Figure 2). CHI was the first insulin secretion disorder to be linked directly to a mutation in the K_{ATP} channel, in this case to the SUR subunit (Thomas et al., 1995). CHI is a rare disease and rates can range from 1 in 50,000 to as high as 1 in 3,000 live births depending on the degree of consanguinity in the population (Fournet and Junien, 2003). Mutations in K_{ATP} contribute about 50% of all CHI cases, and most of these are due to mutations in the SUR1 gene (Tornovsky et al., 2004). Because the

defect is present from birth, brain damage due to severe and prolonged hypoglycemia is a constant threat. Currently one treatment option for CHI management is the pancreatic K_{ATP} channel activator, diazoxide, but it is often ineffective. When patients are unresponsive to pharmacological treatments they undergo partial or complete pancreatectomy, which introduces a life-time of iatrogenic diabetes and malabsorption issues.

Mutations in Kir6.2 or SUR1 can lead to CHI. Channel under-activity can be due, broadly, to either defects of channel activity or channel trafficking (Figure 2) (Shyng et al., 1997b; Shyng et al., 1998; Pratt et al., 2009). The typical defect in CHI mutant channels with dysfunctional activity is loss or attenuation of Mg·nucleotide stimulation (Huopio et al., 2002). Attenuated PIP_2 response has also been reported to cause CHI (Lin et al., 2006b). One might predict that increased ATP inhibition would also be a mechanism of CHI-mutant channels, but to date no such report exists. Loss of K_{ATP} surface expression can be caused by point mutations throughout either subunit. The underlying reasons for decreased surface expression may be numerous: protein misfolding leading to improper RKR-shielding or quaternary arrangement, decreased stability either immediately upon translation or at the plasma membrane, etc.

The finding that SU drugs can act as chaperones for select K_{ATP} trafficking mutants opens up the possibility that new classes of drugs might be developed to treat these children. Currently, prescribing SU for the management of trafficking-defective CHI patients is implausible: although the drugs are predicted to improve expression of the channel, they also effectively block channel activity thereby negating the primary reason for their use. Further, although the first mutations sensitive to the SU chaperone effect displayed normal electrophysiological properties (Yan et al., 2004), subsequent findings indicate other trafficking mutants may harbor dramatic channel activity defects (Lin et al., 2006a; Pratt et al., 2009). Therefore, at least two hurdles must be overcome in order for new classes of K_{ATP} chaperones to be developed: 1) any

potential therapeutic must possess protein-chaperoning in the absence of channel activity effects and 2) genotype specific testing would be required before any individualized drug trial to insure the mutant channel does not exhibit untoward properties. While brute force drug screening is one option to identify new compounds, insight into the structural changes brought about by mutations and by SU binding has the potential to direct a more methodical search.

Monogenic Diabetic Disorders

Mutations that cause channel over-activity will effectively block any metabolic status signal from triggering insulin granule release (Figure 2)—causing forms of neonatal diabetes mellitus, a rare disease affecting about 1 in 400,000 live births (Shield, 2000). The majority of K_{ATP} mutations that fall in this category result in life-long endocrine pancreas dysfunction, PNDM (de Wet et al., 2007; Shimomura et al., 2010); however, there are several reports of patients with symptoms that remit over time, called Transient Neonatal Diabetes Mellitus (TMDM) (Gloyn et al., 2005; Vaxillaire et al., 2007). The pancreatic isoforms of K_{ATP} subunits are expressed in many tissue types throughout the body, especially CNS and peripheral neurons and skeletal muscle, and so cases with the most severe channel defects present with a more serious clinical phenotype that reflects cellular dysregulation in these extra-pancreatic sites: Developmental delay with Epilepsy and Neonatal Diabetes (DEND syndrome) (Proks et al., 2005b; Proks et al., 2006). The molecular mechanisms that lead to K_{ATP} over-activity include decreased ATP sensitivity (through disruption of ligand binding) (Shimomura et al., 2010), decreased 'apparent' ATP sensitivity (secondary to increased intrinsic P_o) (Proks et al., 2004) and increased Mg·ATP stimulation (Babenko et al., 2006). By and large, the degree of channel dysfunction correlates with the clinical phenotype (Hattersley and Ashcroft, 2005), but exceptions exist including ones in which the discrepancy can be explained by effects the mutations also have on channel trafficking (Lin et al., 2006a; Pratt et al., 2009). The most extreme examples of PNDM-activating mutations that

are attenuated by channel expression include R74W and E128K, which have such severe trafficking defects they actually present as the opposite disease, CHI.

Understanding the underlying cause of monogenic diabetes has led to a shift in clinical treatments. Previously, PNDM patients were treated exclusively with insulin – a relatively expensive, painful and difficult-to-manage therapy. This was because patients were (and may still be in some cases) misdiagnosed as having type I diabetes mellitus (DM) and because the etiology just wasn't understood. If a neonate presents with symptoms of DM before the age of six months, type I DM is unlikely and that child's DNA needs to be checked for mutations in SUR1 and/or Kir6.2 (Edghill et al., 2006; Flanagan et al., 2006). Now that we know β-cells are intact and K_{ATP} channel over-activity can be attenuated with SU, many individuals have been successfully transitioned off of insulin and onto oral SUs (Babenko et al., 2006; Pearson et al., 2006; Tonini et al., 2006). Importantly, SU treatment has led to improvement in cognitive and motor deficits in a child with DEND, as well (Slingerland et al., 2006; Slingerland et al., 2008).

K_{ATP} in Disease: Others

Briefly, K_{ATP} channels have been implicated in many other disease processes. Type II, so called 'adult onset,' diabetes mellitus is the mother of all diabetes in terms of the number of people affected, the absolute financial toll it takes on society and the man-hours of research dedicated to it. Of course the causes of type II DM are multi-factorial in terms of genetics and environment, but given the central role K_{ATP} plays in insulin secretion one may predict it also contributes to type II DM. It turns out that a common variant of the KCNJ11 (Kir6.2) gene (E23K) was found to be associated with type II DM in large scale SNP studies (Hani et al., 1998; Gloyn et al., 2003). Subsequent analysis showed strong allelic association of E23K with a second haplotype variant in ABCC8 (S1396A) making it more complicated to determine which one (or the combination) was detrimental in disease progression (Florez et al., 2004; Hamming et al., 2009).

Non-diabetic disease states associated with K_{ATP} channel dysfunction and disregulation include: dilated cardiomyopathy (Bienengraeber et al., 2004), hypokalemic periodic paralysis (Jovanovic et al., 2008) and adrenergic atrial fibrillation (Olson et al., 2007).

Conclusion

Hopefully, this introduction to K_{ATP} physiology, biochemistry and molecular biology has adequately served to highlight the current state of K_{ATP} research as well as the important clinical consequences continued exploration can provide. Despite all we know, one consistent shortfall throughout K_{ATP} literature is an ignorance of the specific interactions between Kir6.X and SUR that determine channel function. I was lucky, therefore, to join the Shyng lab just as two mutations in SUR1 were being characterized that were identified from patients with CHI (Yan et al., 2007). Both mutations (R74W and E128K) cause CHI through severe disruption of K_{ATP} trafficking to the plasma membrane. However, they have proven to be vastly more interesting than mere trafficking-mutants: when channel expression is rescued using SU chemical chaperones they behave like PNDM-causing mutants, the phenotype opposite to CHI [Chapter 2 (Pratt et al., 2009)]. They are unique, also, in the mechanism by which their channel activities are affected — both appear to cause functional uncoupling between SUR1 and Kir6.2 (Chapter 3). These mutations, therefore, present an exceptional opportunity to probe the elusive SUR1-Kir6.2 interface through biochemical and electrophysiological means (Chapters 3 and 4). Although a complete understanding of their effects continues to be a work in progress, strides have been made in our understanding of how SUR1 modulates Kir6.2 as a consequence of these studies.

Table and Figure Legends

Table 1. Distribution and select sensitivities of Kir6.X and SUR and K_{ATP} isoforms. Isoform distribution referenced from: neuromuscular.wustl.edu/mother/chan.html. Relative potassium channel opener sensitivities of specific SUR isoforms referenced from (Babenko et al., 1998); sensitivity rank order is +++ > ++ > + and – indicates no response. ATP sensitivity values of SUR1//Kir6.2 and SUR2//Kir6.2 referenced from (Inagaki et al., 1995a; Inagaki et al., 1996).

Figure 1. K_{ATP} subunits and structure (A) Schematic of SUR1 and Kir6.2 topology with select structural element indicated. Abbreviations: transmembrane domain (TMD), Loop 0 (L0), nucleotide binding domain (NBD), membrane spanning helix 1 and 2 (M1 and M2). **(B)** Select stimulatory and inhibitory ligands of K_{ATP}; the primary subunit with which each interacts can be inferred by whether it is located below the SUR or Kir6.2 schematics of (A). **(C)** Tertiary structure of K_{ATP} includes four pore-forming Kir6.2 subunits and four accessory SUR1 subunits (left). Low resolution EM structure of K_{ATP} channel with Kir6.2 (blue), SUR1 core domain (red) and SUR1-TMD0 (yellow) fit within as viewed from above and within the plane of the plasma membrane (middle, right) (Mikhailov et al., 2005). This model supports functional data indicating TMD0 lies in close opposition to Kir6.2.

Figure 2. Role of K_{ATP} in β-cell insulin release. Hyperglycemia causes an increase in the [ATP]/[ADP] ratio within β-cells. **(A)** Under normal circumstances (WT), this leads to closure of K_{ATP} channels (red) and membrane depolarization, opening of VGCCs (blue) and stimulation of insulin granule exocytosis (black circles). **(B)** Activating mutations in K_{ATP} lead to Permanent Neonatal Diabetes Mellitus (PNDM, left) in which K_{ATP} does not close sufficiently in response to increased [ATP]/[ADP] and insulin is not released under hyperglycemic conditions. Inactivating mutations in K_{ATP} lead to Congenital Hyperinsulinism (CHI) and can be caused by K_{ATP} mutations that reduce either K_{ATP} activity (middle) or surface expression (right) such that

decreased K_{ATP} channel conduction results in insulin exocytosis under hypo- and hyperglycemic conditions.

Figure 3. Kir structure and Kir6.2 ligand binding sites (A and B) Ribbon diagrams of single subunit (A) and tetrameric structure (B) of Kir channel and nomenclature of Kir subunits. Unstructured region shown as dotted line [Figure A and B modified from (Clarke et al., 2010)]. **(C)** Space filling homology model of Kir6.2 channel with adjacent PIP_2 (yellow) and ATP (red) binding sites highlighted (Haider et al., 2007).

Figure 4. Single channel recordings and properties of K_{ATP}, Kir6.2ΔC and K_{ATP}-mini channels. (A) Schematic of modified K_{ATP} subunits **(B)** Representative trace of a WT K_{ATP} single channel recording with an expanded time scale (red, boxed segment of upper trace) to illustrate the 'fast' (Burst) and 'slow' (Inter-burst) events [Figure modified from (Pratt et al., 2009)]. **(C)** Single channel records from Kir6.2ΔC channels (top) and K_{ATP}-mini channels (bottom). Expanded time scales in red. Scale bars were not represented in original publication [Figure modified from (Babenko and Bryan, 2003)]. **(D)** Relationship between ATP-sensitive inhibition and intrinsic channel P_o for K_{ATP}, Kir6.2ΔC and K_{ATP}-mini channels. Symbols describing each channel types are shown to the right of traces in (B) and (C), and values used are from (Babenko and Bryan, 2003).

Figure 5. K_{ATP} inactivation phenotype associated with Kir6.2 inter-subunit instability. (A) Lin et al. characterized two inactivation mutations in Kir6.2 (E229A and R314A) that have unstable currents in nucleotide-free solution but can be re-activated following ATP exposure. (B) The inactivation of E229A (shown) and R314A could also be reversed by exposure to 10μM PIP_2. Note also, ATP inhibition is decreased with PIP_2 exposure. (C) Inactivation can be overcome by re-establishing ion-pairs between subunits by expressing channels composed of

SUR1 plus Kir6.2-dimers with E229 and R314 mutants as indicated in the schematic on the right. Only inter-subunit ion-pairs are possible in channels formed by this Kir6.2-dimer. (Figures modified from(Lin et al., 2003))

Figure 6. Model of PIP_2 mechanism of action. PIP_2 in the plasma membrane is thought to interact with N- and C-terminal residues of Kir6.2 (including the slide helix, shown as colored rectangle) to induce conformational changes that get transduced into pore opening. Contributions by SUR1 are not described by this model [Figure modified from (Enkvetchakul et al., 2007)].

Figure 7. Amphipathic helices in SUR1 and Kir6.2 and a proposed model of SUR1-mediated modulation of Kir6.2 (A) Wheel diagrams of amphipathic 'sliding' helix in SUR1-L0 and 'slide' helix in Kir6.2. Their matching hydrophobic moments (vectors) both point toward the lipophilic face. **(B)** Model of proposed interactions between TMD0-L0 and Kir6.2 N-terminus and M1. Positive interactions (i.e., leading to increased P_o) are shown in red; Negative interactions (i.e., leading to decreased P_o) are shown in blue. The C-domain from an adjacent Kir6.2 subunit contributing residues to the ATP binding site (I182, K185, G334) is shown in light grey. Figures in (A) and (B) have been modified from (Babenko, 2005).

Figure 8. Sulfonylurea binding and inhibition of K_{ATP} (A) Dose-response curve for tolbutamide inhibition. High- (SUR1) and low-affinity (Kir6.2) contributions are indicated [figure modified from (Gribble et al., 1997b)]. **(B)** Schematic of SU binding site and how two SU molecular structures are proposed to fit into one or both sites [figure modified from (Grell et al., 1998)]. **(C)** Location of two mutations within SUR1 that disrupt binding at the 'A' (Y230A) and 'B' (S1238Y) sites of the bipartite SU binding site shown on the topology model of SUR1 from Figure 1.

Subunit Isoforms

	Tissue Distribution	Potassium Channel Opener Sensitivities		
		Diazoxide	Pinacidil	Cromakalim
Kir6.1	Smooth mm			
Kir6.2	Pancreas, heart			
SUR1	Pancreas, neurons (CNS/PNS), heart	+++	+	+
SUR2A	Heart, skeletal mm.	--	++	++
SUR2B	Brain, Liver, Skeletal mm., smooth mm.	+++	++	++

Channel Isoforms

	ATP IC_{50}
Kir6.2 + SUR1	~10uM
Kir6.2 + SUR2A	~100uM

EBP Chapter 1
Table 1

A

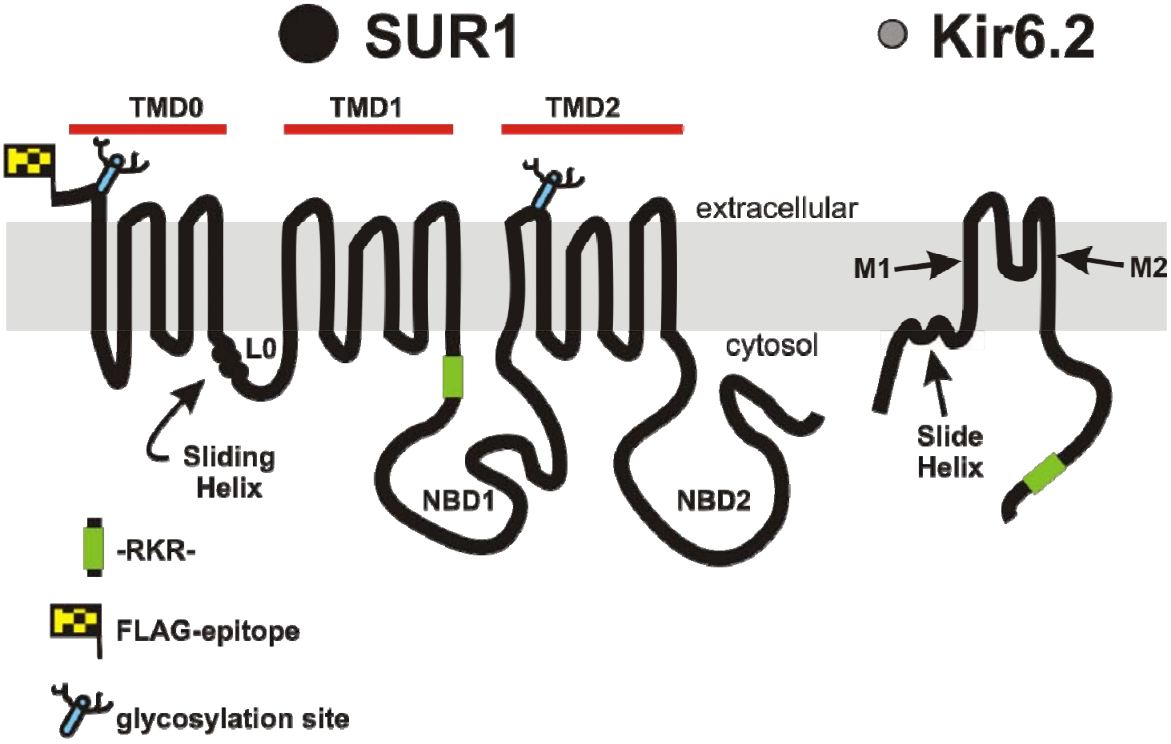

B

Stimulatory:	Mg• nucleotide Potassium Channel Openers (Diazoxide)	PIP_2
Inhibitory:	Sulfonylureas (Glibenclamide, Tolbutamide)	ATP

C

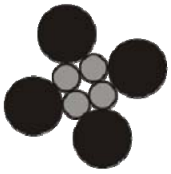

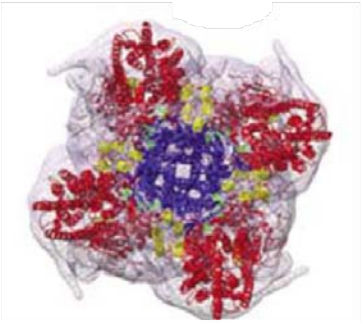

View from Above

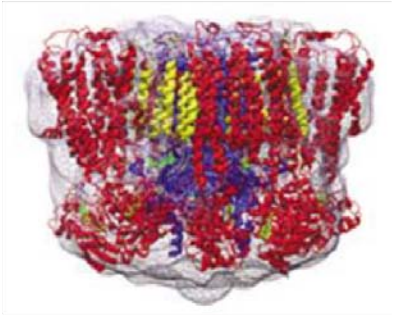

View from the Side

EBP Chapter 1
Figure 1

A

Response to:

High Blood Glucose

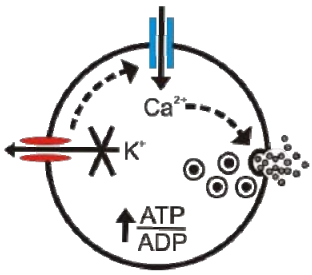

WT

B

Response to:

High Blood Glucose

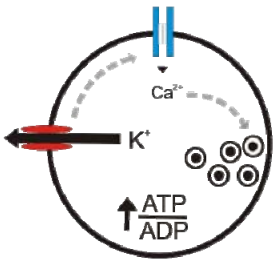

PNDM

Activating K_{ATP} Mutations

High or Low Blood Glucose

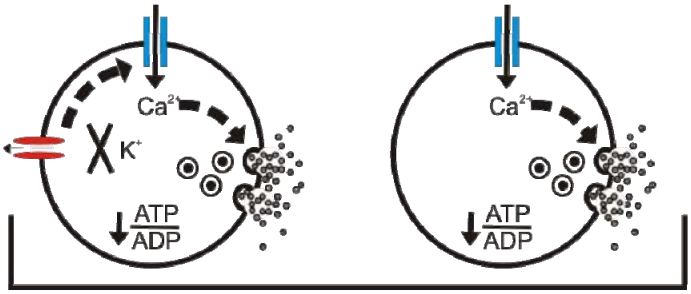

CHI

Inactivating K_{ATP} Mutations

EBP Chapter 1
Figure 2

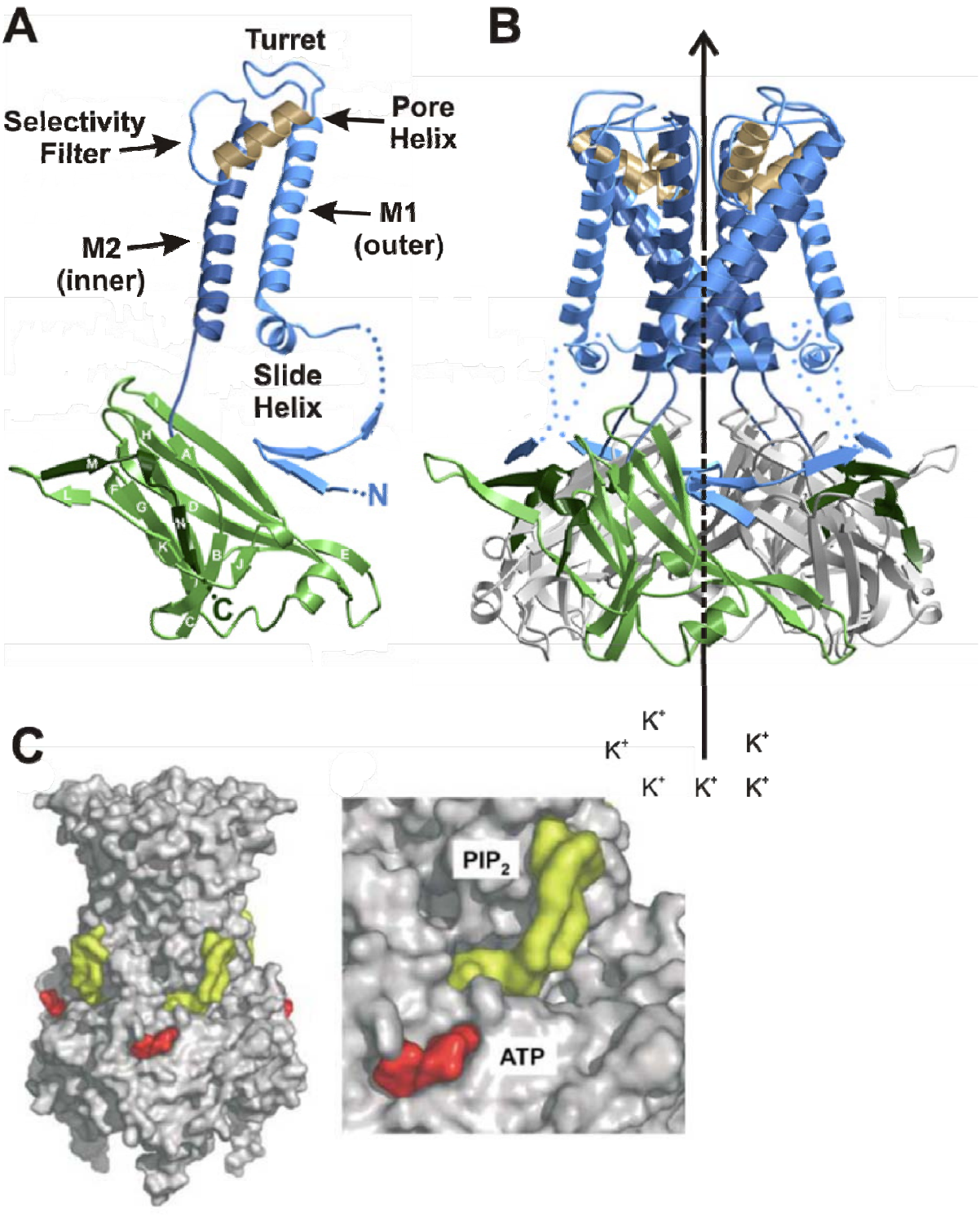

EBP Chapter 1
Figure 3

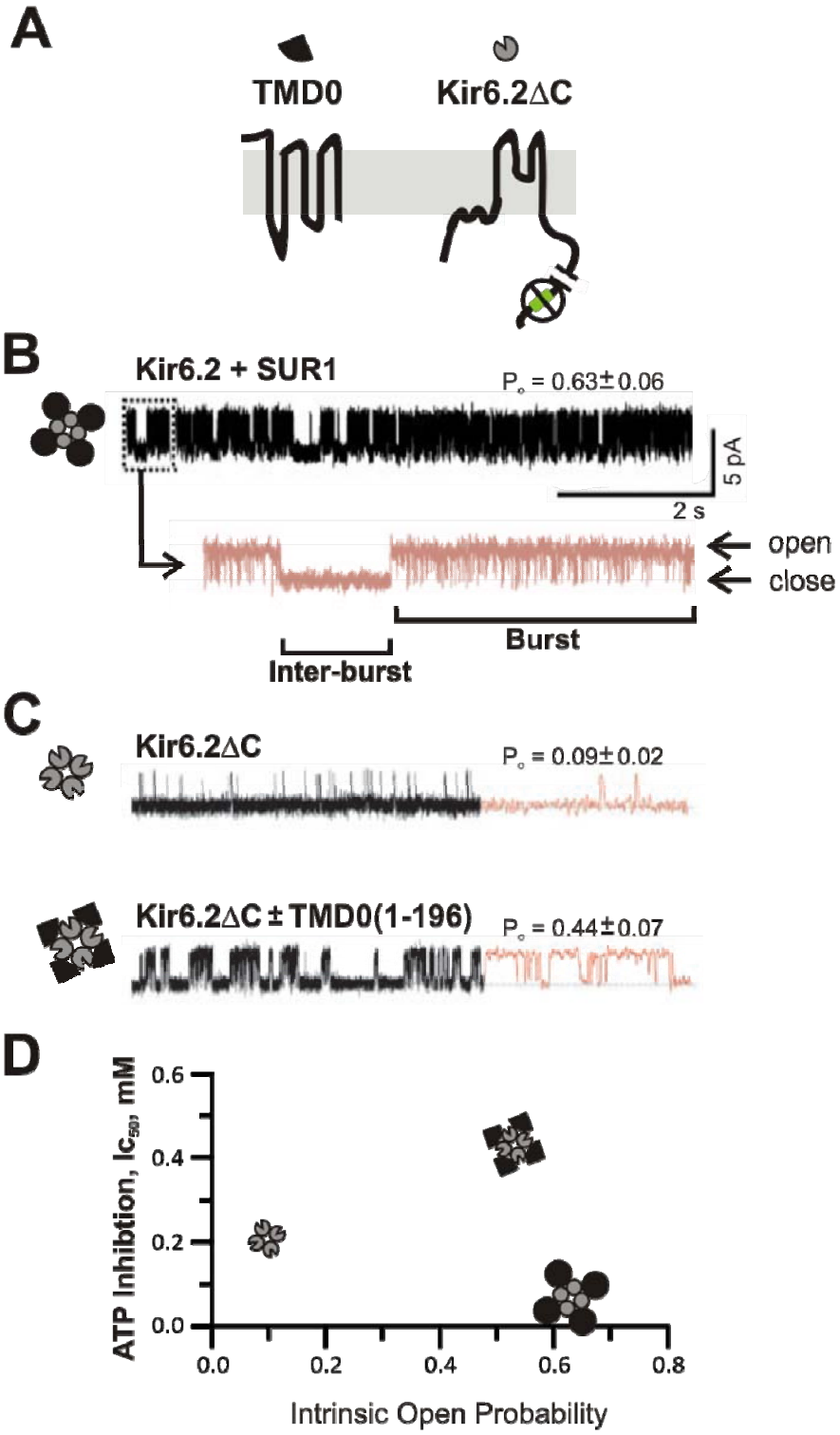

EBP Chapter 1
Figure 4

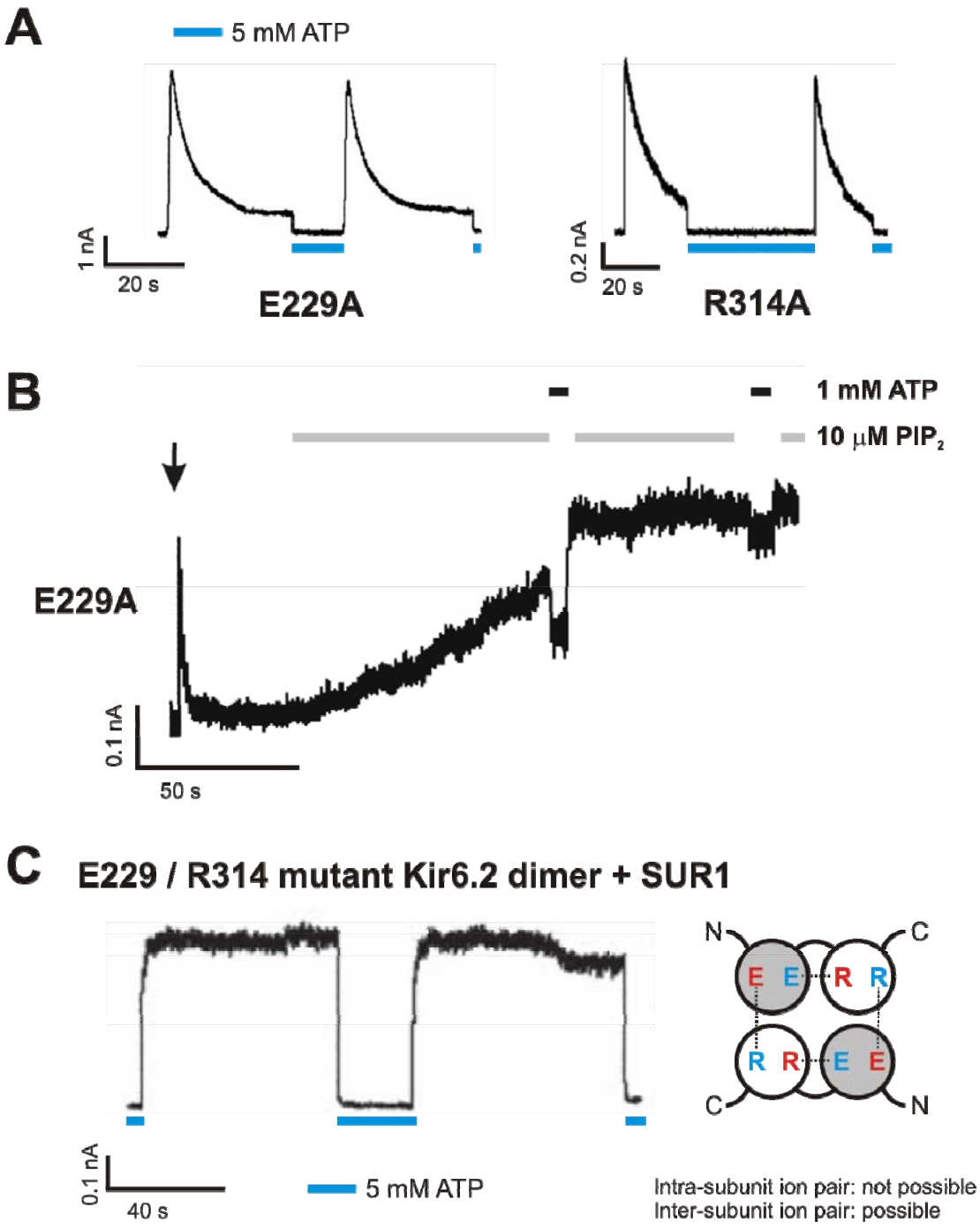

EBP Chapter 1
Figure 5

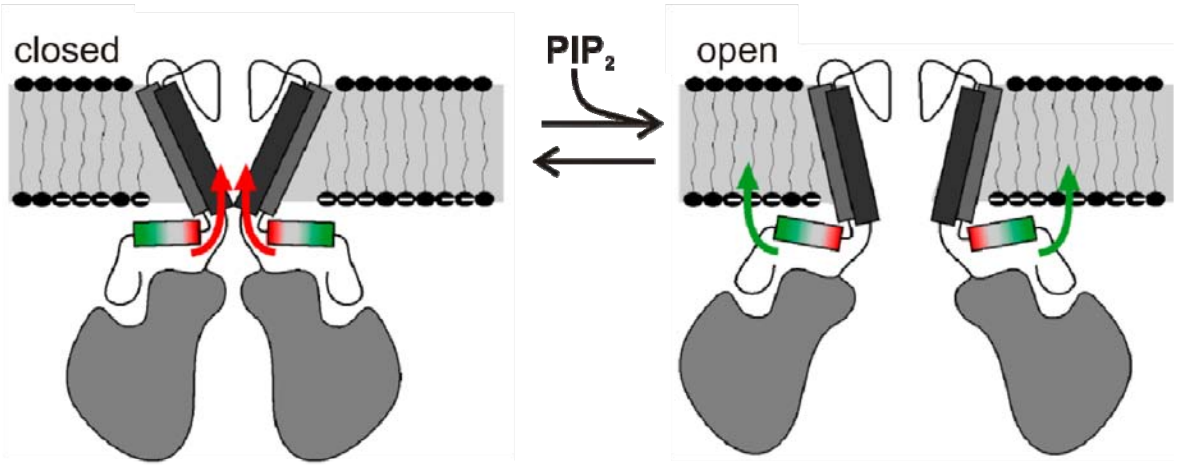

EBP Chapter 1
Figure 6

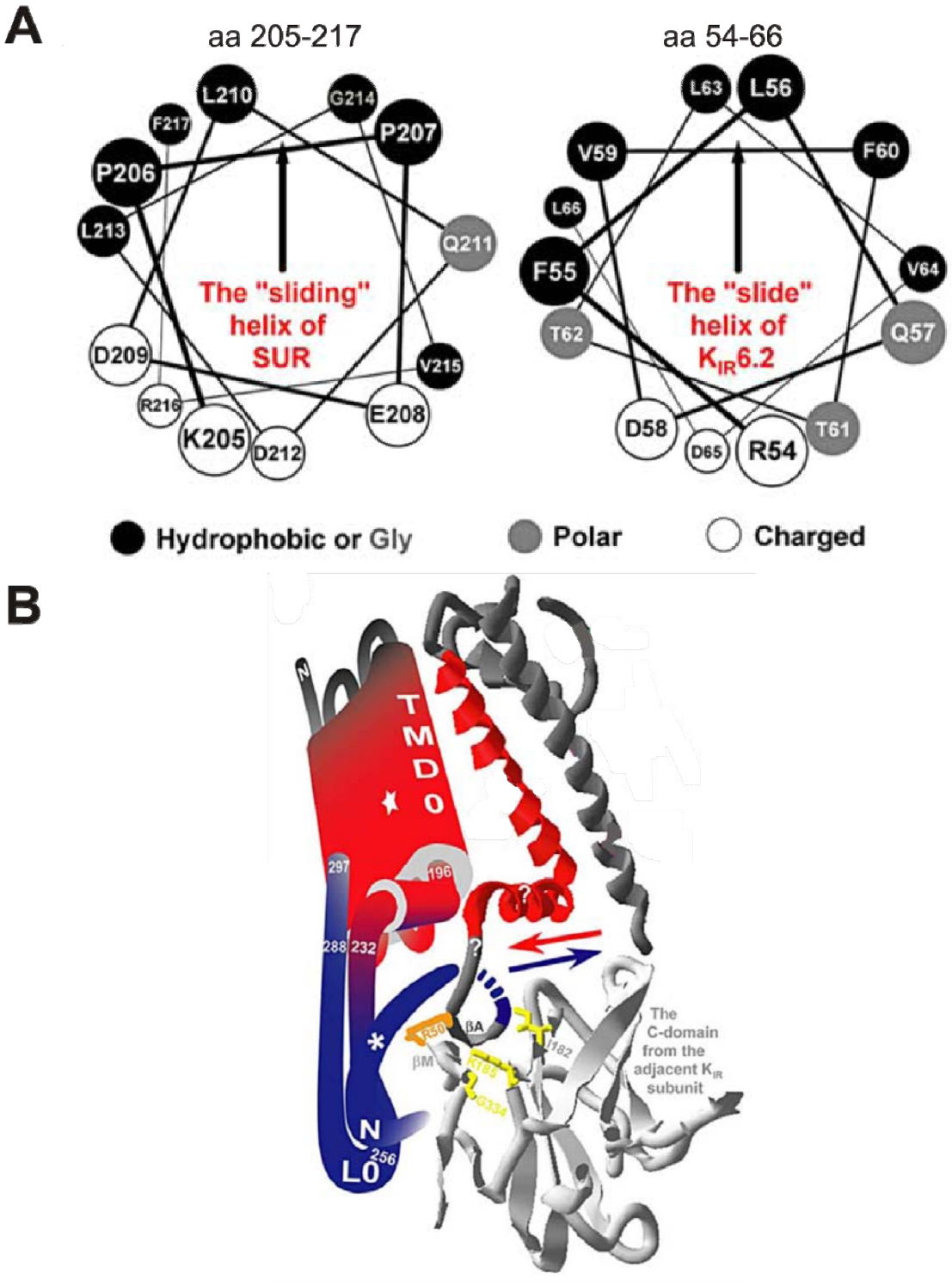

EBP Chapter 1
Figure 7

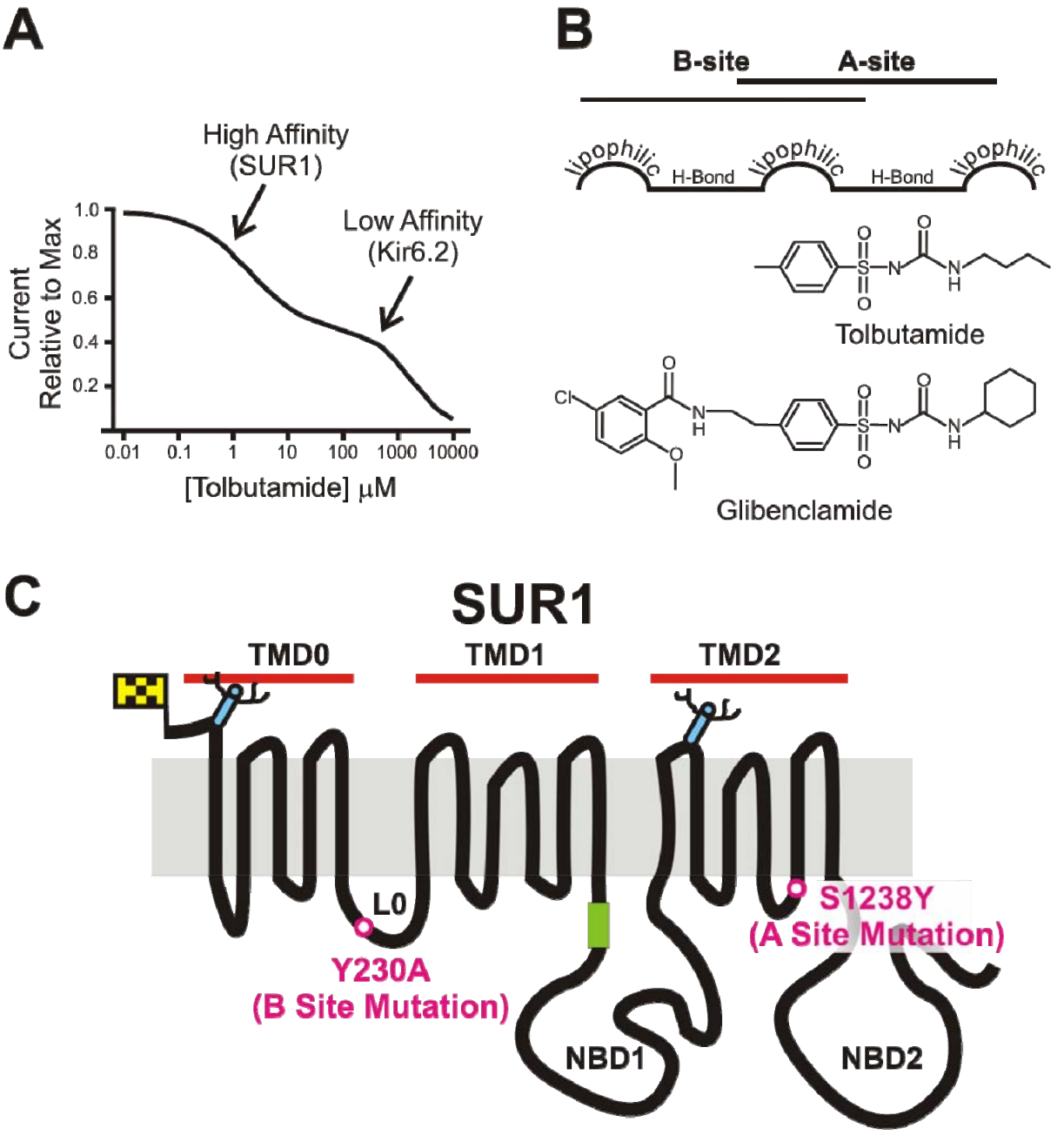

EBP Chapter 1
Figure 8

CHAPTER 2

Sulfonylurea Receptor 1 Mutations That Cause Opposite Insulin Secretion Defects with Chemical Chaperone Exposure

Emily B. Pratt[‡], Fei-Fei Yan[‡], Joel W. Gay[‡], Charles A. Stanley[§], and Show-Ling Shyng[‡]

[‡]Center for Research on Occupational and Environmental Toxicology, Oregon Health & Science University

[§]Division of Endocrinology/Diabetes, The Children's Hospital of Philadelphia

EB Pratt and FF Yan contributed equally to this work

Corresponding Author: Show-Ling Shyng

Chapter 2 is a manuscript that appears as it was published in:

Journal of Biological Chemistry, March 20, 2009, Volume 284, p. 7951-7959

In this chapter I performed the experiments in Figures 2, 3, 4, 6, 7A and 7B, Supplemental 1, 2 and 3. J. Gay performed the molecular biology. FF Yan performed western blots, chemiluminescence and immunohistochemistry in Figure 5, and insulin secretion assays in Figure 7C. Yu-Wen Lin and SL Shyng performed voltage-clamp recording in Figure 1. I also participated in writing the manuscript.

Abstract

The β-cell ATP-sensitive potassium (K_{ATP}) channel composed of sulfonylurea receptor SUR1 and potassium channel Kir6.2 serves a key role in insulin secretion regulation by linking glucose metabolism to cell excitability. Mutations in SUR1 or Kir6.2 that decrease channel function are typically associated with congenital hyperinsulinism, whereas those that increase channel function are associated with neonatal diabetes. Here we report that two hyperinsulinism-associated SUR1 missense mutations, R74W and E128K, surprisingly reduce channel inhibition by intracellular ATP, a gating defect expected to yield the opposite disease phenotype neonatal diabetes. Under normal conditions, both mutant channels showed poor surface expression due to retention in the endoplasmic reticulum, accounting for the loss of channel function phenotype in the congenital hyperinsulinism patients. This trafficking defect, however, could be corrected by treating cells with the oral hypoglycemic drugs sulfonylureas, which we have shown previously to act as small molecule chemical chaperones for K_{ATP} channels. The R74W and E128K mutants thus rescued to the cell surface paradoxically exhibited ATP sensitivity 6- and 12-fold lower than wild-type channels, respectively. Further analyses revealed a nucleotide-independent decrease in mutant channel intrinsic open probability, suggesting the mutations may reduce ATP sensitivity by causing functional uncoupling between SUR1 and Kir6.2. In insulin-secreting cells, rescue of both mutant channels to the cell surface led to hyperpolarized membrane potentials and reduced insulin secretion upon glucose stimulation. Our results show that sulfonylureas, as chemical chaperones, can dictate manifestation of the two opposite insulin secretion defects by altering the expression levels of the disease mutants.

Introduction

The β-cell ATP-sensitive potassium (K_{ATP}) channels are essential for triggering glucose-stimulated insulin secretion as they couple metabolic signals to electrical signals . Each channel is a complex of four regulatory sulfonylurea receptor 1 (SUR1) subunits, encoded by ABCC8, and four pore-forming Kir6.2 inwardly rectifying potassium channel subunits, encoded by KCNJ11 (Aguilar-Bryan and Bryan, 1999). Mutations in ABCC8 or KCNJ11 that perturb the expression and/or gating of the channel lead to channel dysfunction and insulin secretion disorders. Whereas a net loss in channel activity results in congenital hyperinsulinism (CHI), a net gain of channel function causes permanent neonatal diabetes mellitus (PNDM) (Ashcroft, 2005).

SUR1 and Kir6.2 co-assemble in the endoplasmic reticulum (ER) to form channel complexes; successful assembly overcomes the arginine-lysine-arginine (RKR) ER retention motif in SUR1 and Kir6.2 to permit channel trafficking to the plasma membrane (Neagoe and Schwappach, 2005; Heusser et al., 2006). Quality surveillance mechanisms are in place to prevent misfolded or unassembled channel subunits from exiting the ER where the retained proteins are eventually degraded by the ubiquitin-proteasome pathway (Yan et al., 2005). In the plasma membrane, channel activities are regulated by intracellular ATP and Mg·ADP (Aguilar-Bryan and Bryan, 1999). ATP inhibits channel activity by binding to Kir6.2, whereas MgA·DP stimulates channel activity by interacting with the nucleotide binding domains (NBDs) of SUR1 (Nichols, 2006). A Kir6.2 C-terminal truncation mutant lacking the last 36 amino acids and the -RKR- ER retention signal (Kir6.2ΔC) can form channels that are still sensitive to ATP inhibition even in the absence of SUR1 (Tucker et al., 1997). However, the ATP sensitivity of Kir6.2ΔC channels is substantially lower than wild-type (WT) channels, indicating SUR1 hypersensitizes Kir6.2 to ATP inhibition (Tucker et al., 1997; Enkvetchakul et al., 2000). Furthermore, SUR1

markedly increases the intrinsic open probability (P_o) of Kir6.2 channels in the absence of intracellular nucleotides (Nichols, 2006). Recent studies have shown that the first transmembrane domain of SUR1, known as TMD0, is sufficient to increase the P_o of Kir6.2ΔC channels (Babenko and Bryan, 2003; Chan et al., 2003). Interestingly, TMD0 further reduces the ATP sensitivity of the Kir6.2ΔC channel, suggesting other SUR1 domains are necessary to hypersensitize Kir6.2 channels to ATP inhibition (Babenko and Bryan, 2003; Proks et al., 2006). Precisely how TMD0 couples to Kir6.2 to modulate channel gating remains to be elucidated.

Characterized by persistent insulin secretion despite severe hypoglycemia in neonates and infants, CHI frequently results from loss of function K_{ATP} channel mutations (Dunne et al., 2004). These mutations typically reduce channel activity by preventing channel expression at the cell surface, diminishing channel response to stimulation and/or reducing channel P_o (Ashcroft, 2005). By contrast, mutations from the opposite disease phenotype, PNDM, increase channel activity via reduced channel sensitivity to ATP inhibition or enhanced channel response to Mg·ADP stimulation (Ashcroft, 2005). We have previously shown that channel trafficking defects caused by CHI mutations in the TMD0 of SUR1 can be overcome by the oral hypoglycemic drugs sulfonylureas, which act as chemical chaperones to increase the biogenesis efficiency of these mutant channels (Yan et al., 2004; Yan et al., 2006; Yan et al., 2007). Here, we report two mutants, R74W and E128K, which, upon rescue to the cell surface, surprisingly revealed reduced ATP sensitivity-gating defects. Such defects are typically associated with PNDM mutations. Indeed, sulfonylurea-rescued surface expression of these two channels in insulin-secreting cells caused hyperpolarized membrane potentials and blunted insulin secretion in high glucose. Interestingly, unlike previously reported ATP-insensitive mutants, which tend to have increased intrinsic P_o, the R74W and E128K mutants showed reduced intrinsic P_o. The finding suggests R74W and E128K diminish channel ATP sensitivity by a distinct mechanism that likely involves functional uncoupling between SUR1 and Kir6.2.

Results

The R74W and E128K Mutations Reduce Channel Sensitivity to ATP. Previously, we reported several CHI-associated SUR1 mutations that reduce surface expression of K_{ATP} channels could be rescued to the cell surface efficiently by sulfonylureas such as glibenclamide and tolbutamide (Yan et al., 2004; Yan et al., 2006; Yan et al., 2007). These mutations are all in the TMD0 of SUR1 (amino acids 1–196) and include G7R, N24K, F27S, R74W, A116P, E128K, and V187D. The functional properties of rescued A116P and V187D mutant channels had been characterized in detail and shown to be normal (Yan et al., 2004). To test if the other five rescued TMD0-SUR1 mutant channels also have normal nucleotide sensitivities, we performed inside-out patch clamp recordings from COSm6 cells co-transfected with Kir6.2 and WT-SUR1 or mutant-SUR1. Cells were treated with 300 μM tolbutamide overnight followed by 2 h washout to increase mutant channel expression at the cell surface before recording. Note tolbutamide was used in this and subsequent functional experiments because of its low affinity and reversible binding to K_{ATP} channels to allow rapid washout. Of the five mutants, G7R, N24K, and F27S had WT-like or slightly increased ATP sensitivity, and either normal or reduced Mg·ADP response that is commonly associated with CHI mutations (Fig. 1) (Shyng et al., 1998). To our surprise, however, two of the mutants, R74W and E128K, exhibited significantly reduced ATP sensitivities (Fig. 2, *A* and *B*). The R74W mutation has been reported in two focal cases (disease causing a paternally derived mutation that was expressed due to loss of heterozygosity for the maternal allele) (Suchi et al., 2006). The disease in both cases was similar to other focal cases: severe neonatal onset hypoglycemia, failed medical therapy with diazoxide, required surgery, and cured by local resection of the lesion (Suchi et al., 2006). R74W was also reported as a compound heterozygous mutation with another mutation, R1215Q, in a patient with diffuse HI who failed medical therapy with diazoxide and required a near-total pancreatectomy (Henwood et al., 2005; Yan et al., 2007). The E128K mutation occurred in homozygous form in

a child with diffuse hyperinsulinism, severe neonatal onset hypoglycemia, failed diazoxide therapy, and required near-total pancreatectomy for control of hypoglycemia (Yan et al., 2007).

The reduced ATP sensitivity-gating defect is typically linked to PNDM and has never been reported in CHI mutations. To ensure the altered ATP sensitivities were not due to the rescue procedure, we examined ATP inhibition in cells not pretreated with tolbutamide. Although expression levels of R74W and E128K mutants were very low, sufficient currents in a small fraction of transfected cells (identified by co-transfected GFP) were detected. ATP inhibition was as ineffective as in the tolbutamide-rescued channels (Fig. 2*C*), indicating the defect is intrinsic to the mutant channels.

Mechanisms of Reduced ATP Inhibition in R74W and E128K Channels. Several studies have shown that PNDM-causing SUR1 or Kir6.2 mutations can reduce channel ATP sensitivity by enhancing channel response to Mg-nucleotide stimulation (Proks et al., 2005a; de Wet et al., 2007). In inside-out patches, Mg·ADP stimulated channel activity in both R74W and E128K mutants (Fig. 3*A*); however, because the mutants were much less sensitive to nucleotide inhibition, it is difficult to directly compare their Mg·ADP sensitivities to WT channels. We therefore tested the effect of R74W or E128K on channel ATP sensitivity in the background of SUR1-NBD mutations such as G1479D and G1479R in NBD2 and K719M in NBD1, which are known to abolish channel response to Mg·ADP stimulation (Shyng et al., 1997b). In the E128K/G1479R double mutants, ATP sensitivity was as reduced as the E128K mutant; the R74W/G1479D double mutant also showed significantly reduced ATP sensitivity, although to a lesser degree than the R74W single mutant (Fig. 3, *B* and *C*). We also combined E128K with NBD1 mutation K719M (E128K/K719M), and the resulting channels were as insensitive to ATP as E128K (not shown). These results indicate that, even if the mutations increased Mg-

nucleotide stimulation, this effect alone could not explain the reduced ATP sensitivity in R74W and E128K.

Another mechanism that could lead to a reduced apparent channel ATP sensitivity is increased intrinsic P_o (Enkvetchakul et al., 2000; Proks et al., 2004; Proks et al., 2007). The recently identified PNDM-causing SUR1 F132L mutation is an example, so are many Kir6.2 mutations reported earlier (Enkvetchakul et al., 2000; Proks et al., 2004). To examine this possibility, we first measured the P_o of the R74W and E128K channels expressed in COSm6 cells by single channel recording. These experiments show the mutant channels indeed have altered P_o (Fig. 4, A and B). Unexpectedly, however, the average P_o values for R74W and E128K (0.35±0.08 and 0.18±0.06, respectively) were significantly lower than that of WT channels (0.63±0.06; Fig. 4B). Of note, 10 out of 11 patches of the E128K mutant had consistently lower P_o with only one outlier showing a P_o of 0.69 (Fig. 4B). The R74W mutant exhibited more variable P_o ranging from 0.01 to 0.88 (Fig. 4B). Two recordings representing both ends of the R74W P_o spectrum are shown in Fig. 4A. We cannot rule out that in some patches more than one channel might be present; alternatively, the variation might arise from differences in the cellular state such as membrane phosphoinositide levels (Shyng and Nichols, 1998). As a control, we also analyzed the P_o of the F132L mutant. Consistent with that reported previously (Proks et al., 2007), the P_o of F132L (0.71±0.05) tends to be higher than that of WT (Fig. 4), although the difference did not reach statistical significance. As a parallel approach, we also estimated channel P_o by stationary noise analyses of macroscopic currents. The P_o values thus derived are 0.84±0.02 (n=10), 0.71±0.06 (n=9), and 0.35±0.05 (n=9) for WT, R74W, and E128K, respectively. These numbers, while all considerably higher, are nevertheless in general agreement with the trend observed in single channel recording experiments, with the P_o of R74W and E128K significantly lower than that of WT ($p<0.05$). The higher P_o estimated by noise analyses could be attributed to underestimation of noise as a result of filtering (Neher and Stevens, 1977; Sigworth, 1980;

Dempster, 2001; Lin et al., 2006b). Together, our data point to reduced intrinsic channel open probabilities for the R74W and the E128K mutant.

Because Kir6.2 channels formed in the absence of SUR1 (using a C-terminally truncated Kir6.2 lacking the last 36 amino acids thus the -RKR- ER retention signal; referred to as Kir6.2ΔC) have lower P_o and ATP sensitivity than those formed by co-expression with SUR1 (Enkvetchakul et al., 2000; Babenko and Bryan, 2003; Chan et al., 2003), we reasoned the mutations may disrupt functional coupling between SUR1 and Kir6.2. Using the same single channel recording condition (Kint/1 mM EDTA), we found the P_o of Kir6.2ΔC channels to be 0.04±0.01 and the IC_{50} of ATP inhibition 379±53 μM, with a Hill coefficient of 0.97±0.12. These values represent the limit at which the mutations could affect channel P_o and ATP sensitivity if the mutations exert their effects by uncoupling SUR1 and Kir6.2.

Mutant Channel Biogenesis Defects and Correction by Sulfonylureas in Insulin-secreting Cells. The reduced ATP sensitivity of the R74W and E128K mutant channels predicts that, were the channels able to overcome their trafficking defect, they would be insensitive to metabolic stimuli and would cause β-cell dysfunction resembling neonatal diabetes. To test this, we first confirmed the trafficking and gating phenotypes of the mutants in INS-1 cells (clone 832/13) (Hohmeier et al., 2000). INS-1 cells were infected with Kir6.2 and WT SUR1 or mutant-SUR1 recombinant adenoviruses and treated overnight or not with sulfonylureas. SUR1 constructs with a FLAG-epitope (fSUR1) at the extracellular N terminus were used to facilitate surface detection; the epitope does not affect channel behavior (not shown) (Yan et al., 2007). Western blots showed that, without glibenclamide treatment, the R74W and E128K mutant fSUR1 was seen only as a lower band corresponding to the core-glycosylated form in the ER, in contrast to WT fSUR1 seen as both a lower band and an upper band corresponding to the mature complex-glycosylated form found post medial-Golgi (Zerangue et al., 1999). In cells treated with

glibenclamide, abundant upper mutant fSUR1 band was detected, verifying the sulfonylurea rescue effects (Fig. 5*A*; similar results were obtained with 300 μM tolbutamide, not shown). In surface-immunostaining experiments, α-FLAG antibody clearly identified surface expression of WT fSUR1 in both control and sulfonylurea-treated cells (Fig. 5*B*). By contrast, surface R74W- and E128K-fSUR1 was only easily detectable following overnight tolbutamide treatment. Channel surface expression was further quantified using chemiluminescence assays. Following 24 h treatment with 5 μM glibenclamide, the expression level of R74W and E128K mutants increased from 9% to 90% and 9% to 80% that of WT, respectively (Fig. 5*C*).

The trafficking and rescue characteristics of R74W and E128K were also confirmed in rat islets. Islets were transduced with the K_{ATP} subunit adenoviruses for 24 h followed with or without 5 μM glibenclamide treatment for 12 h. The sulfonylurea rescue effect was appraised via the presence of complex-glycosylated fSUR1 protein on Western blots. As shown in Fig. 5D, the SUR1 mutants exhibited the same processing defects that were ameliorated by glibenclamide treatment.

Expression of R74W or E128K Mutant Alters INS-1 Cell Responses to Glucose Stimulation. Having established the sulfonylurea-dependent expression of mutant channels in INS-1 cells, we next determined if expression of the mutants at the cell surface alters membrane electrical properties. Channel activity was first assessed in intact cells using the on-cell voltage clamp (-50 mV membrane potential) configuration. INS-1 cells infected with the K_{ATP} subunit recombinant viruses were exposed to 12 mM glucose media for 3 h before recording. Surface expression of mutant channels was rescued by overnight treatment with 300 μM tolbutamide. Tolbutamide was removed during the high glucose stimulation to allow for washout prior to recording. In uninfected cells or cells expressing exogenous WT K_{ATP} channel subunits, little channel activity was detected (Fig. 6*A*). No channel opening was observed in any of the

uninfected cells (*n*=19); the majority of cells overexpressing exogenous WT channels also had no activity, but occasionally some single channel openings were detected (two of seven). In contrast, all cells infected with the R74W or E128K channel subunits and pretreated with tolbutamide had high on-cell activities (Fig. 6*A*). Consistent with the on-cell activity, upon patch excision into the inside-out patch clamp configuration, channels from cells infected with mutant subunits and pretreated with tolbutamide had significantly reduced ATP sensitivity compare with channels from WT-infected cells (Fig. 6*B*), further confirming surface expression of the mutant channels.

Cells that were infected with R74W or E128K but not rescued by tolbutamide were also tested; a small fraction of each mutant displayed some on-cell channel activity but less than that observed in tolbutamide-treated cells and decreased channel ATP sensitivity upon patch excision (supplemental Fig. S1), indicating some mutant channels were able to traffic to the plasma membrane without pharmacologic chaperone. We suggest that this may be a consequence of heterologous overexpression. These results are in line with our hypothesis that mutant channels are hyperactive under high glucose conditions.

We then tested if expression of mutant channels altered the relationship between glucose and membrane potential using whole cell patch clamp recording. Resting membrane potential (RMP) at 12 mM glucose was determined following whole cell break-in in the current clamp mode (Fig. 7A). Our prior work has shown that membrane potential upon break-in before dialysis (initial RMP) is similar to that measured by perforated patch clamp recording (Lin et al., 2005). Cells were exposed to 200 μM diazoxide, a K_{ATP} channel opener, after the membrane potential had reached steady state to confirm whole cell seal quality and observe the full extent of K_{ATP}-dependent hyperpolarization (not shown). The average initial RMPs with and without tolbutamide pretreatment are shown in Fig. 7B. There is no significant difference between

control cells and cells infected with WT subunits (the initial RMPs are -16.4±3.5mV and -20.7±4.8 mV, respectively). In contrast, both R74W- and E128K-expressing cells receiving tolbutamide pretreatment were significantly more hyperpolarized at 12mM glucose. The initial RMP was -33±3.8 mV for R74W and -54±4.0 mV for E128K. In some mutant virus-infected cells without tolbutamide pretreatment the initial RMP at 12 mM glucose also appeared more hyperpolarized than uninfected or WT-infected cells (see supplemental Fig. S2), although the averaged initial RMP was still more depolarized than that seen in cells receiving tolbutamide pretreatment (Fig. 7B). The occasional more hyperpolarized initial RMP in mutant virus-infected cells not treated with tolbutamide could be attributed to the tolbutamide-independent “leak” mutant channel expression, as evidenced by chemiluminescence assay results (Fig. 5C) and increased on-cell activity coupled with decreased channel ATP sensitivity (supplemental Fig. S1) in a fraction of the non-rescued cells. This interpretation is further substantiated by good correlation between such leak expression and blunted membrane potential response to glucose (supplemental Fig. S3). Taken together, these results are in line with the idea that expression of the R74W or E128K mutant channels at the INS-1 cell surface render the cell membrane potentials unable to depolarize in response to glucose stimulation.

Lastly, we determined if rescue of the R74W or E128K mutant channels to the cell surface would cause defective insulin secretion in response to glucose stimulation. Insulin release during a 2 h static incubation in basal (3 mM) or high (12 mM) glucose was compared for the same experimental groups tested in the above electrophysiology studies. Because prolonged tolbutamide pretreatment to rescue mutant channel surface expression may desensitize cells to subsequent glucose stimulation by affecting their insulin secretory capacity (Gullo et al., 1991; Kawaki et al., 1999) and confound data interpretation, we optimized the tolbutamide pretreatment such that no reduction in subsequent glucose stimulated insulin secretion was observed in uninfected control cells. We found that pretreating INS-1 cells with tolbutamide for 4

h rescued mutant surface expression without affecting insulin secretory capacity. Using this experimental paradigm, we observed that secretion in 12 mM glucose was significantly reduced in tolbutamide-rescued, mutant-infected cells compared with uninfected or WT-infected cells (Fig. 7*C*). In agreement with the electrophysiological data, INS-1 cells infected with mutant channel viruses but not treated with tolbutamide also caused a somewhat reduced insulin secretion response to high glucose, again due to tolbutamide-independent leak expression of mutant channels at the cell surface. These data led us to conclude that rescue of the CHI-causing R74W or E128K mutant K_{ATP} channels by sulfonylureas inverses the β-cell dysfunction phenotype to diabetic.

Discussion

Studies of K_{ATP} channel mutations from patients with hyperinsulinism or diabetes have led to the general view that mutations from hyperinsulinemic patients cause reduced channel function owing to inability of the mutant to express at the cell surface and/or to open during hypoglycemia, whereas those from neonatal diabetes patients cause enhanced channel function by rendering the channel insensitive to the increased ATP/ ADP ratio during glucose stimulation (Ashcroft, 2005). In this work, we present the novel finding of two SUR1 mutations that cause severe hyperinsulinism in patients by preventing channel expression at the cell surface, surprisingly, also render the channel insensitive to ATP inhibition. The diabetes-inducing gating defects were clearly revealed after the mutant channels were rescued to the cell surface by their pharmacological chaperones sulfonylureas. As predicted by the reduced ATP sensitivity-gating defects, expression of mutant channels at the surface of INS-1 cells resulted in insensitivity of the cell to glucose stimulation consistent with a diabetes-like phenotype.

Mechanisms of Reduced ATP Sensitivities in the Mutant Channels. Our results indicate that the decreased ATP sensitivities of R74W and E128K are not due to enhanced Mg·ADP

stimulation, at least alone, because elimination of channel Mg·ADP response by mutations in the nucleotide binding folds did not restore their ATP sensitivity to the level of WT channels (Fig. 3). Furthermore, we found that, rather than increasing channel intrinsic P_o, the R74W and E128K mutations significantly lowered the average intrinsic P_o (Fig. 4). These properties are unlike the previously reported ATP-insensitive mutants and place the R74W and E128K mutants in a distinct category in terms of the underlying mechanisms for loss of ATP sensitivity. Studies by others have indicated that TMD0 physically couples to Kir6.2 to modulate channel gating and facilitate surface expression (Babenko and Bryan, 2003; Chan et al., 2003). However, the chemical interactions between TMD0 and Kir6.2 critical for such modulation have not been defined. That the E128K mutant has poor surface expression, lower P_o, and reduced ATP sensitivity closer to those seen in Kir6.2ΔC channels suggests the mutation likely disrupts the functional coupling between TMD0-SUR1 and Kir6.2. The R74W mutation might also disrupt functional interactions between TMD0-SUR1 and Kir6.2; however, this disruption would be predicted to be less pronounced as the mutation only caused mild reduction in ATP sensitivity and P_o. It is possible that Arg-74 and Glu-128 form interactions with residues in Kir6.2 that are critical for the cross-talk between the two subunits. Interestingly, comparison between channels formed by Kir6.2ΔC only and channels formed by co-expression of TMD0-SUR1 with Kir6.2ΔC showed that TMD0-SUR1 further decreases the ATP sensitivity of Kir6.2ΔC channels by ~6-fold (Babenko and Bryan, 2003; Proks et al., 2007). Because TMD0-SUR1 decreases whereas full-length SUR1 increases the ATP sensitivity of Kir6.2ΔC, the hypersensitizing effect of full-length SUR1 on channel ATP sensitivity must require domains other than TMD0 (Babenko and Bryan, 2003). This, however, does not exclude a role of TMD0 in mediating the hypersensitizing effect of full-length SUR1 on channel ATP sensitivity. In fact, the reduced ATP sensitivities observed in the R74W and E128K mutants indicate TMD0 is necessary for normal channel ATP

sensitivity. A possible scenario is that TMD0 serves as a conduit between other SUR1 domains and Kir6.2 to transduce this hypersensitization.

If R74W and E128K cause functional uncoupling between TMD0-SUR1 and Kir6.2, one might ask if the mutations also result in reduced physical association between the two subunits. Several SUR1-TMD0 mutations have been reported to reduce physical association between TMD0 and Kir6.2 in co-immunoprecipitation experiments, including CHI-causing A116P and V187D mutations and PNDM-causing F132L mutation (Chan et al., 2003; Proks et al., 2007). The former two do not affect the gating properties of the channel (Yan et al., 2004), whereas the F132L mutation reduces ATP sensitivity by increasing channel intrinsic P_o (Proks et al., 2007). These studies suggest that physical association, as assessed by co-immunoprecipitation, does not necessarily correlate with the functional relationship between TMD0 and Kir6.2. It would not be surprising if R74W and E128K do not affect the extent of co-immunoprecipitation between SUR1 and Kir6.2, because there are likely multiple chemical interactions retained (such as those mediated by Ala-116, Val-187, and Phe-132) to allow association of the two subunits.

The Interplay between Channel Expression and Gating in Determining Disease Phenotype. Our study highlights the importance of mutant channel expression level at the cell surface in determining disease phenotype. R74W and E128K, like all other neonatal diabetes-causing mutations, render K_{ATP} channels less sensitive to ATP inhibition during glucose stimulation, and yet they were identified in patients with severe hyperinsulinism, because they also prevent channels from being expressed at the cell membrane. When brought to the INS-1 cell surface by chemical chaperones, the effects of their reduced ATP sensitivity on short circuiting cell response to glucose stimulation became apparent, with the extent of defects correlated with the extent of ATP insensitivities observed in the mutants (Fig. 7). Interestingly, our recent study comparing dominant *versus* recessive forms of CHI associated with K_{ATP}

channel mutations found that, whereas recessive CHI is associated with mutations that often prevent channel expression at the cell surface, dominant CHI is associated with heterozygous mutations that do not compromise channel surface expression but do impair the ability of channels to open in low glucose (Pinney et al., 2008). The R74W was identified in one patient with diffuse disease who also carries an R1215Q mutation that reduces channel sensitivity to Mg·ADP and two patients with focal disease (Shyng et al., 1998; Henwood et al., 2005; Suchi et al., 2006), and E128K was identified as a disease-causing homozygous mutation in a patient with diffuse disease (Yan et al., 2007). In β-cells of these patients, the mutant channel expression level at the surface is likely so low that their gating defects are completely hidden. This is in contrast to dominant heterozygous CHI causing mutations and PNDM-causing heterozygous mutations in which sufficient mutant subunits co-assemble with WT subunits in the octameric channel complex and traffic to the cell surface to manifest their gating defects (Lin et al., 2006a).

Sulfonylureas, Insulin Secretion Diseases and Therapy. The therapeutic utility of sulfonylureas has recently been extended beyond type II diabetes to some patients with PNDM or developmental delay, epilepsy, and neonatal diabetes syndrome caused by K_{ATP} channel mutations (Ashcroft, 2005; Hattersley and Ashcroft, 2005). Moreover, the finding that sulfonylureas could enhance K_{ATP} channel biogenesis efficiency and overcome channel trafficking defects caused by CHI-associated TMD0-SUR1 mutations raises the possibility that these drugs might also have future application to the treatment of some cases of CHI (Yan et al., 2004; Yan et al., 2007). The study we presented here clearly illustrates the complex actions of sulfonylureas and the need to carefully weigh their effects on channel expression and channel gating when treating patients. In this regard, it is important to note that we have found the neonatal diabetes causing mutation F132L also significantly reduces channel expression at the cell surface (57.05±1.75% of WT; n=3), and that sulfonylureas restore mutant channel

surface expression to the same level as WT (109.2±7.05; n=3). Detailed functional analyses of individual disease mutations will be important to develop genotype-specific and mechanism-based therapeutic strategies.

Acknowledgments

We thank Chia-Wei Lin, Malini Kochar and Sarah Haider from Oregon Health & Science University for technical assistance and Dr. Yu-Wen Lin for data sharing.

Materials and Methods

Molecular biology – Rat Kir6.2 cDNA is in pCDNAI/Amp vector and SUR1 or N-terminus FLAG-epitope (DYKDDDDK) tagged SUR1 (fSUR1) in pECE (Cartier et al., 2001). Site-directed mutagenesis was performed using the QuickChange mutagenesis kit (Strategene) and mutations confirmed by sequencing. SUR1 and Kir6.2 recombinant adenoviruses were constructed using the AdEasy kit (Stratagene) as described previously (Lin et al., 2006a; Yan et al., 2007).

Virus infection and insulin secretion assay – INS-1 cells (clone 832/13) were cultured in RPMI-1640 with 11.1 mM D-glucose plus 10% FBS, 100U/ml penicillin, 100 μg/ml streptomycin, 10 mM HEPES, 2 mM glutamine, 1 mM sodium pyruvate, and 50 μM β-mercaptoethanol (Hohmeier et al., 2000). For fSUR1 and Kir6.2 expression, recombinant viruses containing WT or mutant fSUR1 and WT Kir6.2 with desired titers were used to infect cells as described previously (Lin et al., 2005). Cells at ~50% confluency were washed with PBS and incubated for 90 min at 37 °C in OptiMEM (Gibco) containing a mixture of viruses each with a MOI that yielded desired protein expression levels. At the end of the incubation, 2X growth medium was added and the cells cultured at 37 °C until experiments.

Insulin secretion assays were performed as described previously (Lin et al., 2006a). INS-1 cells seeded in 24-well tissue culture plates at ~5 x 10^5 /well were infected with viruses as described above. Twenty-four hours post-infection, the culture medium was replaced by RPMI 1640 with 5 mM glucose and cells incubated for at least 18 hours. Cells were treated with 300 μM tolbutamide during the last four hours of incubation to rescue mutant channel surface expression. Insulin secretion was assayed in HEPES balanced salt solution (HBSS) consisting of (in mM) 114 NaCl, 4.7 KCl, 1 $MgCl_2$, 1.2 KH_2PO_4, 1.16 $MgSO_4$, 20 HEPES, 2.5 $CaCl_2$, 25.5 $NaHCO_3$, and 0.2% bovine serum albumin (pH ~ 7.2). Cells were washed twice with pre-warmed (37^{o}C) HBSS buffer with 3 mM glucose followed by 2-hour incubation in the same buffer prior to stimulation with 0.8 ml/well pre-warmed HBSS buffer containing 3 or 12 mM glucose for 2 hours. The medium was harvested and the amount of insulin determined using Immunochem coated-tube insulin radioimmunoassay (RIA) from ICN Pharmaceuticals (Costa Mesa, CA). Insulin content in the medium was divided by the total cellular insulin content to correct for the number of cells. The resulting value was then normalized to that observed in uninfected cells at 3 mM glucose and expressed as fold-increase in insulin secretion.

Rat pancreatic islet preparation – Animals were treated in accordance with institutional regulations. Rats aged 6 to 8 weeks were injected with 5 mls cold Hanks Balanced Salt Solution (HBSS, Invitrogen) containing 0.3 mg/ml Liberase R1 (Roche Applied Science) from the common bile duct, the distant conjunction to intestine was completely blocked by clamping. Pancreas were then dissected and minced before incubating in a total volume of 10 ml HBSS at 37°C for 30 min to allow digestion to occur. Digestions were stopped with the addition of 45 ml HBSS containing 10% FBS. Tissue suspensions were centrifuged at 1000 rpm for 1 min, supernatants removed, and the pellets resuspended in 50 ml HBSS + 10% Fetal Bovine Serum (FBS). Pancreatic islets were visualized by addition of 0.5 mg/ml diphenylthiocarbazone (Sigma) and were placed individually into fresh HBSS and then into RPMI media containing 5 mM

glucose, 10% FBS, and pen/strep supplements. Approximately 400 islets were maintained for 48hrs at 37°C in a humidified chamber with 5% CO_2 before infection with viruses. Virus infection was carried out as in INS-1 cells described above. About 100 islets matched in size were used for each infection. The MOI of each adenovirus was 10-fold higher than that used for INS-1 cells to achieve the desired protein expression level. Infected islets were treated with sulfonylureas the following day for 12 hours and then harvested with lysis buffer for western blot as described below.

Immunoblotting, immunostaining, and chemiluminescence assays – INS-1 cells or rat islets infected with fSUR1 and Kir6.2 viruses were treated with or without glibenclamide (5 μM) or tolbutamide (300 μM) for 12-24 hours before being processed for immunoblotting or immunofluorescent staining as described previously (Yan et al., 2004; Yan et al., 2007). For immunoblotting, cells were lysed in 20 mM Hepes, pH 7.0/5 mM EDTA/150 mM NaCl/1% Nonidet P-40 with Complete™ protease inhibitors (Roche Applied Science) 48-72 hours post-transfection or infection. Proteins were separated by SDS/PAGE (8%), transferred to nitrocellulose, analyzed by M2 α-FLAG antibody (Sigma) followed by HRP-conjugated α-mouse secondary antibodies (GE Healthcare), and visualized by chemiluminescence (Super Signal West Femto; Pierce). For surface staining, living cells were incubated with α-FLAG M2 mouse monoclonal antibody [10 μg/ml in OptiMEM containing 0.1% bovine serum albumin (BSA)] for one hour at 4°C, washed with ice-cold PBS, then fixed with cold (-20 °C) methanol for 10 min and incubated with Cy-3 conjugated donkey α-mouse secondary antibodies (Jackson) for 30 min at room temperature. After 3x10 min washes in PBS/0.1% BSA and 1x10 min wash in PBS, cells were viewed with an Olympus Fluoview confocal microscope. For chemiluminescence assays, cells were fixed with 2% paraformaldehyde for 30 min at 4°C, preblocked in PBS/0.5% BSA for 30 min, incubated in M2 α-FLAG antibody (10 g/ml) for an hour, washed 4x30 min in PBS/0.5% BSA, incubated in HRP-conjugated α-mouse antibodies for 20 min, and washed

again 4x30 min in PBS/0.5%BSA. Chemiluminescence was quantified using a TD-20/20 luminometer (Turner Designs) following 5 sec incubation in Power Signal Elisa Femto luminol solution (Pierce). All steps after fixation were performed at room temperature. Results of each experiment are the average of two dishes and each data point shown in the figure is the average of 3 experiments.

Patch-clamp recordings – Inside-out patch-clamp recordings in COSm6 and INS-1 cells were performed using an Axopatch 1D amplifier and pClamp9 acquisition software (Axon Inc.) (Yan et al., 2004). Micropipettes were pulled from non-heparinized Kimble glass on a horizontal puller (Sutter Instrument). The bath and pipette solution (K-INT) was: 140 mM KCl, 10 mM K-HEPES, 1 mM K-EGTA, pH 7.4, and pipette resistance was ~1.5 MΩ. For ATP-dose response experiments, 1mM EDTA was added to K-INT to prevent channel rundown (Lin et al., 2003). For MgADP stimulation, free Mg^{2+} concentration was 1mM. All currents were measured at -50 mV membrane potential at room temperature. Whole-cell patch-clamp recording was used to measure INS-1 cell membrane potential (Lin et al., 2005). One day after virus infection, INS-1 cells were preincubated in 5mM glucose RPMI medium for 18 hours followed by incubation in 12 mM glucose for three hours before recording (Lin et al., 2005; Lin et al., 2006a). During recording, cells were bathed in Tyrode's solution consisting of (in mM): 137 NaCl, 5.4 KCl, 1.8 $CaCl_2$, 0.5 $MgCl_2$, 5 HEPES, 3 $NaHCO_3$, 0.16 NaH_2PO_4, with 12 mM glucose. Pipette solution contained (in mM): 10 KCl, 130 K^+-gluconate, 10 HEPES, 1 EGTA, 3 $MgCl_2$ and 5 ATP.

Data analysis – ATP dose response curve fitting was performed with Origin6.1. Single channel open probability (P_o) analysis was carried out using the pCLAMP9 automated channel-event detector and *via* amplitude histogram examination. Briefly, data collected within the first 90s of inside-out patch excision were binned by amplitude using 0.05 pA increments. Histograms were fit with Gaussian distributions and the area-under-the-curve (AUC) for each was determined. P_o

was calculated as $AUC_{channel\text{-}open}$ / ($AUC_{channel\text{-}open}$ + $AUC_{channel\text{-}closed}$). For estimation of channel open probability by stationary noise analysis, short recordings (~1second) of macroscopic currents in K-INT/EDTA or K-INT/EDTA plus 5mM ATP at -50mV were used. For the mutants that are relatively insensitive to ATP inhibition, we reversed the polarity of currents observed in K-INT plus 10mM $BaCl_2$ at +50mV and used that as the baseline. Currents were sampled at 50 kHz and filtered at 5 kHz. Mean current (I) and variance (σ^2) in the absence of ATP were obtained by subtraction of the mean current and variance of the baseline. Single channel current (i) was assumed to be -3.6 pA at -50mV in symmetrical K-INT solution (corresponding to single channel conductance of 72 picosiemens). P_o was then calculated using the following equation: $P_o = 1 - (\sigma^2/(i \times I))$ (Shyng et al., 1997a; Dempster, 2001).

All data are presented as means ± standard error of the mean (SEM). Statistical analysis was performed using independent two-population two-tailed Student's *t*-test, with $p<0.05$ considered statistically significant.

Figure Legends

Figure1. Nucleotide sensitivities of TMD0 mutants G7R, N24K, and F27S. COSm6 cells transfected with Kir6.2 and WT or mutant SUR1 were treated with 300 μm tolbutamide overnight followed by a 2-h washout prior to the recording to rescue mutant channel surface expression. Channel sensitivity to ATP and MgADP was measured by inside-out patch clamp recordings. Recordings in this and subsequent figures were made at -50 mV, and inward currents are shown as upward deflections. **(A)** Representative traces of WT and mutant channels showing channel inhibition by ATP and stimulation by MgADP. Patches were exposed to various concentrations of ATP and ADP as indicated by the *bars* above the recordings. Free [Mg^{2+}] was 1 mm in all solutions. *Scale bars*: WT: 200 pA, 10 s; G7R: 200 pA, 10 s; N24K: 20 pA, 10 s; F27S: 50 pA, 10 s. **(B)** Quantification of channel response to ATP and MgADP. Currents in 0.1 mm ATP or 0.1 mm ATP plus 0.5 mm ADP were normalized to currents in nucleotide-free solution. The ATP sensitivity of N24K is significantly higher than WT while the MgADP sensitivity of both N24K and F27S are significantly lower than WT channels (*, $p < 0.05$; Student's *t* test). Increased sensitivity to ATP inhibition and decreased sensitivity to MgADP stimulation are both expected to reduce channel function and are consistent with the CHI disease phenotype. Each *bar* represents the mean ± S.E. of 3-7 patches.

Figure 2. R74W and E128K decrease channel sensitivity to ATP inhibition. ATP sensitivity was measured by inside-out patch clamp recording in COSm6 cells transfected with Kir6.2 and WT or mutant SUR1. **(A)** Representative traces of WT and mutant channels from cells treated with 300 μm tolbutamide overnight followed by 2-h washout prior to the recording. *Scale bars*: WT: 500 pA, 5 s; R74W and E128K: 50 pA, 5 s. **(B)** ATP dose-response relationships. Parameters describing best-fit curves to the Hill equation ($I_{rel} = 1/(1 + ([ATP]/IC_{50})^H)$), including the [ATP] necessary for half-maximal inhibition (IC_{50}) and Hill coefficient (H), are shown. *Error bars* represent ± S.E. of 3-7 patches. Note the IC_{50} values obtained using the K-INT/EDTA

solution are higher than those reported by others as inclusion of EDTA significantly reduces rundown by minimizing Mg^{2+}-dependent breakdown of membrane phosphoinositides (Lin et al., 2003). **(C)** Representative traces of WT and mutant channels from cells that have not been pretreated with tolbutamide, indicating the decrease in ATP sensitivity observed in (A) and (B) is not due to the chemical chaperone rescue procedure. *Scale bars*: WT: 500 pA, 10 s; R74W and E128K: 20 pA, 10 s.

Figure 3. Reduced ATP sensitivity in R74W and E128K is independent of MgADP stimulation. (A) Representative traces from COSm6, inside-out voltage clamp recordings showing MgADP response in WT and mutant channels. Note 0.5 mm ATP was present during 0.5 mm MgADP stimulation. Free [Mg^{2+}] was 1 mm in all solutions. *Scale bars*: WT: 50 pA, 10 s; R74W: 50 pA, 10 s; E128K: 500 pA, 10 s. **(B)** and **(C)** ATP sensitivity is still reduced in R74W and E128K containing SUR1-NBD mutations G1479D or G1479R. (B) Representative recordings of WT and double-mutant channels. *Scale bars*: WT: 300 pA, 5 s; RW/GD (R74W/G1479D): 100 pA, 5 s; EK/GR (E128K/G1479R): 100 pA, 5 s. (C) ATP dose-response relationships. Parameters describing best-fit curves are given as in Figure 2B. All cells were pretreated with 300 μm tolbutamide to increase surface expression. *Error bars* represent ± S.E. of 3-11 patches.

Figure 4. R74W and E128K reduce channel intrinsic open probability. (A) Inside-out single channel recordings were made in COSm6 cells co-transfected with K_{ATP} subunits. Intrinsic open probability (P_o) was determined in Kint/1 mm EDTA solution to prevent rundown. Representative traces are shown as 10 s of recording and the first 1 s of each expanded (indicated by the *dotted box*), with the P_o given parenthetically. Recordings were digitized at 50 kHz and filtered at 2 kHz. *Scale bars*: 5 pA and 2 s for the 10-s records, 5 pA and 200 μs for the expanded records. **(B)** Average P_o values ± S.E. are shown in the *bar graph*. The distribution of individual P_o values

is displayed; the total number of patches analyzed is shown *above each bar* (*, $p < 0.05$, Student's *t* test; *error bars* represent ± S.E.).

Figure 5. R74W and E128K surface expression was rescued by sulfonylurea treatment in insulin-secreting cells. Processing and surface expression of K_{ATP} channels was assessed in INS-1 cells infected with Kir6.2 and WT or mutant fSUR1 adenoviruses. **(A)** Western blot of fSUR1. The complex-glycosylated mature form of fSUR1 is indicated by the *open arrow* and the core-glycosylated immature form by the *solid arrow*. The *upper band* is undetectable in untreated R74W- and E128K-infected cells, indicating defective channel processing and trafficking. Sulfonylurea treatment, however, restores upper band expression. The same blot was probed for α-tubulin to confirm equal loading of protein samples. **(B)** Surface immunostaining with FLAG-antibody of fSUR1 showed that R74W and E128K mutant channels are only detected at the cell surface following tolbutamide treatment. **(C)** K_{ATP} surface expression in INS-1 cells was quantified using chemiluminescence assays. Under control conditions, R74W and E128K both express at 9% of WT. Sulfonylurea treatment greatly improves R74W and E128K expression to 90 and 80%, respectively. *Error bars* represent ±S.E. of three experiments. **(D)** Islets isolated from rat pancreas were cultured for 48 h and then infected with K_{ATP} subunit-encoding adenoviruses. Exogenous K_{ATP} biogenesis was tracked by Western blot of FLAG epitope. The *upper band* of fSUR1 was only detected following 5 μm glibenclamide treatment. A nonspecific band in the E128K blot is shown to serve as a loading control.

Figure 6. R74W and E128K have inappropriate channel openings in intact cells following high glucose stimulation. (A) On-cell voltage clamp recordings were made in INS-1 cells co-infected with the K_{ATP} subunit-encoding adenoviruses and pretreated with 300 μm tolbutamide to rescue mutant surface expression followed by 3-h washout in 12 mm glucose medium. High

glucose stimulation should cause a rise in intracellular ATP and inhibition of K_{ATP} channels. Representative current traces showing that both uninfected control and WT-infected cells had little or no channel activity; however, both R74W and E128K had robust channel openings. *Scale bars*: 10 s. **(B)** Membrane patches were excised into inside-out configuration from WT- or mutant-infected and tolbutamide-pretreated INS-1 cells after on-cell recording shown in (A) to test channel ATP sensitivity. Representative traces show that channels from mutant-infected and tolbutamide rescued cells have decreased ATP sensitivity compared with channels from WT-infected and tolbutamide pretreated cells. *Scale bars*: WT: 50 pA, 10 s; R74W: 100 pA, 10 s; E128K: 50 pA, 10 s.

Figure 7. R74W or E128K expression at the plasma membrane results in a diabetes phenotype. INS-1 cells were co-infected with the K_{ATP} subunit-encoding adenoviruses followed by pretreatment with 300 μm tolbutamide and washout to rescue surface expression where indicated. **(A)** and **(B)** Initial and post-break-in steadystate membrane potentials following 12 mm glucose stimulation were determined by whole cell current clamp recordings. Representative traces are shown in (A). *Scale bars* represent 10 s of recording, and the *downward arrow* specifies the time of break-in. The initial spike is an artifact going from on-cell to whole cell mode. The average membrane potential values are shown in (B). Each *bar* represents the mean ± S.E. of 11-30 cells. *, $p < 0.05$; $^{\#}$, $p < 0.01$, Student's *t* test. **(C)** Insulin secretion at basal (3 mm) and 12 mm glucose in uninfected controls and WT-, R74W-, or E128K-infected INS-1 cells. R74W- and E128K-infected cells pretreated with 300 μm tolbutamide for 4 h to rescue surface expression had significantly less insulin secretion relative to control or WT-infected cells. In R74W- or E128K-infected cells without tolbutamide rescue, insulin secretion was also reduced likely due to some leak expression of the mutants, although the extent of reduction was less than tolbutamide-rescued cells. *, $p < 0.05$; $^{\#}$, $p < 0.01$, Student's *t* test. Each *bar* represents the mean ± S.E. of three to five experiments.

Supplemental Figure 1. Examples of inside-out patch clamp recordings showing that in a small fraction of mutant-infected INS-cells without tolbutamide rescue, sufficient mutant channels were able to traffic to the surface to cause a decrease in channel sensitivity to ATP inhibition. Scale bars—WT: 500pA, 10s; R74W: 100pA, 10s; E128K:100pA, 10s.

Supplemental Figure 2. Examples of recordings showing the range of membrane potentials at 12mM glucose seen for mutant-infected INS-cells that were not pretreated with tolbutamide. Initial resting membrane potential measurements were examined using whole-cell current-clamp recording in **(A)** R74W- or **(B)** E128K-infected cells. Arrows represent time of break-in. Scale bars: 10s.

Supplemental Figure 3. On-cell activity is correlated with initial resting membrane potential (RMP) in mutant K_{ATP}-infected INS-1 cells. Data from cells in which both on-cell activity (expressed as NP_o: the number of channels in the patch N times the open probability P_o of each channel) and initial RMP was collected is shown; data from cells treated with tolbutamide to rescue channel expression and cells not treated are combined. The on-cell activity was determined using voltage-clamp recording with a holding potential of +50mV. Subsequently, whole-cell current-clamp was used to determine the initial RMP. Note the difference in the scale of the x-axis.

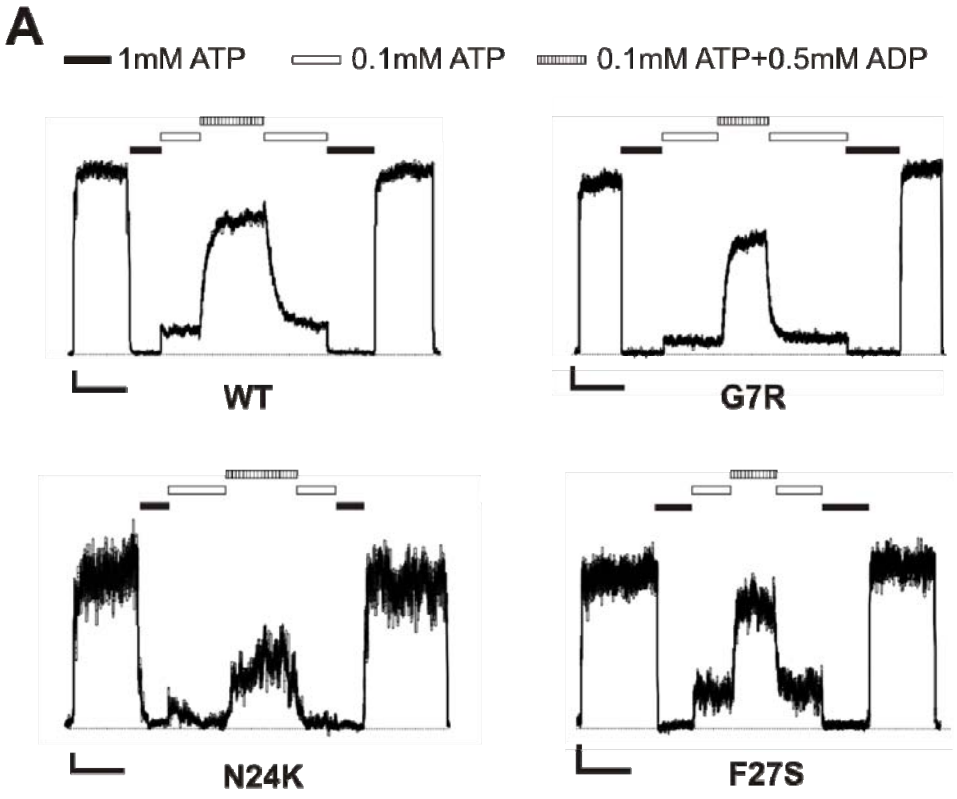

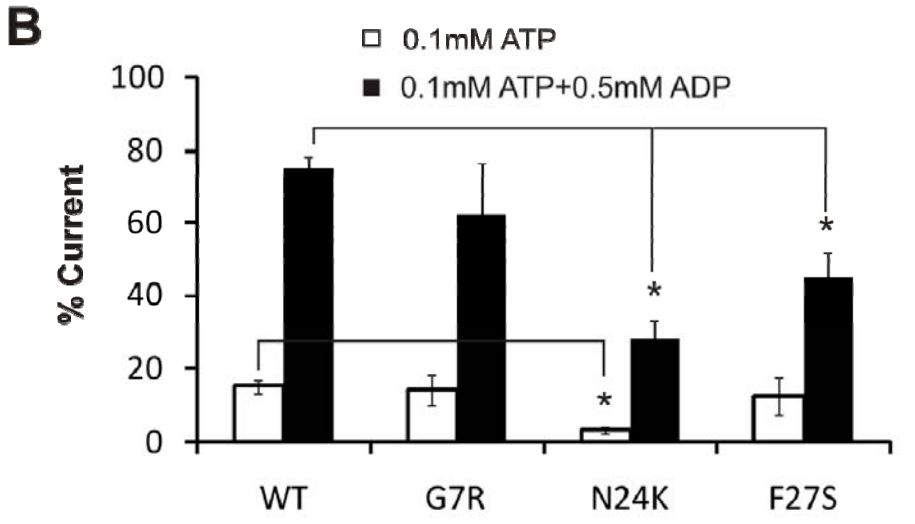

EBP Chapter 2
Figure 1

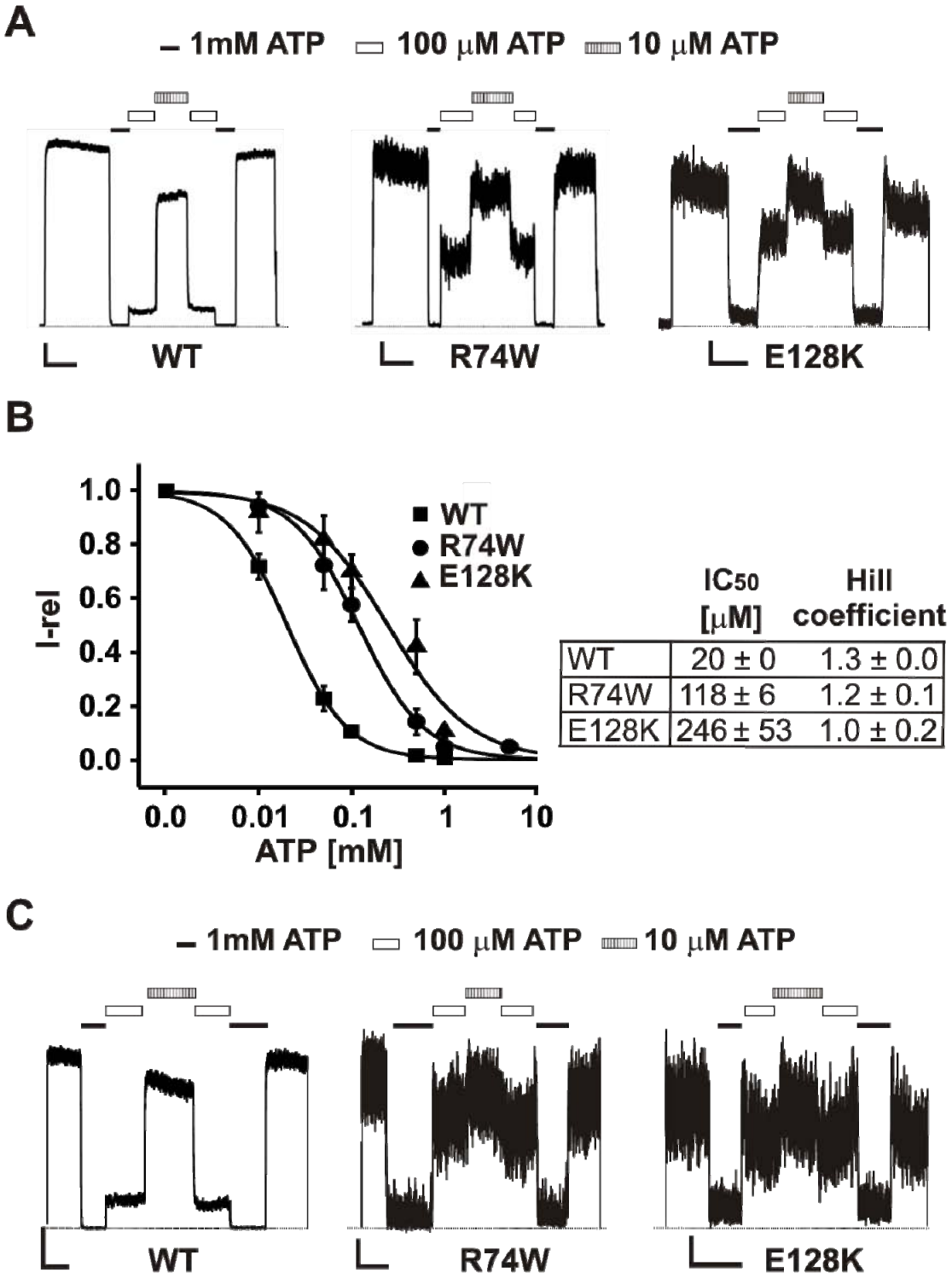

EBP Chapter 2
Figure 2

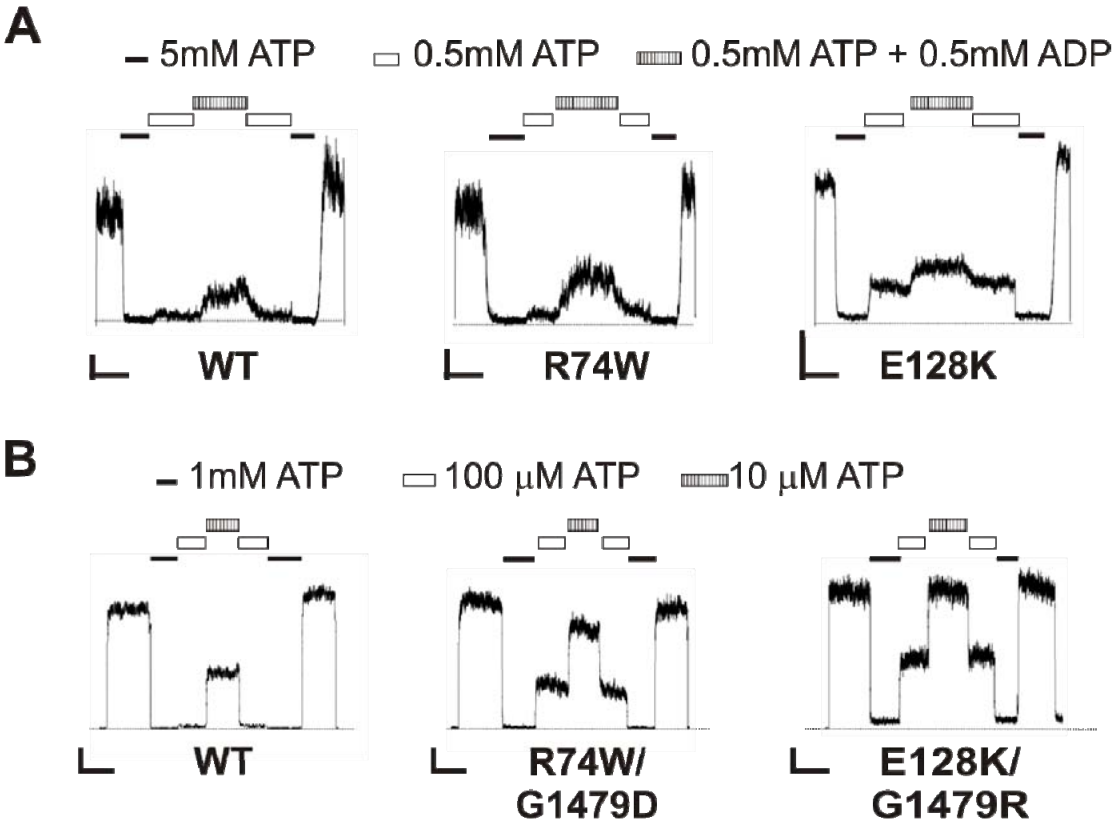

C

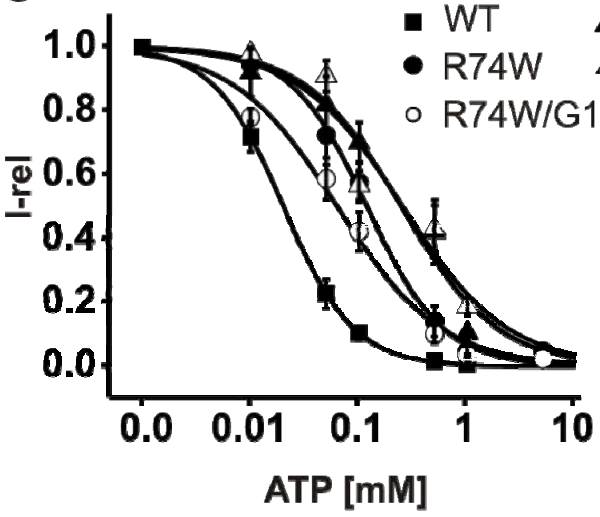

	IC50 [μM]	Hill coefficient
WT	20 ± 0	1.3 ± 0.0
RW	118 ± 6	1.2 ± 0.1
RW/GD	**63 ± 9**	**0.9 ± 0.1**
EK	246 ± 53	1.0 ± 0.2
EK/GR	**253 ± 78**	**0.9 ± 0.2**

EBP Chapter 2
Figure 3

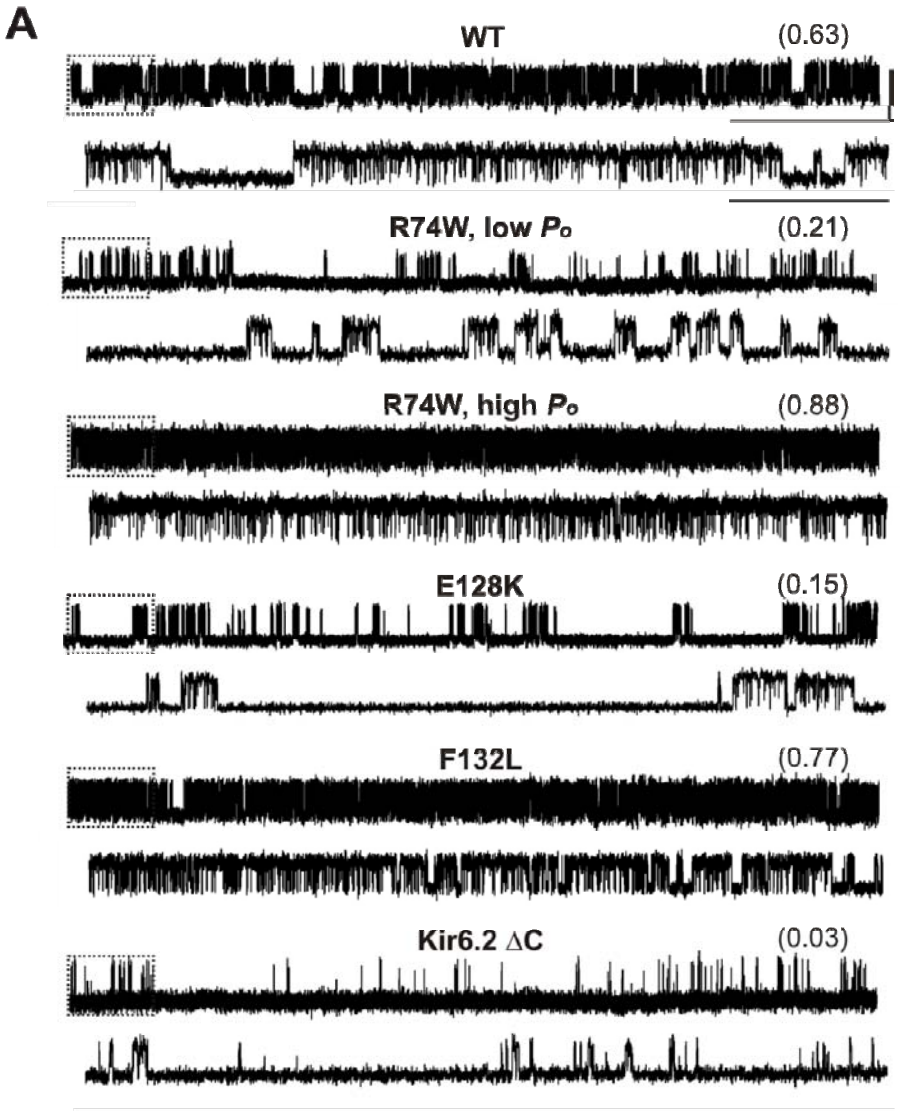

EBP Chapter 2
Figure 4

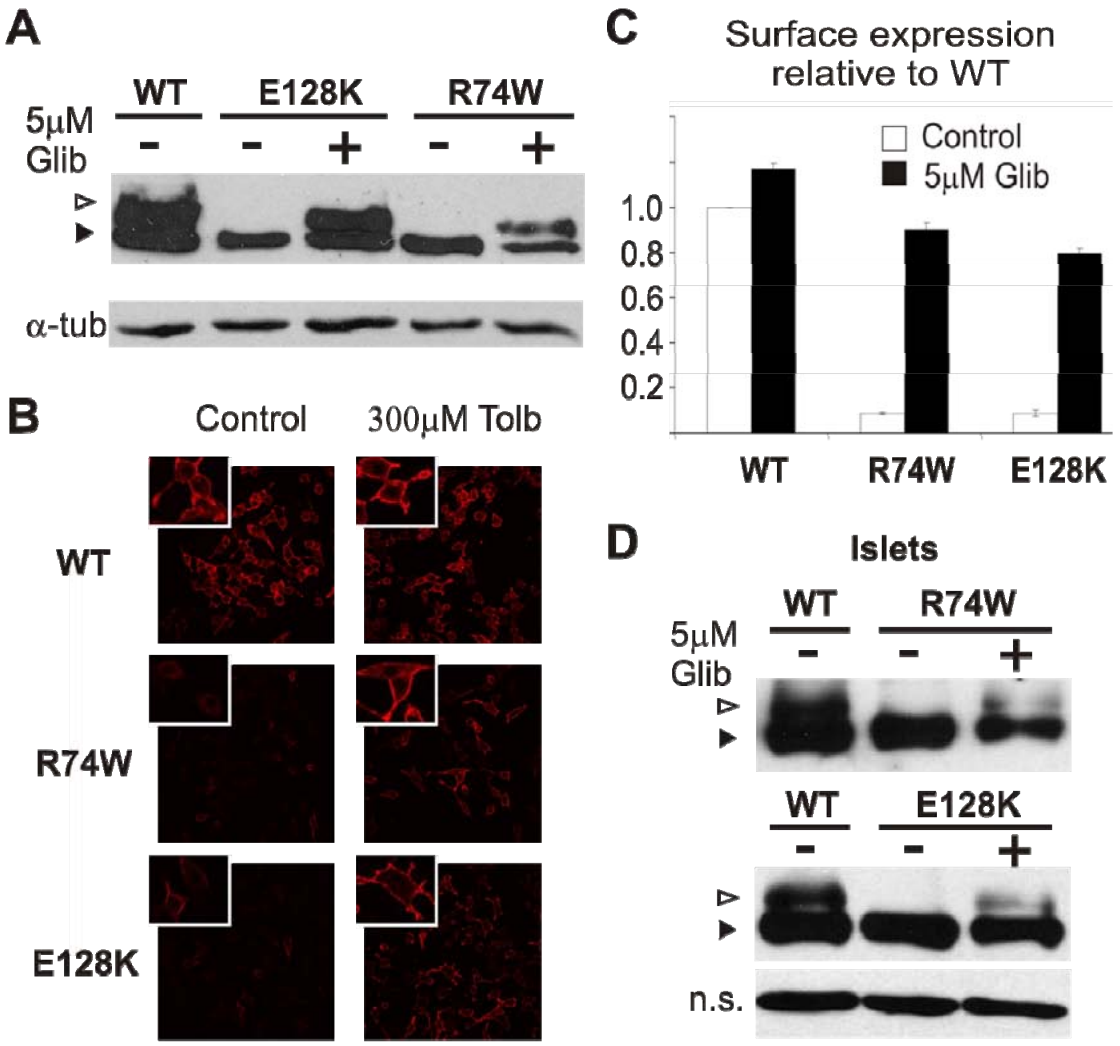

EBP Chapter 2
Figure 5

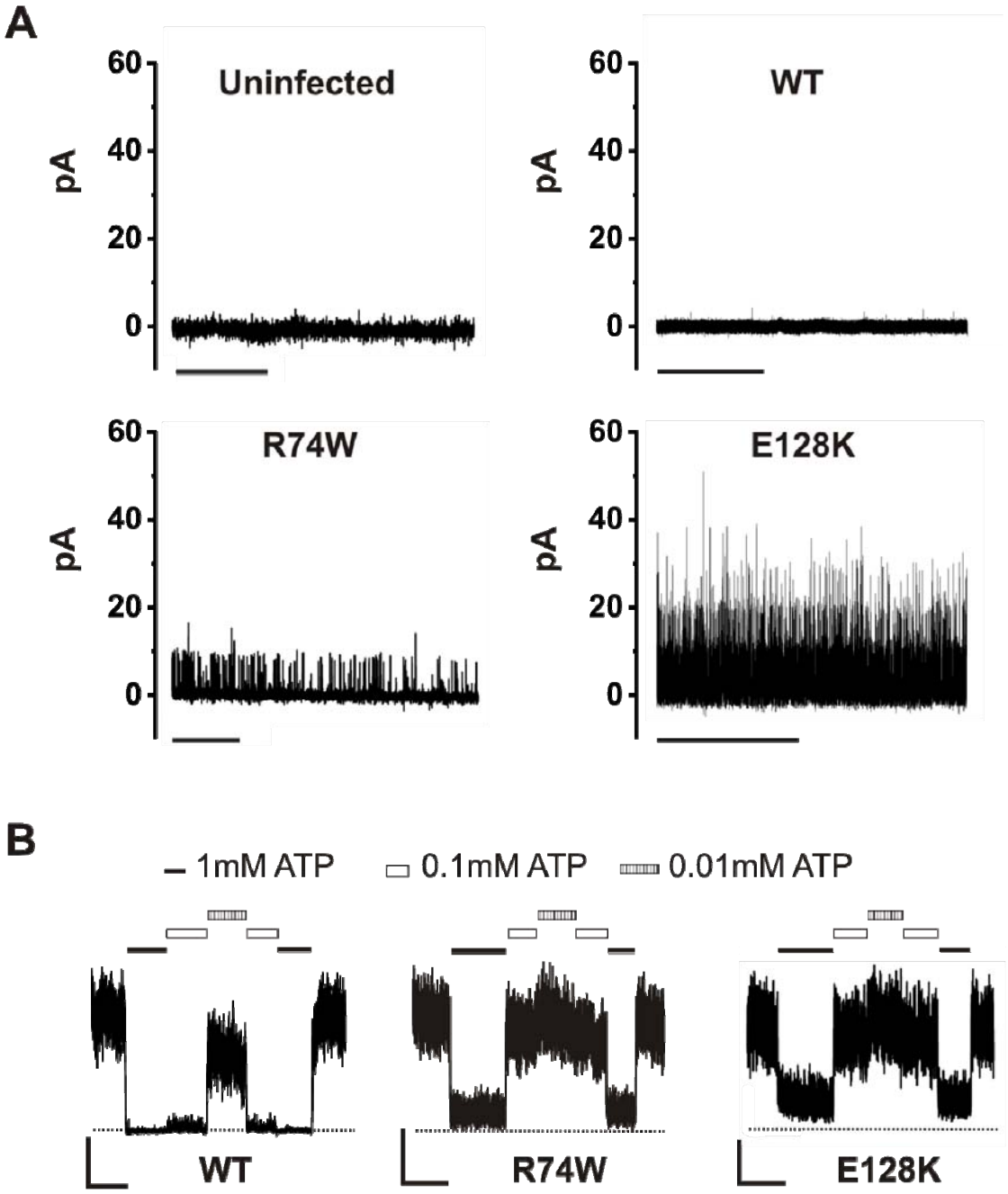

EBP Chapter 2
Figure 6

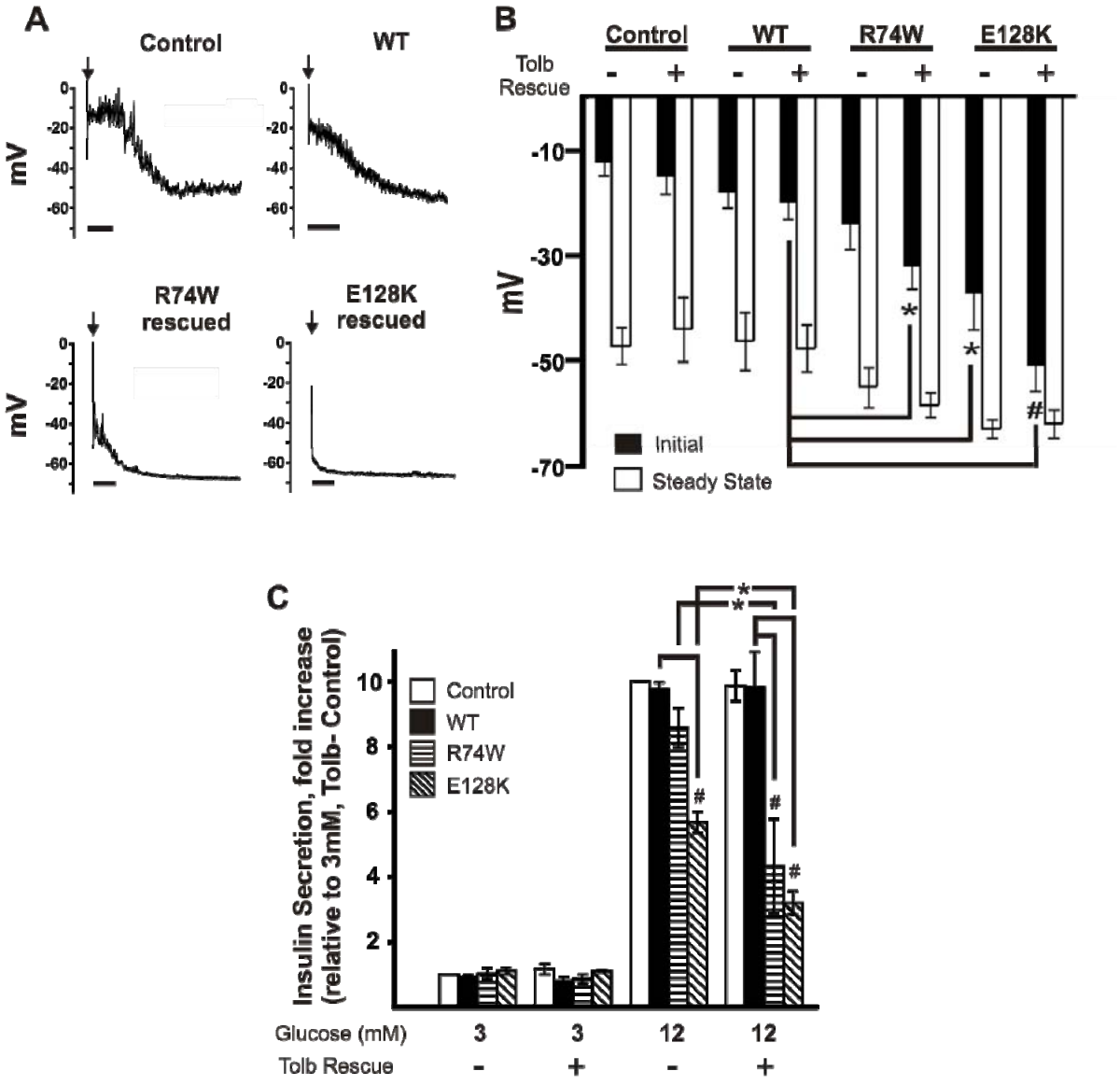

EBP Chapter 2
Figure 7

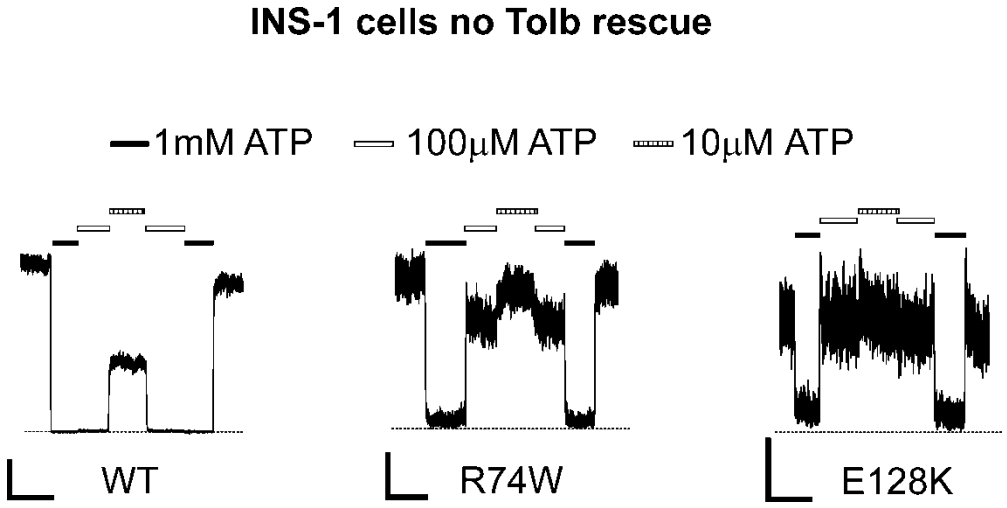

EBP Chapter 2
Supplemental Figure 1

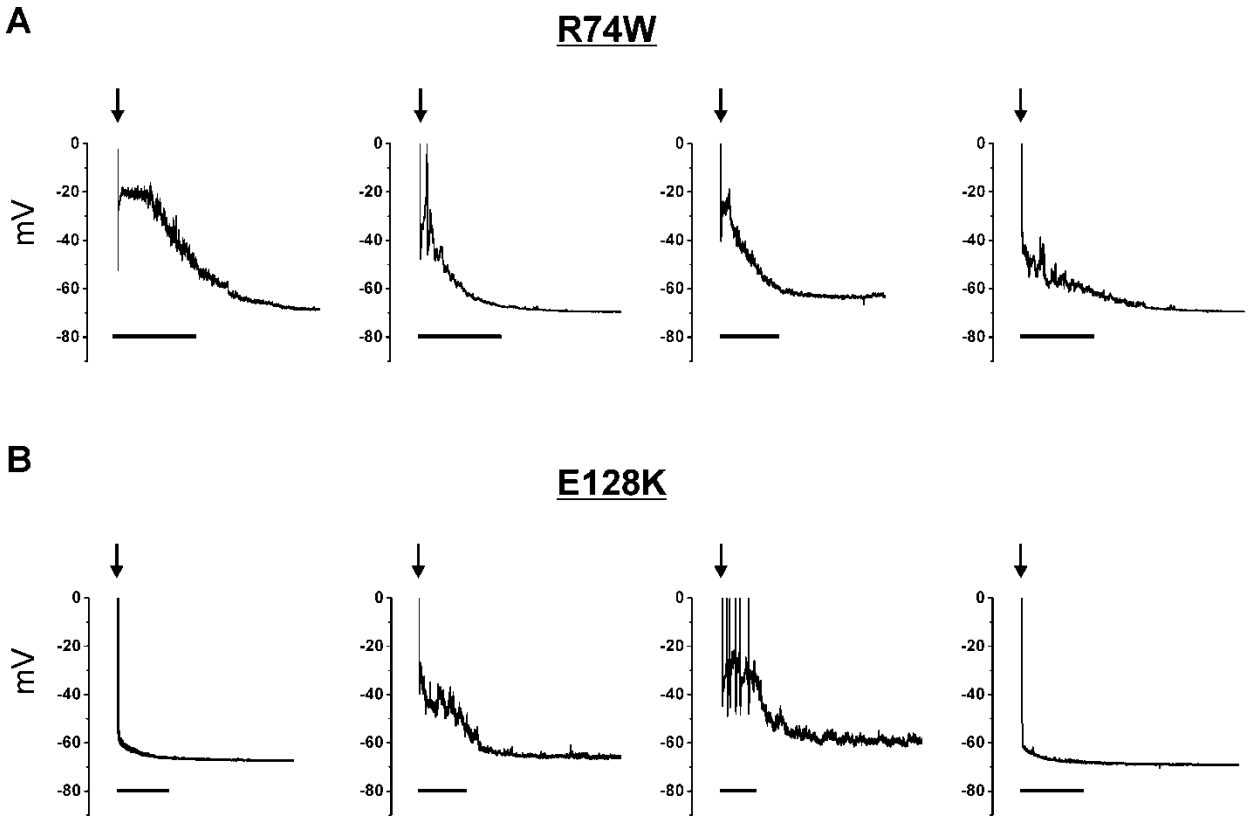

EBP Chapter 2
Supplemental Figure 2

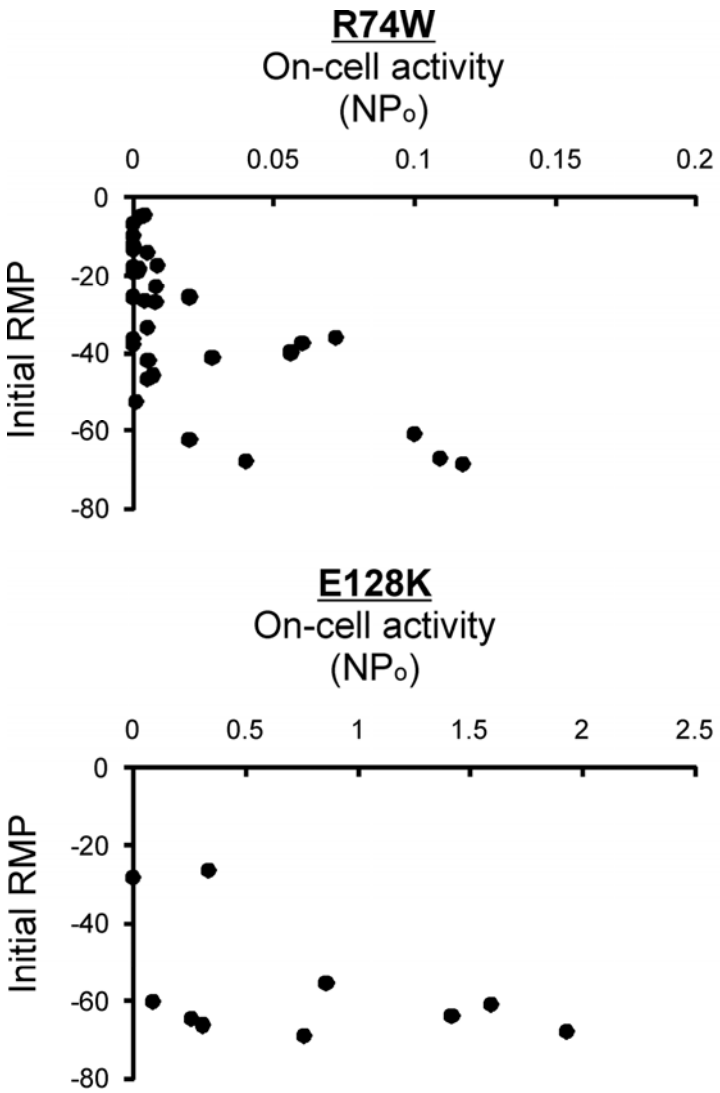

EBP Chapter 2
Supplemental Figure 3

CHAPTER 3

N-terminal Transmembrane Domain of SUR1 Controls Gating of Kir6.2 by Modulating Channel Sensitivity to PIP_2

Emily B. Pratt, Paul Tewson, Cathrin E. Bruederle, William R. Skach, and Show-Ling Shyng

Department of Biochemistry and Molecular Biology, Oregon Health & Science University

Corresponding Author: Show-Ling Shyng

Chapter 3 is a manuscript that appears as it has been submitted for publication to:

Journal of General Physiology, submitted October 2010

In this chapter I performed the experiments in Figures 1B and 1D, 2, 3A and 3B, 4, 5 and 6. P Tewson performed the molecular biology. Qing Zhou performed the western blot (upper) in Figure 1C. C Bruederle performed the western blot (lower) in Figure C and the immunohistochemistry in Figure 3C. I also participated in writing the manuscript.

Abstract

Functional integrity of pancreatic ATP-sensitive potassium (K_{ATP}) channels depends on the interactions between pore-forming subunits inward rectifier potassium channel 6.2 (Kir6.2) and regulatory subunits sulfonylurea receptor 1 (SUR1). Previous studies have shown that the N-terminal transmembrane domain of SUR1 (TMD0) alone is sufficient to interact with Kir6.2 and confer the high intrinsic open probability (P_o) and bursting patterns of activity observed in full-length K_{ATP} channels. However, the nature of TMD0-Kir6.2 interactions that underlie gating modulation is not well understood. Using two previously described disease-causing mutations in TMD0 (R74W and E128K) as starting points, we performed amino acid substitution studies to understand the structural roles of these residues in K_{ATP} channel function in the context of full-length as well as TMD0-SUR1. Our results revealed that although R74W and E128K in full-length SUR1 both decrease surface channel expression and reduce sensitivity to ATP inhibition, they arrive there via distinct mechanisms. Mutation of R74 uniformly reduced TMD0 protein levels, suggesting that R74 is necessary for integrity of transmembrane domain structure. In contrast, E128 mutations retained TMD0 protein levels but reduced functional coupling between TMD0 and Kir6.2 in mini-K_{ATP} channels formed by TMD0 and Kir6.2. Importantly, E128K full-length channels, despite having a greatly reduced P_o, exhibit little response to phosphatidylinositol 4,5-bisphosphate (PIP_2) stimulation. This is reminiscent of Kir6.2 channel behavior in the absence of SUR1, and suggests that TMD0 controls Kir6.2 gating by modulating Kir6.2 interactions with PIP_2. Further supporting this notion, an E128W mutation in full-length channels resulted in an inactivation phenotype that is prevented or reversed by exogenous PIP_2. These results identify a critical determinant in SUR1-TMD0 that controls Kir6.2 gating by controlling channel sensitivity to PIP_2.

Introduction

The pancreatic β-cell ATP-sensitive potassium (K_{ATP}) channel is a member of the inwardly rectifying potassium (Kir) channel family (Inagaki et al., 1995a). It plays a key role in regulating insulin secretion by coupling cell metabolism to cell excitability (Aguilar-Bryan and Bryan, 1999; Nichols, 2006). The channel is a hetero-octameric structure composed of two different subunit types (Clement et al., 1997; Inagaki et al., 1997; Shyng and Nichols, 1997). Four Kir6.2 subunits line the conduction pathway and are similar in topology and sequence to other members of the Kir channel family. ATP and phosphatidylinositol 4,5-bisphosphate (PIP_2) interact with Kir6.2 to inhibit or stimulate channel activity respectively (Tucker et al., 1997; Baukrowitz et al., 1998; Shyng and Nichols, 1998). Surrounding Kir6.2 are four sulfonylurea receptor 1 (SUR1) subunits, which are required for K_{ATP} trafficking and function. SUR1 is a member of the ABC transporter superfamily and contains the canonical ABC transporter core domain [two 6-spanning transmembrane domains (TMDs) and two cytoplasmic nucleotide binding folds (NBF)] plus a unique 5-spanning N-terminal TMD (TMD0) and a large cytosolic linker (L0) (Figure 1A) (Inagaki et al., 1995a; Tusnady et al., 1997; Conti et al., 2001). SUR1 imparts K_{ATP} channels with sensitivities to MgADP-stimulation and to pharmacological agents such as sulfonylureas and diazoxide (Nichols et al., 1996; Gribble et al., 1997a). In addition, SUR1 modifies properties of K_{ATP} by increasing the open probability (P_o) of Kir6.2 and hypersensitizing the channel to nucleotide inhibition (Tucker et al., 1997; Babenko et al., 1999a; Enkvetchakul et al., 2000). Despite advances in our understanding of the distinctive roles of SUR1 and Kir6.2 in K_{ATP} function, significant knowledge gaps remain with regard to the mechanisms of coupling between SUR1 and Kir6.2 that give rise to the gating properties of K_{ATP} channels.

K_{ATP} subunits can be manipulated to create unnatural yet useful channel variants to study channel structure-functional relationships. Both Kir6.2 and SUR1 have a tripeptide ER-retention motif RKR that becomes shielded only upon proper formation of K_{ATP} quaternary structure

(Zerangue et al., 1999). Deletion of the last 36 amino acids of Kir6.2 (Kir6.2ΔC36) removes its RKR motif and leads to surface expression of homotetrameric Kir6.2 channels in the absence of SUR1 (Tucker et al., 1997; Zerangue et al., 1999). These channels differ from wild-type (WT) SUR1-Kir6.2 channels in several respects (Tucker et al., 1997; Babenko et al., 1999a; Enkvetchakul et al., 2000; Babenko and Bryan, 2003; Chan et al., 2003). First, although they are sensitive to ATP inhibition, the half-maximal inhibition concentration (IC_{50}) is ~10-fold higher than WT channels (Tucker et al., 1997). Second, they exhibit a markedly reduced intrinsic P_o, i.e., spontaneous activity in the absence of nucleotides in isolated membrane patches, in comparison to WT channels (P_o ~0.1 versus ~0.6 for WT). In addition, they have altered single channel kinetics with brief openings separated by relatively long periods of closure, in contrast to WT channels which demonstrate bursts of activity with fast open and close events separated by longer closed intervals. Interestingly, co-expression of Kir6.2ΔC36 with TMD0 results in "mini-K_{ATP} channels" with bursting behavior and intrinsic P_o that are similar to WT. However, ATP-sensitivity of mini-K_{ATP} channels remains lower than that of WT; in fact, it is even lower than that of Kir6.2ΔC36 channels. K_{ATP}-mini channels also lack response to MgADP stimulation or pharmacological regulation (Babenko and Bryan, 2003; Chan et al., 2003). Thus TMD0 is sufficient to confer WT channels' bursting properties and high P_o, but the portions of SUR1 responsible for ATP hypersensitization and other SUR1-endowed gating properties lie outside TMD0. The mechanism whereby TMD0 modulates the gating pattern of Kir6.2 has not been determined, although it has been proposed that intramembrane interactions reposition the Kir6.2 outer helix to achieve the effects (Babenko and Bryan, 2003).

A key determinant of K_{ATP} channels' intrinsic P_o is membrane phosphoinositides, in particular PIP_2. Current evidence suggests that PIP_2 interacts with positively charged residues in the N- and C-cytoplasmic domains of Kir6.2 near the lipid-cytoplasm interface to stabilize channel opening (Shyng et al., 2000; Cukras et al., 2002a, b; Haider et al., 2007). Activation of K_{ATP}

channels by PIP_2 also leads to a concomitant decrease in channel sensitivity to ATP (Baukrowitz et al., 1998; Shyng and Nichols, 1998) which binds to a pocket formed by residues from the N- and C-cytoplasmic domains of two adjacent Kir6.2 subunits to inhibit channel activity (Antcliff et al., 2005). Although ATP and PIP_2 may interact with overlapping residues, they are not thought to be competitive ligands (Antcliff et al., 2005; Haider et al., 2007; Stansfeld et al., 2009). Rather, PIP_2 decreases the apparent channel sensitivity to ATP inhibition via allosteric effects. To date, most mutagenesis and modeling studies addressing the mechanism of PIP_2 regulation have focused on the Kir6.2 subunit. However, it has been well documented that SUR1 increases Kir6.2 response to PIP_2 (Baukrowitz et al., 1998; Enkvetchakul et al., 2000). Thus, how SUR1 modulates channel response to PIP_2 is an important question yet to be resolved.

Mutations in SUR1 or Kir6.2 that cause loss of K_{ATP} channel gating or expression result in congenital hyperinsulinism while gain-of-function mutations cause neonatal diabetes (Ashcroft, 2005). Recently, we reported two interesting mutations (R74W and E128K) in the TMD0 domain of SUR1 identified in congenital hyperinsulinism that cause loss of channel function by preventing channel trafficking to the cell surface, but that upon rescue by sulfonylureas to the cell surface (Yan et al., 2004; Yan et al., 2006; Yan et al., 2007)reveal channel gating defects expected to cause the opposite disease, neonatal diabetes (Pratt et al., 2009). The R74W and E128K mutant channels show reduced channel sensitivity to ATP inhibition. However, unlike most ATP-insensitive mutants in which an increased P_o underlies the reduction in apparent ATP-sensitivity by allosteric effects, the R74W and E128K mutants display decreased P_o (Pratt et al., 2009). These alterations resemble differences between WT and Kir6.2ΔC36 channels (Enkvetchakul et al., 2000) and suggest that R74 and E128 may be involved in SUR1 TMD0-Kir6.2 interactions. In this study we systematically replaced residues 74 and 128 with other amino acids (referred to as R74X and E128X) in full-length and mini K_{ATP} channels to probe

their structural and functional roles in the coupling between TMD0 and Kir6.2. We show that R74W reduces physical coupling between the two subunits by reducing stability of the TMD0 protein, indicating that R74 is critical for TMD0 structure. In contrast, E128K disrupts functional coupling between TMD0 and Kir6.2 by abrogating the effects of SUR1 on channel response to PIP_2. The latter finding provides novel insight into the mechanism whereby TMD0 of SUR1 modulates Kir6.2 gating. In Kir channels, PIP_2 plays a central role in determining channel activity (Hilgemann et al., 2001; Yi et al., 2001) and diverse modulators affect Kir channel activity via PIP_2 interactions (Baukrowitz et al., 1998; Shyng and Nichols, 1998; Fan and Makielski, 1999; Liou et al., 1999; Du et al., 2004). We propose that TMD0 confers the intrinsic gating property of K_{ATP} channels by modulating interactions between Kir6.2 and PIP_2.

Results

In full-length K_{ATP}, position R74 is sensitive to substitution by non-charge conserving amino acids. Nine amino acids with diverse side chain properties (Chothia, 1976; Kyte and Doolittle, 1982) were swapped for arginine 74 of SUR1. COSm6 cells were transiently transfected with WT Kir6.2 along with WT or mutant SUR1 with an extracellular, N-terminal FLAG epitope (fSUR1). Forty-eight hours later, cells underwent chemiluminescence assay (see Methods sections) such that antibody directed against the FLAG epitope was detected using ECL substrate reacting with horseradish peroxidase-conjugated secondary antibody. Quantification of the luminescence produced by this reaction is proportional to expression of K_{ATP} channels on the cell surface (Margeta-Mitrovic et al., 2000; Taschenberger et al., 2002). Surface expression for every R74X mutant tested, except the charge-conserving R74K mutation, was significantly reduced to below 40% of WT (Figure 1B). Surface expression quantified by chemiluminescence was confirmed by western blot experiments. SUR1 has two N-linked glycosylation sites (at residues N10 and N1050) that are core glycosylated in the ER and

acquire complex carbohydrate during transit through the Golgi (Raab-Graham et al., 1999). K_{ATP} channel trafficking can therefore be monitored by the relative abundance of core- and complex-glycosylated SUR1. Complex-glycosylated SUR1 serves as a proxy measure of surface expression, although some fraction of "mature" protein may reflect channels in transit from Golgi to the plasma membrane and endosomal trafficking. Figure 1C (top) shows representative immunoblots using α-SUR1 antibody. R74K, which had 74 ± 4% surface expression relative to WT by chemiluminesence (Figure 1B) shows both upper and lower glycosylation bands. In contrast, R74A and R74Y (2±1% and 4±2% surface expression by chemiluminesence, respectively) showed mostly core-glycosylated band with very little complex-glycosylated SUR1 protein.

Next, to assess how each residue substitution effected ATP-sensitive inhibition of K_{ATP} channel activity, inside-out patch, voltage-clamp recordings were performed in transiently transfected COSm6 cells. Because of significantly reduced surface expression in most mutants, cells were pretreated with 300 μM tolbutamide overnight which partially corrects the trafficking defect caused by mutations in the TMD0 of SUR1, including R74W (Yan et al., 2004; Yan et al., 2007; Pratt et al., 2009) and all R74X mutants with the exception of R74D (Supplemental Figure 1). Because R74D had no detectable surface expression before or after tolbutamide exposure, it was excluded from patch-clamp analysis. Tolbutamide was washed out for two hours prior to recording. Representative traces for several mutants are shown in Figure 2A. Macroscopic currents were exposed to ATP (3, 1, 0.3, 0.1 and 0.01 mM) and the amount of current inhibition relative to the maximum channel activity in the absence of ATP was fit to a Hill function ($I_{rel}=1/(1+([ATP]/IC_{50})^H)$). I_{rel} is the current relative to maximum, i.e., nucleotide-free Kint/EDTA (see Methods for discussion of EDTA use); IC_{50} is the concentration of ATP that causes half-maximal inhibition; and H is the Hill coefficient (Figure 2B, left). As with trafficking, the charge-conserving mutant R74K had minimal effect on ATP sensitivity. Additionally, mutation to

glutamate (charge-reversal), cysteine and alanine resulted in negligible differences (IC_{50} = 15±1, 20±1 and 24±3 μM, respectively) indicating that although each mutation decreases steady-state surface expression (Figure 1A, top), functional interactions between SUR1 and Kir6.2 are preserved. In contrast, replacement of R74 with aromatic residues resulted in a significant right-shift in ATP-sensitive inhibition [IC_{50} = 60±8, 89±14, 118±6 μM for phenylalanine, tyrosine, and tryptophan (Pratt et al., 2009), respectively].

R74 mutations in SUR1-TMD0 constructs reduce steady-state protein levels and disrupt surface expression of mini-K_{ATP} channels. Assessing the specific effects of R74X mutations on TMD0 is possible using a version of SUR1 that is truncated after amino acid 198. Steady-state levels of FLAG-tagged TMD0 harboring R74X were assessed via western blot. R74 substitution had substantial effects on TMD0 levels. R74K substitution had the greatest expression with 70% of WT; all other R74 substitutions tested (alanine, phenylalanine, tyrosine and tryptophan) resulted in significantly decreased TMD0 levels, less than 25% of WT (Figure 3A and B, top). We also looked at the ability of R74X fTMD0 to reach the cell surface when co-expressed with Kir6.2ΔC36. By immunofluorescent staining using α-FLAG antibody, no surface protein of R74K or R74W TMD0 was detected above background signal, although WT mini-channels were clearly visible (Figure 3C). The above observations suggest that R74 is important for structural integrity of TMD0. Mutation at this position leads to instability and rapid degradation of TMD0, thus diminishing physical association with Kir6.2 to produce mini-K_{ATP} channels.

Effects of amino acid substitution at E128 of SUR1 on full-length channel biogenesis and ATP-sensitivity. As with R74, we performed amino acid substitution studies at position E128 and assessed both surface expression (Figure 1) and ATP-sensitive inhibition (Figure 2) of each mutant. Broadly, E128X mutants showed better surface expression than R74X mutants. Of the

E128X channels tested charge-reversal mutations (E128R and K) impeded surface expression most strongly (8% and 6% of WT, respectively). Interestingly, charge-conserving E128D also showed relatively poor surface expression, only 38% that of WT channels. Next, we tested the ATP-sensitivity of E128X mutant channels. Again, cells were pretreated with 300 μM tolbutamide overnight to improve the surface expression of each E128X mutant (Supplemental Figure 1) followed by 2 h washout prior to recording. Replacement of E128 with cysteine resulted in normal ATP-induced inhibition (IC_{50} = 23±1 μM), but other amino acid substitutions significantly decreased ATP sensitivity (Figure 2A). Interestingly, substitution of E128 with tryptophan resulted in a unique inactivation phenotype making it difficult to determine the ATP-sensitivity (see Figure 6 below).

E128 mutations in SUR1-TMD0 constructs disrupt functional coupling between TMD0 and Kir6.2. The finding that E128X substitutions affect K_{ATP} channel surface expression and ATP-sensitivity in a pattern distinct from R74X substitutions suggests different roles of the two residues in channel structure and function. To further investigate the structural and functional role of E128, we analyzed the E128X-TMD0 proteins and the resulting mini-K_{ATP} channels when co-expressed with Kir6.2ΔC36. Western blots of fTMD0 showed that amino acid substitutions at E128 had much less effect on steady state levels of the protein compared to mutation at R74 as quantified by densitometry (Figure 3A and B, bottom). Also in contrast to R74X, E128K fTMD0 was detected at the cell surface of COSm6 cells when it was co-transfected with Kir6.2ΔC36 (Figure 3C) indicating it forms intact mini-K_{ATP} channels suitable for electrophysiological analysis.

Previously, we reported that full-length K_{ATP} channels harboring E128K-SUR1 subunits have decreased intrinsic open probability [P_o = 0.18 versus 0.63 for WT; (Pratt et al., 2009)]. We tested whether the same would be true for mini-K_{ATP} channels with E128K substitution as such

results would be a clear indication that E128K disrupts functional coupling between TMD0 of SUR1 and Kir6.2. Single channel recordings made from COSm6 cells co-transfected with E128K- fTMD0 and Kir6.2ΔC36 showed that indeed, the average intrinsic P_o of E128K mini-K_{ATP} channels was significantly lower than WT mini-channels (P_o = 0.17±0.04 for E128K versus 0.60±0.06 for WT, $p < 0.05$) (Figure 4A, B). Further, the E128K channels exhibited short bursts of activity separated by relatively long closures, distinguishing them from channels composed of Kir6.2ΔC36 alone. Mini-channels with a previously described mutation (F132L, identified in patients with severe neonatal diabetes) that increases open probability were also recorded as a positive control (Proks et al., 2006; Proks et al., 2007). These results demonstrate that E128K in the context of both full-length protein and TMD0 alone reduces functional coupling between SUR1 and Kir6.2 with regard to intrinsic P_o and single channel kinetics.

In K_{ATP} channels, ATP-sensitivity is normally negatively correlated with intrinsic P_o through allosteric effects (see Introduction) (Enkvetchakul et al., 2000; Enkvetchakul and Nichols, 2003). Following this relationship, in mini-K_{ATP} channels TMD0 increases the P_o of Kir6.2ΔC36 leading to a decrease in the ATP-sensitivity conferred by Kir6.2ΔC36 [IC_{50} ~138 μM for Kir6.2ΔC36 and ~309 μM for TMD0+ Kir6.2ΔC36 (Chan et al., 2003)]. As E128K abrogates the effect of TMD0-SUR1 on the open probability of Kir6.2, we predicted that mini-K_{ATP} channels with the E128K mutation will also have ATP-sensitivity more similar to Kir6.2ΔC36 than to TMD0+Kir6.2ΔC36 channels. COSm6 cells expressing WT, E128K or F132L mini-channels or Kir6.2ΔC36 alone were recorded in the absence and presence of 1 mM ATP (Figure 4C). The F132L mini-channels were included as a control here as they have been shown to have increased P_o and decreased ATP-sensitivity compared to WT mini-K_{ATP} channels (Proks et al., 2007). As predicted, the E128K mini channels were inhibited to a similar extent as Kir6.2ΔC36 channels (~85%) while the WT and F132L mini channels were inhibited by only 52% and 15%

respectively (compare Figures 4B and C). The above results support the hypothesis that E128K directly uncouples functional interactions between TMD0 and Kir6.2, which leads to a decrease in intrinsic P_o and an increase in ATP sensitivity (compare to WT mini-K_{ATP}) like that of Kir6.2ΔC36 channels.

E128K attenuates response of full-length channels to PIP_2. The intrinsic open probability of Kir channels is thought to be determined by channel interactions with membrane phosphoinositides, in particular PIP_2: the stronger the interactions the higher the P_o (Logothetis et al., 2007a; Xie et al., 2007). In K_{ATP} channels, PIP_2 increases the P_o and allosterically decreases apparent ATP-sensitivity (Baukrowitz et al., 1998; Shyng and Nichols, 1998; Fan and Makielski, 1999). Previous studies have shown that while Kir6.2 interacts with PIP_2 directly, SUR1 enhances Kir6.2 response to PIP_2 (Baukrowitz et al., 1998; Shyng and Nichols, 1998; Enkvetchakul et al., 2000). In inside-out patches, application of PIP_2 to the bath solution rapidly increases WT channel activity to maximal P_o and decreases channel sensitivity to ATP inhibition. In contrast, Kir6.2ΔC36 channels show relatively small increase in P_o and decrease in ATP-sensitivity. We hypothesize that SUR1 modulates the P_o of Kir6.2 via TMD0 by enhancing channel response to PIP_2. Moreover, E128 is essential for this modulation such that mutation to lysine (E128K) diminishes the effect of TMD0 on the P_o of Kir6.2 (Figure 4). Accordingly, we predicted that the E128K channel will have reduced sensitivity to PIP_2. Indeed, we found that K_{ATP} channels harboring the E128K mutation were much less responsive to PIP_2 both in terms of increase in current amplitude and decrease in ATP-sensitivity compared to WT (Figure 5A). After 30 seconds of exposure to 5 μM PIP_2, WT current increased 1.53 ± 0.12-fold relative to current prior to PIP_2 exposure whereas E128K channel current increased only 1.07 ± 0.10-fold (Fig.5B). An additional 30-seconds exposure to 5 μM PIP_2 did not minimize this difference. The lack of current increase upon PIP_2 exposure in E128K is striking when one considers the starting P_o of E128K is so much lower than WT such that WT P_o has the potential to increase

from ~0.6 to 1.0 while E128K P_o has the potential to increase from ~0.2 to 1.0. Moreover, the marked decrease in ATP-sensitivity following PIP_2 exposure seen in WT channels was also abrogated in the E128K mutant (Figure 5A and C). The reduced response to PIP_2 in the E128K channels resembles that seen in Kir6.2ΔC36 channels, providing evidence that E128K disrupts the ability of SUR1 to enhance channel response to PIP_2.

The E128W mutation in SUR1 causes inactivation in full-length channels that can be recovered by PIP_2 and by exposure and subsequent removal of ATP. Additional evidence supporting the involvement of E128 in mediating channel response to PIP_2 came from the intriguing phenotype presented by the E128W mutation. As mentioned above, mutation of E128 to a tryptophan causes the current to undergo spontaneous decay in the absence of nucleotides, which we refer to as inactivation (Figure 6). Exposure to high concentrations of ATP (1, 3 or 5 mM) reset E128W channels such that increasing the length of ATP exposure resulted in more current when the patch was re-exposed to nucleotide-free solution (Figure 6A and B). Further, exposure of the E128W patches to PIP_2 slowed or reversed the inactivation as well as potentiated the ATP-induced 'resetting' of channel activity (Figure 6C). The time- and ATP concentration-dependence of reactivation as well as the PIP_2 responsiveness are reminiscent of other inactivation mutations that we have described in previous studies caused by mutations in Kir6.2 that disrupt inter-Kir6.2 subunit interactions (Shyng et al., 2000; Lin et al., 2003; Lin et al., 2008). We have proposed that in the Kir6.2 inactivation mutants, disruption of inter-Kir6.2 subunit interactions destabilize the channels' PIP_2-bound open state and that application of exogenous PIP_2 shifts the equilibrium of channels towards the PIP_2-bound open state to prevent and reverse inactivation (Lin et al., 2003). ATP, which has been proposed to bind to a site coordinated by specific N- and C-terminal residues from adjacent Kir6.2 subunits, reestablishes the subunit-subunit interface, allowing channels to bind PIP_2 and, when the ATP inhibitory effect is removed, to open briefly (Lin et al., 2003). The results that E128W causes

similar inactivation which can be overcome by PIP_2 lend strong support to the proposal that E128 plays a critical role in the coupling between SUR1 and Kir6.2 in a PIP_2-dependent manner. In addition, the ATP-dependent recovery from inactivation in the E128W mutant suggests that conformational changes in Kir6.2 brought about by binding of ATP reestablish functional coupling between TMD0-SUR1 and Kir6.2, manifested as increased channel activity (i.e. P_o) when ATP inhibition is removed.

Discussion

Biochemical, functional and structural studies to date have provided clear evidence that TMD0 of SUR1 interacts with Kir6.2 to modulate channel trafficking and gating (Schwappach et al., 2000; Babenko and Bryan, 2003; Chan et al., 2003; Mikhailov et al., 2005). However, the molecular basis and signaling mechanism by which TMD0 exerts its effect remain poorly understood. Mutations in TMD0 offer potential for probing these problems. R74W and E128K are just such mutations as they cause dramatic impediments to channel trafficking and gating. Here we studied full-length and mini-channels to learn more about the functional role of R74 and E128 and show that R74W and E128K disrupt channel function by different mechanisms. More importantly, our results indicate TMD0 controls gating of the Kir6.2 pore by modulating PIP_2 sensitivity.

Role of R74. Replacement of R74 by any non-conserved residue in full-length channels led to substantial impairment of surface expression (Figure 1A). That these mutations cause a dramatic reduction in TMD0 protein levels suggest an important role of R74 in structural integrity of this protein domain. While the exact location of R74 with respect to the membrane has not been determined experimentally, *in silico* calculations [using the TOPCONS algorithm (Bernsel et al., 2009)] predict that residue R74 resides at the cytosolic-end of the second TM segment of TMD0 (Supplemental Figure 2). Studies of membrane integration of proteins have shown that

the aromatic amino acids tryptophan and tyrosine are frequently found at the membrane-water interface where they interact favorably with the lipid headgroups while another aromatic residue phenylalanine favors placement deeper into the lipophilic environment of the membrane (Killian and von Heijne, 2000). Charged amino acids are more likely to be found in cytoplasmic, aqueous environments (Heijne, 1986). However, positively charged amino acids lysine and arginine which have relatively long aliphatic side-chains are also seen at the interface where the aliphatic chain is localized to the hydrophobic part of the lipid bilayer while the charged side-chains interact with negatively charged lipid phosphate groups (Killian and von Heijne, 2000; Hessa et al., 2005). The relevance of these patterns of TM segment properties to the results presented here comes into play when hypothesizing the structural changes R74X substitutions have on TMD0 conformation. One might expect that substitution of TM-flanking R74 by non-conserved amino acids to induce a shift of TM2 boundary or disrupt normal membrane integration. Accordingly, with the exception of lysine, all other amino acids used in the R74X screen (A, H, C, W, F, Y, L, D or E) are predicted to shift the boundary of TM1 and TM2 (as well as TM3 for R74D and R74E) by TOPCONS (Supplemental Figure 2). The decrease in full-length K_{ATP} channel surface expression of R74X mutants (Figure 1) and instability of TMD0 (Figure 3) are consistent with these substitutions having an effect on protein folding and structure.

Interestingly, sulfonylureas acting as chemical chaperones partially overcome the trafficking defect in R74X full length K_{ATP} channels. While the mechanism by which sulfonylureas overcome this defect is not yet known, one possibility is that binding of sulfonylureas allows the mutant channel to escape the ER quality control mechanism to reach the cell surface. Regardless, this rescue strategy provides us the opportunity to analyze the ATP sensitivity of most mutants. These results show that mutation of R74 reduce ATP-sensitivity of the channel. Unfortunately however, unlike E128 mutations (see discussion below), R74 mutations in TMD0

failed to express at the cell surface when co-transfected with Kir6.2ΔC36 making it difficult to address the question of whether the gating defects are caused directly by changes in the functional coupling between TMD0 and Kir6.2 or involve indirect effects on SUR1 structure outside TMD0.

Role of E128. Full-length channels bearing E128X mutations are in general expressed at a higher level at the cell surface than R74X channels (Figure 1). Moreover, mutations at residue 128 have less effect on TMD0 protein levels and E128K-TMD0 can form mini-channels with Kir6.2ΔC36 that traffic to the cell surface. These results suggest E128 is not as critical for folding of TMD0 as R74. Consistent with this idea, the TOPCONS-predicted TM structure of TMD0 does not change with any E128 substitution, in contrast to substitutions at R74 (Supplemental Figure 2). However, the E128K mutation in both full-length and mini-K_{ATP} channels decrease open probability and ATP-sensitivity thereby indicating E128 contributes to functional coupling with Kir6.2.

Strikingly, E128K renders full-length channels much less sensitive to PIP_2 stimulation, recapitulating that seen in Kir6.2ΔC36 channels. To our knowledge, this is the first SUR1 mutation reported to reduce channel sensitivity to PIP_2. The finding is important because although SUR1 has been implicated in K_{ATP} channel gating regulation by PIP_2 the mechanisms are unknown (Baukrowitz et al., 1998; Enkvetchakul et al., 2000; Song and Ashcroft, 2001). Our study identifies a residue critical to this regulation. How might E128 contribute to channel interaction with PIP_2? The current model is that the charged phosphoinositol headgroup of PIP_2 binds to Kir6.2 via a patch of positively-charged residues in the cytoplasmic domain near the plasma membrane (Nishida and MacKinnon, 2002; Enkvetchakul and Nichols, 2003; Kuo et al., 2003). This portion of Kir6.2 is “pulled” toward the membrane resulting in a stabilized open conformation. Because E128 is negatively charged, it probably does not participate directly in

PIP_2 (or ATP) binding. Alternatively, we propose that E128 interacts directly with Kir6.2 near the membrane interface to stabilize the channel pore complex in a PIP_2-bound open state (see Figure 7A). This is consistent with the predicted location of E128 within the short second cytoplasmic loop adjacent to the lipid bilayer. The idea that TMD0 increases the P_o of Kir6.2 by enhancing channel-PIP_2 interactions differs from a previous model in which intramembrane interactions between TMD0 and Kir6.2 reposition the Kir6.2 outer helix to achieve the gating effect (Babenko and Bryan, 2003).

The detrimental effect of E128K on channel interaction with PIP_2 offers a clear explanation for how the mutation might reduce P_o in full-length and mini-K_{ATP} channels. It is well accepted that PIP_2 is a primary determinant of channel open probability. However, the effect of E128K on ATP-sensitivity and PIP_2-mediated regulation are more complex. Previous studies have shown that while TMD0 confers Kir6.2 with the high intrinsic P_o observed in full-length channels, it does not confer the hypersensitizing effect of SUR1 on ATP inhibition (Babenko and Bryan, 2003; Chan et al., 2003). Accordingly, the mini-K_{ATP} channels composed of TMD0 and Kir6.2ΔC36 are even less sensitive to ATP inhibition than Kir6.2ΔC36 channels, following the model that increased P_o (due to enhanced PIP_2 response) allosterically reduces ATP-sensitivity. Mini-K_{ATP} channels with the E128K mutation also follow this relationship, i.e., they show reduced P_o and increased ATP-sensitivity relative to WT mini-channels (similar to that seen for Kir6.2ΔC36). Although the P_o : ATP sensitivity relationship might predict that in full-length channels the E128K mutant should show increased ATP-sensitivity relative to WT, this is, however, not the case. Rather, E128K full-length channels actually have reduced ATP-sensitivity. Thus, by abolishing the ability of TMD0 to enhance Kir6.2 response to PIP_2 the E128K mutation abrogates the ability of structures downstream of TMD0 to hypersensitize Kir6.2 to ATP inhibition. Future identification of residues responsible for the hypersensitizing effect of SUR1 on Kir6.2 ATP

sensitivity will be critical for understanding precisely how E128K uncouples SUR1 from Kir6.2 with respect to regulation by both PIP_2 and ATP.

Implications for the mechanism by which TMD0 modulates the gating of Kir6.2. The observation that E128W gives rise to an inactivation phenotype previously observed in several Kir6.2 mutations that are predicted to alter inter-Kir6.2 subunit interface suggests multiple mutation sites can disrupt normal channel gating via a converging mechanism that is sensitive to both PIP_2 and ATP. Recent crystallographic work by Clarke et al. describes an unappreciated role for the intracellular domain (including the membrane-tethered slide helix) in modulating the ion conduction pore of Kir channels (Clarke et al., 2010). Namely, a 'twist' conformation in which the slide helix and cytoplasmic domain rotate relative to the transmembrane and pore helices is associated with a non-conducting pattern of ions within the selectivity filter. The transmission of intracellular conformation-change into channel opening (involving rearrangement of cytoplasmic subunit-subunit interfaces) occurred in the absence of appreciable changes in TM segment amino acid-backbones. This study highlights the importance of intracellular subunit-subunit interactions in Kir channel gating and helps explain how mutations of Kir6.2 residues predicted to lie at the inter-Kir6.2 subunit interface (such as E229, R314 and R301) cause inactivation. The finding is especially provocative when considered in the context of the SUR1/Kir6.2 K_{ATP} channel complex because it opens up the possibility that SUR1 can modulate Kir6.2 conduction primarily through cytoplasmic domain interfaces, such as that mediated by E128. The inactivation phenotype of E128W might, therefore, represent transition between two distinct ends of a spectrum of conformations described by Clarke et al. in which SUR1 goes from being coupled (before inactivation and reactivated conducting state) to uncoupled (inactivated low-conducting state). The act of ATP-binding could then reactivate the channel by drawing Kir6.2 subunits together in the case of Kir6.2 inactivation mutations (Lin et al., 2003), and SUR1 and Kir6.2 back together in the case of E128W, to establish inter-subunit interactions necessary for

stabilizing (if only briefly) the open conformation (see Figure 7B). Increasing the concentration of PIP_2 in the membrane could shift the equilibrium towards the PIP_2-bound open state by mass action thereby slowing and reversing inactivation as well as boosting the ATP-induced resetting of the channel in both Kir6.2 and E128W-SUR1 inactivation mutants (Figure 6C; 7B).

In summary, our study shows that R74 and E128 have different roles in TMD0 structure-function. Whereas R74 is important for TMD0 structure stability, E128 plays a critical role in the functional coupling between TMD0-SUR1 and Kir6.2 by controlling channel response to PIP_2. The finding that TMD0 controls Kir6.2 gating via PIP_2 is in line with the concept that in Kir channels diverse modulators affect channel gating by modulating channel interactions with membrane phospholipids (Logothetis et al., 2007a; Xie et al., 2007).

Acknowledgments

We thank Jeremy Bushman and Dr. Qing Zhou for helpful discussions and Joel Gay, Dr. Pei-Chun Chen and Dr. Yoshihiro Matsumura for technical assistance. This work was supported by grants from NIDDK to EBP (F30DK081305) and to SLS (DK066485).

Materials and Methods

Molecular biology – Rat Kir6.2 cDNA constructs including the full-length WT subunit and a truncation mutant lacking the C-terminal 36 amino acids (Kir6.2ΔC36) are in pCDNAI/Amp plasmid (Lin et al., 2008). Hamster SUR1 constructs are in pECE and include full-length subunits with an N-terminus FLAG-epitope (DYKDDDDK) (fSUR1) or the first transmembrane domain only (amino acids 1-198) with (fTMD0) or without (TMD0) the FLAG-epitope. The FLAG epitope does not change biochemical or functional properties of the channel (Cartier et al.,

2001). Site-directed mutagenesis was performed using the QuickChange mutagenesis kit (Strategene) and mutations were confirmed by direct sequencing.

Immunoblotting – COSm6 cells were maintained in DMEM with 10% FBS and 1% Pen/Strep. Cells plated on 35mm dishes and ~70% confluent were transfected with fSUR1 (0.6 μg) and Kir6.2 (0.4 μg) [or fTMD0 (1 μg) and Kir6.2ΔC36 (1 μg)] plasmids using Fugene®6 (Roche). The amount of cDNA was adjusted to maintain 1:1 molar ratio of SUR1 to Kir6.2. Cells were processed 48-72 h after transfection and following 12-18 h of sulfonylurea treatment where indicated [tolbutamide (300 μM)] (Sigma) (Yan et al., 2004; Yan et al., 2007). Cells were lysed in a buffer containing 20 mM Hepes, pH 7.0, 5 mM EDTA, 150 mM NaCl, 1% Triton-X with Complete™ protease inhibitors cocktail tablet (Roche). Protein concentrations were determined using Bio-Rad Lowry assay. Equal amount of protein from each sample was separated by SDS/PAGE, transferred to nitrocellulose, analyzed by mouse M2 α-FLAG antibody (Sigma) or rabbit α-SUR1 generated against the C-terminal peptide (KDSVFASFVRADK) (Yan et al., 2007) followed by HRP-conjugated α-mouse or α-rat secondary antibodies (GE Healthcare), and visualized by chemiluminescence (Super Signal West Femto; Pierce).

Chemiluminescence assays – Forty-eight hours after transfection, cells in 35mm dishes were fixed with 2% paraformaldehyde for 30 min, pre-blocked in PBS/0.5% BSA for 30 min, incubated in M2 α-FLAG antibody (10 μg/ml) for an hour, washed 4x30 min in PBS/0.5% BSA, incubated in HRP-conjugated α-mouse antibodies for 20 min, and washed again 4x30 min in PBS/0.5% BSA. Chemiluminescence was quantified using a TD-20/20 luminometer (Turner Designs) following 10 sec incubation in Power Signal ELISA Femto luminol solution (Pierce). Results of each experiment are the average of two 35mm dishes and each data point shown in figures is the average of ≥3 experiments.

Immunofluorescence staining – COSm6 cells were co-transfected with WT and mutant fSUR1 TMD0 and WT Kir6.2ΔC36. After 24 h cells were plated onto glass cover slips, grown for 24 h, and incubated with α-FLAG M2 mouse monoclonal antibody (10 µg/ml OptiMEM containing 0.1% BSA) for 1 h at 4°C to label surface channels. Cells were then washed with ice-cold PBS, fixed with cold (–20 °C) methanol for 10 min, and incubated with Alexa 488 goat α-mouse secondary antibody (Molecular Probes) for 45 min at room temperature. After three washes with PBS cells were mounted and viewed with a Zeiss LSM710 3-spectral confocal microscope and a 63x1.4NA objective (Carl Zeiss, Jena, Germany).

Patch-clamp recordings – Inside-out patch-clamp recordings in COSm6 cells were performed using an Axopatch 1D amplifier and pClamp9 acquisition software (Axon Inc.) (Yan et al., 2004). For macroscopic recordings, micropipettes were pulled from non-heparinized Kimble glass (Fisher Scientific) on a horizontal puller (Sutter Instrument) and had resistances of ~1.5-2.0 MΩ. Micropipettes for single channel recordings were pulled from either non-heparinized Kimble glass or borosilicate electrodes (Sutter Instruments), coated with Sylgard-148® (Sigma) and polished by microforge and had resistances of ~2-6 MΩ. The bath and pipette solution (Kint) was: 140 mM KCl, 10 mM K-HEPES, 1 mM K-EGTA, pH 7.4. 1mM EDTA was added to Kint to prevent channel rundown (Lin et al., 2003). All currents were measured at -50 mV membrane potential (+50 holding potential) at room temperature. When recording from cells expressing mutant channels with very little basal surface expression, the cells were pretreated with 300 µM tolbutamide overnight to augment expression.

Data analysis – Data are presented as means ± standard error of the mean (SEM). Statistical analysis was performed using independent two-population, two-tailed Student's *t*-test, with $p < 0.05$ considered statistically significant. Single channel open probability (P_o) analysis was carried out using the pCLAMP9 automated channel-event detector. When a decrease in

channel activity was noted, only activity recorded within the first 60 sec of inside-out patch excision was used for analysis. TMD0 sequence alignment was performed using PRALINE (Simossis and Heringa, 2005). Transmembrane topology predictions were performed using TOPCONS (Bernsel et al., 2009). Densitometry was performed using ImageJ (Rasband and Maryland).

Figure Legends

Figure 1. Expression studies of fSUR1 R74X and E128X K_{ATP} channels. (A) Schematic of fSUR1 structure including topological domains and the placement of residues R74 and E128 (stars), glycosylation sites (branches), extracellular FLAG-epitope (flag) and the –RKR– ER-retention motif (rectangle). The end of the TMD0 (amino acid 198) construct used in subsequent experiments is shown by the break. (B) Chemiluminescence assays were performed to quantitatively assess how surface expression of K_{ATP} channels is effected by different amino acids at position 74 of SUR1. Surface expression is shown relative to WT channel expression. Error bars represent SEM; n=3-6 for each condition. (C) Representative immunoblots using αer-SUR1 antibody to detect expression of fSUR1 protein in cells co-transfected with Kir6.2 and either fSUR1 R74X (top) or E128X (bottom) cDNAs. SUR1 protein undergoes differential glycosylation such that core-glycosylated protein (lower band, arrow) becomes complex-glycosylated (upper band, arrow head) upon trafficking through the Golgi; thus, the amount of upper band is a proxy for the extent of K_{ATP} surface expression. (D) Chemiluminescence assays performed to assess surface expression of E128X K_{ATP} channels. Surface expression is shown relative to WT channel expression. Error bars represent SEM; n=3-6 for each condition.

Figure 2. Functional studies of fSUR1 R74X and E128X K_{ATP} channels. (A) Representative traces from inside-out, voltage-clamp experiments performed in COSm6 cells transfected with WT Kir6.2 and WT, R74X (top) or E128X (bottom) SUR1. [ATP] is indicated above each trace

(black line—1 mM, dotted line—0.1 mM, white bar—0.01 mM) and zero current by the dotted lines. Scale bars: horizontal—10 sec; vertical—1000 pA for WT and E128C, 200 pA for the rest. (B) ATP sensitivity expressed as half-maximal inhibitory concentration (IC_{50}) for each R74X (left) and E128X (right) mutant. IC_{50} values are from best fits using the Hill equation (Irel= 1/ (1+ ([ATP]/ IC_{50})^H)). Five ATP concentrations were tested (3, 1, 0.3, 0.1 and 0.01 mM). n = 3-11 patches for each ATP concentration tested. Note the axes have different ranges for each mutagenesis set—a dotted line denotes the 0.1 mM value on each.

Figure 3. Biochemical and immunohistological studies of TMD0 harboring select R74X or E128X mutations. (A) Representative immunoblots of FLAG-tagged SUR1 TMD0 constructs with either R74X (top) or E128X (bottom) mutations expressed in COSm6 cells. Blots were probed for fTMD0 (α-FLAG) followed by α-tubulin as a loading control. (B) Densitometry analysis was performed on the blots in (A) to quantify R74X (top) or E128X (bottom) fTMD0 protein levels relative to WT fTMD0. n = 3. (C) Cells co-transfected with WT, R74W, R74K or E128K fTMD0 and Kir6.2ΔC36 were fixed and probed with α-FLAG antibody 48 h post-transfection to detect surface expression of K_{ATP} mini-channels. A rim of surface staining was detected in WT- and E128K-transfected cells (green, inset images), but not in either R74W- or R74K-transfected cells. Cell nuclei were DAPI-stained (blue). Scale bar: 50 mm, and 10 mm for insets.

Figure 4. E128K mini-K_{ATP} channels have decreased intrinsic open probability. (A) Representative traces from inside-out, voltage-clamp recordings made from COSm6 cells transfected with Kir6.2ΔC36 with and without WT, E128K or F132L fTMD0 to form mini-K_{ATP} channels. Each trace is 10 sec long (upper) with 1 sec expanded (dashed box, lower) to illustrate bursting properties. The scale bar near the WT trace is 5 pA and applies to all traces. (B) Average intrinsic P_o of each channel type is given ± SEM. Distribution of individual data

points and number of patches analyzed are also shown. The average P_o of E128K mini-K_{ATP} channels is significantly different from WT mini-K_{ATP} channels and Kir6.2ΔC36 channels (*p < 0.05, student's t-test). (C) Average current of mini-K_{ATP} and Kir6.2ΔC36 channels in 1mM ATP relative to maximal current in nucleotide-free Kint/EDTA solution. Number of inside-out patches tested is given; error bars represent SEM.

Figure 5. E128K full-length K_{ATP} channels have decreased PIP_2 responsiveness. (A) Traces from inside-out, voltage-clamp recordings from COSm6 cells transfected with Kir6.2 and WT (upper) or E128K (lower) SUR1. Patches were exposed to 1 mM (black line) or 3 mM (white bar) ATP or 5 μM PIP_2 (striped bar). Scale bars: WT—1 min, 1000 pA; E128K—1 min, 100 pA. Zero current is indicated by the dotted lines. (B) Average fold change of currents in ATP-free Kint/EDTA solution following one or two sequential 30 sec exposures to 5 μM PIP_2. (C) Average fold change of ATP-inhibited current (relative to Kint/EDTA before any treatment) in three different ATP concentrations following one or two sequential 30 sec exposures to 5 μM PIP_2. Error bars represent SEM; n=8 (WT) and 12 (E128K) patches (*p < 0.05, student's t-test).

Figure 6. Traces from E128W SUR1 K_{ATP} channels—an inactivation mutant. (A) Representative trace of inside-out, voltage-clamp experiment showing inactivation and the ability of ATP to 'reset' the current upon reentry into ATP-free Kint/EDTA solution. For this and (C), the time of patch excision is denoted by the arrow, 3 mM ATP exposure by the black lines and the zero current level by the dotted lines. The max current for this record is indicated by the star. Scale bars: vertical—200 pA; horizontal—1 min. Note the break in trace during which ATP was applied. (B) The ability of high concentrations (1-5 mM) of ATP to reset the E128W K_{ATP} channel is illustrated by this scatter plot. Each symbol represents a different trace with several exchanges between ATP-containing and ATP-free Kint/EDTA solutions (the values for the trace in (A) are black squares). A total of 12 traces are represented. The amount of current upon

reexposure to Kint/EDTA (y-axis) is dependent on the length of time the patch is exposed to ATP (x-axis). The collective data set is well represented by an exponential fit. (C) Representative trace showing that exposure of the E128W K_{ATP} channels to 5 μM PIP_2 (striped bars) can decrease/reverse inactivation as well as increase the efficacy of ATP (black lines, 5 mM) to reset the channel. PIP_2 also decreases the ability of ATP to inhibit channel activity as seen following the second PIP_2 exposure. Scale bars: vertical—200 pA; horizontal—1 min.

Figure 7. Proposed model for the role of E128 in SUR1-Kir6.2 coupling. (A) Cartoon illustrating proposed physical relationships between SUR1, Kir6.2 and PIP_2 in the WT, E128K mutant and the Kir6.2ΔC36 channels. (B) The E128W mutation destabilizes the channel in the SUR1-Kir6.2 coupled, PIP_2-bound open state, leading to channel inactivation. These structural changes can be overcome by increasing membrane PIP_2, or by ATP binding to the channel which recovers coupling between SUR1 and Kir6.2 allowing channels to enter PIP_2-bound open state briefly before inactivation occurs again. Note that the four states presented should not be taken as detailed kinetic gating states of the channel, and that the transitions between the states are indicated only to illustrate the recovery effects of PIP_2 and ATP on inactivated channels.

Supplemental Figure 1. Quantification of SU rescue effect. COSm6 cells co-transfected with WT Kir6.2 and WT, R74X (top) or E128X (bottom) SUR1 were treated overnight with 300mM tolbutamide prior to chemiluminescence assays. Basal surface expression (from Figure 1)—black bars; tolbutamide rescue—white bars. Error bars represent SEM; n ≥ 3 for each condition.

Supplemental Figure 2. (A) TMD0 is highly conserved between human SUR1 and SUR2, and among species. The alignment was performed using PRALINE, residues 44 through 150 of TMD0 are shown. R74 and E128 and A116P (black boxes) and predicted TM segments (grey boxes, predictions by TOPCONS) are shown. Species include: human (hu), hamster (h), danio

rerio/zebra fish (dr) and canine (c). The degree of conservation between sequences is calculated on a scale of 1-9 below the sequences. Cytoplasmic (in) or extracellular (out) loops are also indicated. (B) TOPCONS prediction software was used to determine possible effects of R74X mutations on transmembrane segment topology of TMD0. Deviations from hypothetical WT TM-segment spans are indicated in the table. (C) A schematic of the membrane topology of WT SUR1 TMD0 (amino acids 1-198, end noted by break) is shown highlighting R74 and E128 (stars), FLAG-epitope (flag) and glycosylation site (branch).

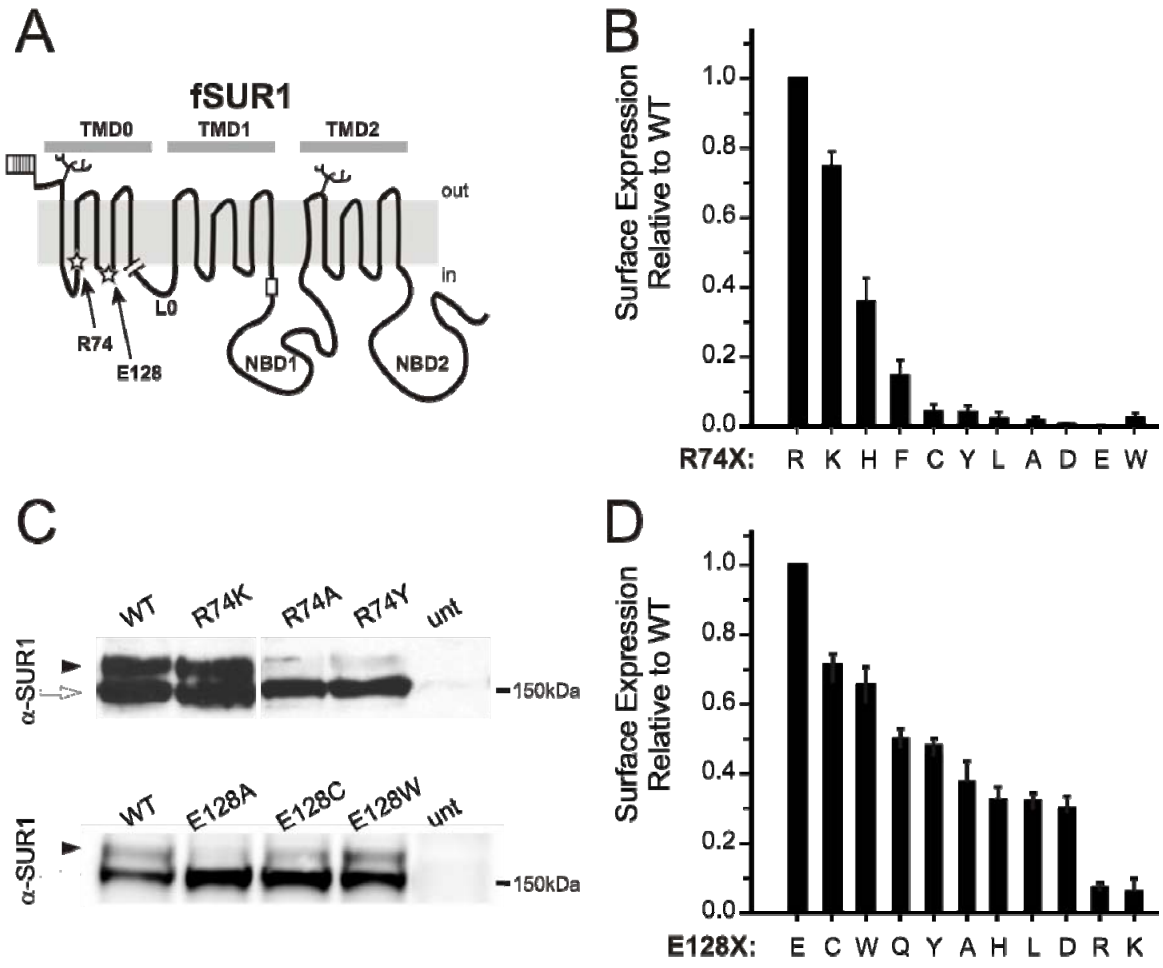

EBP Chapter 3
Figure 1

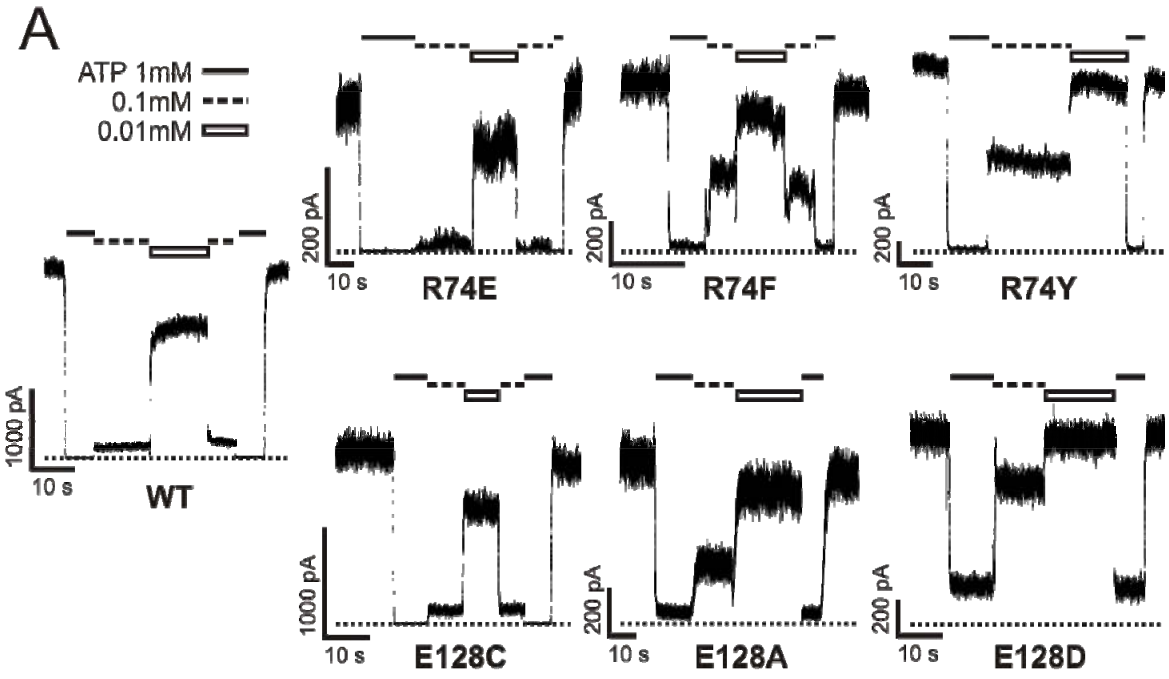

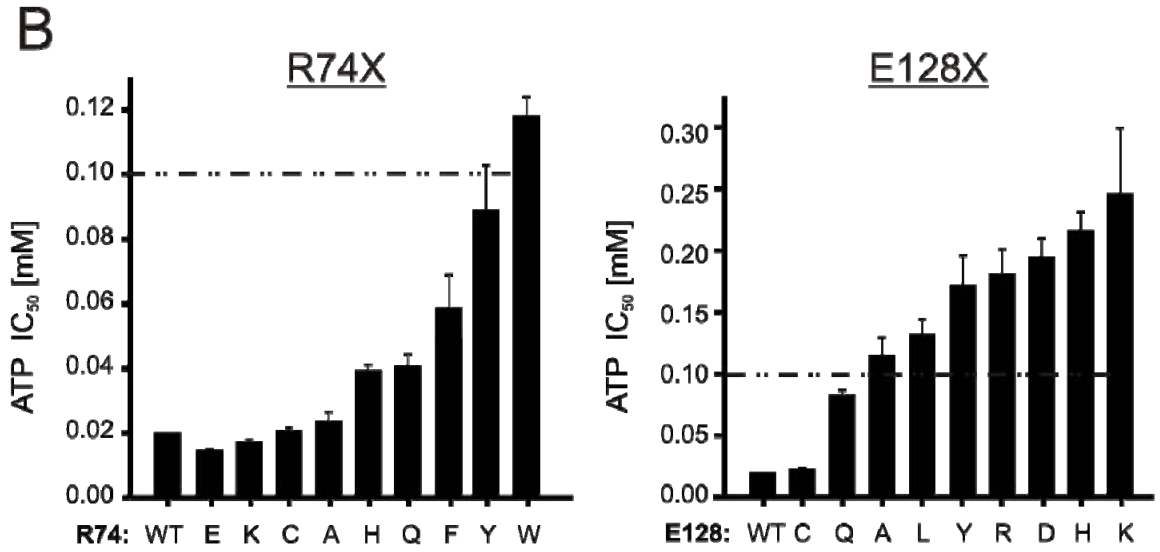

EBP Chapter 3
Figure 2

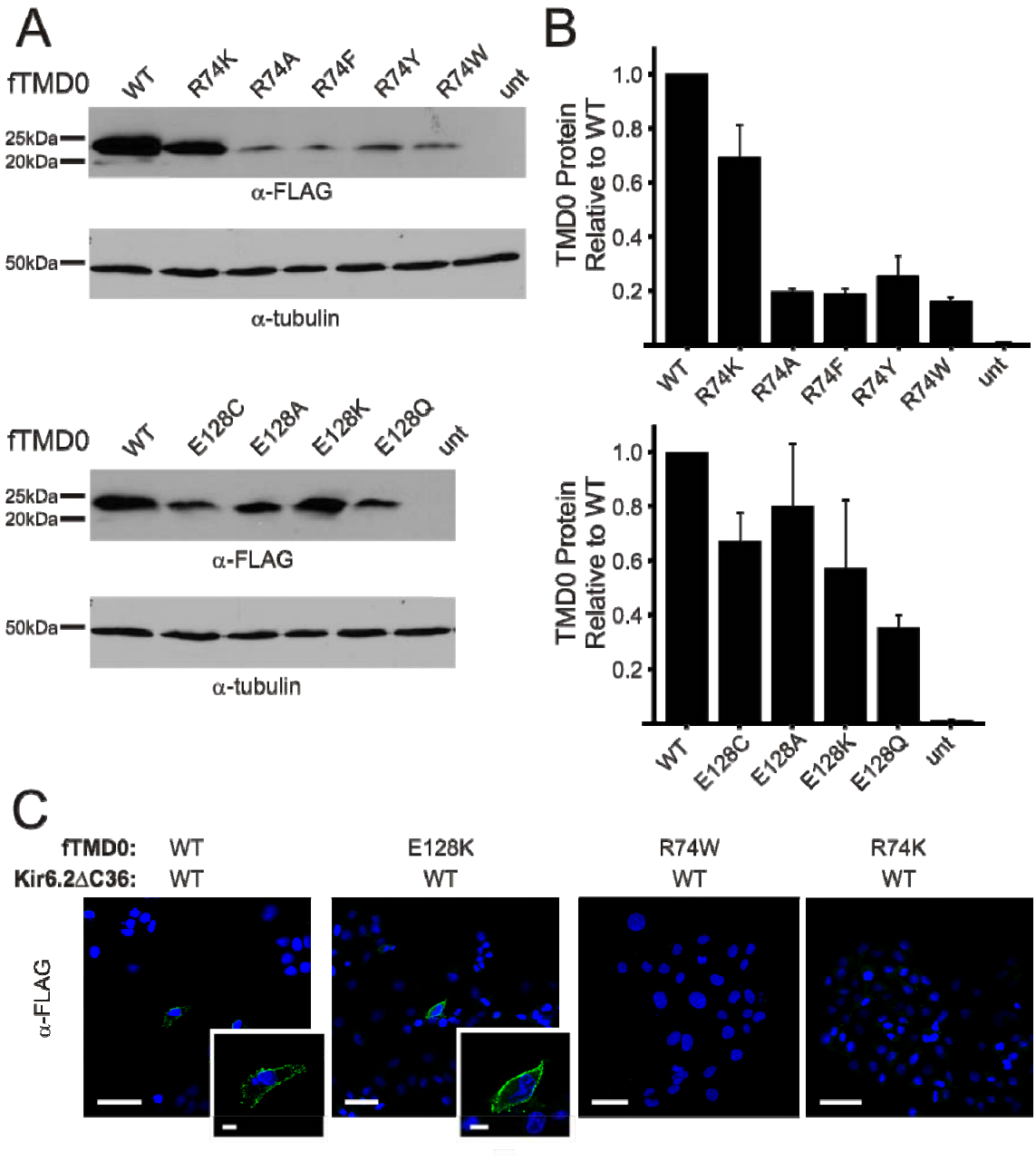

EBP Chapter 3
Figure 3

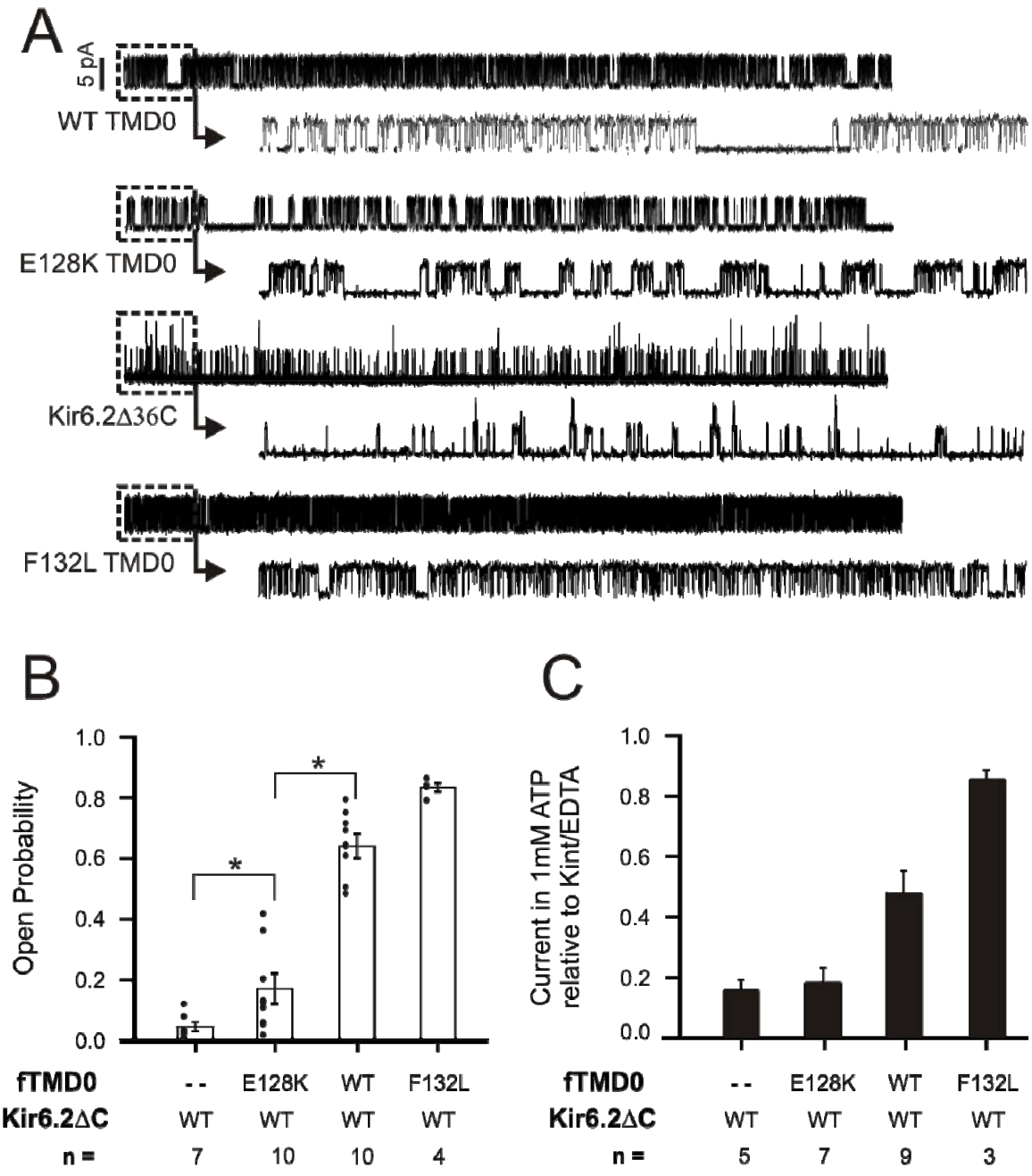

EBP Chapter 3
Figure 4

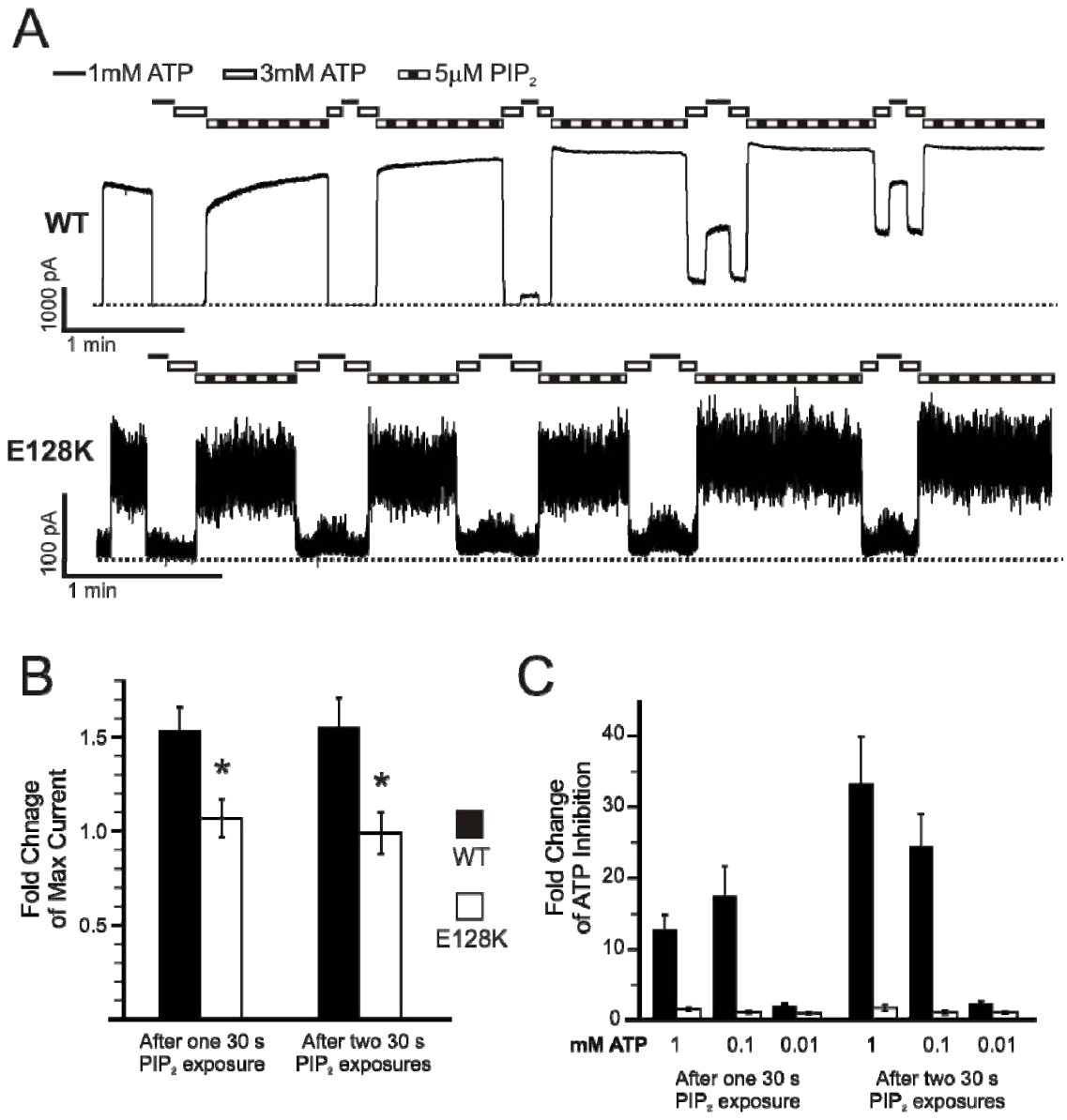

EBP Chapter 3
Figure 5

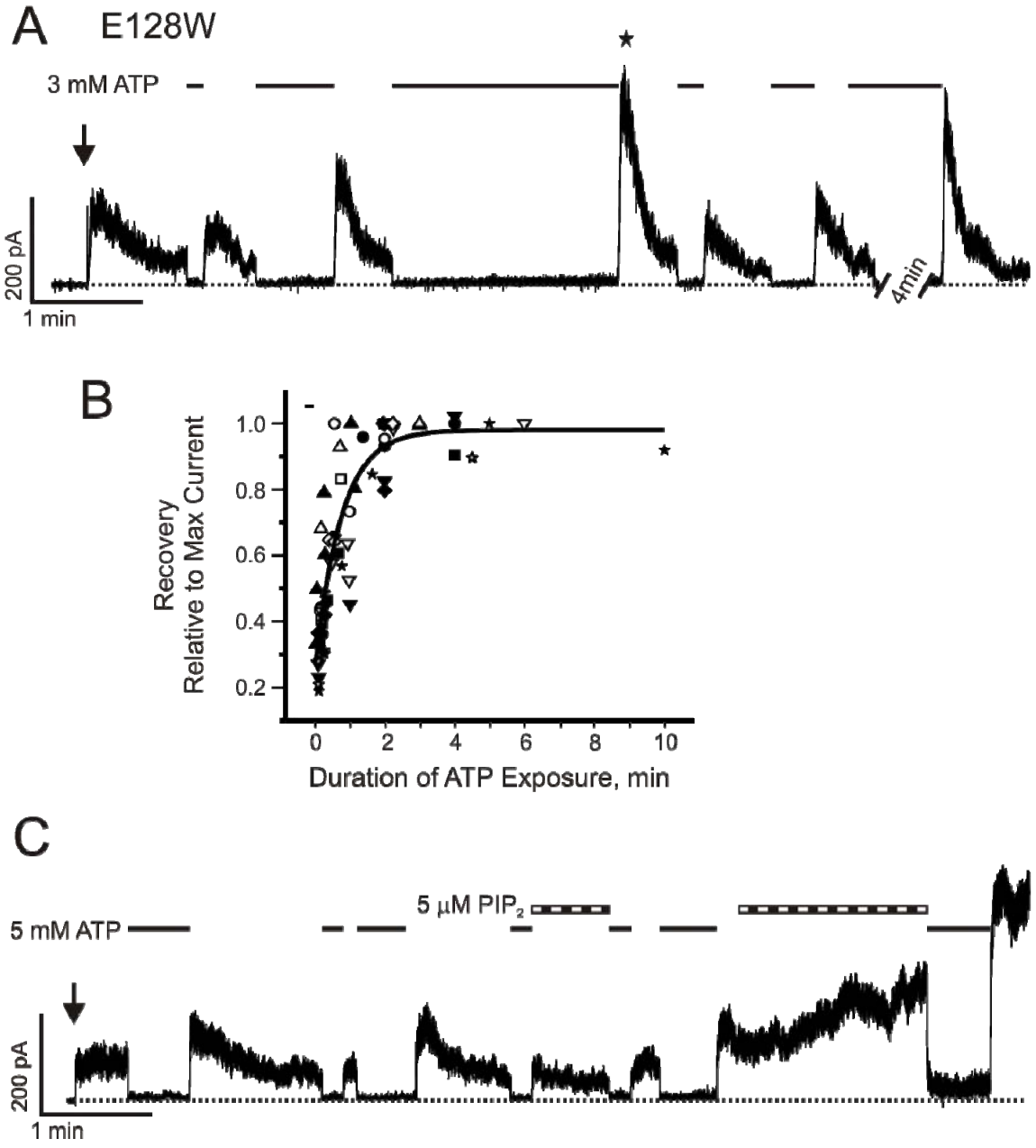

EBP Chapter 3
Figure 6

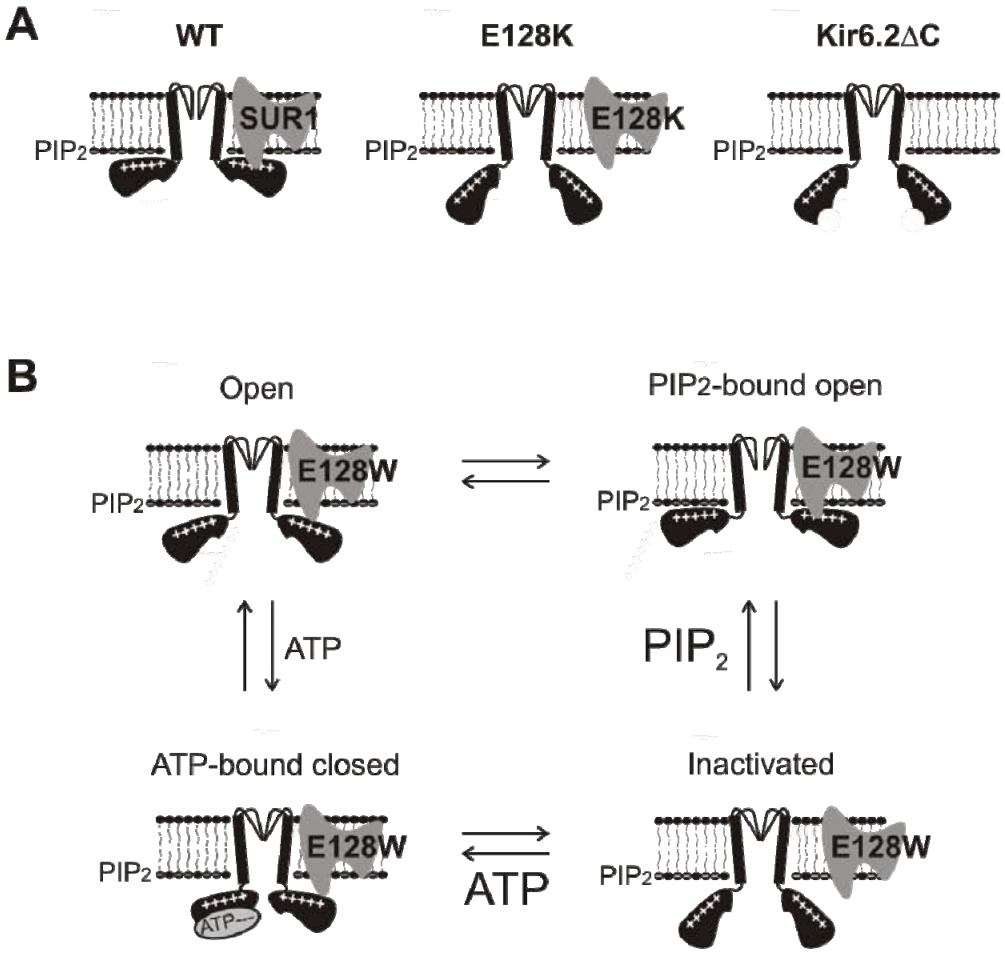

EBP Chapter 3
Figure 7

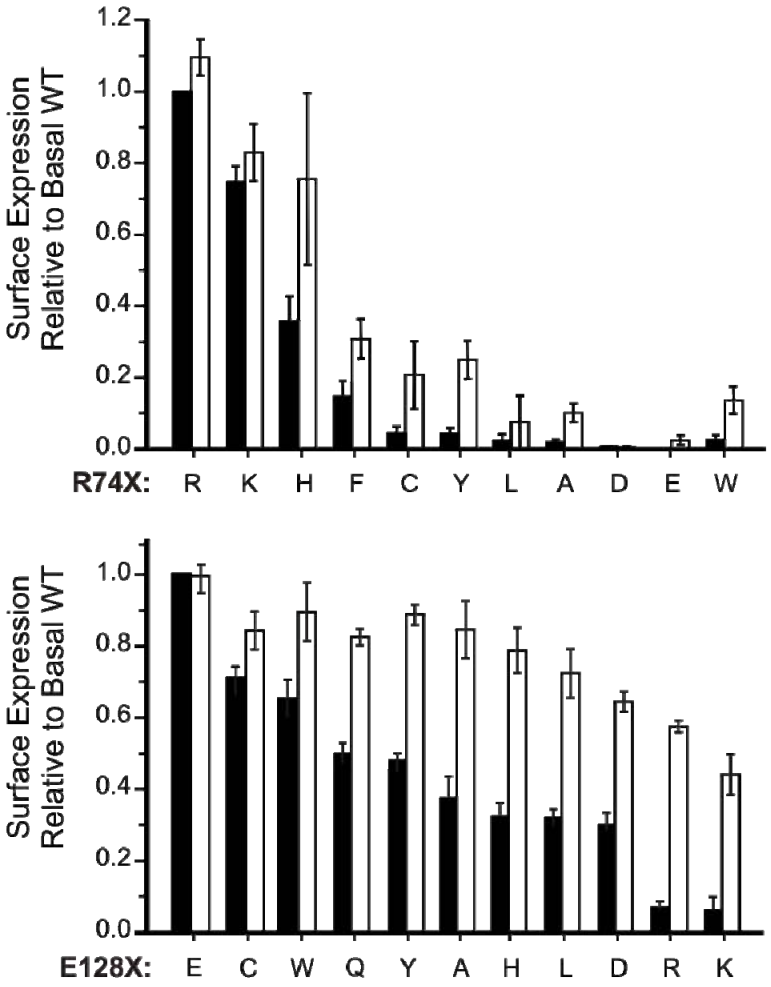

EBP Chapter 3
Supplemental Figure 1

A

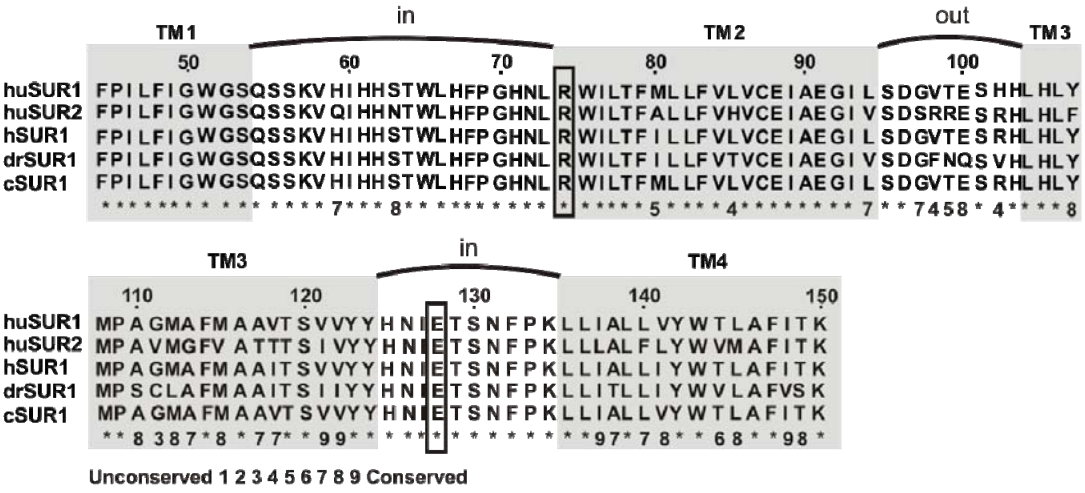

B

TOPCONS Transmembrane Segment Predictions

	TM1	TM2	TM3	TM4	TM5
WT	33-53	74-94	104-124	135-155	167-187
E128X	--	--	--	--	--
R74K	--	--	--	--	--
R74H	31-51	72-92	--	--	--
R74F	31-51	72-92	--	--	--
R74C	31-51	72-92	--	--	--
R74Y	31-51	72-92	--	--	--
R74L	31-51	72-92	--	--	--
R74A	31-51	72-92	--	--	--
R74W	31-51	72-92	--	--	--
R74D	31-51	73-93	103-123	--	--
R74E	31-51	73-93	103-123	--	--

C

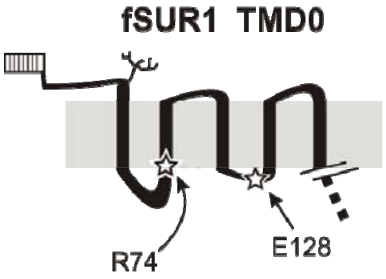

EBP Chapter 3
Supplemental Figure 2

CHAPTER 4

TOWARD UNDERSTANDING KIR6.2-SUR1 INTERACTIONS

Experiments shown and discussed in this chapter have not been published. I performed all of the experiments in Chapter 4 unless otherwise noted.

Abstract

The overarching theme of this thesis is to understand which and how SUR1-Kir6.2 interactions influence K_{ATP} function. An essential role of SUR1 E128K for TMD0-Kir6.2 coupling has been shown in Chapters 2 and 3; the obvious question is "does E128 participate in a direct physical interaction with Kir6.2?" This question was addressed by performing a screen of select positively charged residues in Kir6.2 looking for a site that could normalize E128K's decreased ATP-inhibition by re-establishing a proposed salt-bridge. An obvious interaction-partner for E128 was not found; however, interesting results flourished as a consequence of this screen. For instance, rather than ATP acting as an inhibitory factor, K_{ATP} channels doubly mutant for E128K and Kir6.2 residues known to disrupt PIP_2-mediated effects were seemingly stimulated by ATP. I propose this is due to profound channel instability in which ligand binding (ATP or PIP_2) can re-establish a semi-normal conformation in which spontaneous activity briefly occurs following ligand unbinding. Also, Q52, a residue in Kir6.2 near the slide helix, has proved to be essential for regulating K_{ATP} ATP-sensitivity and may be involved in SUR1 hypersensitization. Quite satisfyingly, while investigating the importance of Q52 an actual SUR1-Kir6.2 inter-subunit interaction was identified with E203, a residue near the L0 sliding helix. Their physical association is proposed to be maintained via electrostatic interactions and their proximity is supported by cysteine crosslinking data. In addition to the search for specific sites of interaction between SUR1 and Kir6.2, I embarked on another screen of all charged residues in SUR1's TMD0 and L0 domains to better appreciate the influence SUR1 has on K_{ATP} activity. The sliding helix of SUR1 has proven to be a zone of consequence; mutations of residues throughout it cause defects in ATP-inhibition, ADP-stimulation, PIP_2-stimulation and surface expression. Data described in this chapter will serve as springboards for more in-depth structure-function analysis relating SUR1 to Kir6.2.

Introduction

The presence of sulfonylurea receptor 1 (SUR1) has dramatic effects on the pore-forming inward rectifier potassium channel 6.2 (Kir6.2) subunit of K_{ATP}. In addition to providing requisite interactions that permit trafficking of K_{ATP} to the cell surface (Inagaki et al., 1995a), SUR1 dramatically hypersensitizes Kir6.2's intrinsic ATP inhibition (referred to as SUR1 hypersensitization hereinafter) (Shyng et al., 1997b; Tucker et al., 1997) and instills the channel with Mg·nucleotide-based stimulation and pharmacological sensitivities (Inagaki et al., 1995a; Gribble et al., 1997b; Shyng et al., 1997b; Schwanstecher et al., 1998). Also, patterns of single channel bursting properties vary with the presence and absence of SUR1 (Tucker et al., 1997). TMD0 is sufficient to bring about WT-like single-channel bursting properties of Kir6.2ΔC (Babenko and Bryan, 2003; Chan et al., 2003); however, regions beyond TMD0 control SUR1 hypersensitization, Mg·nucleotide stimulation and drug responsiveness.

In previous chapters, I and others have used two disease causing mutations in TMD0 to investigate how SUR1 modulates Kir6.2. With regard to SUR1 hypersensitization, Babenko has proposed that L0 of SUR1 is involved in this property based on experiments using mini-K_{ATP} channels with successively longer extensions into L0 (Babenko and Bryan, 2003; Babenko, 2005) (Chapter 1, section "SUR1 TMD0-L0" and Figure 7). I contend that the unusual phenotype of the SUR1 E128K mutation lends support to the hypothesis that SUR1's hypersensitizing region lies outside of TMD0. To be precise, in full-length K_{ATP} E128K results in decreased ATP inhibition, but in mini-K_{ATP} E128K has increased ATP inhibition versus WT mini-K_{ATP} (Chapter 3, Figure 4), therefore the basis for E128K's disruption of ATP inhibition in full-length K_{ATP} must lie outside TMD0. I propose that E128K dislocates SUR1's hypersensitization region via an allosteric mechanism. To verify this proposition, we need to identify the specific portion(s) of SUR1 responsible for SUR1 hypersensitization.

The extensive examination of SUR1 E128 has been especially fruitful. In addition to explaining how the mutation causes CHI (trafficking defect (Pratt et al., 2009)), work presented in Chapter 3 suggests a broader mechanism for how SUR1 modifies Kir6.2 activity through PIP_2 interactions. More remains to be understood about what the functional consequences of E128K are and how the E128K phenotype arises. For example, what is the sulfonylurea sensitivity of E128K? More pressing, what is the exact molecular mechanism by which E128K defects arise? I hypothesized an electrostatic interaction with Kir6.2 was involved and tested several residues in Kir6.2 based on rationale detailed in the Results section. Although such an interaction has yet to be found, I present data of a most astonishing phenotype: when certain mutations in Kir6.2 are expressed with SUR1 E128K, the presence of typically inhibitory ATP causes increased current.

To fully comprehend how K_{ATP} operates, the regions and residues of Kir6.2 that are acted upon by SUR1 are just as important to elucidate. In terms of preserving global interactions with SUR1 such that hetero-octameric channels can form and function at the plasma membrane, the first 44 amino acids can be truncated from Kir6.2 before completely preventing K_{ATP} trafficking (Babenko et al., 1999b). The same is true for deletion of Kir6.2's last 35 amino acids to make Kir6.2ΔC, which can still interact with SUR1 to form octameric channels (Tucker et al., 1997). Numerous disease-causing mutations arising in Kir6.2 have illuminated structural elements within and between Kir6.2 subunits that are important for proper channel activity. For example, Q52R was first identified in a patient with DEND and has since been shown to cause decreased apparent ATP-affinity by augmenting the channels' intrinsic P_o (Proks et al., 2004). Interestingly, when this mutation was introduced into the Kir6.2ΔC channel, it did not affect P_o (Tammaro et al., 2006). This SUR1-dependence begs the question: what part of SUR1 contributes to the Kir6.2 Q52R phenotype and does it do so by directly engaging Q52?

Mutagenesis and electrophysiological studies are the primary means by which to examine structural and functional associations between SUR1 and Kir6.2. Homology models are of limited value when it comes to SUR1 because no high-resolution structure exists for the portions of SUR1 (TMD0 and L0) that are thought to most closely associate with Kir6.2. Accordingly, I used a reverse genetics approach to actively search for sites of interaction between Kir6.2 and E128 of SUR1 through electrophysiological and biochemical techniques. Additionally, I embarked upon a second screen of charged residues throughout TMD0-L0 to gain insight into how these residues affect SUR1's influence on K_{ATP} function. Results from these two initially independent approaches united in the identification of what may be the first defined structural SUR1-Kir6.2 inter-subunit interaction. Charge reversal mutations and cysteine crosslinking studies of SUR1 E203 and Kir6.2 Q52 provide strong evidence that these two residues intermingle in a meaningful way. Further, I have found that the sliding helix of L0 is a stretch of amino acids highly sensitive to genetic disruption by all measures employed.

Results

E128K diminishes SU-sensitive inhibition. Because E128K causes decreased ATP inhibition and PIP_2 stimulation, I wanted to test whether this mutation disrupts other ligand-mediated responses. In chapter 2 I tested whether E128K affected Mg·ADP-sensitive stimulation of K_{ATP} and found it was not lost; however it is difficult to fully assess Mg·ADP responsiveness because ATP sensitivity is so low compared to WT (Chapter 2, Figure 3A). In Chapter 2 I also performed current-clamp experiments in mutant-infected INS-1 cells to confirm the E128K channels were hyperactive following glucose pretreatment (Chapter 2, Figure 7). Not discussed in that chapter was the attenuated tolbutamide response observed in these records. That is, after establishing the whole-cell configuration in current-clamp mode, I exposed the cells to 300μM tolbutamide and assessed K_{ATP} channel inhibition, as revealed by depolarization. Reliably, E128K-infected

cells were less responsive to tolbutamide treatment than WT-infected cells (Figure 1A). To more directly determine SU-sensitive inhibition of the E128K channels I performed inside-out patch voltage-clamp experiments using transfected COSm6 cells. Mutant and WT channels were exposed to different concentrations of tolbutamide. Tolbutamide inhibition was attenuated at all concentrations tested, significantly so at the highest concentrations (for 100 and 1000μM, 43±3 and 84±3 reduction of current for E128K versus 51±2 and 99±1 for WT) (Figure 1B). This result is consistent with the finding that E128K causes functional uncoupling between K_{ATP} subunits.

Kir6.2 screen for SUR1 E128-interacting residues. E128K causes functional uncoupling between SUR1-TMD0 and Kir6.2. This conclusion is based on properties of full-length K_{ATP} channels [decreased P_o and ATP, PIP_2 and tolbutamide sensitivity relative to WT (Chapters 2, 3 and 4)] and mini-K_{ATP} channels [P_o and ATP inhibition approaching Kir6.2ΔC-values versus WT mini-K_{ATP} (Chapter 3)]. A very appealing hypothesis to explain this finding is that E128 is involved in a direct structural interaction with Kir6.2; the simplest type of interaction to imagine is an electrostatic one in which the negatively charged glutamic acid is involved in a salt-bridge with a positively charged residue in Kir6.2.

To test this hypothesis, I performed a screen of positively charged residues in regions of Kir6.2 that I deemed to have the highest probability of participating in this hypothetical interaction. Figure 2 includes a sequence alignment of rat Kir6.2 (the construct I used for my experiments) versus human Kir6.2 and illustrates which residues were included in this screen. Each site was mutated and then expressed with either WT or E128K SUR1. ATP sensitivity was assessed for the single and double mutants.

I determined regions of Kir6.2 that had “the highest probability of participating” in an E128-Kir6.2 interaction using the following logic. The N-terminus of Kir6.2 is a provocative region to consider

because it has been shown to be necessary for association with SUR1 (Schwappach et al., 2000) and inhibition by SU (Reimann et al., 1999). However, the most proximal section of the Kir6.2 N-terminus was not included because as many as 44 amino acids can be truncated from the N-terminus of Kir6.2 in the presence of SUR1 without eliminating trafficking of the channels, suggesting the most important points of contact between Kir6.2 and SUR1 lie downstream of residue 44 (Babenko et al., 1999b). Likewise, the last 35 amino acids of Kir6.2 were not included because they, too, can be deleted (to make Kir6.2ΔC35) and functional TMD0-Kir6.2 interactions remain, as seen by mini-K_{ATP} channels. Residues that lie within and between M1 and M2 would be inaccessible to E128 [which is predicted to lie within a cytosolic loop (see Chapter 3, Supplemental Figure 2)] and so were not screened. Additionally, I used previous studies performed in Colin Nichols lab looking at what happened when positive residues in both the N- and C-terminal regions of Kir6.2 were mutated to alanine to further eliminate unlikely targets (Shyng et al., 2000; Cukras et al., 2002a). That is, I predicted any Kir6.2 residue involved in an electrostatic interaction with E128 would have a phenotype similar to E128A [deceased ATP-sensitive inhibition (Chapter 3, Figure 2)] when mutated to alanine. Therefore, positive-to-neutral (alanine) substitutions that resulted in normal ATP inhibition (noted by ☒ in Figure 2) as reported by the Nichols group were also excluded from the screen. Finally, most residues that constitute the predicted ATP-binding pocket in Kir6.2 (noted by ● in Figure 2, R201 and R50 were included in the screen) or are known to be involved in a different salt-bridge interaction [i.e., the Kir6.2 R314:E229 salt-bridge (Lin et al., 2003), noted by orange bars] were also left out of my screen. These restrictions left 11/41 lysines and arginines to screen in the rat Kir6.2 (K47, R50, R54, K67, R176, R177, R192, R201, R206, K222 and R301). Two of these residues (K222 and R301) have yet to be tested. K222 is predicted to lie well away from the plasma membrane using a homology model developed by fellow graduate student Jeremy Bushman. R301, however, could be informative to test because it is proposed to be important for Kir6.2 inter-subunit stability (Lin et al., 2008) and it is located near the top (i.e., close to the

plasma membrane) of the C-terminus (Haider et al., 2007) in the vicinity of where short inter-TM segment loops (and thus E128) probably lies.[1]

In addition to the 9 positive residues described above, several other residues were included in this screen for various reasons. Glutamines (polar) and histidines (polar, capable of becoming protonated under certain conditions) near-by and within the slide helix (H46, Q52, Q57, H70) were included because the prevailing hypothesis in the field is that the N-terminal domain of Kir6.2 is intimately situated near TMD0 and the slide helix, in particular, contributes to regulation of K_{ATP} channel activity. V59 (within the slide helix), P69 and T71 (predicted to lie near the cytoplasmic end of M1) substitutions were also tested with E128K, bringing the total number of residues screened to 16.

Direct E128K-Kir6.2 interaction not found. Each of the 13 Kir6.2 residues described above were mutated to negatively charged glutamic acid (and some also to aspartic acid), with two exceptions. V59 was mutated to two previously described disease-causing residues [V59M and V59G (Proks et al., 2004; Sagen et al., 2004)], and P69 was mutated to arginine. Next, COSm6 cells were co-transfected with mutant Kir6.2 and either WT or E128K SUR1 plasmids. Inside-out patch, voltage-clamp recordings were performed to determine the ATP-sensitive inhibition of single and double mutants (1, 0.1 and 0.01 mM ATP were tested in most cases). The prediction is that a residue responsible for electrostatic interaction with E128 of SUR would cause significant shift toward ATP-insensitivity when mutated to a negatively charged amino acid and expressed with WT SUR1, but would behave like WT (normal ATP inhibition) when co-expressed with E128K SUR1 because the ionic interaction would be re-established. Cells expressing the E128K mutation were pre-treated with 300μM tolbutamide overnight to facilitate expression at the plasma membrane. Figure 3 shows results for ATP inhibition studies. No

[1] R16, within the excluded N-terminus, might also be interesting to test because it has a decreased ATP-sensitivity when mutated to alanine, and lies in an un-resolved region of the homology model.

residue tested in this screen demonstrated this predicted pattern of activity. However, several interesting observations were made.

The majority of mutations did, indeed, have decreased ATP inhibition when expressed with WT SUR1; but usually the difference between WT and double-mutant was toward even greater insensitivity when co-expressed with E128K, indicating the two residues possibly cause ATP-insensitivity through different, additive mechanisms and are not partners in an inter-subunit salt-bridge. Kir6.2 mutations in which co-expression of E128K caused more severe ATP insensitivity relative to the single mutant are indicated by the downward arrows in Figure 3 (K47E, R50E, Q52E, K67E/D, P69R, T71E, R201E). Two mutants did not have detectable currents either on their own or when co-expressed with E128K despite pre-treatment with 300μM tolbutamide (R177E, R206D). Another mutant, R54E, had WT-like ATP-sensitivity as a single mutant and when it was co-expressed with E128K was still inhibited by ATP although the currents were very small (smaller than E128K alone even with 300μM tolbutamide pre-treatment) making it difficult to properly assess ATP inhibition. Preliminary results show the R54E//E128K channel surface expression was like WT upon pretreated with 5μM glibenclamide when tested by chemiluminescence (data not shown, n=1, basal expression was not tested). The small current amplitude in the face of presumably near-normal surface expression indicates this residue pair does not re-establish any hypothetical E128-salt bridge.

ATP activates select E128K//Kir6.2 double mutants. Strikingly, several double mutants displayed *increased* activity with the application of ATP (H46E, Q57E, R176E, R192E and R206E, indicated by stars in Figures 2 and 3). Traces of H46E, Q57E, R176 and R192 are shown in Figure 4 and traces of R206E are shown in Figure 5; the placement of each residue on a Kir6.2 homology model developed by Jeremy Bushman is shown in Figure 6. All of these 'ATP-activation' mutations showed small currents (usually distinguishable single channel

openings) in nucleotide-free Kint/EDTA except the H46E//E128K and R206E//E128K pairs which usually had current on isolation of the membrane patch but rapidly inactivated in nucleotide-free Kint/EDTA and only became active again in high concentrations of ATP (1mM). Also, longer ATP exposure times brought about current that enhances over time for some of the ATP-activation pairs (see H46E//E128K and R192E//E128K traces).

PIP_2 (or the lack of PIP_2) may be involved in this shocking activation phenotype because 3 of 5 ATP-activation mutations identified have previously been implicated in PIP_2 efficacy (R176, R192 and R206). R176 and R206 lie near the plasma membrane on the cytoplasmic surface of Kir6.2's C-terminus, however, R192 lies further within the cell at a Kir6.2-Kir6.2 subunit interface (Figure 6B) and has an inactivation phenotype on its own (Shyng et al., 2000; Lin et al., 2003). Given my finding that E128K also disrupts PIP_2 stimulation (Chapter 3, Figure 5), I wanted to look at the effect PIP_2 would have on these ATP-activation pairs. Preliminary experiments were carried out using the R206E//E128K double mutant; 5μM PIP_2 was found to stimulate channel activity but not to the same degree as ATP (Figure 5B). PIP_2 application did not appear to enhance the ATP-activation observed (however longer or more concentrated applications need to be tested).

One possible explanation for the ATP-activation is that it is a result of an imbalance between ATP inhibition (via Kir6.2) and Mg·ATP stimulation (via SUR1). To test this possibility I performed a preliminary experiment in which one of the Kir6.2 ATP-activation mutants, R176E, was co-expressed with SUR1 E128K and a third mutation (G1479R) located in the second NBD to abolish Mg-ATP stimulation (Shyng et al., 1997b). The R176//E128K/G1479R triple mutant channel was still more active in the presence of 1 mM ATP than in Kint/EDTA (data not shown, n=2).

Another PIP_2-affecting residue included in this screen (K67) had a possibly related phenotype. K67X significantly decreases intrinsic P_o of K_{ATP} presumably because of lost PIP2 interactions. Although it is unlikely E128K interacts with this residue as ATP-sensitive inhibition for K67E [and several other mutations at this site tested (R, C, A and D)] was increased relative to WT and not decreased as predicted for an E128-interacting residue (Figure 7A and B), doubly mutant K67E//E128K and K67D//E128K showed some stimulation of current in the presence of 100μM ATP (indicated by the spiral in Figures 2 and 3). Both double mutants tested were inhibited by 1mM ATP, but currents were greater-than-control in the presence of 100 μM ATP (Figure 7C). Double mutants harboring E128K and K67C or A or R were not tested. A similar phenotype was noted in several recordings made from H70E//E128K, but the currents were very small and this mutant should be further studied before any conclusions are stated (data not shown).

Kir6.2 Q52 may be a critical residue in the establishment of SUR1 hypersensitization. The effect of E128K on the Q52E mutant does not fit with a model in which the two residues interact since Q52E//E128K has an ATP-sensitivity similar to E128K alone and not WT-like as my hypothesis predicted, but this turned out to be a very interesting residue to investigate, nonetheless. There is suggestion in the literature that Q52 might interact with or be affected by SUR1. Q52R is a very strongly activating mutation that was first identified in a patient with DEND syndrome (Proks et al., 2004). It has significantly increased intrinsic P_o (~0.8 versus 0.6 for WT) that is SUR1-dependent. That is, in Kir6.2ΔC channels, the Q52R mutation did not change the P_o (Tammaro et al., 2006). Predictably, the very high P_o of Q52R results in a right-shift of the ATP-inhibition dose-response curve, i.e., decreased apparent affinity and ATP inhibition. When I mutated this residue to the opposite charge (Q52E), the resultant channel had significantly increased ATP-sensitive inhibition (IC_{50} predicted to be ~2μM based on an incomplete dose-response curve including only 1, 0.1 and 0.01mM ATP, versus the WT IC_{50} of ~20μM) (Figure 7A). I have not collected single channel records of Q52E full-length channels,

but I predict it to have significantly deceased P_o. Q52E was made in the Kir6.2Δ35C background and single channel records were collected from transfected COSm6 cells; although the average P_o of the Q52E channel was less than WT Kir6.2Δ35C channels, it was not significantly so (0.02 ± 0.006, n=3 versus 0.05 ± 0.014, n=5, respectively; p=0.23, student's t-test) (data not shown).

Several independent yet intersecting pieces of data led me to hypothesize that Q52 is intimately related to SUR1 hypersensitization. First, I am not aware of any report of a K_{ATP} mutation that causes significant *increase* of ATP-sensitive inhibition, much less one in which the same residue can switch between hyper- and hypo-sensitivity phenotypes. Second, Q52R's phenotype is reportedly SUR1-dependant. Third, Q52 is not proposed to be part of the ATP-binding site, but it is very close to R50 which is believed to interact directly with the γ-phosphate portion of ATP (Trapp et al., 2003). Fourth, Q52 resides just proximal to the Kir6.2 slide helix (Chapter 1, Figure 7) and is, therefore, well positioned to modulate slide-helix functionality. Finally, this portion of the Kir6.2 N-terminal is hypothesized to participate in the SUR1-L0 stimulation of mini-K_{ATP} channel activity (Chapter 1, Figure 7). For these reasons I broadened my investigation of SUR1 for potential sites of interaction with Q52 in hopes of identifying SUR1's 'hypersensitizing' residues.

I used a similar paradigm to identify Q52-interacting residues as I did for the E128K screen (i.e., ATP-sensitivity was used as a proxy for predictions about interactions); however, given that glutamine has a polar side-chain I tested both positively- and negatively-charge SUR1 residues. Further distinguishing the Q52-screen from the E128-screen was how single mutations at each site affected channel activity. All substitutions at E128, less cysteine, cause deceased ATP-sensitivity presumably through TMD0-Kir6.2 uncoupling. However, Q52 phenotypes are more diverse: Q52R has minimal ATP inhibition and high P_o, Q52E has increased ATP inhibition and

low P_o indicating this site has an adaptive role in determining K_{ATP} P_o; I therefore tested SUR1 residues with both Q52E and Q52R (Figure 8B and 8C).

Somewhat surprisingly, the E128K mutation proved to be the only one that altered both Q52E and Q52R ATP inhibition and was, in fact, dominant in both Q52E//E128K and Q52R//E128K channels. As stated above, however, the Q52E//E128K phenotype does not endorse a possibility that these two residues engage physically. In support of this, cysteine-crosslinking studies using Q52C//E128C channels did not show evidence of crosslinking (Figure 9C, bottom). Electrostatic interactions between E128 and Q52 side chains are not supported by my data; further, they do not even appear close enough to do so. However, E128K does disrupt whichever residue(s) in SUR1 is necessary for the dramatic phenotypes of Q52E/R.

SUR1 E203 can interact with Kir6.2 Q52 and may also be a critical residue in the establishment of SUR1 hypersensitization. Which residues *are* necessary for the Q52E/R phenotype? To answer this question I utilized SUR1 mutants created for another functional screen being carried out in parallel to the Kir6.2 screen (TMD0-L0 screen described below). Several mutant SUR1 constructs were co-expressed with Kir6.2 Q52E or Q52R in COSm6 cells and ATP-sensitivities were tested (Figure 8B and 8C). One combination in particular stands out – SUR1 E203K : Kir6.2 Q52E. This double-mutant channel had extremely left-shifted ATP-sensitive inhibition, 100-fold higher than WT (IC_{50} 180 ± 5nM, n=2-5 per ATP concentration tested) (Figure 9A and 9B). On its own, the ATP sensitivity of E203K appears to be slightly higher than WT (predicted IC_{50} ~12 μM, based on only three ATP concentrations) (see Figure 11).

To test the hypothesis that SUR1 E203 and Kir6.2 Q52 might directly interact, I mutated each site to cysteine and performed cysteine-crosslinking studies. I co-transfected COSm6 cells with

WT or Q52C Kir6.2 plus WT or E203C SUR1 plasmids and performed inside-out patch voltage-clamp recordings. An oxidizing environment (needed to drive the reactive thiol groups of the cysteine side-chains into a disulfide linkage) was created by exposing membrane patches to 0.2% hydrogen peroxide (H_2O_2). A reducing environment (to break any potential disulfide bridges) was created by exposing membrane patches to 5 mM dithiothreitol (DTT). Figure 9C shows representative traces from Q52C//E203C, Q52C, E203C and WT patches[2]. Upon exposure of the Q52C//E203C double mutant to 0.2% H_2O_2 a rapid and robust inhibition of current was observed. This inhibition was not reversible with removal of H_2O_2 or, importantly, with application of either 1 mM ATP or 5 μM PIP_2. However, exposure of the patch to 5 mM DTT did result in increased current. Further, application of 5 μM PIP_2 could stimulate Q52C//E203C currents, but only *after* DTT treatment if the channel was first exposed to H_20_2. This result is consistent with the hypothesis Q52C and E203C side-chains are close enough to participate in inter-subunit interactions. Co-application of 0.2% H_2O_2 with 1 mM ATP (or application of 0.2% H_2O_2 to channels already inhibited by 1 mM ATP) did not attenuate this lasting inhibition (data not shown) suggesting the ability to establish a disulfide bridge between Q52C and E203C is not state-dependent. Control experiments performed on WT and E203C single mutants did not result in any inhibition by 0.2% H_2O_2, but 5 mM DTT did occasionally cause reversible current block (Figure 9C, Bottom). Singly mutant Q52C channels consistently showed inhibition with 0.2% H_2O_2 that was slower and not as complete as with Q52C//E203C channels (Figure 9C). As with the double mutant, it was not reversible by H_2O_2 removal or application of 1 mM ATP; in contrast, however, 5 mM DTT did not increase channel activity and, importantly, 5 μM PIP_2 could strongly increase Q52C currents after 0.2% H_2O_2 inhibition and before subsequent 5 mM DTT exposure. These findings suggest H_2O_2 is causing Q52C channel inhibition by a mechanism other than disulfide-bridge formation seen in Q52C//E203C.

[2] The ATP-sensitivity of the mutants was also determined (predicted IC_{50}'s based on three ATP concentrations for WT, Q52C, E203C, Q52C//E203, Q52C//E128C are 15±1, 13±1, 5±1, 10±1, 57±3 μM, respectively).

Notably, as stated above, I also tested Q52C//E128C channels for crosslinking capability and found that the presence of E128C completely blocked any H_2O_2-induced inhibition of Q52C; Q52C//E128C behaved like WT channels in terms of H_2O_2 (little to no effect) and DTT (reversible current block) responses (Figure 9C, bottom).

The SUR1 L0 'sliding helix' is a hot-spot for disruption of K_{ATP} activities and expression. I hypothesized that E128K in SUR1 TMD0 participates in inter-subunit interactions, but I did not believe E128K could possibly be the only residue in SUR1 united with Kir6.2. For reasons discussed in Chapter 1 (including mini-K_{ATP} channel properties and the low resolution crystal structure of full-length K_{ATP}) I wanted to take a closer look at residues throughout TMD0 and L0. I constructed a screen of all charged residues (positive: glutamic and aspartic acid, negative: lysine and arginine) in the predicted cytoplasmic regions of TMD0-L0, 33 residues in all (Figure 10). Each charged residue was neutralized (mutated to alanine) or made into an oppositely charged amino acid (D and E were mutated to K, K and R were mutated to E). Both functional (ATP-, ADP- and PIP_2-sensitivity) and expression (chemiluminescence) properties of mutant channels were tested. With the substantial help of Dr. Qing Zhou and Joel Gay, most of this data has now been collected.

Each of the tests performed were done using WT Kir6.2- plus mutant SUR1-transfected COSm6 cells. ATP inhibition was tested in two separate PCR-clones to confirm the observed phenotype was due to the experimental mutation and not an unintended nucleotide substitution introduced during the PCR reaction. When two clones were shown to have indistinguishable ATP inhibition, only one clone was used in all subsequent tests.

By all measures, the sliding helix (aa205-217) contains multiple important residues with the potential to significantly disrupt K_{ATP} activity and/or trafficking. The averaged data of ATP

inhibition from each of the channels I recorded from is shown in Figure 11. K205A/E, D209A/K, D212A/K and R216A/E all showed much reduced ATP inhibition.

Figure 12 shows the averaged data of ADP stimulation from each of the channels I recorded from. The concentration of free Mg^{2+} was kept at 1 mM for each nucleotide solution tested. E203K, K205A/E, D209A/K all appear to have increased sensitivity to stimulation by 0.5 mM ADP in the presence of 0.1 mM ATP. In contrast, R216A/E and D212A/K all seem to have reduced ADP stimulation; however, one should note that the inhibition by both 1 and 0.1 mM ATP is much greater for each of these mutants than by Mg·ATP (compare red and blue bars between Figures 11 and 12 for these residues). This discrepancy suggests R216A/E and D212A/K channels do retain the ability to be stimulated by Mg·nucleotide, substantially so.

PIP_2 sensitivity has also been tested for several of the mutants in this screen (Figure 13) and it appears that R193E's and K205E's current increases in the presence of 5μM PIP_2 more than WT. Generally, mutations that show more pronounced PIP_2 stimulation are thought to have decreased sensitivity to the endogenous levels of PIP_2 present in the membrane patch (which is accompanied by a parallel decease in intrinsic P_o); therefore, when they are exposed to exogenous PIP_2 they have more opportunity to grow current because the P_o has a greater range over which to increase.

The ability of the TMD0-L0 mutants to traffic to the plasma membrane was tested by chemiluminescence assay (Figure 14). Like the functional screening, residues in the sliding helix appear to be critical for WT-like expression. In addition to the mutations already discussed in Chapters 2 and 3 (R74A/E and E128A/K), K57E in TMD0 diminished basal expression to below 50% of control. In L0, D209K, D212A/K, D216A and D310K have basal expression below 50% of control. Overnight treatment with 5μM glibenclamide could substantially improve

expression of E128A/K, D212A/K and R216E. In the cases of R74A and R74E, glibenclamide was not tested, but the less effective SU chaperone rescue by 300 μM tolbutamide is shown (blue bars).

Discussion

A substantial body of work exists to support a fundamental role of the N-terminal domains of SUR1 (TMD0 and L0) in K_{ATP} regulation. Placement of TMD0-L0 near Kir6.2 implicates it in the formation of a transduction pathway through which conformational changes in SUR1 can be transmitted to Kir6.2 where they eventually translate into conduction properties of the pore. Uncoupling of SUR1 from Kir6.2 occurs when E128K is introduced. The finding that tolbutamide inhibition is reduced in the E128K channel is predicted if TMD0 is, in fact, required for the transduction of SUR1-based signals to Kir6.2. E128K is far away from the predicted tolbutamide binding site [which includes the “A”-site of bipartite SU binding pocket (Chapter 1, Figure 8)] and therefore it is unlikely tolbutamide binding is affected, although this idea has not been directly tested through SU-binding assays.

In addition to providing a conduit for SUR1-based signals to reach Kir6.2, it is clear that TMD0 changes the intrinsic properties of Kir6.2. Again, studies utilizing E128K to uncouple TMD0 from Kir6.2 have guided a new way of thinking about the mechanism by which SUR1 modulates K_{ATP} activity. Membrane PIP_2 is central to SUR1’s engagement with Kir6.2, yet there must be physical interactions between the two subunits that bring about changes in PIP_2 affinity or efficacy. As E128K is the only SUR1 mutation described to break the functional interactions between TMD0 and Kir6.2, it was used as a starting point to probe for certain subunit-subunit interfaces. A screen of positively charged residues throughout the N- and C-termini of Kir6.2 was performed using E128K as bait. Although none of the residues tested seem to be involved in a cross-subunit salt-bridge with E128K, several of them did invite further investigation.

Especially interesting was a phenotype common to 5 of the Kir6.2 residues screened termed ATP-activation. The currents stimulated by 1 mM ATP in each of these ATP-activation pairs was small, often small enough to differentiate single channel openings. Current (I) is dependent on three factors by the following relationship: $I=n*P_o*\gamma$, where n is the number of channels present, P_o is the fraction of time each channel is open and γ the single channel conductance of each channel opening. The very small currents seen in each of the ATP-activation pairs could be due to decreased expression or decreased channel openings but not an adjustment in γ because single channel openings can be observed and, thus, γ can be calculated, and was normal. I have not tested by western blot or chemiluminescence the possibility that expression (n) has been attenuated. Whether expression is effected or not, channel openings seem to be rare events as judged by the brief channel openings that can be distinguished within the activation events and the increase in current with longer ATP exposure.

How ATP can stimulate K_{ATP} to open when the channel has evolved to be inhibited by nucleotides is an intriguing question. Based on the preliminary results using the G1479R NBD mutant, it appears not be a matter of SUR1-mediated Mg·nucleotide stimulation. More evidence to negate NBD-based stimulation is the fact that these experiments are performed in Mg-free conditions and, therefore, minimal Mg-nucleotide stimulation can occur. To explain these ATP-activation pairs, I favor a hypothesis that involves open state instability and broad ATP-induced conformational changes. The combined E128K-induced disruption of PIP_2 interactions with its concomitant TMD0-Kir6.2 uncoupling in the face of additional Kir6.2-induced PIP_2-interruption leads to dramatic channel instability such that it cannot maintain spontaneously open conformations. The presence of ATP can temporarily reinstate a semi-normal channel configuration, analogous to its effect on inactivation mutations [like E128W (Chapter 4, Figure 6)]. **I hypothesize that the activity observed in these double mutants is not activation by ATP, per se, but rather brief/unstable openings of the normally spontaneously active**

channel following unbinding of ATP. Further, I propose that ATP affinity is greatly reduced (recall, the ATP-binding site is composed of both N- and C-termini of adjacent Kir6.2 subunits), therefore the presence of ATP and its stabilizing effect is short. In this scheme, upon unbinding of ATP the channel transitions from an ATP-bound closed state to a very briefly lived ATP-unbound open state before breaking down into an inactivated state.

One prediction that results from this hypothesis is that ATP binding is necessary to reestablish a channel capable of conduction. Preliminary experiments to test this have been carried out using two ATP-activation pairs (R206E//E128K and R176E//E128K) along with a third mutation in the ATP-binding site, R50E. ATP was not observed to change these triple-mutant channels, whether it be to stimulate or inhibit the spontaneous activity observed (data not shown). If this hypothetical mechanism is correct, one may be able to force an ATP-activation pair channel to remain closed by keeping ATP in its binding site as often as possible. For instance, if the time between transitions of ATP-unbound/closed to ATP-bound/closed can be sufficiently shortened (perhaps by application of very high concentrations of ATP (e.g., >10 mM)], the channel may not have time to open (and inactivate).

Another fascinating result that came out from the Kir6.2 screen was that residue Q52 can both reduce (Q52R) and increase (Q52E) ATP-sensitive inhibition. Q52 is proposed to be near but not part of the Kir6.2 ATP-binding site. It is unlikely Q52E/R effects are through direct modification of ATP binding because, surely, mutating it to the negatively charged glutamic acid would decrease interactions with the negatively charged ATP molecule, opposite from what is observed. That Q52R effects have been reported to be SUR1-dependent made it an inviting target to use in my search for SUR1-Kir6.2 interactions. Further, that it's phenotype is charge-dependent makes it, perhaps, more rational to use as electrostatic bait than E128K which has the same phenotype whether mutated to oppositely charged (K or R) or charge-conserving (D)

amino acids (Chapter 3, Figures 1 and 2). Indeed, a charged residue in SUR1 was identified that can not only significantly enhance the ATP-sensitive inhibition by Q52E, but can also be physically crosslinked to Q52 when both are mutated to cysteine. The Q52E//E203K double mutant increased ATP-sensitivity 100-fold. That two mutations were necessary to profoundly increase ATP inhibition of K_{ATP} may speak to the fact that, to date, no CHI-causing mutation has been described whose underlying mechanism of action is increased ATP-sensitive inhibition. CHI is caused, instead, by trafficking mutations and decreased Mg·ATP stimulation. After more thorough analysis of how this double mutant effects other K_{ATP} properties (P_o, Mg-nucleotide stimulation, drug sensitivities, expression), it would be interesting to test its effect on insulin secretion. The prediction, of course, is that insulin secretion would greatly increase under low-glucose conditions. This may be an especially difficult experiment to carry out in INS-1 cells (like was performed for E128K and R74W in Chapter 2, Figure 7C) because each singly-mutant subunit would have to compete with endogenous WT subunits for channel composition. Until a way to knock-out or knock down both endogenous subunits is developed (perhaps using siRNA technology paired with primary cultures of β-cells from knock-out lines), this proof-of-principle experiment will go untested.

Nonetheless, this interacting pair is very exciting because it suggests a particular site of interaction between SUR1 and Kir6.2 that may contribute to the SUR1 hypersensitization. E203K is located in the L0 domain of SUR1 just proximal to the proposed 'sliding helix' (see Introduction, Figure 7 and this chapter, Figure 9), which fits with previous reports that mini-K_{ATP} channels with an extended TMD0-L0 truncation (aa1-232) result in even higher P_o than shorter (aa1-198) or longer (aa1-256/288) TMD0 constructs (Babenko and Bryan, 2003; Babenko, 2005). It is interesting that residue 203 is not conserved between SUR1 (E203) and SUR2 (K203) and SUR2 does not hypersensitize Kir6.2 to ATP as strongly as SUR1 (IC_{50} = ~20μM versus ~100 μM for SUR1 and SUR2A, respectively) (Inagaki et al., 1996). If residue 203 in

SUR is important for SUR hypersensitization, mutation of SUR2 K203 to E should shift ATP-sensitivity toward that of SUR1.[3]

E203 is very near the SUR1-L0 sliding helix, a region found to be exquisitely sensitive to genetic disruption by my TMD0-L0 charged residues screen (Figures 10, 11, 12 and 13). The Babenko model of SUR1-Kir6.2 interaction states the sliding helix is intimately involved in signal transduction and there could be flexibility in the relationship it has with Kir6.2. That is, perhaps the sliding helix behaves in a manner similar to that suggested for Kir6.2's slide helix and can move parallel or rotate relative to the plane of the membrane (Clarke et al., 2010). If this is the case, it is tempting to speculate that more E203K:Q52E-like interactions exist for residues throughout the sliding helix and that they may be state-dependent. That is, if the sliding helix moves relative the Kir6.2 to effect channel conduction, maybe we can identify which amino-acids they mingle with using cysteine-crosslinking. Further, perhaps the identity of a sliding helix-Kir6.2 interaction will change depending on the conformational/gating state of the channel (e.g., does the ability to crosslink change in the presence of ATP?). This is all speculation at this point, of course, and the experiments to test these ideas are outside the scope of this dissertation.

One thing that can be stated, however, based on results from the TMD0-L0 screen is that the zone within SUR1 considered responsive to the SU chaperoning effect should be expanded to include L0. A previous screen of CHI-causing mutations (due to trafficking defects) distributed throughout SUR1 found only those located within TMD0 were sensitive to the SU chaperone effect; notably, the screen did not include any mutations within L0 (Yan et al., 2007). Understanding how SU exert their chaperoning effects is not well understood, but is presumed

[3] Note that I tested Kir6.2 Q52E//SUR2 channels and found the ATP sensitivity to be identical to Q52E//SUR1 channels (IC_{50}=2±1 μM based on 3 ATP concentrations); however WT SUR2's starting IC_{50} was 60 μM in my experiments and so the combined Kir6.2 Q52E//SUR2 K203 channel was 30-fold more sensitive to ATP than WT Kir6.2//SUR2 channels.

to facilitate tertiary and quaternary structure formation of SUR and K_{ATP}, respectively. One possibility is that SU act analogous to ATP in the inactivation mutations—it somehow acts to bring proper inter-subunit interfaces together. I have one very preliminary yet provocative piece of data to support this idea. I serendipitously noticed that the E128K channel was significantly stimulated by PIP_2 [recall, E128K causes loss of PIP_2 stimulation of current (Chapter 3, Figure 5)] if the channels were recorded from without first washing out the 300 μM tolbutamide (used to improve surface expression) (data not shown). Follow up experiments are needed, but this result suggests that SU, too, can act to re-couple SUR1 with Kir6.2. Recall, also, that SU is known to interact with Kir6.2 both physically [Kir6.2 is photo-labeled using radioactive SU compounds (Gros et al., 1999)] and functionally (low affinity SU inhibition is thought to occur directly through Kir6.2 (Gribble et al., 1997b). It is a stretch, perhaps to suggest properties of plasma membrane K_{ATP} channels are the same as channel subunits in the ER, but this is a provocative idea.

Clearly the TMD0 and L0 domains of SUR1 will be fertile grounds to study as we work toward the long-term goal of specifying inter-subunit interactions. Broad based screens including those presented here will (and have!) provide data on which hypothesis driven experiments can be designed.

Materials and Methods

All experimental methods used in this chapter were performed as previously described in Chapters 2 and 3.

Figure Legends

Figure 1. Tolbutamide sensitivity of E128K-expressing cells. (A) Representative traces of whole-cell current-clamp recordings from INS-1 cells infected with WT or E128K SUR1 and WT Kir6.2 adenovirus. After break-in (arrows) and establishing a stable baseline, the KCO 200 μM diazoxide was applied followed by 300 μM tolbutamide. Blunted responsiveness to channel inhibition by tolbutamide was noted in several E128K-infected cells. **(B)** Inside-out patch, voltage-clamp recordings were performed on COSm6 cells transfected with WT or E128K SUR1 and WT Kir6.2 to more directly test the ability of tolbutamide to inhibit E128K channel function. At every concentration tested, E128K had less average current than WT, with the differences reaching statistical significance at 100 μM and 1 mM. *$p<0.05$, student's t-tests. The number of patches tested is indicated by the key.

Figure 2. Rat versus human Kir6.2 sequence alignment and key to screen for E128-interacting residues. Structural elements and residues included or not in this screen are indicated. Sites of non-identity are designated by either "+" (conserved) or "-" (not conserved) between the sequences. Positively charged residues are bolded. Reasons for inclusion or exclusion of residues are depicted by symbols above the sequences, results from the screen are depicted by symbols below the sequences.

Figure 3. Results from E128-interacting screen. COSm6 cells transfected with WT or E128K SUR1 plus WT or mutant Kir6.2 were tested by inside-out voltage-clamp. Average response to three ATP concentrations (0.01, 0.1 and 1 mM) are shown in the bar graphs for each single Kir6.2 mutant and its corresponding E128K double mutant (indicated by +). Inhibition of current was calculated relative to maximum current in nucleotide-free Kint/EDTA solution. Mutations are separated according to their location on the N- (top) or C-terminus (bottom) of Kir6.2. The

relative change in ATP inhibition upon introduction of E128K is indicated by symbols below each data set (see key). “nc” means no current was detected.

Figure 4. ATP-activation phenotypes observed with co-expression of E128K. Representative inside-out patch voltage-clamp records from 4 of the 5 “ATP-activation” pairs identified in the E128-interacting screen. Recordings are all from COSm6 cells and control solution is Kint/EDTA. An expanded section of the H46E//E128K (top) trace is indicated by the dotted box.

Figure 5. R206E//E128K ATP-activation pair traces. Representative inside-out patch voltage-clamp records from COSm6 cells transfected with Kir6.2 R206E and SUR1 E128K showing activation in the presence of 1 or 5 mM ATP or 10 μM PIP_2. Unlike all other records shown in this chapter, the lower trace was transfected with double the amount of cDNA (with a concomitant increase in Fugene6© transfection reagent).

Figure 6. Placement of ATP-activation mutations in Kir6.2. (A) Each of the five identified ATP-activation mutants are shown in a different color on a homology model of Kir6.2 developed by Jeremy Bushman. **(B)** The interface between adjacent Kir6.2 subunits (one in grey, the other in magenta) is shown highlighting the placement of several residues at the interface between two subunits. Unless otherwise noted, each of the residues belongs to the magenta subunit.

Figure 7. K67X mutations cause increased ATP inhibition and an unusual activation phenotype when expressed with E128K. (A) Representative inside-out patch voltage-clamp records from COSm6 cells transfected with WT SUR1 and WT or K67X Kir6.2. **(B)** Average current inhibition in 0.01 mM ATP for each of the Kir6.2 K67X mutants tested. Inhibition is shown relative to maximum current in nucleotide-free Kint/EDTA solution. Error bars represent the SEM. **(C)** Representative traces from K67E//E128K (top) and K67D//E128K (bottom)

channels expressed in COSm6 cells. In both cases, an increase in current to greater-than-control levels is seen in 0.1 mM ATP, although the channels are clearly inhibited by 1 mM ATP. The portion of the K67E//E128K trace surrounded by the dotted box is expanded. Arrows represent the time of inside-out patch excision.

Figure 8. Kir6.2 Q52E and Q52R cause opposite ATP inhibition phenotypes. (A) Representative inside-out patch voltage-clamp records from COSm6 cells transfected with WT SUR1 and WT or Q52E or Q52R Kir6.2. **(B)** Q52E was expressed with several different SUR1 mutants and double-mutant channel ATP-sensitive inhibitions were tested using three ATP concentrations [0.01, 0.1 and 1 mM, indicated by the same colors used in (A)]. Average ATP inhibition relative to nucleotide-free Kint/EDTA solution is shown. ATP responses for Q52E, E128K and WT channels are shown for comparison. **(C)** Q52R was expressed with several SUR1 mutations just as in (B).

Figure 9. Kir6.2 Q52X and SUR1 E203X are capable of establishing ionic and covalent bonds. (A) Representative inside-out patch voltage-clamp record from COSm6 cells transfected with Kir6.2 Q52E and SUR1 E203K. **(B)** ATP-dose response of the Q52E//E203K channel versus WT. Six ATP concentrations (0.01, 0.1, 1, 10, 100 and 1000 μM) were tested. Best-fit (using the Hill equation) is shown, as are the IC_{50}s and the number of patches used to test each ATP concentration. Error bars represent SEM. **(C)** Representative traces from cysteine-crosslinking experiments using the subunit combinations indicated below each trace. The zero current base line is shown by the dotted lines. Note that each of the traces in (C) have the same time-axis scale.

Figure 10. Hamster versus human SUR1 sequence alignment and key to SUR1 TMD0-L0 screen. Structural elements and residues included in this screen are indicated. All charged

residues are bolded. Sites of non-identity are designated by either "+" (conserved) or "-" (not conserved) between the sequences. Residues included in the screen are shown by pink (experiments performed by EBP) or blue (experiments performed by Dr. Qing Zhou) bars.

Figure 11. ATP inhibition of mutants included in the SUR1 TMD0-L0 screen. Average current in three different concentrations of ATP (0.01, 0.1 and 1 mM) is shown relative to maximum current in nucleotide-free Kint/EDTA solution. Results from charge reversal (top) and neutralization (bottom) at the same residue are separated but lined up vertically. The number of patches testes is indicated beside each data set and error bars represent SEM. Note that only experiments carried out by EBP are included in these graphs.

Figure 12. Mg·ADP stimulation of mutants included in the SUR1 TMD0-L0 screen. Average current in three 1 mM ATP, 0.1 mM ATP or 0.1 mM ATP plus 0.5 mM ADP is shown relative to maximum current in nucleotide-free Kint solution. All solutions were supplemented with MgCl to keep the free Mg^{2+} concentration at 1 mM. Results from charge reversal (top) and neutralization (bottom) at the same residue are separated but lined up vertically. The number of patches tested is indicated beside each data set and error bars represent SEM. Note that only experiments carried out by EBP are included in these graphs.

Figure 13. PIP_2 stimulation of mutants included in the SUR1 TMD0-L0 screen. Average current following one (grey) or two (black) 30 second exposures to 5 μM PIP_2 is shown relative to maximum current in nucleotide-free Kint/EDTA solution. Results from charge reversal (top) and neutralization (bottom) at the same residue are separated but lined up vertically. The number of patches tested is indicated beside each data set and error bars represent SEM. Note that only experiments carried out by EBP are included in these graphs.

Figure 14. Surface expression of mutants included in the SUR1 TMD0-L0 screen. Chemiluminescence experiments were performed to quantify basal and SU-rescued surface expression of mutants. Results from charge reversal (top) and neutralization (bottom) at the same residue are separated but lined up vertically. The number of patches tested is indicated beside each data set and error bars represent SEM. Note that only experiments carried out by EBP are included in these graphs.

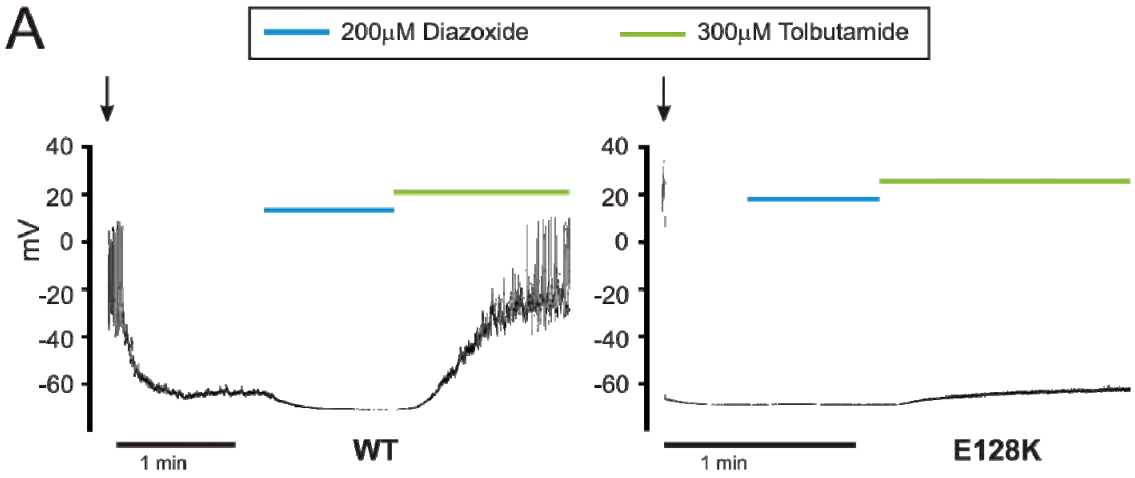

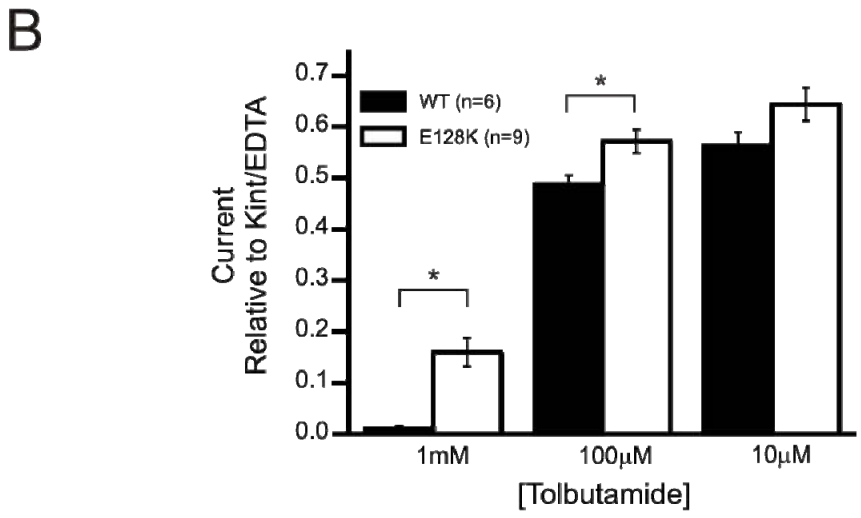

(File: EBP E128K R74K IO Tolb Sens.xls; Tab: 8-30-10)

EBP Chapter 4
Figure 1

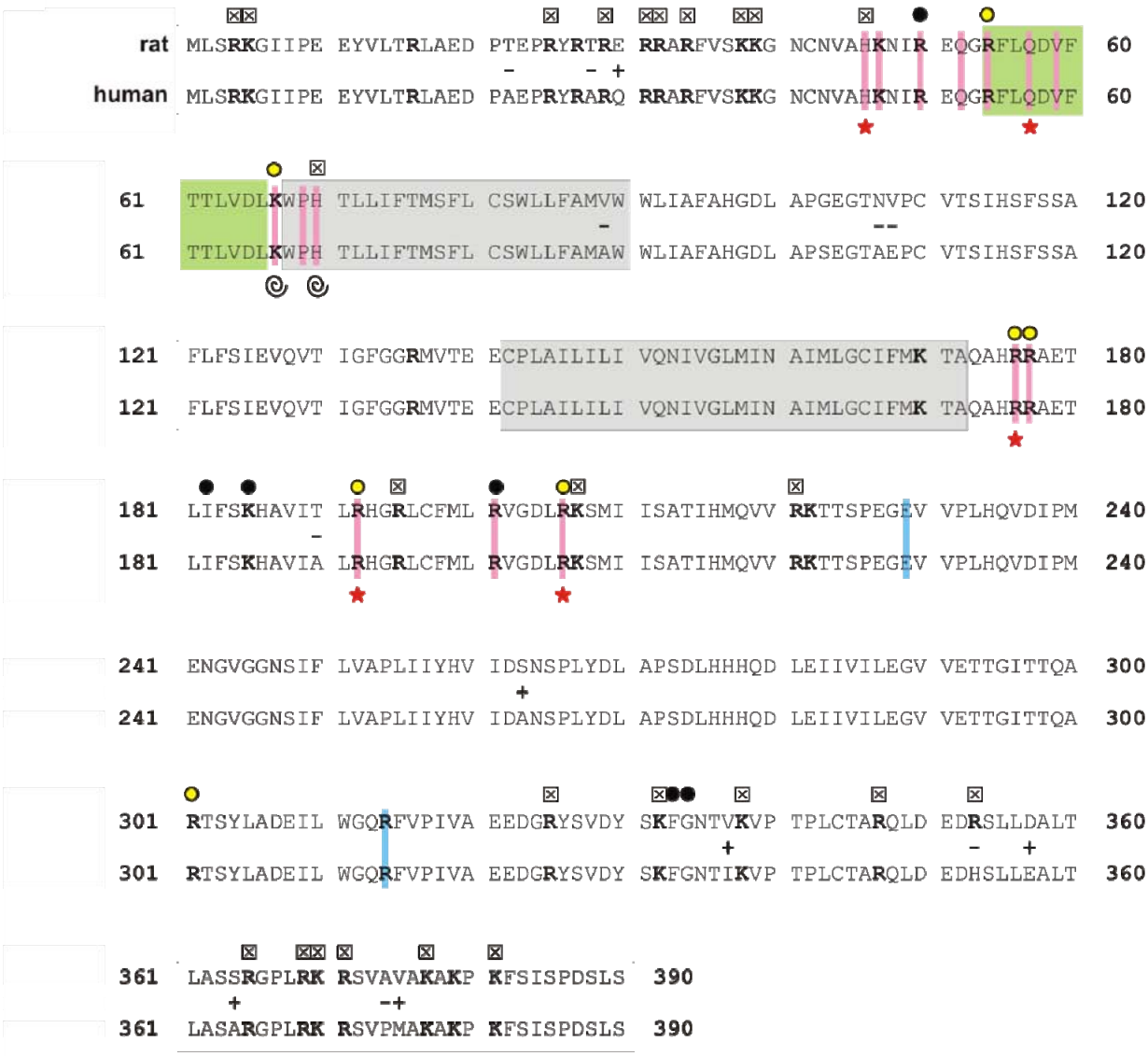

Slide Helix

M1 or M2 Helix

E229 : R314 ion pair

Not included in screen

Included in SUR1 E128K // Kir6.2 screen

Above Sequences

- PIP_2-residue
- ATP binding site residue
- Alanine substitution has normal ATP IC_{50} or Rb^+ efflux

Below Sequences (expressed w/ E128K)

- 100μM ATP > K_{int}/EDTA Current
- Activation of Current with ATP

Between Sequences

- \- Non-conserved residue
- \+ Conserved residue

EBP Chapter 4
Figure 2

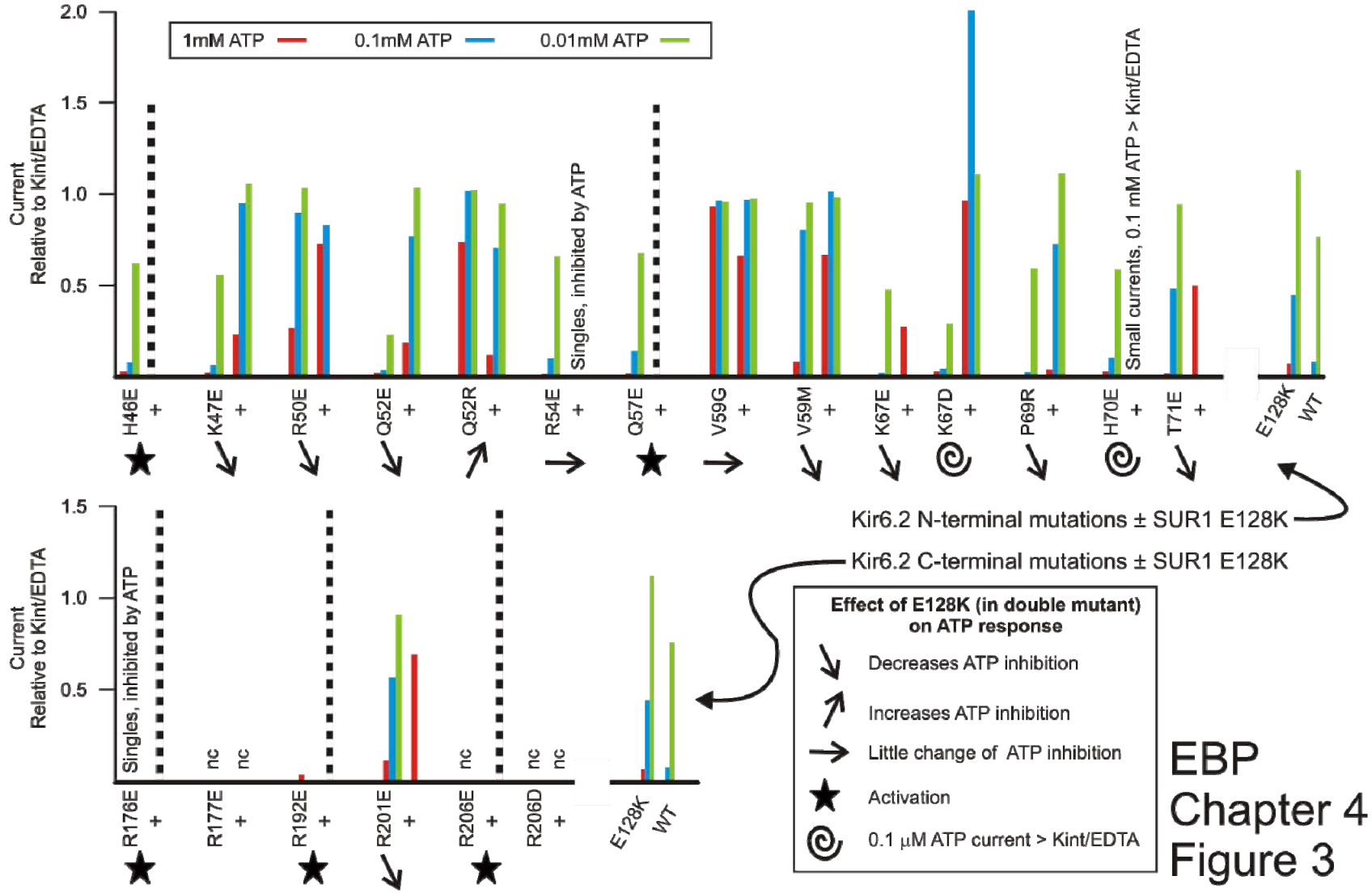

EBP
Chapter 4
Figure 3

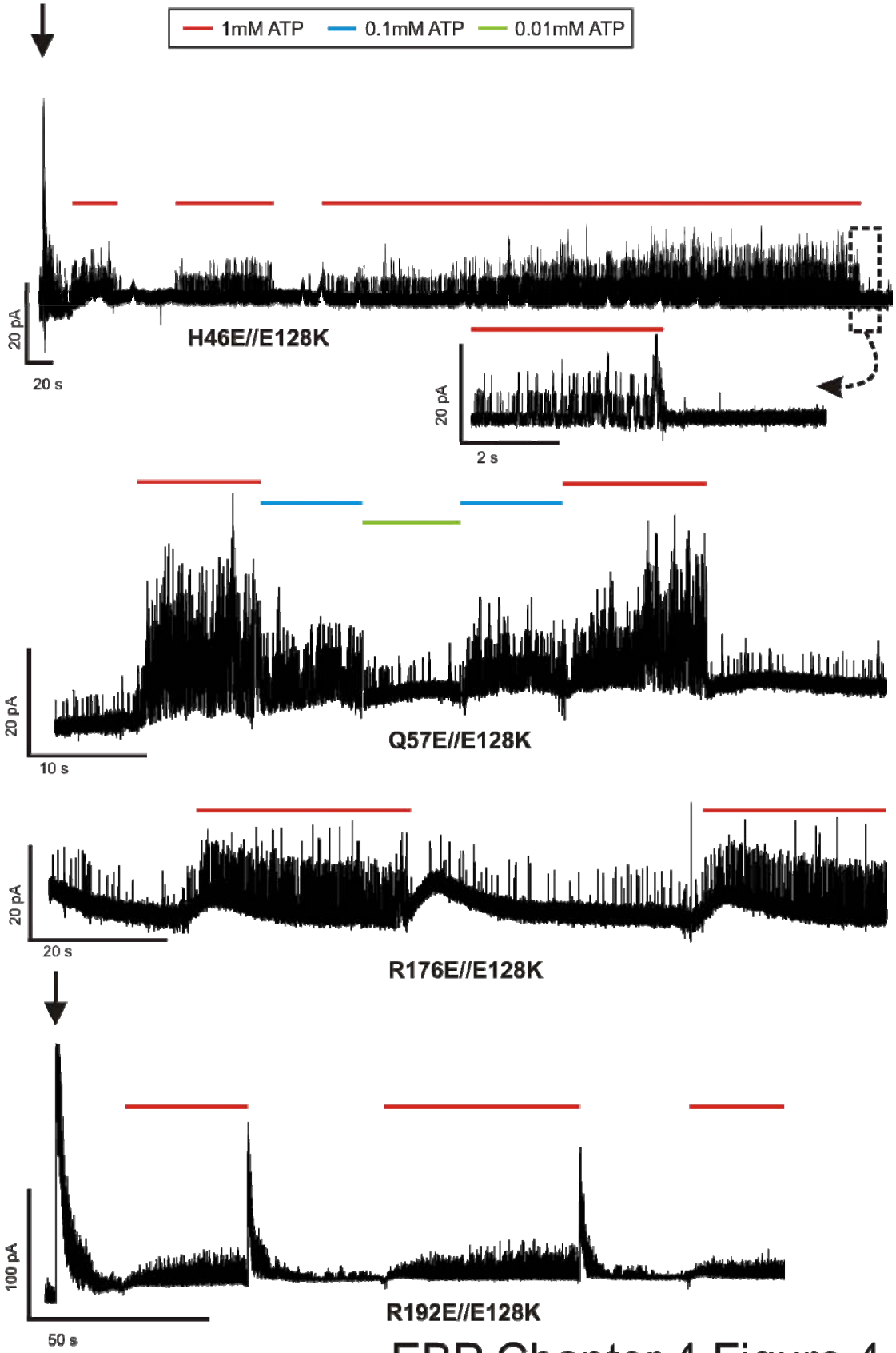

EBP Chapter 4 Figure 4

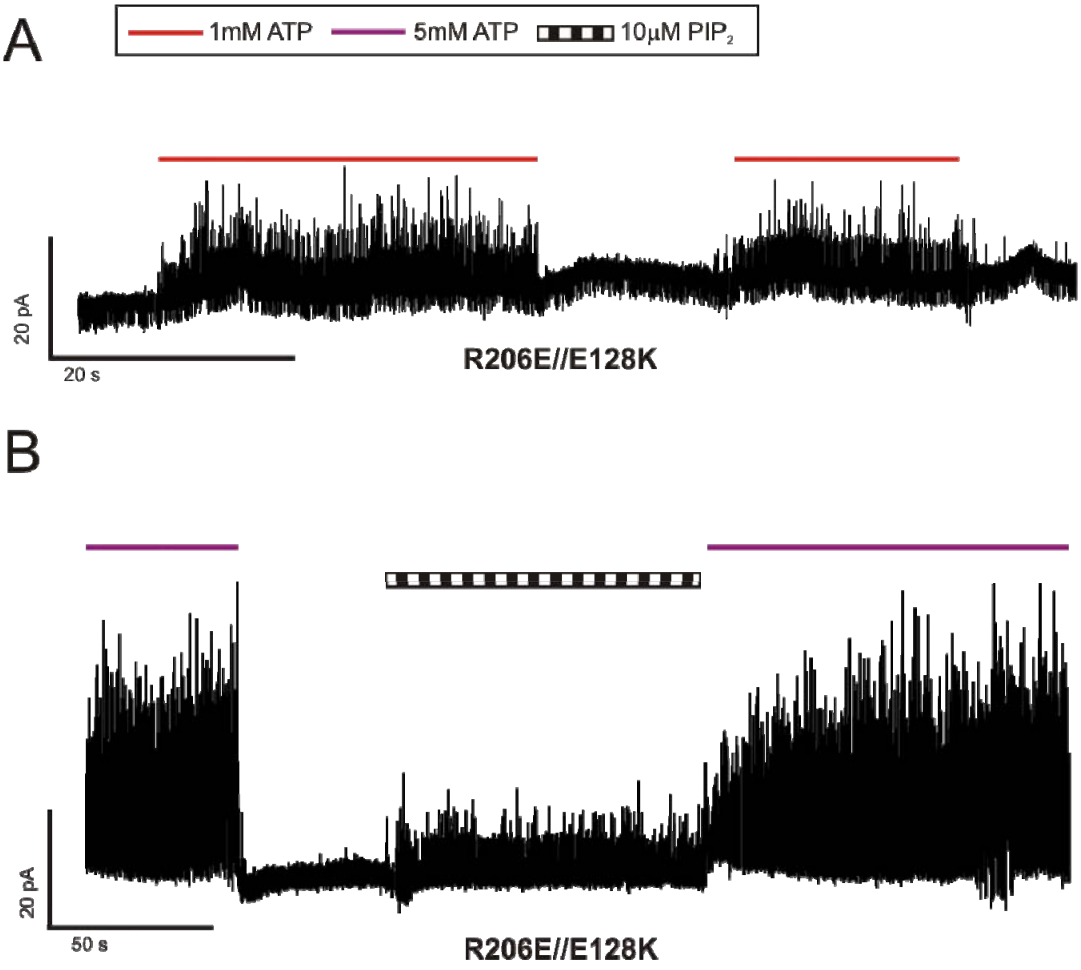

EBP Chapter 4
Figure 5

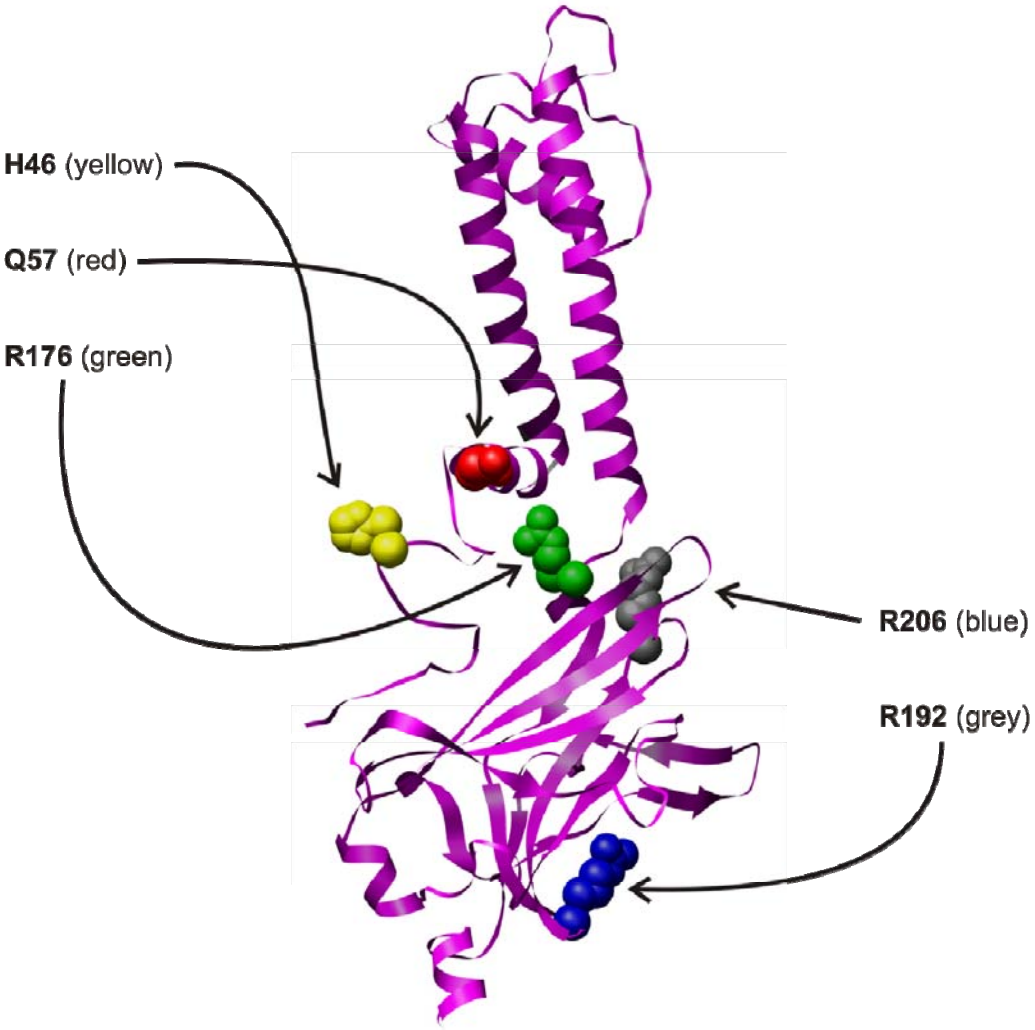

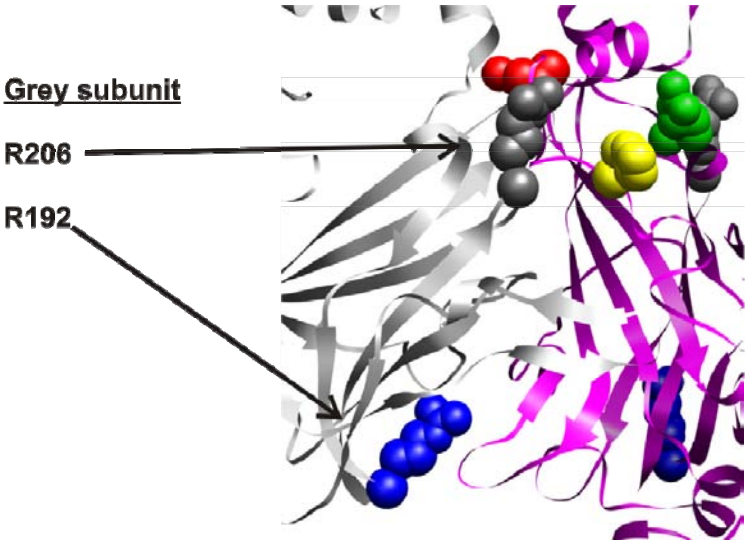

EBP Chatper 4 Figure 6

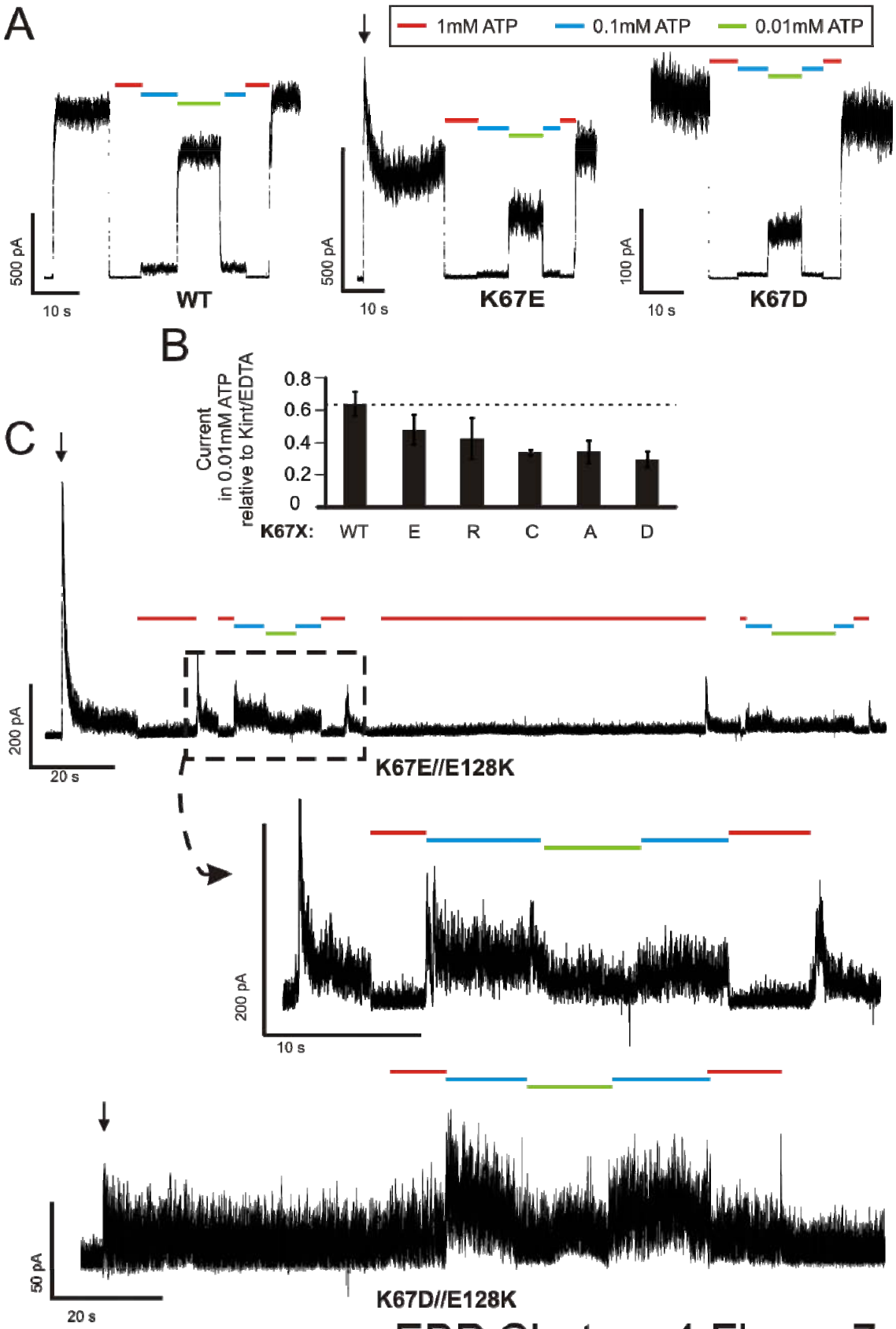

EBP Chatper 4 Figure 7

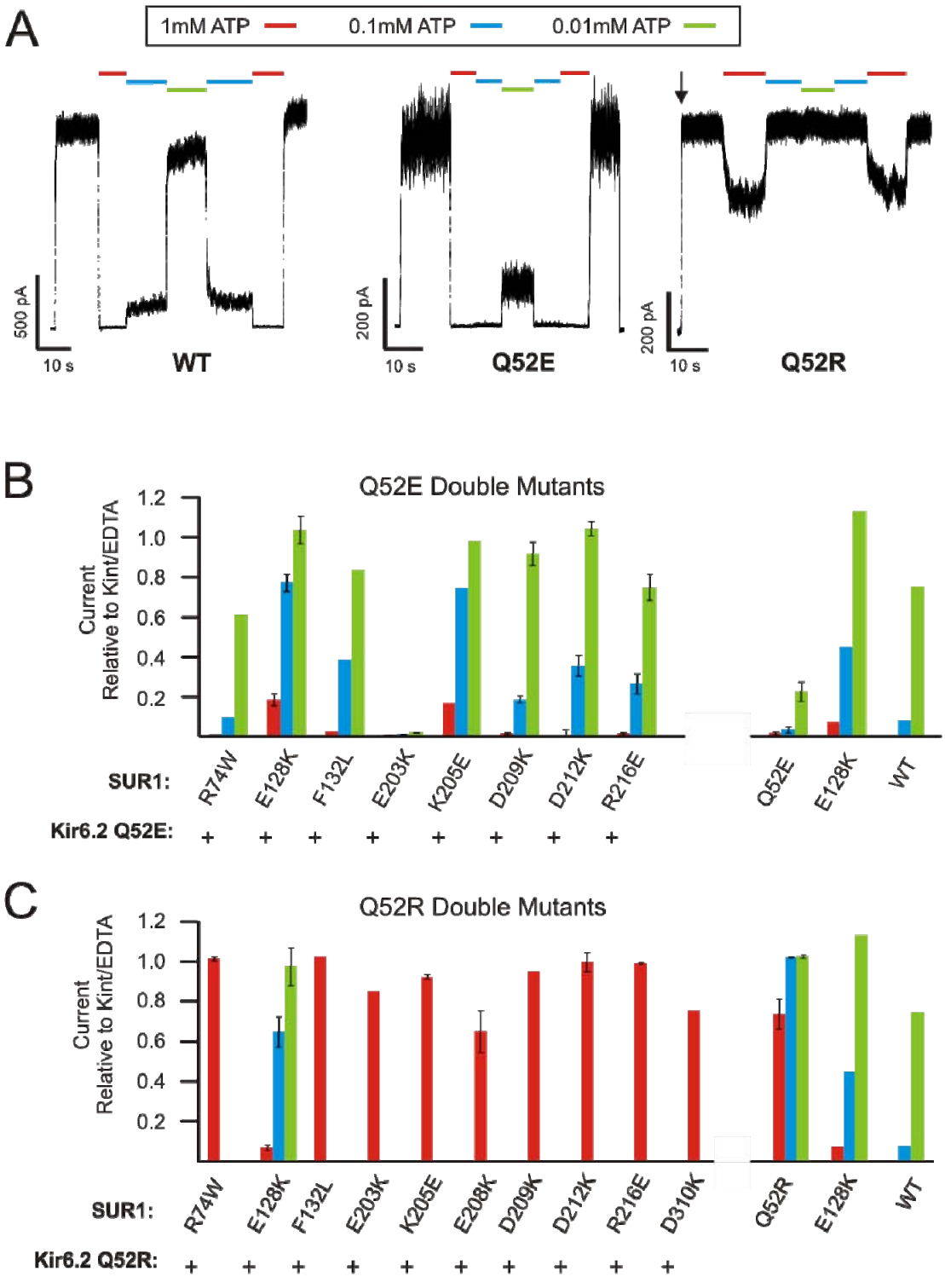

EBP Chapter 4
Figure 8

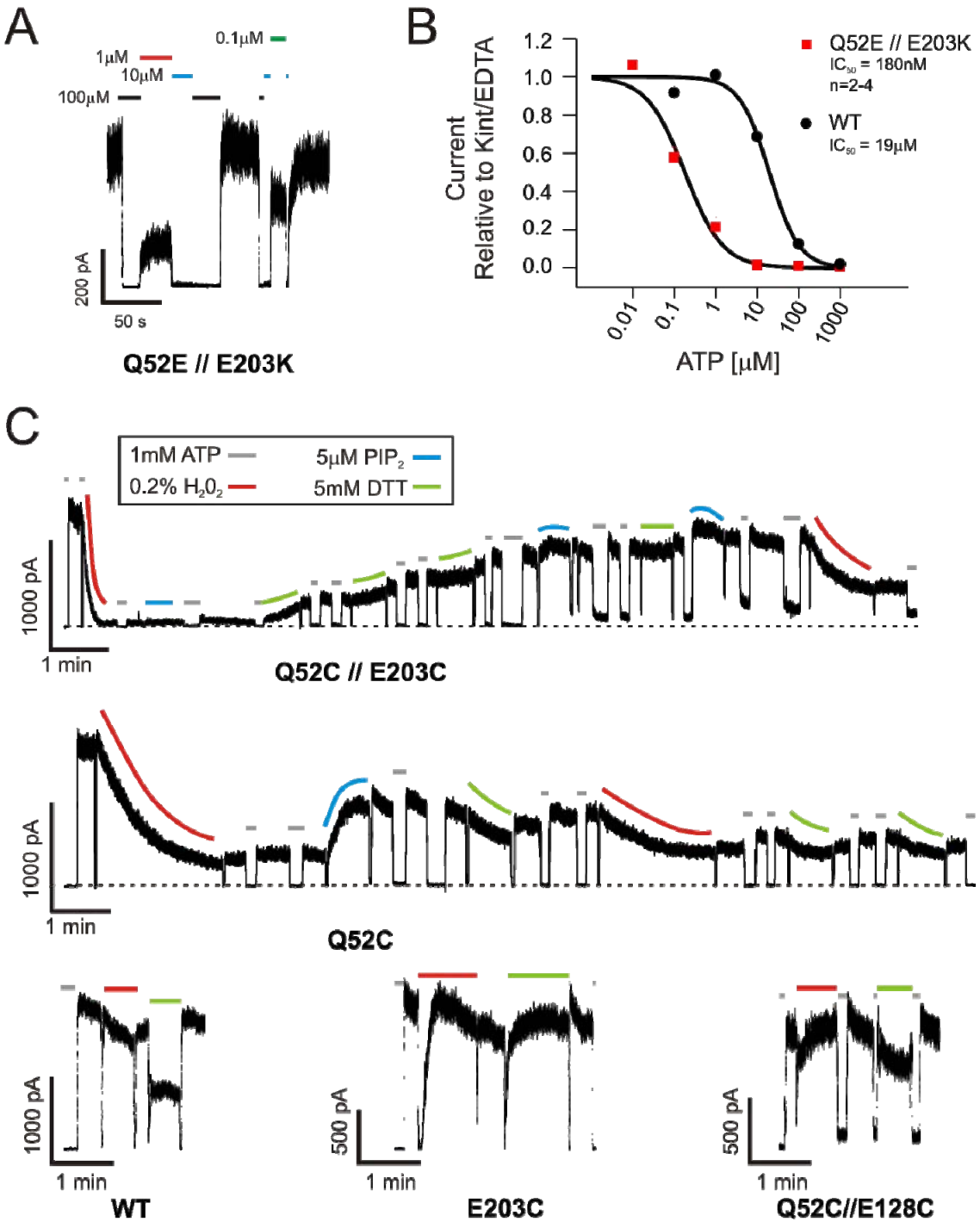

EBP Chapter 4
Figure 9

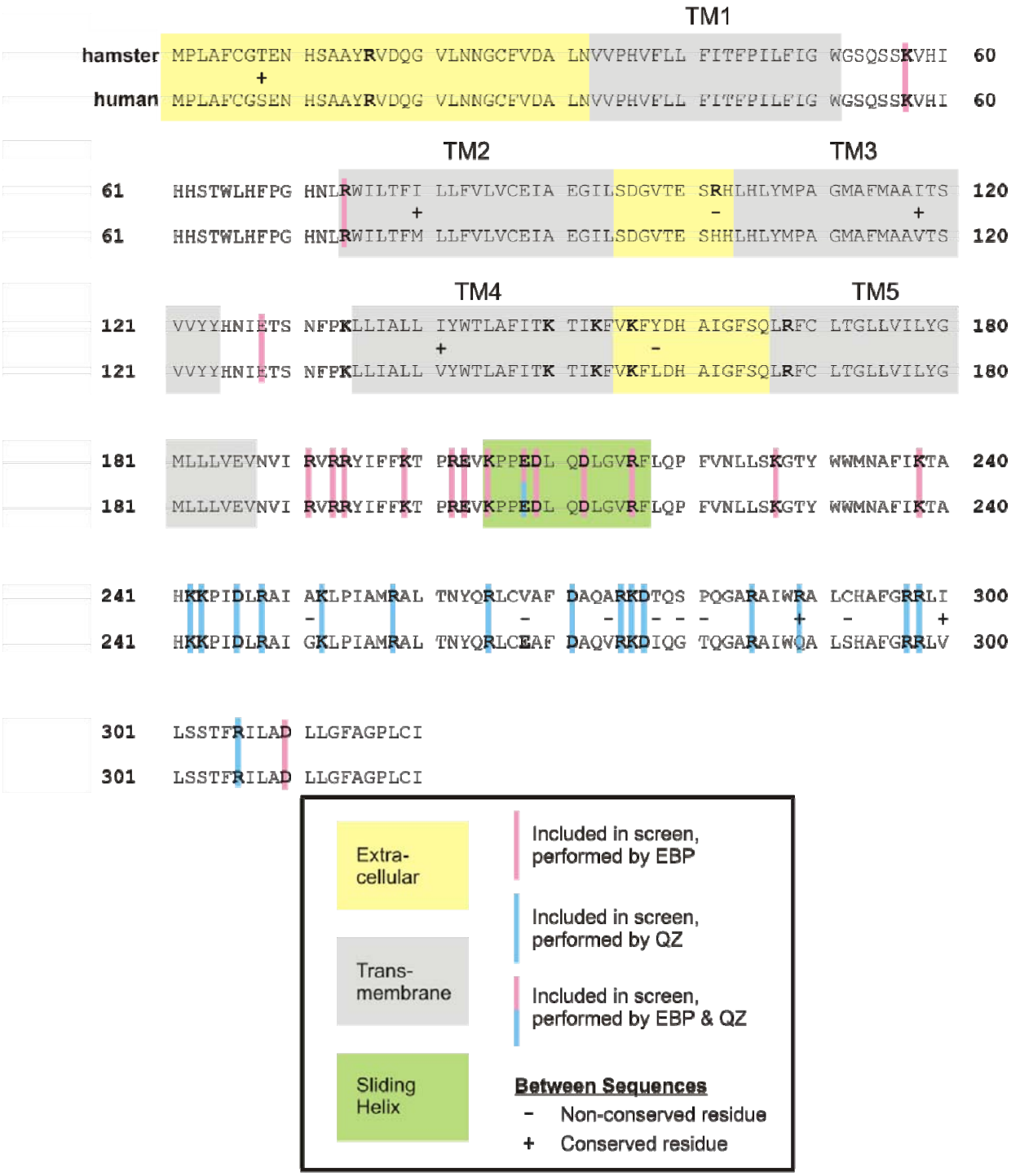

EBP Chapter 4
Figure 10

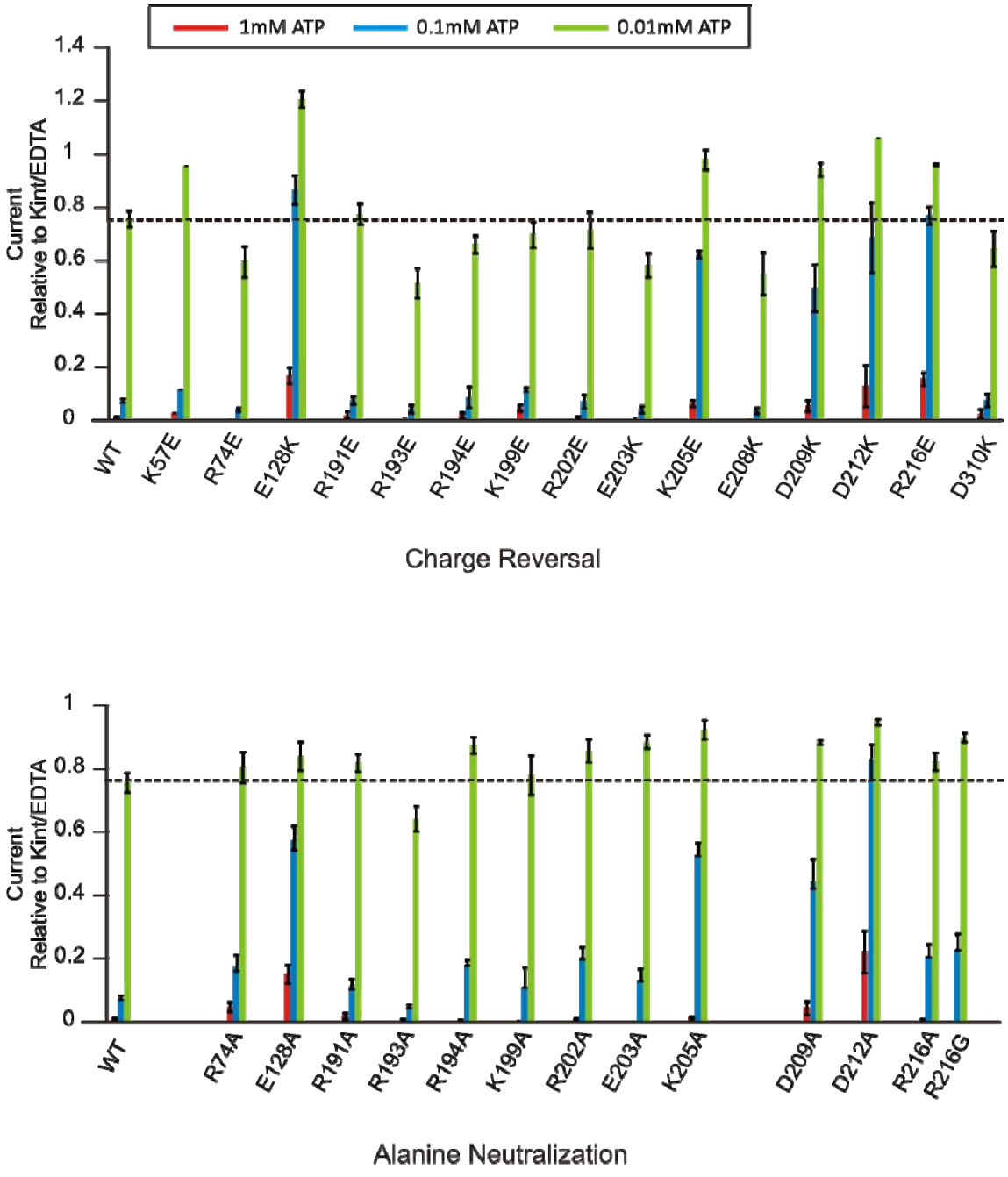

EBP Chapter 4
Figure 11

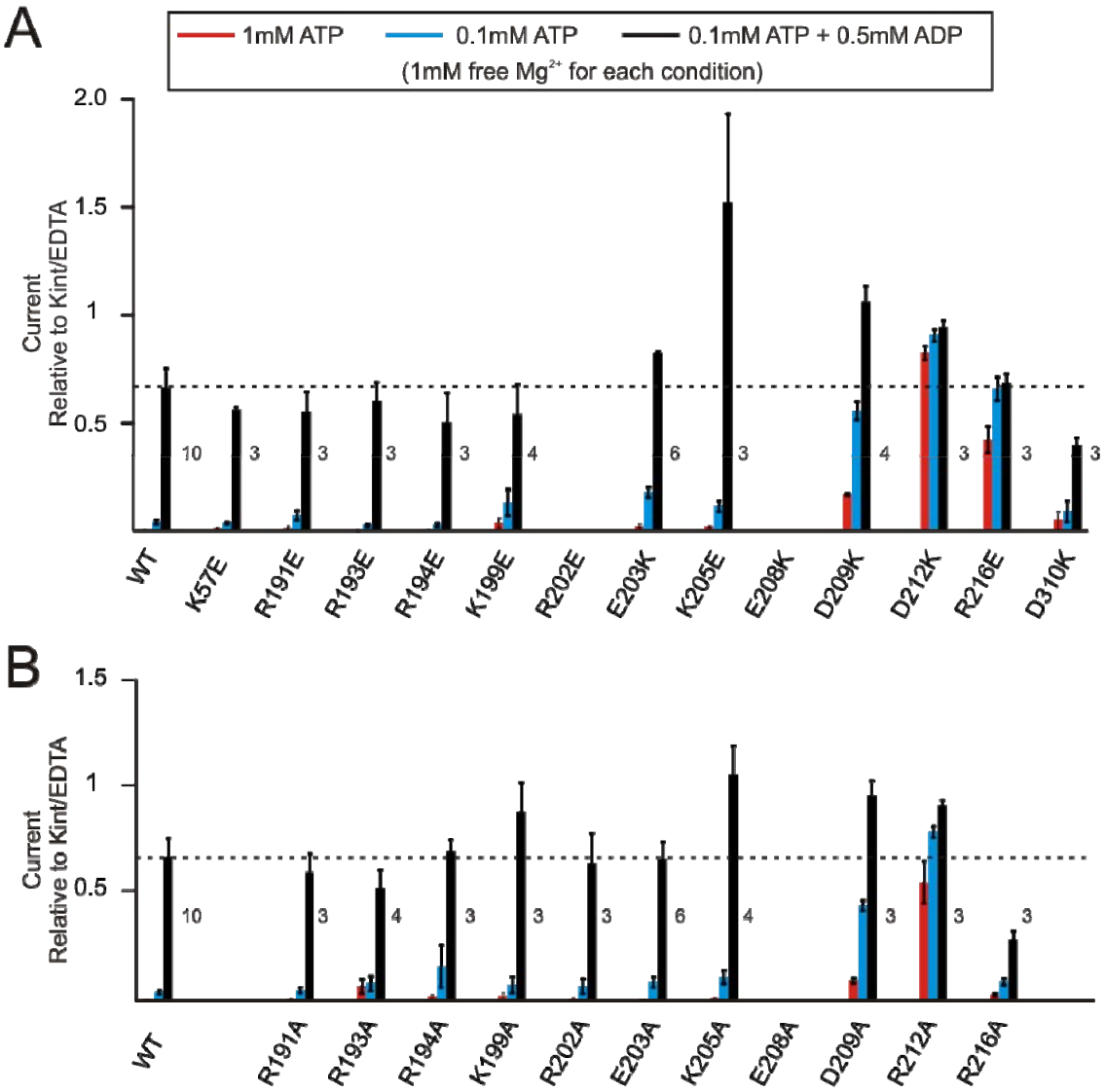

EBP Chapter 4
Figure 12

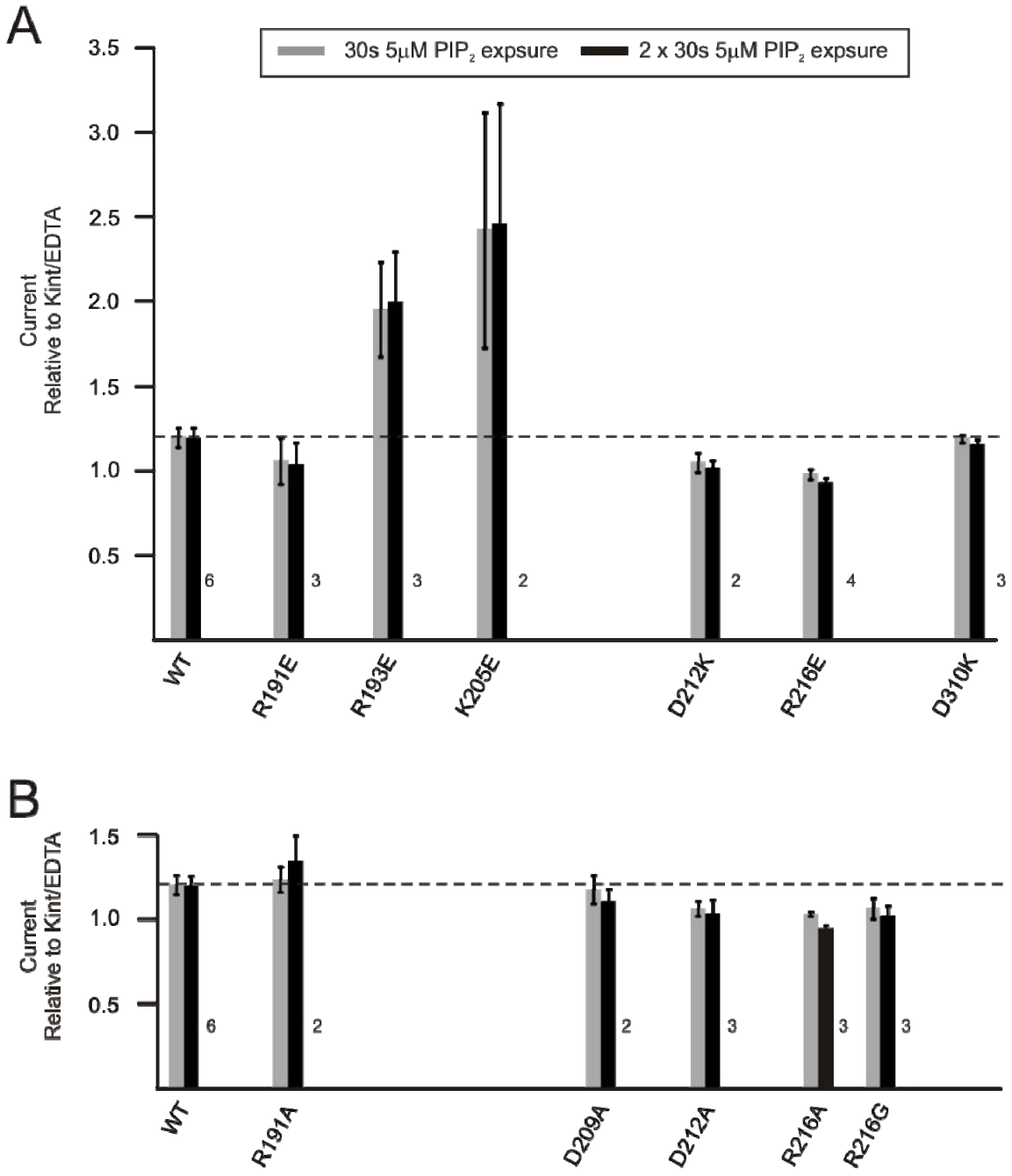

EBP Chapter 4
Figure 13

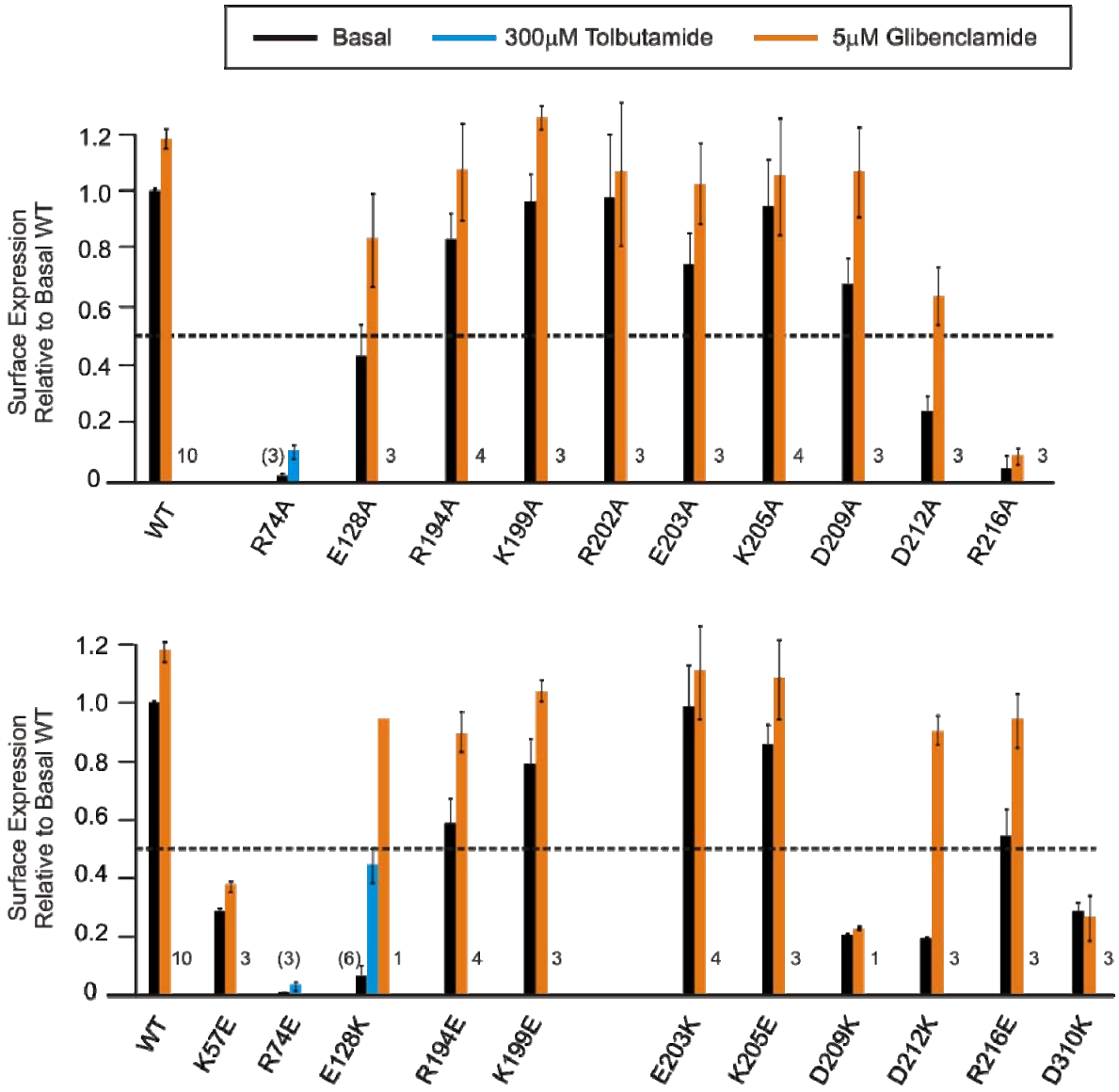

EBP Chapter 4
Figure 14

CHAPTER 5: CONCLUSIONS

Work presented in this dissertation advances the field of K_{ATP} physiology. Clarification of functional and physical interactions between the two heterologous subunits of K_{ATP} has been exceedingly slow compared to what we know about how the Kir6.2 subunit performs in the absence of SUR1. Based on data outlined in Chapters 2-4, several contributions have been made toward this end. A previously unappreciated mechanism of SUR1-influence involving PIP_2 has been elucidated. One new physical connection between Kir6.2 and SUR1 has been identified (Q52 : E203) and a once hypothetical role for SUR1's sliding helix has been validated through electrophysiological and biochemical means. Additionally, progress in understanding disease mechanisms and probable complications of drug development are addressed. A unique phenotype was discovered for two separate CHI-causing mutations in which severe disruption of both trafficking and activity were found, i.e., these dysfunctions are not mutually exclusive. That a single disease variant can result in multiple different problems means the utility of potential new chaperoning drugs may be compromised for certain populations of CHI patients. The body of work reported will launch several new areas of inquiry.

Clinical Implications

Drug Discovery

Failed trafficking is now a well established mechanism of disease for CHI with examples of Kir6.2 and SUR1 mutations that greatly decrease surface expression of K_{ATP} (Cartier et al., 2001; Partridge et al., 2001; Crane and Aguilar-Bryan, 2004; Yan et al., 2007). In fact, trafficking defects have also been linked to PNDM-associated mutations, and even suggested to mitigate symptoms of what would otherwise be diagnosed as DEND (Lin et al., 2006a). Clearly, the balance between expression and activity must be taken into account when explaining how a

given K_{ATP} mutant causes disease. In theory, eventually expression should trump activity such that even the most severely activating mutation will be disguised by its absence from where it matters most—the plasma membrane. Therefore, from a purely basic science point of view it was satisfying to identify two mutations where this was exactly the case: SUR1 E128K and R74W (Pratt et al., 2009). My contributions to this proof-of-principle were multiple electrophysiological assays that showed decreased nucleotide sensitivities and a direct association between hyperpolarized membrane potentials and surface expression. Given the prelude to this publication discussed above, it now seems inevitable that just such mutations would be discovered; however, their existence does color aspects of future research.

Most importantly, and not nearly as satisfying, for children and loved ones affected by CHI mutations, the future of drug development becomes more complicated by this finding. Merely increasing K_{ATP} surface expression will not treat all cases of trafficking-defective CHI. What was already a rare disease with unlikely prospects of orphan drug (Congress, 1983) development seems even more far away. Not to put too fine a pessimistic point on it, even within the broader class of CHI-trafficking mutations, it appears no one chemical chaperone will successfully facilitate trafficking of every genetic variant. That is, to date the most effective and non-specific chaperone drugs identified (SU compounds) improve expression of only a subset of trafficking mutants. Within SUR1, all known trafficking mutations that are sensitive to SU treatment are located in TMD0 and L0 domains [(Yan et al., 2007), Chapter 4]. Kir6.2 trafficking rescue seems to be less domain-specific (Lin et al., 2006a), yet Kir6.2 also may be less susceptible to extreme loss of expression as there are far fewer CHI-trafficking mutants described for Kir6.2 than for SUR1 (Crane and Aguilar-Bryan, 2004; Marthinet et al., 2005).

Disease Mechanisms

In terms of authenticating hypothetical disease mechanisms, the identification of the double mutant Kir6.2 Q52E//SUR1 E203K may prove to be the first hyperinsulinism K_{ATP} channel in which *increased* ATP-sensitivity is the underlying cause (Chapter 4). Of course, more electrophysiological (especially Mg·nucleotide stimulation) and cell biology experiments (insulin secretion) need to be performed before we can confidently characterize Q52E//E203K channels as CHI-like. Nonetheless, one can speculate that the reason no such CHI cause has been reported is that mutations in both subunits are necessary to profoundly affect K_{ATP} in this way. Importantly, in order for any such hypersensitive double mutant channel to cause disease its subunits must first compete for assembly with any WT alleles that express; what's more, the relative placement of SUR1 and Kir6.2 would have to be precise in order to juxtapose the two residues, as presumably, they need to be 'interacting' to cause their extreme hypersensitivity. Follow-up experiments will need to be performed to determine if, in fact, juxtaposition is necessary and whether just one Q52E//E203K pair are sufficient to cause hypersensitivity. It is thought that a single binding event between ATP and K_{ATP} is sufficient to induce channel closure (Enkvetchakul et al., 2000; Craig et al., 2008), so the latter may prove to be true.

Basic Science Implications

The presence of SUR increases sensitivity of the channel to ATP inhibition, termed SUR1 hypersensitization. In accordance with the general state of K_{ATP} research, the specific interactions between SUR1 and Ki6.2 that determine this property are unknown. At least two different anatomic-based mechanisms have been put forward to account for SUR1 hypersensitization; both hypothesized mechanisms involve reorientation of the Kir6.2 non-canonical ATP binding site. The first proposes assembly with SUR1 leads to widening of the external aperture of the crevice that binds ATP to improve access of the binding site to ligand

(Dabrowski et al., 2004). A second proposes SUR1 interactions reposition the Kir6.2 amino-terminus such that R50 can more-tightly interact with the -phosphate of ATP (Babenko and Bryan, 2002; Babenko, 2005). These models need not be mutually exclusive. But what portions of SUR1 account for the "SUR1 interactions" in whatever model proves to be authenticated?

Although the presence of the SUR1 core domain is essential to induce SUR1 hypersensitization [as indicated by the fact that mini-K_{ATP} channels composed of varying lengths of TMD0-L0 truncations of SUR1 do not show SUR1 hypersensitization (Babenko and Bryan, 2003)], TMD0-L0 has been proposed to be central to SUR1-Kir6.2 transduction mechanism (Babenko, 2005). This is based in part on the fact that portions of SUR1 with the greatest reported influence on K_{ATP} P_o are TMD0 and L0. That is, given the near-universal inverse relationship between P_o and ATP sensitivity for K_{ATP} (the higher a channel's P_o, the lower that channel's ATP-sensitivity) it is plausible that SUR1 hypersensitivity relies on or is interconnected with this feature. My findings with regard to E128K and the Q52//E203 pair support a multi-dimensional model in which no *one* residue or cluster of residues can account for SUR1 hypersensitization, rather SUR1 domains participate in a coordinated manner to bring about this property. Consider the following as justification. The Q52//E203 interaction described in Chapter 4 represents what may be the illusive L0-Kir6.2 interface described in Babenko's model (Chapter 1, Figure X). That the Q52E//E203K double mutant causes *hyper*-hypersensitivity lends support to the involvement of both residues in the property. Owing to the proximity between Q52 and R50, the involvement of Q52//E203 is especially harmonious with the model presented by Banbenko and Bryan in which the placement of R50 shifts to bring about SUR1 hypersensitization. However, based on the finding that E128K seems to be the only residue able to exert a (dominant) influence on the phenotypes of both Kir6.2 Q52E and Q52R, **I predict that an architectural configuration involving E128K and Kir6.2 must first assemble in order to bring Q52 and E203 close enough to interact and/or cause SUR1 hypersensitivity.** The involvement of E128 may be

allosteric [despite serious effort, any direct E128-Kir6.2 interaction has yet to be found (Chapter 4, Figure 3)]. If a multi-dimensional network of connectivity is predicated on the influence of E128, interaction between Q52 and E203 is predicted to disappear in the presence of E128K. Satisfyingly, very recent data collected by my colleague, Dr. Qing Zhou, indicates the triple mutant channel Q52E//E128K/E203K has an IC_{50} of ~65 μM (personal communication, data not shown), significantly higher than Q52E//E203K [~200 nM (Chapter 4, Figure 9)] and suggesting Q52E and E203K are unable to interact.

In a related aside, it is curious that Q52R expressed with WT SUR1 (which, presumably, should constitute an equal-but-opposite salt-bridge interaction between Q52R and E203) does not also lead to extreme ATP-sensitivity. Perhaps substitution with the positively charges arginine transforms residue 52 into one capable of interacting with membrane PIP_2 (Figure 1), leading instead to the high P_o/low ATP-sensitivity/DEND phenotype (Proks et al., 2004). A competition for Q52R-binding exists between PIP2 and E203. If Q52R is expressed with WT SUR1, PIP_2 wins. If Q52R is expressed with E128K SUR1, E203 wins (or at least, PIP2 loses). This would explain why the E128K mutation has a dominant effect on both Q52E and Q52R (Chapter 4, Figure 8), and also why the Q52R mutation is SUR1-dependent (i.e., Q52R Kir6.2ΔC does not have increased P_o relative to WT Kir6.2ΔC). Experiments to test this hypothesis (e.g., neomycin studies of WT versus Q52R versus Q52R//E128K) await investigation.

Closing Thoughts

An immense body of work generated by scientists worldwide has resulted in a broad understanding of K_{ATP} channels where there was painfully little just 15 years ago. However, for all we know, there remain major gaps. When I began work on this dissertation 6 years ago I felt the most conspicuous need for clarification lay at the at the interface of what makes K_{ATP} so

unique – two extremely divergent proteins working in synchrony. It has been my goal during this time to shine a ray of light on what are certainly fleeting and nuanced interactions between SUR1 and Kir6.2. In part because so little was available on which to build testable hypotheses, I chose to use take a 'shotgun' approach to the question of which residues in SUR1 and Kir6.2 govern their intimate interactions and I have been fortunate to have had a modicum of success.

Continued search for the physical links between subunits will prove to be vital for developing models of communication as well as potentially directing drug development. Until an adequate high resolution crystal structure of an intact K_{ATP} channel becomes available, brute force methods similar to ones described in this dissertation will inevitably lead to intriguing results. Indeed, when I began these experiments I had no idea that a new role for PIP_2 in SUR1-regulation of K_{ATP} would present itself. Nor was I expecting to serendipitously stumble upon what may be key residues involved in SUR1 hypersensitization. All this is to say that the profession of scientist requires much more than hard facts and tangible proof; faith in the scientific process is essential.

Figure Legend

Figure 1. Hypothetical change in the conformation of Kir6.2 Q52R in the presence and absence of SUR1. Using the Kir6.2 homology model developed by Jeremy Bushman, I have replaced the glutamine at residue 52 with arginine. I propose substitution of Q52R generates a new PIP_2 interaction site at the residue. However, based on the differential phenotype of WT//Q52R and E128K//Q52R, the position of Q52R relative to the plasma membrane varies depending on the presence or absence of SUR1, or with WT versus E128K SUR1. In WT channels, Q52R is unavailable for interaction with SUR1 because competition from PIP_2 draws Q52R upward (left). In the absence of SUR1 (i.e., Kir6.2ΔC channels) or when co-expressed with E128K SUR1, the placement of Q52R is such that it cannot reach PIP_2 (right).

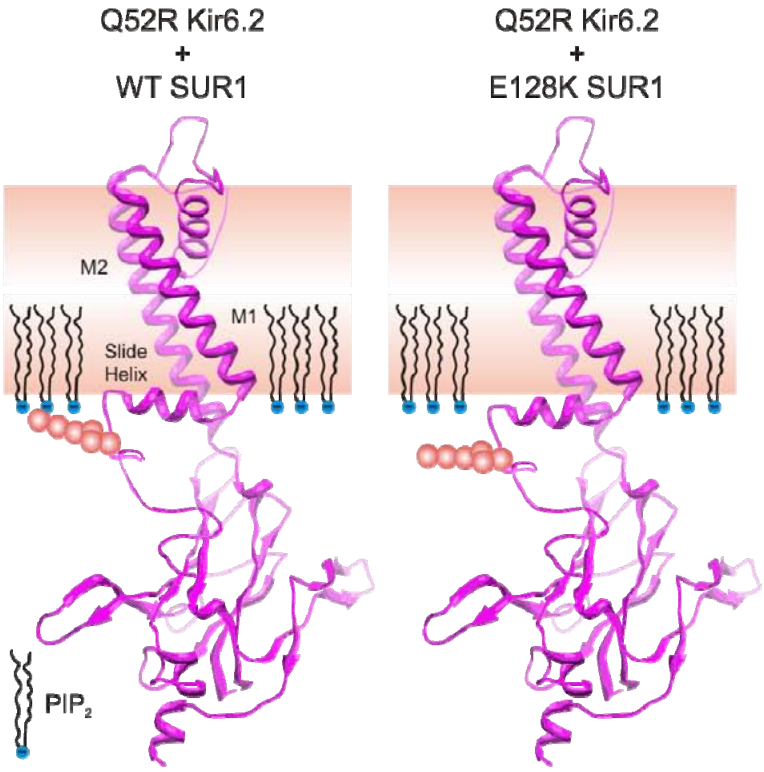

EBP Chapter 5
Figure 1

References Cited

Aguilar-Bryan, L., and J. Bryan. 1999. Molecular Biology of Adenosine Triphosphate-Sensitive Potassium Channels. *Endocr Rev*. 20:101-135.

Aguilar-Bryan, L., C.G. Nichols, S.W. Wechsler, J.P.t. Clement, A.E. Boyd, 3rd, G. Gonzalez, H. Herrera-Sosa, K. Nguy, J. Bryan, and D.A. Nelson. 1995. Cloning of the beta cell high-affinity sulfonylurea receptor: a regulator of insulin secretion. *Science*. 268:423-426.

Antcliff, J.F., S. Haider, P. Proks, M.S. Sansom, and F.M. Ashcroft. 2005. Functional analysis of a structural model of the ATP-binding site of the K(ATP) channel Kir6.2 subunit. *Embo J*. 24:229-239.

Ashcroft, F.M. 2005. ATP-sensitive potassium channelopathies: focus on insulin secretion. *J Clin Invest*. 115:2047-2058.

Ashfield, R., F.M. Gribble, S.J. Ashcroft, and F.M. Ashcroft. 1999. Identification of the high-affinity tolbutamide site on the SUR1 subunit of the K(ATP) channel. *Diabetes*. 48:1341-1347.

Ayyagari, R., A. Nestorowicz, Y. Li, S. Chandrasekharappa, C. Chinault, P. van Tuinen, R.J. Smith, J.F. Hejtmancik, and M.A. Permutt. 1996. Construction of a YAC contig encompassing the Usher syndrome type 1C and familial hyperinsulinism loci on chromosome 11p14-15.1. *Genome Res*. 6:504-514.

Babenko, A.P. 2005. K(ATP) channels "vingt ans apres": ATG to PDB to Mechanism. *J Mol Cell Cardiol*. 39:79-98.

Babenko, A.P., L. Aguilar-Bryan, and J. Bryan. 1998. A view of sur/KIR6.X, KATP channels. *Annu Rev Physiol*. 60:667-687.

Babenko, A.P., and J. Bryan. 2002. SUR-dependent modulation of KATP channels by an N-terminal KIR6.2 peptide. Defining intersubunit gating interactions. *J Biol Chem*. 277:43997-44004.

Babenko, A.P., and J. Bryan. 2003. SUR domains that associate with and gate KATP pores define a novel gatekeeper. *J Biol Chem*. 26:26.

Babenko, A.P., G. Gonzalez, L. Aguilar-Bryan, and J. Bryan. 1999a. Sulfonylurea receptors set the maximal open probability, ATP sensitivity and plasma membrane density of KATP channels. *FEBS Lett*. 445:131-136.

Babenko, A.P., G. Gonzalez, and J. Bryan. 1999b. The N-terminus of KIR6.2 limits spontaneous bursting and modulates the ATP-inhibition of KATP channels. *Biochem Biophys Res Commun*. 255:231-238.

Babenko, A.P., M. Polak, H. Cave, K. Busiah, P. Czernichow, R. Scharfmann, J. Bryan, L. Aguilar-Bryan, M. Vaxillaire, and P. Froguel. 2006. Activating mutations in the ABCC8 gene in neonatal diabetes mellitus. *N Engl J Med*. 355:456-466.

Bakos, E., R. Evers, G. Calenda, G.E. Tusnady, G. Szakacs, A. Varadi, and B. Sarkadi. 2000. Characterization of the amino-terminal regions in the human multidrug resistance protein (MRP1). *J Cell Sci*. 113 Pt 24:4451-4461.

Baukrowitz, T., U. Schulte, D. Oliver, S. Herlitze, T. Krauter, S.J. Tucker, J.P. Ruppersberg, and B. Fakler. 1998. PIP2 and PIP as determinants for ATP inhibition of KATP channels. *Science*. 282:1141-1144.

Beech, D.J., H. Zhang, K. Nakao, and T.B. Bolton. 1993. K channel activation by nucleotide diphosphates and its inhibition by glibenclamide in vascular smooth muscle cells. *Br J Pharmacol*. 110:573-582.

Beguin, P., K. Nagashima, M. Nishimura, T. Gonoi, and S. Seino. 1999. PKA-mediated phosphorylation of the human K(ATP) channel: separate roles of Kir6.2 and SUR1 subunit phosphorylation. *EMBO Journal*. 18:4722-4732.

Bernsel, A., H. Viklund, A. Hennerdal, and A. Elofsson. 2009. TOPCONS: consensus prediction of membrane protein topology. *Nucl. Acids Res.* 37:W465-468.

Bienengraeber, M., A.E. Alekseev, M.R. Abraham, A.J. Carrasco, C. Moreau, M. Vivaudou, P.P. Dzeja, and A. Terzic. 2000. ATPase activity of the sulfonylurea receptor: a catalytic function for the KATP channel complex. *Faseb J*. 14:1943-1952.

Bienengraeber, M., T.M. Olson, V.A. Selivanov, E.C. Kathmann, F. O'Cochlain, F. Gao, A.B. Karger, J.D. Ballew, D.M. Hodgson, L.V. Zingman, Y.P. Pang, A.E. Alekseev, and A. Terzic. 2004. ABCC9 mutations identified in human dilated cardiomyopathy disrupt catalytic KATP channel gating. *Nat Genet*. 36:382-387.

Bloc, A., T. Cens, H. Cruz, and Y. Dunant. 2000. Zinc-induced changes in ionic currents of clonal rat pancreatic -cells: activation of ATP-sensitive K+ channels. *J Physiol*. 529 Pt 3:723-734.

Branstrom, R., C.A. Aspinwall, S. Valimaki, C.G. Ostensson, A. Tibell, M. Eckhard, H. Brandhorst, B.E. Corkey, P.O. Berggren, and O. Larsson. 2004. Long-chain CoA esters activate human pancreatic beta-cell KATP channels: potential role in Type 2 diabetes. *Diabetologia*. 47:277-283.

Branstrom, R., I.B. Leibiger, B. Leibiger, B.E. Corkey, P.O. Berggren, and O. Larsson. 1998. Long chain coenzyme A esters activate the pore-forming subunit (Kir6. 2) of the ATP-regulated potassium channel. *J Biol Chem*. 273:31395-31400.

Bryan, J., A. Crane, W.H. Vila-Carriles, A.P. Babenko, and L. Aguilar-Bryan. 2005. Insulin secretagogues, sulfonylurea receptors and K(ATP) channels. *Current pharmaceutical design*. 11:2699-2716.

Bryan, J., W.H. Vila-Carriles, G. Zhao, A.P. Babenko, and L. Aguilar-Bryan. 2004. Toward linking structure with function in ATP-sensitive K+ channels. *Diabetes*. 53 Suppl 3:S104-112.

Cartier, E.A., L.R. Conti, C.A. Vandenberg, and S.L. Shyng. 2001. Defective trafficking and function of KATP channels caused by a sulfonylurea receptor 1 mutation associated with persistent hyperinsulinemic hypoglycemia of infancy. *Proc Natl Acad Sci U S A*. 98:2882-2887.

Chan, K.W., H. Zhang, and D.E. Logothetis. 2003. N-terminal transmembrane domain of the SUR controls trafficking and gating of Kir6 channel subunits. *Embo J*. 22:3833-3843.

Chang, T.J., W.P. Chen, C. Yang, P.H. Lu, Y.C. Liang, M.J. Su, S.C. Lee, and L.M. Chuang. 2009. Serine-385 phosphorylation of inwardly rectifying K+ channel subunit (Kir6.2) by AMP-dependent protein kinase plays a key role in rosiglitazone-induced closure of the K(ATP) channel and insulin secretion in rats. *Diabetologia*. 52:1112-1121.

Chothia, C. 1976. The nature of the accessible and buried surfaces in proteins. *J Mol Biol*. 105:1-12.

Chutkow, W.A., M.C. Simon, M.M. Le Beau, and C.F. Burant. 1996. Cloning, tissue expression, and chromosomal localization of SUR2, the putative drug-binding subunit of cardiac, skeletal muscle, and vascular KATP channels. *Diabetes*. 45:1439-1445.

Clarke, O.B., A.T. Caputo, A.P. Hill, J.I. Vandenberg, B.J. Smith, and J.M. Gulbis. 2010. Domain Reorientation and Rotation of an Intracellular Assembly Regulate Conduction in Kir Potassium Channels. *Cell*. 141:1018-1029.

Clement, J.P.t., K. Kunjilwar, G. Gonzalez, M. Schwanstecher, U. Panten, L. Aguilar-Bryan, and J. Bryan. 1997. Association and stoichiometry of K(ATP) channel subunits. *Neuron*. 18:827-838.

Congress, U. 1983. The Orphan Drug Act. *In* U.S. Congress, editor.

Conti, L.R., C.M. Radeke, S.L. Shyng, and C.A. Vandenberg. 2001. Transmembrane topology of the sulfonylurea receptor SUR1. *J Biol Chem*. 276:41270-41278.

Cook, D.L., and C.N. Hales. 1984. Intracellular ATP directly blocks K+ channels in pancreatic B-cells. *Nature*. 311:271-273.

Craig, T.J., F.M. Ashcroft, and P. Proks. 2008. How ATP inhibits the open K(ATP) channel. *J Gen Physiol*. 132:131-144.

Crane, A., and L. Aguilar-Bryan. 2004. Assembly, maturation, and turnover of K(ATP) channel subunits. *J Biol Chem*. 279:9080-9090.

Cukras, C.A., I. Jeliazkova, and C.G. Nichols. 2002a. The role of NH(2)-terminal positive charges in the activity of inward rectifier K(ATP) channels. *J Gen Physiol*. 120:437-446.

Cukras, C.A., I. Jeliazkova, and C.G. Nichols. 2002b. Structural and functional determinants of conserved lipid interaction domains of inward rectifying kir6.2 channels. *J Gen Physiol*. 119:581-591.

Dabrowski, M., A. Tarasov, and F.M. Ashcroft. 2004. Mapping the architecture of the ATP-binding site of the KATP channel subunit Kir6.2. *J Physiol*. 557:347-354.

de Wet, H., M.G. Rees, K. Shimomura, J. Aittoniemi, A.M. Patch, S.E. Flanagan, S. Ellard, A.T. Hattersley, M.S. Sansom, and F.M. Ashcroft. 2007. Increased ATPase activity produced by mutations at arginine-1380 in nucleotide-binding domain 2 of ABCC8 causes neonatal diabetes. *Proc Natl Acad Sci U S A*. 104:18988-18992.

Dean, M., and R. Allikmets. 2001. Complete characterization of the human ABC gene family. *J Bioenerg Biomembr*. 33:475-479.

Dempster, J. 2001. Laboratory Computer: A Practical Guide for Physiologists and Neuroscientists. Academic Press, San Diego, CA.

Doyle, D.A., J. Morais Cabral, R.A. Pfuetzner, A. Kuo, J.M. Gulbis, S.L. Cohen, B.T. Chait, and R. MacKinnon. 1998. The structure of the potassium channel: molecular basis of K+ conduction and selectivity. *Science*. 280:69-77.

Drain, P., L. Li, and J. Wang. 1998. KATP channel inhibition by ATP requires distinct functional domains of the cytoplasmic C terminus of the pore-forming subunit. *Proc Natl Acad Sci U S A*. 95:13953-13958.

Du, X., H. Zhang, C. Lopes, T. Mirshahi, T. Rohacs, and D.E. Logothetis. 2004. Characteristic interactions with phosphatidylinositol 4,5-bisphosphate determine regulation of kir channels by diverse modulators. *J Biol Chem*. 279:37271-37281.

Duhault, J., and R. Lavielle. 1991. History and evolution of the concept of oral therapy in diabetes. *Diabetes Res Clin Pract*. 14 Suppl 2:S9-13.

Dunne, M.J., K.E. Cosgrove, R.M. Shepherd, A. Aynsley-Green, and K.J. Lindley. 2004. Hyperinsulinism in infancy: from basic science to clinical disease. *Physiol Rev*. 84:239-275.

Edghill, E.L., R.J. Dix, S.E. Flanagan, P.J. Bingley, A.T. Hattersley, S. Ellard, and K.M. Gillespie. 2006. HLA genotyping supports a nonautoimmune etiology in patients diagnosed with diabetes under the age of 6 months. *Diabetes*. 55:1895-1898.

Enkvetchakul, D., I. Jeliazkova, J. Bhattacharyya, and C.G. Nichols. 2007. Control of inward rectifier K channel activity by lipid tethering of cytoplasmic domains. *J Gen Physiol*. 130:329-334.

Enkvetchakul, D., G. Loussouarn, E. Makhina, S.L. Shyng, and C.G. Nichols. 2000. The kinetic and physical basis of K(ATP) channel gating: toward a unified molecular understanding. *Biophys J*. 78:2334-2348.

Enkvetchakul, D., and C.G. Nichols. 2003. Gating mechanism of KATP channels: function fits form. *J Gen Physiol*. 122:471-480.

Fan, Z., and J.C. Makielski. 1997. Anionic phospholipids activate ATP-sensitive potassium channels. *J Biol Chem*. 272:5388-5395.

Fan, Z., and J.C. Makielski. 1999. Phosphoinositides decrease ATP sensitivity of the cardiac ATP-sensitive K(+) channel. A molecular probe for the mechanism of ATP-sensitive inhibition. *J Gen Physiol*. 114:251-269.

Flanagan, S.E., E.L. Edghill, A.L. Gloyn, S. Ellard, and A.T. Hattersley. 2006. Mutations in KCNJ11, which encodes Kir6.2, are a common cause of diabetes diagnosed in the first 6 months of life, with the phenotype determined by genotype. *Diabetologia*. 49:1190-1197.

Florez, J.C., N. Burtt, P.I. de Bakker, P. Almgren, T. Tuomi, J. Holmkvist, D. Gaudet, T.J. Hudson, S.F. Schaffner, M.J. Daly, J.N. Hirschhorn, L. Groop, and D. Altshuler. 2004. Haplotype structure and

genotype-phenotype correlations of the sulfonylurea receptor and the islet ATP-sensitive potassium channel gene region. *Diabetes*. 53:1360-1368.

Fournet, J.C., and C. Junien. 2003. The genetics of neonatal hyperinsulinism. *Horm Res*. 59 Suppl 1:30-34.

Fu, Y., W. Tian, E.B. Pratt, L.B. Dirling, S.L. Shyng, C.K. Meshul, and D.M. Cohen. 2009. Down-regulation of ZnT8 expression in INS-1 rat pancreatic beta cells reduces insulin content and glucose-inducible insulin secretion. *PloS one*. 4:e5679.

Gloyn, A.L., F. Reimann, C. Girard, E.L. Edghill, P. Proks, E.R. Pearson, I.K. Temple, D.J. Mackay, J.P. Shield, D. Freedenberg, K. Noyes, S. Ellard, F.M. Ashcroft, F.M. Gribble, and A.T. Hattersley. 2005. Relapsing diabetes can result from moderately activating mutations in KCNJ11. *Hum Mol Genet*. 14:925-934.

Gloyn, A.L., M.N. Weedon, K.R. Owen, M.J. Turner, B.A. Knight, G. Hitman, M. Walker, J.C. Levy, M. Sampson, S. Halford, M.I. McCarthy, A.T. Hattersley, and T.M. Frayling. 2003. Large-scale association studies of variants in genes encoding the pancreatic beta-cell KATP channel subunits Kir6.2 (KCNJ11) and SUR1 (ABCC8) confirm that the KCNJ11 E23K variant is associated with type 2 diabetes. *Diabetes*. 52:568-572.

Grell, W., R. Hurnaus, G. Griss, R. Sauter, E. Rupprecht, M. Mark, P. Luger, H. Nar, H. Wittneben, and P. Muller. 1998. Repaglinide and related hypoglycemic benzoic acid derivatives. *J Med Chem*. 41:5219-5246.

Gribble, F.M., S.J. Tucker, and F.M. Ashcroft. 1997a. The essential role of the Walker A motifs of SUR1 in K-ATP channel activation by Mg-ADP and diazoxide. *Embo J*. 16:1145-1152.

Gribble, F.M., S.J. Tucker, and F.M. Ashcroft. 1997b. The interaction of nucleotides with the tolbutamide block of cloned ATP- sensitive K+ channel currents expressed in Xenopus oocytes: a reinterpretation. *J Physiol*. 504:35-45.

Gribble, F.M., S.J. Tucker, S. Seino, and F.M. Ashcroft. 1998. Tissue specificity of sulfonylureas: studies on cloned cardiac and beta- cell K(ATP) channels. *Diabetes*. 47:1412-1418.

Gros, L., A. Virsolvy, G. Salazar, D. Bataille, and P. Blache. 1999. Characterization of low-affinity binding sites for glibenclamide on the Kir6.2 subunit of the beta-cell KATP channel. *Biochem Biophys Res Commun*. 257:766-770.

Gullo, D., A.M. Rabuazzo, M. Vetri, C. Gatta, C. Vinci, M. Buscema, R. Vigneri, and F. Purrello. 1991. Chronic exposure to glibenclamide impairs insulin secretion in isolated rat pancreatic islets. *J Endocrinol Invest*. 14:287-291.

Haider, S., A.I. Tarasov, T.J. Craig, M.S. Sansom, and F.M. Ashcroft. 2007. Identification of the PIP(2)-binding site on Kir6.2 by molecular modelling and functional analysis. *Embo J*. 26:3749-3759.

Hambrock, A., C. Loffler-Walz, U. Russ, U. Lange, and U. Quast. 2001. Characterization of a mutant sulfonylurea receptor SUR2B with high affinity for sulfonylureas and openers: differences in the coupling to Kir6.x subtypes. *Mol Pharmacol*. 60:190-199.

Hamming, K.S., D. Soliman, L.C. Matemisz, O. Niazi, Y. Lang, A.L. Gloyn, and P.E. Light. 2009. Coexpression of the type 2 diabetes susceptibility gene variants KCNJ11 E23K and ABCC8 S1369A alter the ATP and sulfonylurea sensitivities of the ATP-sensitive K(+) channel. *Diabetes*. 58:2419-2424.

Hani, E.H., P. Boutin, E. Durand, H. Inoue, M.A. Permutt, G. Velho, and P. Froguel. 1998. Missense mutations in the pancreatic islet beta cell inwardly rectifying K+ channel gene (KIR6.2/BIR): a meta-analysis suggests a role in the polygenic basis of Type II diabetes mellitus in Caucasians. *Diabetologia*. 41:1511-1515.

Hattersley, A.T., and F.M. Ashcroft. 2005. Activating mutations in kir6.2 and neonatal diabetes: new clinical syndromes, new scientific insights, and new therapy. *Diabetes*. 54:2503-2513.

Heijne, G. 1986. The distribution of positively charged residues in bacterial inner membrane proteins correlates with the trans-membrane topology. *Embo J*. 5:3021-3027.

Henquin, J.C. 1992. The fiftieth anniversary of hypoglycaemic sulphonamides. How did the mother compound work? *Diabetologia*. 35:907-912.

Henwood, M.J., A. Kelly, C. Macmullen, P. Bhatia, A. Ganguly, P.S. Thornton, and C.A. Stanley. 2005. Genotype-phenotype correlations in children with congenital hyperinsulinism due to recessive mutations of the adenosine triphosphate-sensitive potassium channel genes. *J Clin Endocrinol Metab*. 90:789-794.

Hessa, T., H. Kim, K. Bihlmaier, C. Lundin, J. Boekel, H. Andersson, I. Nilsson, S.H. White, and G. von Heijne. 2005. Recognition of transmembrane helices by the endoplasmic reticulum translocon. *Nature*. 433:377-381.

Heusser, K., H. Yuan, I. Neagoe, A.I. Tarasov, F.M. Ashcroft, and B. Schwappach. 2006. Scavenging of 14-3-3 proteins reveals their involvement in the cell-surface transport of ATP-sensitive K+ channels. *J Cell Sci*. 119:4353-4363.

Hibino, H., A. Inanobe, K. Furutani, S. Murakami, I. Findlay, and Y. Kurachi. 2010. Inwardly rectifying potassium channels: their structure, function, and physiological roles. *Physiol Rev*. 90:291-366.

Hilgemann, D.W., S. Feng, and C. Nasuhoglu. 2001. The complex and intriguing lives of PIP2 with ion channels and transporters. *Sci STKE*. 2001:RE19.

Hohmeier, H.E., H. Mulder, G. Chen, R. Henkel-Rieger, M. Prentki, and C.B. Newgard. 2000. Isolation of INS-1-derived cell lines with robust ATP-sensitive K+ channel-dependent and -independent glucose-stimulated insulin secretion. *Diabetes*. 49:424-430.

Huopio, H., S.L. Shyng, T. Otonkoski, and C.G. Nichols. 2002. K(ATP) channels and insulin secretion disorders. *Am J Physiol Endocrinol Metab*. 283:E207-216.

Inagaki, N., T. Gonoi, J.P. Clement, C.Z. Wang, L. Aguilar-Bryan, J. Bryan, and S. Seino. 1996. A family of sulfonylurea receptors determines the pharmacological properties of ATP-sensitive K+ channels. *Neuron*. 16:1011-1017.

Inagaki, N., T. Gonoi, J.P.t. Clement, N. Namba, J. Inazawa, G. Gonzalez, L. Aguilar-Bryan, S. Seino, and J. Bryan. 1995a. Reconstitution of IKATP: an inward rectifier subunit plus the sulfonylurea receptor. *Science*. 270:1166-1170.

Inagaki, N., T. Gonoi, and S. Seino. 1997. Subunit stoichiometry of the pancreatic beta-cell ATP-sensitive K+ channel. *FEBS Lett*. 409:232-236.

Inagaki, N., J. Inazawa, and S. Seino. 1995b. cDNA sequence, gene structure, and chromosomal localization of the human ATP-sensitive potassium channel, uKATP-1, gene (KCNJ8). *Genomics*. 30:102-104.

Inagaki, N., Y. Tsuura, N. Namba, K. Masuda, T. Gonoi, M. Horie, Y. Seino, M. Mizuta, and S. Seino. 1995c. Cloning and functional characterization of a novel ATP-sensitive potassium channel ubiquitously expressed in rat tissues, including pancreatic islets, pituitary, skeletal muscle, and heart. *J Biol Chem*. 270:5691-5694.

Inanobe, A., T. Matsuura, A. Nakagawa, and Y. Kurachi. 2007. Structural diversity in the cytoplasmic region of G protein-gated inward rectifier K+ channels. *Channels (Austin, Tex*. 1:39-45.

Isomoto, S., C. Kondo, M. Yamada, S. Matsumoto, O. Higashiguchi, Y. Horio, Y. Matsuzawa, and Y. Kurachi. 1996. A novel sulfonylurea receptor forms with BIR (Kir6.2) a smooth muscle type ATP-sensitive K+ channel. *J Biol Chem*. 271:24321-24324.

Janbon, M., Chaptal, J., Vedel, A. and Schaap J. 1942. Accidents hypoglycemiques graves par un sulfamidothiazol (le VK ou 2254 RP). *Montpellier Med.* 21-22:441-444.

Jovanovic, S., Q. Du, S. Mukhopadhyay, R. Swingler, R. Buckley, J. McEachen, and A. Jovanovic. 2008. A patient suffering from hypokalemic periodic paralysis is deficient in skeletal muscle ATP-sensitive K channels. *Clin Transl Sci*. 1:71-74.

Kawaki, J., K. Nagashima, J. Tanaka, T. Miki, M. Miyazaki, T. Gonoi, N. Mitsuhashi, N. Nakajima, T. Iwanaga, H. Yano, and S. Seino. 1999. Unresponsiveness to glibenclamide during chronic treatment induced by reduction of ATP-sensitive K+ channel activity. *Diabetes*. 48:2001-2006.

Killian, J.A., and G. von Heijne. 2000. How proteins adapt to a membrane-water interface. *Trends Biochem. Sci.* 25:429-434.

Koster, J.C., Q. Sha, S. Shyng, and C.G. Nichols. 1999. ATP inhibition of KATP channels: control of nucleotide sensitivity by the N-terminal domain of the Kir6.2 subunit. *J Physiol*. 515:19-30.

Kuo, A., J.M. Gulbis, J.F. Antcliff, T. Rahman, E.D. Lowe, J. Zimmer, J. Cuthbertson, F.M. Ashcroft, T. Ezaki, and D.A. Doyle. 2003. Crystal structure of the potassium channel KirBac1.1 in the closed state. *Science*. 300:1922-1926.

Kyte, J., and R.F. Doolittle. 1982. A simple method for displaying the hydropathic character of a protein. *J Mol Biol*. 157:105-132.

Lawson, K., and M.J. Dunne. 2001. Peripheral channelopathies as targets for potassium channel openers. *Expert Opin Investig Drugs*. 10:1345-1359.

Li, L., J. Wang, and P. Drain. 2000. The I182 region of k(ir)6.2 is closely associated with ligand binding in K(ATP) channel inhibition by ATP. *Biophys J*. 79:841-852.

Lin, C.W., Y.W. Lin, F.F. Yan, J. Casey, M. Kochhar, E.B. Pratt, and S.L. Shyng. 2006a. Kir6.2 mutations associated with neonatal diabetes reduce expression of ATP-sensitive K+ channels: implications in disease mechanism and sulfonylurea therapy. *Diabetes*. 55:1738-1746.

Lin, C.W., F. Yan, S. Shimamura, S. Barg, and S.L. Shyng. 2005. Membrane phosphoinositides control insulin secretion through their effects on ATP-sensitive K+ channel activity. *Diabetes*. 54:2852-2858.

Lin, Y.W., J.D. Bushman, F.F. Yan, S. Haidar, C. MacMullen, A. Ganguly, C.A. Stanley, and S.L. Shyng. 2008. Destabilization of ATP-sensitive potassium channel activity by novel KCNJ11 mutations identified in congenital hyperinsulinism. *J Biol Chem*. 283:9146-9156.

Lin, Y.W., T. Jia, A.M. Weinsoft, and S.L. Shyng. 2003. Stabilization of the Activity of ATP-sensitive Potassium Channels by Ion Pairs Formed between Adjacent Kir6.2 Subunits. *J Gen Physiol*. 122:225-237.

Lin, Y.W., C. MacMullen, A. Ganguly, C.A. Stanley, and S.L. Shyng. 2006b. A novel KCNJ11 mutation associated with congenital hyperinsulinism reduces the intrinsic open probability of beta-cell ATP-sensitive potassium channels. *J Biol Chem*. 281:3006-3012.

Liou, H.H., S.S. Zhou, and C.L. Huang. 1999. Regulation of ROMK1 channel by protein kinase A via a phosphatidylinositol 4,5-bisphosphate-dependent mechanism. *Proc Natl Acad Sci U S A*. 96:5820-5825.

Logothetis, D.E., T. Jin, D. Lupyan, and A. Rosenhouse-Dantsker. 2007a. Phosphoinositide-mediated gating of inwardly rectifying K(+) channels. *Pflugers Arch*. 455:83-95.

Logothetis, D.E., D. Lupyan, and A. Rosenhouse-Dantsker. 2007b. Diverse Kir modulators act in close proximity to residues implicated in phosphoinositide binding. *J Physiol*. 582:953-965.

MacGregor, G.G., K. Dong, C.G. Vanoye, L. Tang, G. Giebisch, and S.C. Hebert. 2002. Nucleotides and phospholipids compete for binding to the C terminus of KATP channels. *Proc Natl Acad Sci U S A*. 99:2726-2731.

Margeta-Mitrovic, M., Y.N. Jan, and L.Y. Jan. 2000. A trafficking checkpoint controls GABA(B) receptor heterodimerization. *Neuron*. 27:97-106.

Markworth, E., C. Schwanstecher, and M. Schwanstecher. 2000. ATP4- mediates closure of pancreatic beta-cell ATP-sensitive potassium channels by interaction with 1 of 4 identical sites. *Diabetes*. 49:1413-1418.

Marthinet, E., A. Bloc, Y. Oka, Y. Tanizawa, B. Wehrle-Haller, V. Bancila, J.-M. Dubuis, J. Philippe, and V.M. Schwitzgebel. 2005. Severe Congenital Hyperinsulinism Caused by a Mutation in the Kir6.2

Subunit of the Adenosine Triphosphate-Sensitive Potassium Channel Impairing Trafficking and Function. *J Clin Endocrinol Metab*. 90:5401-5406.

Masia, R., J.C. Koster, S. Tumini, F. Chiarelli, C. Colombo, C.G. Nichols, and F. Barbetti. 2007. An ATP-binding mutation (G334D) in KCNJ11 is associated with a sulfonylurea-insensitive form of developmental delay, epilepsy, and neonatal diabetes. *Diabetes*. 56:328-336.

Masia, R., and C.G. Nichols. 2008. Functional clustering of mutations in the dimer interface of the nucleotide binding folds of the sulfonylurea receptor. *J Biol Chem*. 283:30322-30329.

Matsuo, M., N. Kioka, T. Amachi, and K. Ueda. 1999. ATP binding properties of the nucleotide-binding folds of SUR1. *J Biol Chem*. 274:37479-37482.

Matsuo, M., K. Tanabe, N. Kioka, T. Amachi, and K. Ueda. 2000. Different binding properties and affinities for ATP and ADP among sulfonylurea receptor subtypes, SUR1, SUR2A, and SUR2B. *J Biol Chem*. 275:28757-28763.

Mikhailov, M.V., J.D. Campbell, H. de Wet, K. Shimomura, B. Zadek, R.F. Collins, M.S. Sansom, R.C. Ford, and F.M. Ashcroft. 2005. 3-D structural and functional characterization of the purified KATP channel complex Kir6.2-SUR1. *Embo J*. 24:4166-4175.

Moreau, C., H. Jacquet, A.L. Prost, N. D'Hahan, and M. Vivaudou. 2000. The molecular basis of the specificity of action of K(ATP) channel openers. *Embo J*. 19:6644-6651.

Neagoe, I., and B. Schwappach. 2005. Pas de deux in groups of four--the biogenesis of KATP channels. *J Mol Cell Cardiol*. 38:887-894.

Neher, E., and C.F. Stevens. 1977. Conductance fluctuations and ionic pores in membranes. *Annu Rev Biophys Bioeng*. 6:345-381.

Nelson, D.A., L. Aguilar-Bryan, and J. Bryan. 1992. Specificity of photolabeling of beta-cell membrane proteins with an 125I-labeled glyburide analog. *J Biol Chem*. 267:14928-14933.

Nichols, C.G. 2006. KATP channels as molecular sensors of cellular metabolism. *Nature*. 440:470-476.

Nichols, C.G., W.J. Lederer, and M.B. Cannell. 1991. ATP dependence of KATP channel kinetics in isolated membrane patches from rat ventricle. *Biophys J*. 60:1164-1177.

Nichols, C.G., S.L. Shyng, A. Nestorowicz, B. Glaser, J.P.t. Clement, G. Gonzalez, L. Aguilar-Bryan, M.A. Permutt, and J. Bryan. 1996. Adenosine diphosphate as an intracellular regulator of insulin secretion. *Science*. 272:1785-1787.

Nishida, M., M. Cadene, B.T. Chait, and R. MacKinnon. 2007. Crystal structure of a Kir3.1-prokaryotic Kir channel chimera. *Embo J*. 26:4005-4015.

Nishida, M., and R. MacKinnon. 2002. Structural basis of inward rectification: cytoplasmic pore of the G protein-gated inward rectifier GIRK1 at 1.8 A resolution. *Cell*. 111:957-965.

Noma, A. 1983. ATP-regulated K+ channels in cardiac muscle. *Nature*. 305:147-148.

Olson, T.M., A.E. Alekseev, C. Moreau, X.K. Liu, L.V. Zingman, T. Miki, S. Seino, S.J. Asirvatham, A. Jahangir, and A. Terzic. 2007. KATP channel mutation confers risk for vein of Marshall adrenergic atrial fibrillation. *Nat Clin Pract Cardiovasc Med*. 4:110-116.

Orie, N.N., A.M. Thomas, B.A. Perrino, A. Tinker, and L.H. Clapp. 2009. Ca2+/calcineurin regulation of cloned vascular K ATP channels: crosstalk with the protein kinase A pathway. *Br J Pharmacol*. 157:554-564.

Partridge, C.J., D.J. Beech, and A. Sivaprasadarao. 2001. Identification and pharmacological correction of a membrane trafficking defect associated with a mutation in the sulfonylurea receptor causing familial hyperinsulinism. *J Biol Chem*. 276:35947-35952.

Pearson, E.R., I. Flechtner, P.R. Njolstad, M.T. Malecki, S.E. Flanagan, B. Larkin, F.M. Ashcroft, I. Klimes, E. Codner, V. Iotova, A.S. Slingerland, J. Shield, J.J. Robert, J.J. Holst, P.M. Clark, S. Ellard, O. Sovik, M. Polak, and A.T. Hattersley. 2006. Switching from insulin to oral sulfonylureas in patients with diabetes due to Kir6.2 mutations. *N Engl J Med*. 355:467-477.

Pegan, S., C. Arrabit, W. Zhou, W. Kwiatkowski, A. Collins, P.A. Slesinger, and S. Choe. 2005. Cytoplasmic domain structures of Kir2.1 and Kir3.1 show sites for modulating gating and rectification. *Nat Neurosci*. 8:279-287.

Pinney, S.E., C. MacMullen, S. Becker, Y.W. Lin, C. Hanna, P. Thornton, A. Ganguly, S.L. Shyng, and C.A. Stanley. 2008. Clinical characteristics and biochemical mechanisms of congenital hyperinsulinism associated with dominant KATP channel mutations. *J Clin Invest*. 118:2877-2886.

Pratt, E.B., F.F. Yan, J.W. Gay, C.A. Stanley, and S.L. Shyng. 2009. Sulfonylurea receptor 1 mutations that cause opposite insulin secretion defects with chemical chaperone exposure. *J Biol Chem*. 284:7951-7959.

Proks, P., J.F. Antcliff, J. Lippiat, A.L. Gloyn, A.T. Hattersley, and F.M. Ashcroft. 2004. Molecular basis of Kir6.2 mutations associated with neonatal diabetes or neonatal diabetes plus neurological features. *Proc Natl Acad Sci U S A*. 101:17539-17544.

Proks, P., A.L. Arnold, J. Bruining, C. Girard, S.E. Flanagan, B. Larkin, K. Colclough, A.T. Hattersley, F.M. Ashcroft, and S. Ellard. 2006. A heterozygous activating mutation in the sulphonylurea receptor SUR1 (ABCC8) causes neonatal diabetes. *Hum Mol Genet*. 15:1793-1800.

Proks, P., C.E. Capener, P. Jones, and F.M. Ashcroft. 2001. Mutations within the P-loop of Kir6.2 modulate the intraburst kinetics of the ATP-sensitive potassium channel. *J Gen Physiol*. 118:341-353.

Proks, P., C. Girard, and F.M. Ashcroft. 2005a. Functional effects of KCNJ11 mutations causing neonatal diabetes: enhanced activation by MgATP. *Hum Mol Genet*. 14:2717-2726.

Proks, P., C. Girard, S. Haider, A.L. Gloyn, A.T. Hattersley, M.S. Sansom, and F.M. Ashcroft. 2005b. A gating mutation at the internal mouth of the Kir6.2 pore is associated with DEND syndrome. *EMBO Rep*. 6:470-475.

Proks, P., K. Shimomura, T.J. Craig, C.A. Girard, and F.M. Ashcroft. 2007. Mechanism of action of a sulphonylurea receptor SUR1 mutation (F132L) that causes DEND syndrome. *Hum Mol Genet*. 16:2011-2019.

Qin, D.Y., M. Takano, and A. Noma. 1989. Kinetics of ATP-sensitive K+ channel revealed with oil-gate concentration jump method. *American Journal of Physiology*. 257:H1624-1633.

Raab-Graham, K.F., L.J. Cirilo, A.A. Boettcher, C.M. Radeke, and C.A. Vandenberg. 1999. Membrane topology of the amino-terminal region of the sulfonylurea receptor. *J Biol Chem*. 274:29122-29129.

Rasband, W.S., ImageJ, U. S. National Institutes of Health, Bethesda,, and U. Maryland, http://rsb.info.nih.gov/ij/, 1997-2009.

Rees, D.C., E. Johnson, and O. Lewinson. 2009. ABC transporters: the power to change. *Nat Rev Mol Cell Biol*. 10:218-227.

Reimann, F., S.J. Tucker, P. Proks, and F.M. Ashcroft. 1999. Involvement of the n-terminus of Kir6.2 in coupling to the sulphonylurea receptor. *J Physiol*. 518:325-336.

Rohacs, T., C.M. Lopes, T. Jin, P.P. Ramdya, Z. Molnar, and D.E. Logothetis. 2003. Specificity of activation by phosphoinositides determines lipid regulation of Kir channels. *Proc Natl Acad Sci U S A*. 100:745-750.

Rorsman, P., and G. Trube. 1985. Glucose dependent K+-channels in pancreatic beta-cells are regulated by intracellular ATP. *Pflugers Arch*. 405:305-309.

Sagen, J.V., H. Raeder, E. Hathout, N. Shehadeh, K. Gudmundsson, H. Baevre, D. Abuelo, C. Phornphutkul, J. Molnes, G.I. Bell, A.L. Gloyn, A.T. Hattersley, A. Molven, O. Sovik, and P.R. Njolstad. 2004. Permanent neonatal diabetes due to mutations in KCNJ11 encoding Kir6.2: patient characteristics and initial response to sulfonylurea therapy. *Diabetes*. 53:2713-2718.

Sakura, H., C. Ammala, P.A. Smith, F.M. Gribble, and F.M. Ashcroft. 1995. Cloning and functional expression of the cDNA encoding a novel ATP- sensitive potassium channel subunit expressed in pancreatic beta-cells, brain, heart and skeletal muscle. *FEBS Lett*. 377:338-344.

Sanchez, J.A., T. Gonoi, N. Inagaki, T. Katada, and S. Seino. 1998. Modulation of reconstituted ATP-sensitive K(+)-channels by GTP-binding proteins in a mammalian cell line. *J Physiol*. 507 (Pt 2):315-324.

Schulze, D., T. Krauter, H. Fritzenschaft, M. Soom, and T. Baukrowitz. 2003. Phosphatidylinositol 4,5-bisphosphate (PIP2) modulation of ATP and pH sensitivity in Kir channels. A tale of an active and a silent PIP2 site in the N terminus. *J Biol Chem*. 278:10500-10505.

Schwanstecher, M., S. Loser, F. Chudziak, and U. Panten. 1994a. Identification of a 38-kDa high affinity sulfonylurea-binding peptide in insulin-secreting cells and cerebral cortex. *J Biol Chem*. 269:17768-17771.

Schwanstecher, M., C. Schwanstecher, C. Dickel, F. Chudziak, A. Moshiri, and U. Panten. 1994b. Location of the sulphonylurea receptor at the cytoplasmic face of the beta-cell membrane. *Br J Pharmacol*. 113:903-911.

Schwanstecher, M., C. Sieverding, H. Dorschner, I. Gross, L. Aguilar-Bryan, C. Schwanstecher, and J. Bryan. 1998. Potassium channel openers require ATP to bind to and act through sulfonylurea receptors. *Embo J*. 17:5529-5535.

Schwappach, B., N. Zerangue, Y.N. Jan, and L.Y. Jan. 2000. Molecular basis for K(ATP) assembly: transmembrane interactions mediate association of a K+ channel with an ABC transporter. *Neuron*. 26:155-167.

Shield, J.P. 2000. Neonatal diabetes: new insights into aetiology and implications. *Horm Res*. 53 Suppl 1:7-11.

Shimomura, K., G.P. de Nanclares, C. Foutinou, M. Caimari, L. Castano, and F.M. Ashcroft. 2010. The first clinical case of a mutation at residue K185 of Kir6.2 (KCNJ11): a major ATP-binding residue. *Diabet Med*. 27:225-229.

Shimomura, K., C.A. Girard, P. Proks, J. Nazim, J.D. Lippiat, F. Cerutti, R. Lorini, S. Ellard, A.T. Hattersley, F. Barbetti, and F.M. Ashcroft. 2006. Mutations at the same residue (R50) of Kir6.2 (KCNJ11) that cause neonatal diabetes produce different functional effects. *Diabetes*. 55:1705-1712.

Shyng, S., T. Ferrigni, and C.G. Nichols. 1997a. Control of rectification and gating of cloned KATP channels by the Kir6.2 subunit. *J Gen Physiol*. 110:141-153.

Shyng, S., T. Ferrigni, and C.G. Nichols. 1997b. Regulation of KATP channel activity by diazoxide and MgADP. Distinct functions of the two nucleotide binding folds of the sulfonylurea receptor. *J Gen Physiol*. 110:643-654.

Shyng, S., and C.G. Nichols. 1997. Octameric stoichiometry of the KATP channel complex. *J Gen Physiol*. 110:655-664.

Shyng, S.L., C.A. Cukras, J. Harwood, and C.G. Nichols. 2000. Structural determinants of PIP(2) regulation of inward rectifier K(ATP) channels. *J Gen Physiol*. 116:599-608.

Shyng, S.L., T. Ferrigni, J.B. Shepard, A. Nestorowicz, B. Glaser, M.A. Permutt, and C.G. Nichols. 1998. Functional analyses of novel mutations in the sulfonylurea receptor 1 associated with persistent hyperinsulinemic hypoglycemia of infancy. *Diabetes*. 47:1145-1151.

Shyng, S.L., and C.G. Nichols. 1998. Membrane phospholipid control of nucleotide sensitivity of KATP channels. *Science*. 282:1138-1141.

Sigworth, F.J. 1980. The variance of sodium current fluctuations at the node of Ranvier. *J Physiol*. 307:97-129.

Simossis, V.A., and J. Heringa. 2005. PRALINE: a multiple sequence alignment toolbox that integrates homology-extended and secondary structure information. *Nucl. Acids Res.* 33:W289-294.

Slingerland, A.S., W. Hurkx, K. Noordam, S.E. Flanagan, J.W. Jukema, L.C. Meiners, G.J. Bruining, A.T. Hattersley, and M. Hadders-Algra. 2008. Sulphonylurea therapy improves cognition in a patient with the V59M KCNJ11 mutation. *Diabet Med*. 25:277-281.

Slingerland, A.S., R. Nuboer, M. Hadders-Algra, A.T. Hattersley, and G.J. Bruining. 2006. Improved motor development and good long-term glycaemic control with sulfonylurea treatment in a patient with the syndrome of intermediate developmental delay, early-onset generalised epilepsy and neonatal diabetes associated with the V59M mutation in the KCNJ11 gene. *Diabetologia*. 49:2559-2563.

Song, D.K., and F.M. Ashcroft. 2001. ATP modulation of ATP-sensitive potassium channel ATP sensitivity varies with the type of SUR subunit. *J Biol Chem*. 276:7143-7149.

Stansfeld, P.J., R. Hopkinson, F.M. Ashcroft, and M.S. Sansom. 2009. PIP(2)-binding site in Kir channels: definition by multiscale biomolecular simulations. *Biochemistry*. 48:10926-10933.

Sturgess, N.C., M.L. Ashford, D.L. Cook, and C.N. Hales. 1985. The sulphonylurea receptor may be an ATP-sensitive potassium channel. *Lancet*. 2:474-475.

Suchi, M., C.M. MacMullen, P.S. Thornton, N.S. Adzick, A. Ganguly, E.D. Ruchelli, and C.A. Stanley. 2006. Molecular and immunohistochemical analyses of the focal form of congenital hyperinsulinism. *Mod Pathol*. 19:122-129.

Suh, B.C., and B. Hille. 2008. PIP2 is a necessary cofactor for ion channel function: how and why? *Annu Rev Biophys*. 37:175-195.

Tammaro, P., C. Girard, J. Molnes, P.R. Njolstad, and F.M. Ashcroft. 2005. Kir6.2 mutations causing neonatal diabetes provide new insights into Kir6.2-SUR1 interactions. *Embo J*. 24:2318-2330.

Tammaro, P., P. Proks, and F.M. Ashcroft. 2006. Functional effects of naturally occurring KCNJ11 mutations causing neonatal diabetes on cloned cardiac KATP channels. *J Physiol*. 571:3-14.

Tanabe, K., S.J. Tucker, M. Matsuo, P. Proks, F.M. Ashcroft, S. Seino, T. Amachi, and K. Ueda. 1999. Direct photoaffinity labeling of the Kir6.2 subunit of the ATP- sensitive K+ channel by 8-azido-ATP. *J Biol Chem*. 274:3931-3933.

Taschenberger, G., A. Mougey, S. Shen, L.B. Lester, S. LaFranchi, and S.L. Shyng. 2002. Identification of a familial hyperinsulinism-causing mutation in the sulfonylurea receptor 1 that prevents normal trafficking and function of KATP channels. *J Biol Chem*. 277:17139-17146.

Thomas, P.M., G.J. Cote, N. Wohllk, B. Haddad, P.M. Mathew, W. Rabl, L. Aguilar-Bryan, R.F. Gagel, and J. Bryan. 1995. Mutations in the sulfonylurea receptor gene in familial persistent hyperinsulinemic hypoglycemia of infancy. *Science*. 268:426-429.

Tonini, G., C. Bizzarri, R. Bonfanti, M. Vanelli, F. Cerutti, E. Faleschini, F. Meschi, F. Prisco, E. Ciacco, M. Cappa, C. Torelli, V. Cauvin, S. Tumini, D. Iafusco, and F. Barbetti. 2006. Sulfonylurea treatment outweighs insulin therapy in short-term metabolic control of patients with permanent neonatal diabetes mellitus due to activating mutations of the KCNJ11 (KIR6.2) gene. *Diabetologia*. 49:2210-2213.

Tornovsky, S., A. Crane, K.E. Cosgrove, K. Hussain, J. Lavie, M. Heyman, Y. Nesher, N. Kuchinski, E. Ben-Shushan, O. Shatz, E. Nahari, T. Potikha, D. Zangen, Y. Tenenbaum-Rakover, L. de Vries, J. Argente, R. Gracia, H. Landau, A. Eliakim, K. Lindley, M.J. Dunne, L. Aguilar-Bryan, and B. Glaser. 2004. Hyperinsulinism of infancy: novel ABCC8 and KCNJ11 mutations and evidence for additional locus heterogeneity. *J Clin Endocrinol Metab*. 89:6224-6234.

Trapp, S., S. Haider, P. Jones, M.S. Sansom, and F.M. Ashcroft. 2003. Identification of residues contributing to the ATP binding site of Kir6.2. *Embo J*. 22:2903-2912.

Tucker, S.J., F.M. Gribble, C. Zhao, S. Trapp, and F.M. Ashcroft. 1997. Truncation of Kir6.2 produces ATP-sensitive K+ channels in the absence of the sulphonylurea receptor. *Nature*. 387:179-183.

Tusnady, G.E., E. Bakos, A. Varadi, and B. Sarkadi. 1997. Membrane topology distinguishes a subfamily of the ATP-binding cassette (ABC) transporters. *FEBS Lett*. 402:1-3.

Uhde, I., A. Toman, I. Gross, C. Schwanstecher, and M. Schwanstecher. 1999. Identification of the potassium channel opener site on sulfonylurea receptors. *J Biol Chem*. 274:28079-28082.

Vaxillaire, M., A. Dechaume, K. Busiah, H. Cave, S. Pereira, R. Scharfmann, G.P. de Nanclares, L. Castano, P. Froguel, and M. Polak. 2007. New ABCC8 mutations in relapsing neonatal diabetes and clinical features. *Diabetes*. 56:1737-1741.

Vila-Carriles, W.H., G. Zhao, and J. Bryan. 2007. Defining a binding pocket for sulfonylureas in ATP-sensitive potassium channels. *Faseb J*. 21:18-25.

Wang, C., K. Wang, W. Wang, Y. Cui, and Z. Fan. 2002. Compromised ATP binding as a mechanism of phosphoinositide modulation of ATP-sensitive K(+) channels. *FEBS Lett*. 532:177-182.

Xie, L.H., S.A. John, B. Ribalet, and J.N. Weiss. 2007. Activation of inwardly rectifying potassium (Kir) channels by phosphatidylinosital-4,5-bisphosphate (PIP2): interaction with other regulatory ligands. *Prog Biophys Mol Biol*. 94:320-335.

Yan, F., C.W. Lin, E. Weisiger, E.A. Cartier, G. Taschenberger, and S.L. Shyng. 2004. Sulfonylureas correct trafficking defects of ATP-sensitive potassium channels caused by mutations in the sulfonylurea receptor. *J Biol Chem*. 279:11096-11105.

Yan, F.F., J. Casey, and S.L. Shyng. 2006. Sulfonylureas correct trafficking defects of disease-causing ATP-sensitive potassium channels by binding to the channel complex. *J Biol Chem*. 281:33403-33413.

Yan, F.F., C.W. Lin, E.A. Cartier, and S.L. Shyng. 2005. Role of ubiquitin-proteasome degradation pathway in biogenesis efficiency of {beta}-cell ATP-sensitive potassium channels. *Am J Physiol Cell Physiol*. 289:C1351-1359.

Yan, F.F., Y.W. Lin, C. MacMullen, A. Ganguly, C.A. Stanley, and S.L. Shyng. 2007. Congenital hyperinsulinism associated ABCC8 mutations that cause defective trafficking of ATP-sensitive K+ channels: identification and rescue. *Diabetes*. 56:2339-2348.

Yi, B.A., D.L. Minor, Jr., Y.F. Lin, Y.N. Jan, and L.Y. Jan. 2001. Controlling potassium channel activities: Interplay between the membrane and intracellular factors. *Proc Natl Acad Sci U S A*. 98:11016-11023.

Zerangue, N., B. Schwappach, Y.N. Jan, and L.Y. Jan. 1999. A new ER trafficking signal regulates the subunit stoichiometry of plasma membrane K(ATP) channels. *Neuron*. 22:537-548.

APPENDIX

THE CELL GIVETH AND THE CELL TAKETH AWAY: AN OVERVIEW OF NOTCH PATHWAY ACTIVATION BY ENDOCYTIC TRAFFICKING OF LIGANDS AND RECEPTORS

Emily B. Pratt[a], Jill S. Wentzell[a], Julia E. Maxson[b], Lauren Courter[a], Dennis Hazelett[c], Jan L. Christian[b]

[a]Center for Research on Occupational and Environmental Toxicology
[b] Department of Cell and Developmental Biology
[c] Department of Integrative Biosciences

Oregon Health and Science University, School of Medicine, Portland, Oregon, USA

EB Pratt and JS Wentzell contributed equally

Corresponding author: Jan L. Christian

Appendix is a manuscript as it appears in the original paper published in the journal Acta Histochemica, January 30, 2010.

I wrote the sections "Receptor endocytosis: a mechanism to restrict ligand-independent Notch activation?" and "Ligand endocytosis: a means of mechanical strain?" JS Wentzell wrote the sections "Ligand endocytosis: required for ligand activation?" and "Receptor endocytosis: required for γ-secretase cleavage of Notch?" JE Maxson wrote the introduction. D. Hazelett and L. Courter prepared the figures. I also revised the manuscript according to the reviews suggestions.

Abstract

Notch signaling is firmly established as a form of cell-to-cell communication that is critical throughout development. Dysregulation of Notch has been linked to cancer and developmental disorders, making it an important target for therapeutic intervention. One aspect of this pathway that sets it apart from others is its apparent reliance on endocytosis by signal-sending *and* signal-receiving cells. The subtle details of endocytosis-mediated molecular processing within both ligand- and receptor-presenting cells that are required for the Notch signal to maintain fidelity remain unclear. The endosomal system has long been known to play an important role in terminating signal transduction by directing lysosomal trafficking and degradation of cell surface receptors. More recently, endocytic trafficking has also been shown to be critical for activation of signaling. This review highlights four models of endocytic processing in the context of the Notch pathway. In ligand-presenting cells, endocytosis may be required for pre-processing of ligands to make them competent for interaction with Notch receptors and/or for exerting a pulling force on the ligand/Notch complex. In receptor-presenting cells, endocytosis may be a prerequisite for Notch cleavage and thus activation and/or it could be a means of limiting ligand-independent Notch activation. Recent advances in our understanding of how and why endocytosis of Notch receptors and ligands is required for activation and termination of signaling during normal development and in disease states are discussed.

Introduction

In the past decade, endocytic trafficking has been shown to be a critical component of many signaling pathways — including the well-studied Notch signaling pathway, which is essential for a wide range of developmental processes. Many features of the Notch signal transduction cascade have been elucidated, but a key question that remains to be fully answered is why endocytic trafficking is required in both signal sending and receiving cells for the pathway to function. This brief review will cover what is known about the role of endocytosis in Notch signaling and will highlight questions remaining in the field.

Several recent reviews provide an in depth description of the core features of Notch signaling (Kopan and Ilagan, 2009; Tien et al., 2009). Briefly, Notch proteins are single pass transmembrane receptors that transduce signals via a unique mechanism involving receptor proteolysis, resulting in the release of an active intracellular Notch fragment. The extracellular domain of the prototypical Notch receptor contains tandem arrays of Epidermal Growth Factor (EGF[1])-like repeats and a conserved negative regulatory region (NRR) that consists of three Lin12/Notch repeats (LNRs) and a heterodimerization (HD) domain (Fig. 1A). The NRR functions to prevent ligand-independent activation of Notch, as illustrated by the fact that mutations within this domain generate a constitutively active receptor, leading to developmental defects and cancers (Greenwald and Seydoux, 1990; Weng et al., 2004). During intracellular

Abbreviations used:
EGF –Epidermal Growth Factor
NRR – negative regulatory region (structural domain of Notch that shields S2 cleavage site in absence of ligand binding and activation)
LNR – Lin12/Notch repeat
HD – heterodimerization domain
NECD – Notch extracellular domain
NICD – Notch intracellular domain (the portion of Notch that traffics and signals to the nucleus)
CSL – CBF/Su(H)/Lag-1
DSL – Delta/Serrate/Lag-2 (family of ligands that activate Notch)
Lgd - lethal giant disks
Hrs - hepatocyte growth factor-regulated tyrosine kinase substrate
ESCRT – endosomal sorting complexes required for transport
S1 cleavage – (furin-mediated cleavage resulting in heterodimerization of Notch)
S2 cleavage – (ADAM/TACE cleavage resulting in release of NECD fragment)
S3 and S4 cleavage – (γ-secretase cleavages resulting in release of NICD fragment)

receptor maturation, mammalian Notch is cleaved at the S1 site within the HD domain by furin, or a related member of the proprotein convertase family. This generates extracellular and transmembrane subunits that are held together by the HD domain (Fig. 1A). Furin cleavage is not required for mammalian Notch to reach the cell surface (Bush et al., 2001), but it is required for activation of Notch signaling. Curiously, *Drosophila* Notch lacks a consensus furin cleavage site and only the uncleaved form is detected on the cell surface (Kidd and Lieber, 2002), suggesting that pathway activation differs between vertebrates and invertebrates.

Ligands of the Delta/Serrate/Lag-2 (DSL) family activate Notch. These ligands are membrane-anchored proteins and thus receptor activation requires cell-cell contact in most circumstances. Ligand binding triggers a sequential cascade of cleavages within Notch, named S2, S3 and S4 (Fig. 1B). The S2 site, which resides within the carboxyl (C)-terminal portion of the HD domain, is cleaved by members of the ADAM/TACE metalloprotease family (Mumm et al., 2000). This cleavage releases the Notch extracellular domain (NECD) from the heterodimer (Figure 1B) (Kopan et al., 1996; Struhl and Adachi, 1998). A recent structural analysis showed that the S2 cleavage site is normally masked by extensive interdomain interactions within the NRR (Gordon et al., 2007). Thus, ligand induced conformational changes in the Notch receptor are presumably required to expose the S2 site for ADAM-mediated cleavage. S2 cleavage is a prerequisite for subsequent intramembranous cleavage of Notch at the S3 and S4 sites by the γ-secretase complex. These cleavages release the Notch intracellular domain (NICD) (Struhl and Adachi, 2000; Fiuza and Arias, 2007). The NICD then translocates to the nucleus, where it interacts with members of the CBF1/Su(H)/Lag-1 (CSL) family of transcription factors, displacing co-repressors and recruiting co-activators to activate transcription of Notch target genes (Fortini and Artavanis-Tsakonas, 1994; Fiuza and Arias, 2007).

Studies in *Drosophila* have shown that dynamin-dependent endocytosis is essential in both the ligand- and receptor-presenting cells for successful transduction of Notch signals (Seugnet et al., 1997), and several models have since been proposed to explain this requirement (illustrated in Figure 2). First, endocytosis has been proposed to direct DSL ligands to an intracellular compartment where they undergo essential post-translational modifications prior to recycling to the cell surface for receptor activation (Fig. 2A) (Wang and Struhl, 2004, 2005). Alternatively, or perhaps in addition, endocytosis of DSL ligand bound to the Notch receptor may be necessary to provide a pulling force that dissociates the Notch heterodimer and/or induces a conformational change, thereby exposing the S2 ADAM cleavage site (Fig. 2B) (Parks et al., 2000; Nichols et al., 2007). In the signal-receiving cell, Notch endocytosis may be required for γ-secretase cleavage of Notch, perhaps because the enzyme complex is primarily active in an intracellular compartment (Fig. 2C) (Gupta-Rossi et al., 2004). Finally, Notch receptor endocytosis and lysosomal targeting may be required to prevent "accidental" ligand-independent activation of Notch (Fig. 2D) (Childress et al., 2006; Gallagher and Knoblich, 2006; Jaekel and Klein, 2006). In the following sections, we present evidence for and against each of these models, which are not mutually exclusive.

Ligand endocytosis: required for ligand activation?

As summarized above, the requirement for endocytosis in signal sending cells might reflect a need to internalize the ligand prior to receptor interaction in order to generate an active ligand and/or a need to internalize the ligand-receptor complex in order to activate signaling. There is good evidence supporting both hypotheses and, indeed, endocytosis in the signal-presenting cell may serve multiple functions. The observation that DSL ligand activation requires a specialized endocytic pathway, rather than simple bulk endocytosis, supports the first model.

However, the precise effect endocytosis is having on ligand activity remains unresolved. Evidence and proposed mechanisms for this model are discussed in this section.

Endocytosis of DSL ligand is triggered by monoubiquitination of its cytoplasmic tail, by the E3 ubiquitin ligases Neuralized and Mindbomb (Wang and Struhl, 2004). Ubiquitination targets DSL ligands for Epsin-mediated endocytosis, which is essential for signaling. Epsin proteins facilitate membrane curvature in addition to targeting membrane proteins for endocytosis. DSL ligands generated in Epsin mutant cells are efficiently transported to the cell surface, but cannot signal to their neighbors (Wang and Struhl, 2004). Because bulk endocytosis, which does not require Epsin function, is insufficient to facilitate DSL-Notch signaling, these results have been interpreted to suggest that Epsin targets ligands to a special endocytic compartment that they must enter to acquire signaling activity.

Recent studies suggest that ligand recycling may be a prerequisite for receptor binding. An ubiquitination-defective mutant form of the mouse Delta homolog, Dll1, can be internalized, albeit not as efficiently as the wild type species, but is unable to recycle back to the cell surface or to bind and activate Notch in neighboring cells (Heuss et al., 2008). While these studies demonstrate the importance of ligand recycling for receptor binding and activation, the mechanism by which this generates a more potent ligand remains a mystery. One possibility is that DSL ligands undergo post-translational modification of the extracellular domain within a specialized intracellular compartment, and that this enhances receptor binding (Fig. 2A). Consistent with this possibility, a potential DSL cleavage fragment is detected in wild type cells, but not in Epsin mutant cells, which cannot endocytose ligands (Wang and Struhl, 2004). A second possibility is that DSL ligands are initially diffuse over the entire surface of the cell, but are recycled to the outside of the cell in a clustered state, and that this enhances the strength of ligand-receptor interactions. If endocytosis-mediated clustering is occurring, interactions of

monomers within endocytic vesicles may promote multimer formation, or monomers could become concentrated and interact upon recycling to localized plasma membrane domains. This model is supported by the finding that soluble forms of Delta are unable to activate Notch unless they are preclustered (Hicks et al., 2002). Finally, ligands may be recycled to specific lipid microdomains that contain essential cofactors, or are otherwise optimized for signal transmission. Lipid rafts are one example of specialized membrane domains that are believed to function as signaling platforms (Lajoie et al., 2009). Mouse Dll1 is partially localized to lipid raft microdomains, whereas an ubiquitin-defective, recycling incompetent form of Dll1 is not (Heuss et al., 2008). The latter ligand is unable to signal, consistent with the idea that localization to particular microdomains is important for signal transmission and is dependent on endocytosis.

It seems likely from these results that at least some DSL ligands must travel through the endocytic pathway in order to become active Notch ligands. This theory does not rule out the potential requirement for endocytosis during interaction with the Notch receptor. It is possible that DSL ligands undergo two rounds of endocytosis, the first to generate an active ligand and the second to generate an active receptor, as discussed below.

Ligand endocytosis: a means of mechanical strain?

A second hypothesis for why endocytosis in the signal-presenting cell is essential is that ligand induced mechanical uncoupling of the extracellular and transmembrane domains of Notch is critical for efficient DSL-Notch signaling. Such a model features the endocytosis of DSL bound to Notch by the ligand-presenting cell, which, in turn generates a pulling force necessary for mechanical uncoupling of the ligand-bound Notch extracellular domain (NECD) from the Notch transmembrane domain (Fig. 2B). This uncoupling subsequently unmasks the S2 ADAM cleavage site and allows Notch receptor processing and, thus, intracellular signaling.

The initial clues for ligand-endocytosis-mediated Notch activation were provided by the observation that endocytosis-deficient clones of cells in *Drosophila* behave in a manner consistent with an inability to either send or receive Notch signals (Seugnet et al., 1997; Parks et al., 2000). In addition, signaling required the separation of the NECD and NICD into cellular compartments within the signal-sending (called 'trans-endocytosis") and signal-receiving cells, respectively, in such clones (Parks et al., 2000). Trans-endocytosis is also seen during Notch activation in mammals (Parks et al., 2000; Nichols et al., 2007): NECD and ligand colocalize in intracellular vesicles of the ligand-sending cell.

A potential structural basis for the mechanical force uncoupling model was recently discovered in the crystal structure of a modified human Notch protein (Gordon et al., 2007). The crystal structure provided clues to the mechanism of auto-inhibition by the extracellular LNR domains that suppress ligand-independent signaling at the plasma membrane (Weinmaster, 1997). The presence of the globular LNR domains in a solvent-inaccessible pocket surrounding the critical S2 cleavage site supports a model in which major conformational changes are necessary to expose the S2 site to allow for metalloprotease cleavage, which is a prerequisite for the subsequent γ-secretase mediated cleavage that generates the active NICD signaling molecule. It is unlikely that minor allosteric effects would be sufficient to disrupt the broad and stable interactions of the S2 cleavage site and LNR domains.

If force generated by the signal-sending cell is required to activate Notch on the receiving cell, then one would predict that endocytosis-deficient DSL ligands would fail to activate Notch. Analysis of endocytosis-incompetent *delta* mutants is indeed consistent with this model (Parks et al., 2006). Delta molecules lacking their intracellular domain (*delta*ΔICD) can traffic to the plasma membrane but are unable to activate Notch. Endocytic localization of *delta*ΔICD is not observed in these situations and it is reasonable to infer that trans-endocytosis fails to occur.

The finding that *delta*ΔICD expressing cells retain their ability to aggregate with Notch expressing cells suggests that DSL endocytosis is not required for ligand-receptor interactions *in vivo*, and hence, that these interactions are not sufficient to activate signaling (with some caveats, see discussion below). Further evidence that *delta*Δ*ICD* can bind endogenous Notch receptors was provided by the demonstration of its ability to act as a dominant negative in several in vivo contexts, including *Drosophila*, *Xenopus* and chicken (Chitnis et al., 1995; Sun and Artavanis-Tsakonas, 1996; Henrique et al., 1997). In these systems *delta*Δ*ICD* induces an overabundance of neuronal tissue — the classic 'neurogenic' phenotype that is characteristic of impaired Notch signaling.

These observations appear superficially at odds with earlier cell culture experiments. Trans-endocytosis observed in *Drosophila* cell culture was shown to involve translocation of full-length Notch into Delta and Serrate expressing cells in the presence of canonical Notch signal activation (Klueg et al., 1998). However, saturation of processing and signaling machinery in the context of overexpression experiments is a potentially serious confound to these experiments. There is, in fact, evidence that some limiting components of the *Drosophila* delta-notch signaling pathway exist that can be titrated out in overexpression studies (Selkoe and Kopan, 2003). It is therefore possible that trans-endocytosis of the NECD fragment also occurred in the above experiments, (and triggered the signal activation) but was not observed due to abundance of unprocessed/full-length Notch.

In an attempt to address this issue more rigorously, Nichols et al. performed a quantitative analysis of the NECD-to-NICD ratio in the ligand-presenting cells in a mammalian cell culture system expressing wild type proteins (Nichols et al., 2007). Their careful examination of relative amounts of mammalian NECD and NICD that undergo trans-endocytosis in the presence or absence of pharmacological inhibition of S2 or S3 cleavage showed that the majority of trans-

endocytosed Notch consists of NECD independent of NICD. These results are consistent with the finding that separation of the two halves of Notch is sufficient to activate signaling (Rand et al., 2000). Still unresolved, however, is whether trans-endocytosis of S1-cleaved Notch occurs prior to or plays a causal role in S2 cleavage. There is good evidence that S2 cleavage does not occur until after ligand binding (Mumm et al., 2000), but the temporal relationship between dissociation of S1-cleaved heterodimeric forms of Notch and S2 processing has yet to be elucidated. It is possible to have NECD trans-endocytosis in the absence of S2 cleavage, but this may not represent the normal sequence of events. Biochemical experiments that follow the short peptide fragment between the S1 and S2 cleavage sites could shed light on this matter. Trans-endocytosis of that peptide fragment would be strong evidence that S2 cleavage occurs in parallel or prior to any mechanical strain; alternatively, shedding of the small peptide into the extracellular space or internalization into the signal-receiving cell would be consistent with S2 cleavage following NECD trans-endocytosis.

Unlike its mammalian homologue, *Drosophila* Notch exists on the cell surface predominantly in the uncleaved, full-length form, and appears to lack a consensus motif for S1 cleavage (Kidd and Lieber, 2002). It follows that S2, rather than S1, cleavage must be necessary for NECD trans-endocytosis in flies, unless there is a smaller population of heterodimeric Notch that constitutes the active form of the receptor. There is experimental evidence for the presence of heterodimeric Notch in *Drosophila*, most notably the finding that divalent cation-chelation leads to the release of NECD even when added in the presence of protease inhibitors (Rand et al., 2000). Because the structural integrity of the LNR domain is dependent on millimolar levels of calcium (Aster et al., 1999), this result is interpreted to mean that calcium chelation disrupts interactions between the LNR and HD domains, leading to release of the S1-cleaved NECD. Importantly, though, it is unclear whether the protease inhibitor cocktail used in these experiments was effective against ADAM metalloproteases and/or γ-secretase. This leaves

open the possibility that calcium chelation merely relieves the structural auto-inhibition by LNR domains and leads to ligand-independent S2 or S3 cleavage (Rand et al., 2000). More experiments are needed to unequivocally determine whether the active form of *Drosophila* Notch undergoes S1 cleavage and heterodimerization. For example, immunopurification and sequencing of trans-endocytosed NECD would demonstrate whether the peptide fragment ends at a putative furin (S1) or metalloprotease (S2) cleavage site.

One caveat of the mechanical strain model with respect to signaling in *Drosophila* is borne out of this controversy surrounding Notch S1 pre-processing: if the functional Notch molecule is not expressed as a heterodimer, the pulling force would not separate but instead unfold and expose a cleavage site for processing, but this appears to be insufficient for Notch signaling in other model systems. In mammals, S1 cleavage and heterodimerization must precede S2 cleavage. Mammalian S1 cleavage-incompetent Notch is only observed to transendocytose as full-length protein and no signal activation is detected (implying S2 and S3 processing are absent) (Nichols et al., 2007). If the ligand-expressing cell does pull on the ligand-receptor complex, ‘stretching out’ of the Notch LNR autoinhibitory domains would still be predicted to occur in these mutants, which would expose the S2 cleavage site for processing and then cause NICD liberation. Perhaps this reflects differences between mammalian and *Drosophila* processing machinery (Kidd and Lieber, 2002). It may be that mammalian Notch is obliged to separate to entirely expose cleavage sites or allow for ADAM/metalloprotease activity whereas the homologous *Drosophila* S2 cleavage machinery has access to, or can act on the unprocessed, full-length receptor. Expression and analysis of mammalian notch — either wild-type forms in the presence of potent furin inhibitors or S1 cleavage-incompetent mutants — in *Drosophila* cell culture could address this discrepancy.

The most difficult experimental observation to reconcile with the mechanical strain model is the discovery of some soluble Notch ligands that have signaling capability. Under this model, soluble ligands that are unable to provide traction are predicted to be antagonists of Notch signaling, and some reports bear this prediction out (Sun and Artavanis-Tsakonas, 1997; Qi et al., 1999; Hicks et al., 2002). However, there are also examples of soluble DSL ligands that activate Notch signaling in a myriad of contexts (Fitzgerald and Greenwald, 1995; Varnum-Finney et al., 1998; Han et al., 2000; Hicks et al., 2002; Chen and Greenwald, 2004). Most soluble ligands, including the one known endogenous example (DSL-1 in *Caenorhabditis elegans*), occur as multimers (DSL-1 is a dimer) or are bound to artificial substrates. This configuration may somehow lead to another form of mechanical strain sufficient for Notch activation. It is equally plausible that these soluble signaling events occur via non-canonical Notch pathways. A recent study of human hematopoietic stem cells suggests soluble and membrane-bound Delta4 have differential effects on cell proliferation via Notch signaling and that soluble ligand signaling can only be partially accounted for by canonical, S3/γ-secretase cleavage (Lahmar et al., 2008).

Receptor endocytosis: required for γ-secretase cleavage of Notch?

Genetic and cell biological studies have identified an important role for the endocytosis of not only the DSL ligands, but also the Notch receptor in generating an active signal. Endocytosis by the signal-receiving cell has been proposed to be required for S3 γ-secretase cleavage of Notch (Fig. 2C), although this remains controversial. Consistent with this possibility, γ-secretase is more enzymatically active at a lower pH characteristic of endosomes and lysosomes, and is found primarily in intracellular compartments, although a small fraction can be detected at the plasma membrane as well (Pasternak et al., 2003). Studies in vertebrates and flies, however, offer conflicting evidence for whether or not γ-secretase cleavage requires endocytosis of Notch.

Further, if receptor endocytosis is necessary, how it influences NICD cleavage and stability is also an area of interest. Evidence against and in favor of a role for endocytosis by the Notch receptor-presenting cell in canonical signal activation is presented in this section.

Genetic studies in *Drosophila* suggest that S3 γ-secretase cleavage occurs at the plasma membrane, rather than intracellularly, and does not require receptor internalization. One such study showed that whereas γ-secretase dependent cleavage of full-length Notch does not occur in *shibire* mutant embryos, which are defective in endocytosis due to loss of Dynamin activity, γ-secretase dependent cleavage of a truncated form of Notch lacking most of the extracellular domain (and mimicking S2-cleaved Notch) proceeds normally in these embryos (Struhl and Adachi, 1998). This suggests that endocytosis is required for S2 cleavage (perhaps through models 1 and/or 2 discussed above), but *not* for S3 cleavage. A second study examined embryos mutant for Nicastrin, an essential component of the γ-secretase complex. Nicastrin is required for S3 cleavage of Notch and, thus, in cells defective for this protein Notch processing stalls following S2 ADAM/TACE-mediated ectodomain shedding. If γ-secretase cleavage occurs intracellularly, one would predict that the S2 cleaved form of Notch would undergo endocytosis and accumulate in γ-secretase containing intracellular vesicles in Nicastrin mutant cells, but instead it is detected primarily at the plasma membrane (Lopez-Schier and St Johnston, 2002).

More recent studies in mammalian cell lines support the model that endosomal entry is essential for γ-secretase mediated activation of Notch. In cultured cells, dynamin-dependent endocytosis was shown to be essential for γ-secretase mediated cleavage of a truncated form of murine Notch that mimics the S2-cleaved form (Gupta-Rossi et al., 2004). These same studies showed that Notch is monoubiquitinated on a juxtamembrane lysine residue, by an as yet unidentified ubiquitin-ligase, and that this is critical for generation and nuclear accumulation of the NICD. Careful analysis of endocytic uptake and subcellular localization of full-length Notch mutants

that cannot be monoubiquitinated revealed that these are retained at the plasma membrane, whereas mutant forms that lack the γ-secretase cleavage motif are internalized, but not cleaved or transported to the nucleus. Collectively, these studies suggest that monoubiquitination takes place at the membrane, and is essential for S2-cleaved Notch to reach internal compartments within the cell where S3 γ-secretase cleavage takes place.

Only recently has a requirement for internalization of endogenous Notch for signaling been examined in detail in *Drosophila*. Vaccari et al (2008) looked at Notch endocytosis, cleavage and pathway activation in a panel of *Drosophila* mutant cells that are defective in various stages of endocytosis. This study revealed that there is a sharp increase in γ-secretase cleavage and pathway activation upon entry into endosomes, indicating that endosomal entry of Notch is required for efficient signaling. Curiously, signaling was not completely abolished in mutants with severely restricted endosomal entry, and this residual activity was shown to be due to an alternate, dynamin-independent internalization route. These alternate pathways may be sufficient for activation of Notch when it is highly overexpressed, which could account for the seemingly conflicting data showing that truncated Notch can still signal in flies that are defective for dynamin-dependent endocytosis (Struhl and Adachi, 1998). Alternatively, it is possible that there is a low level of γ-secretase activity at the plasma membrane that can generate enough activated Notch to trigger signaling when the receptor is overexpressed, but not when it is present at endogenous levels.

To complicate matters, recent studies suggest the rate of endocytosis in a given cell type may influence the site of S3 cleavage and potency of the resultant NICD fragment. Biochemical analysis in a mammalian system has revealed that γ-secretase cleaves Notch at more than one site, generating ligands that differ in their stability, and thus signaling potency. The choice of cleavage site varies according to subcellular location (Tagami et al., 2008). At the plasma

membrane, γ-secretase is more likely to generate a relatively stable NICD fragment containing valine at the amino (N)-terminus, whereas in endosomes, cleavage is likely to occur at a more C-terminal site that generates a less stable fragment containing a serine or threonine residue at the N-terminus. The serine-ended NICD is not only more easily degraded, but also shows reduced activation of Notch signaling. These findings demonstrate that, at least in cell culture, g-secretase cleavage occurs both at the cell surface and in intracellular compartments. Since Notch is important in many tissues for a variety of functions, this complex activation scheme may allow for nuanced regulation of Notch for its diverse functions. It remains to be examined, however, whether there are *in vivo* circumstances in which the rate of endocytosis modulates Notch signaling, much less the mechanism for such a hypothetical shift.

Receptor endocytosis: a mechanism to restrict ligand-independent Notch activation?

Endocytosis has long been described as a means of signal termination for various plasma membrane signaling events. Likewise, Notch endocytosis appears to terminate signaling, and to prevent inappropriate ligand-independent activity. Indeed, HECT-type E3-ubiquitin ligases of the Nedd4 family have been implicated in the targeting of full-length Notch from the plasma membrane to endocytic and then lysosomal vesicles as a part of its natural turnover (Cornell et al., 1999; Qiu et al., 2000; Sakata et al., 2004; Wilkin et al., 2004). However, if endocytosis by the receptor-presenting cell promotes ligand-dependant Notch activation (as discussed in the previous section), could the same set of machinery go awry and lead to ligand-independent Notch activation? This section examines this possibility and discusses research that indicates endocytic function serves a critical role in tamping down spontaneous Notch activation.

Analogous to mutations in the Notch receptor that have shed light on auto-inhibition (Sanchez-Irizarry et al., 2004), examination of proteins involved in endosomal trafficking, sorting, or both

have revealed circumstances in which their dysregulation may lead to 'accidental' Notch signaling in the absence of ligand-receptor interaction. One protein that has been identified as being necessary for proper endosomal trafficking of Notch is lethal giant disks (Lgd). Lgd is a conserved cytosolic protein containing a lipid-interacting, C2 motif. In *lgd* mutant cells, Notch accumulates in early endosomal vesicles marked by expression of Hrs (hepatocyte growth factor-regulated tyrosine kinase substrate) and ectopic pathway activation occurs in a γ-secretase dependent but ligand independent fashion (Childress et al., 2006; Gallagher and Knoblich, 2006; Jaekel and Klein, 2006). Interestingly, overexpression of wild-type Lgd leads to the same ligand-independent activation of canonical Notch signaling, suggesting that Lgd is titrating out one or more other requisite trafficking proteins that are required to target Notch for lysosomal degradation (Klein, 2003). A similar accumulation of Notch in early endosomal vesicles is observed in cells mutant for either *hrs*, which recruits monoubiquitinated plasma membrane proteins to endosomes, or for components of the Endosomal Sorting Complexes Required for Transport (ESCRT) complex that is necessary for maturation of endosomes into multivesicular bodies. Whereas ligand-independent activation of Notch is observed in cells mutant for ESCRT components, for *lgd* or for both, it is not observed in *hrs* or in *hrs/lgd* double mutant cells. This indicates that Lgd functions downstream of Hrs, and that constitutive activation of Notch in *lgd* mutant cells requires transit through an early endosomal compartment. It should be noted that although mutations in *hrs* rescue ligand-independent Notch signaling in *lgd* mutant cells, Hrs is not required for endogenous ligand-induced signaling. Recently, a thorough study of how blockade of endocytosis at discrete stages affects levels of endogenous Notch signaling was performed. Obstruction of Notch trafficking after formation of Hrs-positive early endosomes, but before maturation into lysosomes, resulted in ectopic Notch activation similar to that observed in *lgd* mutants (Vaccari et al., 2008). Taken together, these findings suggest that Lgd normally functions to traffic Notch to the lysosome, and that blockade of endocytic maturation at late stages enables Notch to either enter or accumulate in an

endosomal compartment that promotes excessive g-secretase cleavage and signal activation (Fig. 2D).

The most obvious difference between endogenous Notch activation and the ectopic signaling observed in *lgd* mutants is the dependence of the former, but not the latter, on ligand interaction. This raises the question of whether activation occurs independent of S2 and/or S3 cleavage in *lgd* mutants. As previously discussed, binding of DSL ligands at the cell surface is believed to relieve auto-inhibition mediated by Notch's LNR domains, such that the S2 cleavage event can occur. Given the new appreciation for the structural basis of auto-inhibition (Gordon et al., 2007), it is reasonable to hypothesize that the progressively lower pH found in endocytic vesicles distorts H-bonding networks and electrostatic interactions, thus relieving steric hindrance to allow for S2-, and subsequent S3-cleavage in the absence of ligand. In fact, there is evidence that a sequence of cleavages similar or identical to the canonical ligand-induced signaling is required for the endocytic ligand-independent signal in *lgd* mutants. First, S2 cleavage of Notch has recently been found to depend on post-translational O-linked-glycosylation of the extracellular EGF-repeats of Notch by the *O*-glucosyltransferase Rumi (Acar et al., 2008). Endogenous Notch signaling is lost in *rumi* mutant flies, and loss of *rumi* suppresses ectopic activation of Notch in *lgd* mutant cells. Thus, Rumi function and, by inference, S2 cleavage of Notch are required for both ligand-dependant and ligand-independent Notch signaling. Analysis of flies mutant for both *lgd* and *kuzbanian* (the ADAM protease involved in S2 Notch processing) would clarify the necessity of S2 cleavage in endocytic ligand-independent signaling. The evidence that S3 cleavage is required for endocytic, ligand-independent signaling is more direct since decreasing the dose of presenilin (the enzymatic component of the γ-secretase complex) by half attenuates Notch activation in *lgd* mutant flies (Jaekel and Klein, 2006). Given that γ-secretase may target different cleavage sites within Notch depending on cellular compartmentalization (Tagami et al., 2008), it would be interesting to

compare cleavage site usage in wild type tissue with that in *lgd*, or other endosomal mutants in which Notch is ectopically activated. To this end, western blot and/or proteomic analysis of Notch fragments may shed light on the nature of endosomal, ligand-independent Notch cleavage.

Conclusions

While Notch signaling is, to date, unique in its requirement for endocytosis of both the ligand and the receptor for full pathway activation, it is becoming increasing apparent that cell signaling and endocytic membrane trafficking are intimately connected for many different signaling pathways. For example, there is evidence that presenilins, the catalytic component of the γ-secretase complex, modulate diverse biological processes independent of conventional γ-secretase protease activity — including regulation of protein trafficking (Hass et al., 2009). With this in mind, we cannot rule out the possibility that presenilins participate in directing Notch for internalization via dynamin-independent pathways.

Overlap between Notch signaling components and those of other signaling pathways imply that some of the models described here may have broader influence. For instance, there is a growing list of substrates for which γ-secretase is involved in their regulated intramembrane proteolysis (Beel and Sanders, 2008). One such target for γ-secretase cleavage is amyloid precursor protein (APP), which has been extensively studied for its role in neurodegenerative diseases such as Alzheimer's Disease. It is entirely possible that greater similarities between these two pathways may emerge when the ligand for APP is revealed (Ma et al., 2008). In conclusion, mechanisms for how endocytosis and membrane trafficking activate and restrain the Notch signaling pathway will likely extend beyond the specific proteins we have highlighted in this review.

Acknowledgements

This work was supported in part by a grant from the NIH to JSW, JEM, LC and DH (T32, HD049309) and by grants from the NIH to JLC (RO1 HD37976 and R03 HD058841) and to EBP (5F30DK081305).

Figure legends

Figure 1. Schematic illustration of Notch structure and pathway activation. **(A)** Notch receptors have an extracellular domain composed of reiterated Epidermal Growth Factor (EGF)-like repeats and a conserved negative regulatory region (NRR) consisting of Lin12/Notch repeats (LNRs) and a heterodimerization (HD) domain. The intracellular portion of Notch contains repeated ankyrin (ANK) repeats, nuclear localization signals (NLS) and a PEST domain that controls receptor half life. Vertebrate Notch undergoes S1 cleavage within the secretory pathway to generate the heterodimeric receptor that is found on the cell surface. **(B)** Notch is activated by binding to ligands of the Delta/Serrate/Lag-2 (DSL) family. The ligands are ubiquitinated (green circle) and internalized into signal sending cells before and/or after receptor activation. Activated Notch undergoes sequential cleavage, initially at the S2 site by members of the ADAM family of metalloproteases (blue ball), and then at the S3 and S4 sites by γ-secretase (orange circle). S2 cleavage occurs at the cell surface and releases the Notch extracellular domain (NECD) from the heterodimer. γ-secretase mediated cleavages take place on the plasma membrane and/or in endosomes. These cleavages release the Notch intracellular domain (NICD), which translocates to the nucleus where it interacts with members of the CBF1/Su(H)/Lag-1 (CSL) family of transcription factors, and recruits co-activators (CoA) to activate transcription of Notch target genes. NICD signaling is terminated by lysosomal degradation.

Figure 2. Models for how endocytosis activates Notch signaling. **(A)** Endocytosis as a means of generating active DSL ligand. In this model, DSL ligand is synthesized, and reaches the plasma membrane in an inactive (red) form. E3 ubiquitin ligases monoubiquitinate (Ub) the cytoplasmic tail of DSL, leading to epsin-dependent endocytosis. The ligand is converted to its active form (orange) in an intracellular compartment and then returned to the plasma membrane. The nature of the postranslational modification that activates the ligand is unknown. **(B)** Ligand endocytosis as a means of generating mechanical strain. In this model, endocytosis of DSL ligand (orange) bound to the Notch heterodimer (blue) on adjacent cells generates mechanical strain that unmasks the S2 cleavage site on Notch, enabling it to be cleaved by ADAM/TACE metalloproteases, thereby generating the remaining transmembrane fragment that is the substrate for the γ-secretase complex in the signal receiving cell. The completion of endocytosis results in trans-endocytosis of NECD and DSL into the signal sending cell. **(C)** Notch endocytosis is required for S3 cleavage. Following ligand binding and S2 cleavage, ubiquitination of the cytoplasmic tail of the remaining transmembrane fragment of Notch triggers its endocytosis. The more acidic environment of the endosomes is required for the proteolytic activity of presenilin (Ps), the component of the γ-secretase complex (purple) that cleaves the S3 site to generate active NICD. **(D)** Endocytosis as a means of preventing ligand-independent activation of the Notch receptor. A fraction of full length Notch undergoes ligand independent internalization from the plasma membrane and traffics to endocytic and lysosomal vesicles as part of its natural turnover. Mutations in components of the intracellular trafficking machinery, such as lethal giant discs (Lgd), that obstruct endosomal trafficking at a step after the formation of hepatocyte growth factor-regulated tyrosine kinase substrate (Hrs)-positive endosomes but before maturation into lysosomes, enable Notch to either enter or accumulate in an early endosomal compartment that allows for excessive, ligand independent γ-secretase cleavage of the S3 site to generate the active NICD fragment.

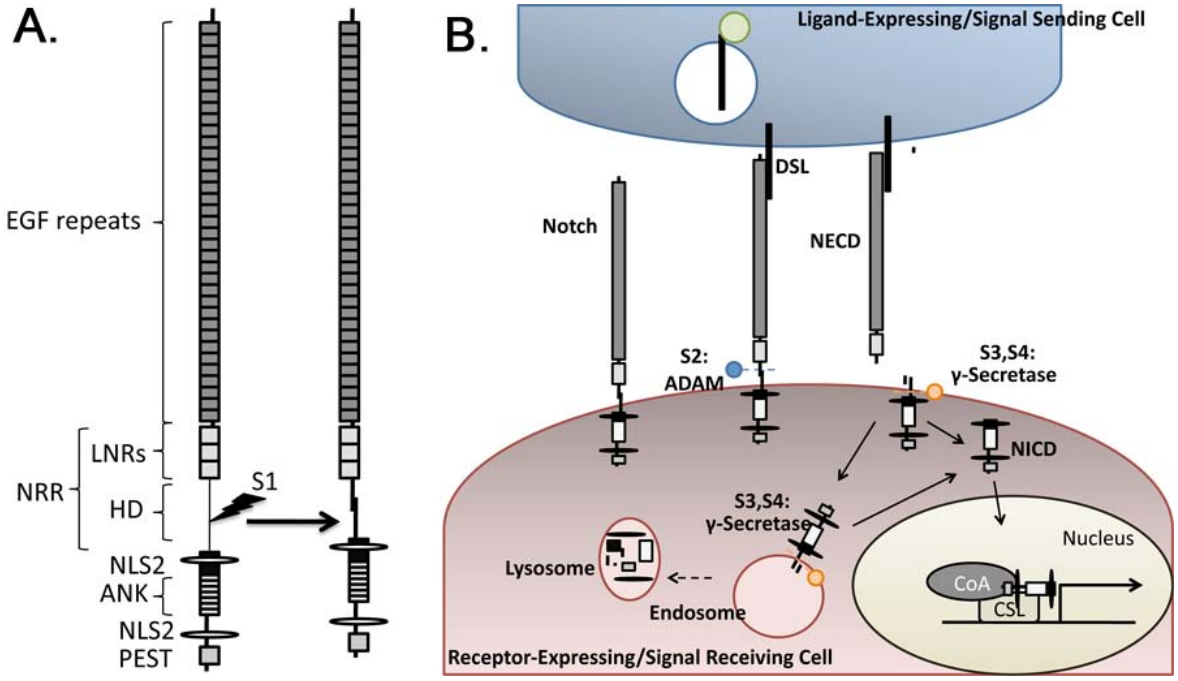

EBP Appendix

Figure 1

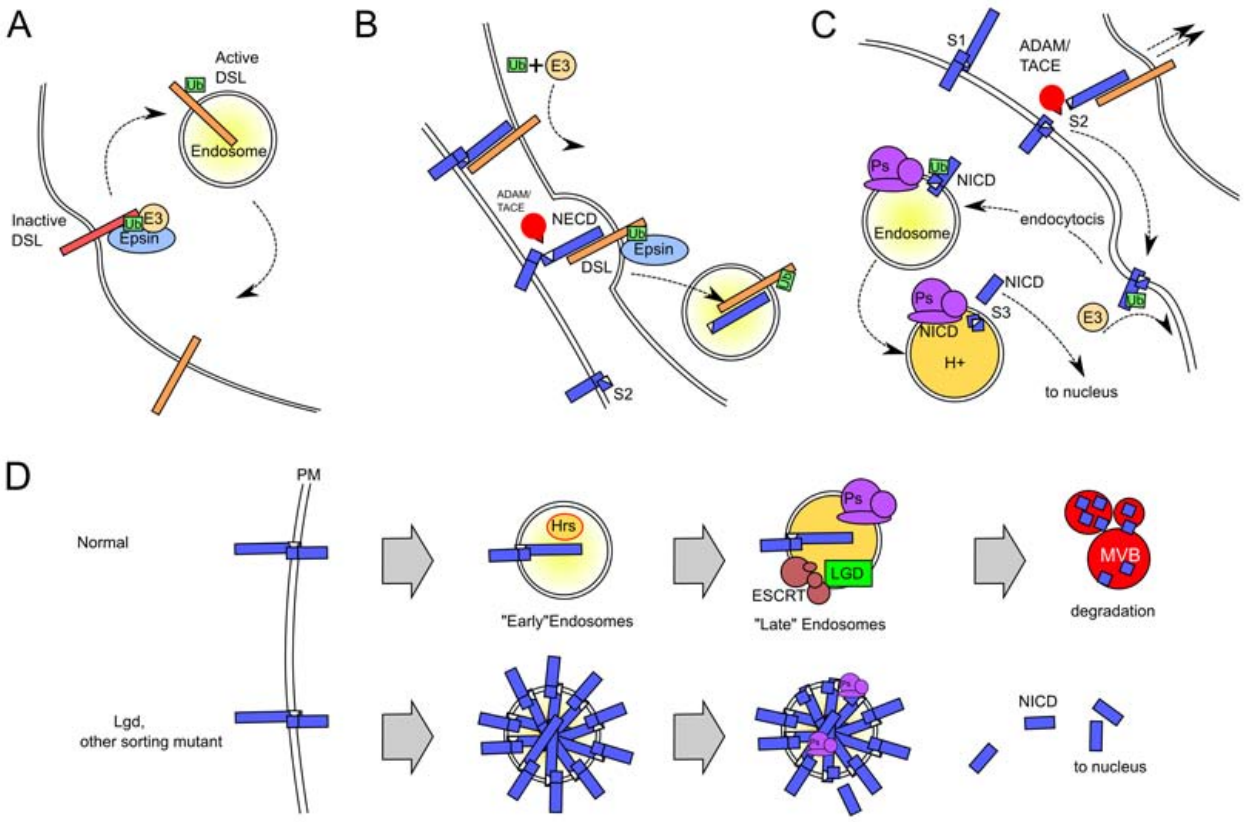

EBP Appendix

Figure 2

References Cited

Acar, M., H. Jafar-Nejad, H. Takeuchi, A. Rajan, D. Ibrani, N.A. Rana, H. Pan, R.S. Haltiwanger, and H.J. Bellen. 2008. Rumi is a CAP10 domain glycosyltransferase that modifies Notch and is required for Notch signaling. *Cell*. 132:247-258.

Aster, J.C., W.B. Simms, Z. Zavala-Ruiz, V. Patriub, C.L. North, and S.C. Blacklow. 1999. The folding and structural integrity of the first LIN-12 module of human Notch1 are calcium-dependent. *Biochemistry*. 38:4736-4742.

Beel, A.J., and C.R. Sanders. 2008. Substrate specificity of gamma-secretase and other intramembrane proteases. *Cell Mol Life Sci*. 65:1311-1334.

Bush, G., G. diSibio, A. Miyamoto, J.B. Denault, R. Leduc, and G. Weinmaster. 2001. Ligand-induced signaling in the absence of furin processing of Notch1. *Dev Biol*. 229:494-502.

Chen, N., and I. Greenwald. 2004. The lateral signal for LIN-12/Notch in C. elegans vulval development comprises redundant secreted and transmembrane DSL proteins. *Dev Cell*. 6:183-192.

Childress, J.L., M. Acar, C. Tao, and G. Halder. 2006. Lethal giant discs, a novel C2-domain protein, restricts notch activation during endocytosis. *Curr Biol*. 16:2228-2233.

Chitnis, A., D. Henrique, J. Lewis, D. Ish-Horowicz, and C. Kintner. 1995. Primary neurogenesis in Xenopus embryos regulated by a homologue of the Drosophila neurogenic gene Delta. *Nature*. 375:761-766.

Cornell, M., D.A. Evans, R. Mann, M. Fostier, M. Flasza, M. Monthatong, S. Artavanis-Tsakonas, and M. Baron. 1999. The Drosophila melanogaster Suppressor of deltex gene, a regulator of the Notch receptor signaling pathway, is an E3 class ubiquitin ligase. *Genetics*. 152:567-576.

Fitzgerald, K., and I. Greenwald. 1995. Interchangeability of Caenorhabditis elegans DSL proteins and intrinsic signalling activity of their extracellular domains in vivo. *Development*. 121:4275-4282.

Fiuza, U.M., and A.M. Arias. 2007. Cell and molecular biology of Notch. *J Endocrinol*. 194:459-474.

Fortini, M.E., and S. Artavanis-Tsakonas. 1994. The suppressor of hairless protein participates in notch receptor signaling. *Cell*. 79:273-282.

Gallagher, C.M., and J.A. Knoblich. 2006. The conserved c2 domain protein lethal (2) giant discs regulates protein trafficking in Drosophila. *Dev Cell*. 11:641-653.

Gordon, W.R., D. Vardar-Ulu, G. Histen, C. Sanchez-Irizarry, J.C. Aster, and S.C. Blacklow. 2007. Structural basis for autoinhibition of Notch. *Nat Struct Mol Biol*. 14:295-300.

Greenwald, I., and G. Seydoux. 1990. Analysis of gain-of-function mutations of the lin-12 gene of Caenorhabditis elegans. *Nature*. 346:197-199.

Gupta-Rossi, N., E. Six, O. LeBail, F. Logeat, P. Chastagner, A. Olry, A. Israel, and C. Brou. 2004. Monoubiquitination and endocytosis direct gamma-secretase cleavage of activated Notch receptor. *J Cell Biol*. 166:73-83.

Han, W., Q. Ye, and M.A. Moore. 2000. A soluble form of human Delta-like-1 inhibits differentiation of hematopoietic progenitor cells. *Blood*. 95:1616-1625.

Hass, M.R., C. Sato, R. Kopan, and G. Zhao. 2009. Presenilin: RIP and beyond. *Semin Cell Dev Biol*. 20:201-210.

Henrique, D., E. Hirsinger, J. Adam, I. Le Roux, O. Pourquie, D. Ish-Horowicz, and J. Lewis. 1997. Maintenance of neuroepithelial progenitor cells by Delta-Notch signalling in the embryonic chick retina. *Curr Biol*. 7:661-670.

Heuss, S.F., D. Ndiaye-Lobry, E.M. Six, A. Israel, and F. Logeat. 2008. The intracellular region of Notch ligands Dll1 and Dll3 regulates their trafficking and signaling activity. *Proc Natl Acad Sci U S A*. 105:11212-11217.

Hicks, C., E. Ladi, C. Lindsell, J.J. Hsieh, S.D. Hayward, A. Collazo, and G. Weinmaster. 2002. A secreted Delta1-Fc fusion protein functions both as an activator and inhibitor of Notch1 signaling. *J Neurosci Res*. 68:655-667.

Jaekel, R., and T. Klein. 2006. The Drosophila Notch inhibitor and tumor suppressor gene lethal (2) giant discs encodes a conserved regulator of endosomal trafficking. *Dev Cell*. 11:655-669.

Kidd, S., and T. Lieber. 2002. Furin cleavage is not a requirement for Drosophila Notch function. *Mech Dev*. 115:41-51.

Klein, T. 2003. The tumour suppressor gene l(2)giant discs is required to restrict the activity of Notch to the dorsoventral boundary during Drosophila wing development. *Dev Biol*. 255:313-333.

Klueg, K.M., T.R. Parody, and M.A. Muskavitch. 1998. Complex proteolytic processing acts on Delta, a transmembrane ligand for Notch, during Drosophila development. *Mol Biol Cell*. 9:1709-1723.

Kopan, R., and M.X. Ilagan. 2009. The canonical Notch signaling pathway: unfolding the activation mechanism. *Cell*. 137:216-233.

Kopan, R., E.H. Schroeter, H. Weintraub, and J.S. Nye. 1996. Signal transduction by activated mNotch: importance of proteolytic processing and its regulation by the extracellular domain. *Proc Natl Acad Sci U S A*. 93:1683-1688.

Lahmar, M., C. Catelain, S. Poirault, M. Dorsch, J.L. Villeval, W. Vainchenker, O. Albagli, and E. Lauret. 2008. Distinct effects of the soluble versus membrane-bound forms of the notch ligand delta-4 on human CD34+CD38low cell expansion and differentiation. *Stem Cells*. 26:621-629.

Lajoie, P., J.G. Goetz, J.W. Dennis, and I.R. Nabi. 2009. Lattices, rafts, and scaffolds: domain regulation of receptor signaling at the plasma membrane. *The Journal of cell biology*. 185:381-385.

Lopez-Schier, H., and D. St Johnston. 2002. Drosophila nicastrin is essential for the intramembranous cleavage of notch. *Dev Cell*. 2:79-89.

Ma, Q.H., T. Futagawa, W.L. Yang, X.D. Jiang, L. Zeng, Y. Takeda, R.X. Xu, D. Bagnard, M. Schachner, A.J. Furley, D. Karagogeos, K. Watanabe, G.S. Dawe, and Z.C. Xiao. 2008. A TAG1-APP signalling pathway through Fe65 negatively modulates neurogenesis. *Nature cell biology*. 10:283-294.

Mumm, J.S., E.H. Schroeter, M.T. Saxena, A. Griesemer, X. Tian, D.J. Pan, W.J. Ray, and R. Kopan. 2000. A ligand-induced extracellular cleavage regulates gamma-secretase-like proteolytic activation of Notch1. *Mol Cell*. 5:197-206.

Nichols, J.T., A. Miyamoto, S.L. Olsen, B. D'Souza, C. Yao, and G. Weinmaster. 2007. DSL ligand endocytosis physically dissociates Notch1 heterodimers before activating proteolysis can occur. *J Cell Biol*. 176:445-458.

Parks, A.L., K.M. Klueg, J.R. Stout, and M.A. Muskavitch. 2000. Ligand endocytosis drives receptor dissociation and activation in the Notch pathway. *Development*. 127:1373-1385.

Parks, A.L., J.R. Stout, S.B. Shepard, K.M. Klueg, A.A. Dos Santos, T.R. Parody, M. Vaskova, and M.A. Muskavitch. 2006. Structure-function analysis of delta trafficking, receptor binding and signaling in Drosophila. *Genetics*. 174:1947-1961.

Pasternak, S.H., R.D. Bagshaw, M. Guiral, S. Zhang, C.A. Ackerley, B.J. Pak, J.W. Callahan, and D.J. Mahuran. 2003. Presenilin-1, nicastrin, amyloid precursor protein, and gamma-secretase activity are co-localized in the lysosomal membrane. *J Biol Chem*. 278:26687-26694.

Qi, H., M.D. Rand, X. Wu, N. Sestan, W. Wang, P. Rakic, T. Xu, and S. Artavanis-Tsakonas. 1999. Processing of the notch ligand delta by the metalloprotease Kuzbanian. *Science*. 283:91-94.

Qiu, L., C. Joazeiro, N. Fang, H.Y. Wang, C. Elly, Y. Altman, D. Fang, T. Hunter, and Y.C. Liu. 2000. Recognition and ubiquitination of Notch by Itch, a hect-type E3 ubiquitin ligase. *J Biol Chem*. 275:35734-35737.

Rand, M.D., L.M. Grimm, S. Artavanis-Tsakonas, V. Patriub, S.C. Blacklow, J. Sklar, and J.C. Aster. 2000. Calcium depletion dissociates and activates heterodimeric notch receptors. *Mol Cell Biol*. 20:1825-1835.

Sakata, T., H. Sakaguchi, L. Tsuda, A. Higashitani, T. Aigaki, K. Matsuno, and S. Hayashi. 2004. Drosophila Nedd4 regulates endocytosis of notch and suppresses its ligand-independent activation. *Curr Biol*. 14:2228-2236.

Sanchez-Irizarry, C., A.C. Carpenter, A.P. Weng, W.S. Pear, J.C. Aster, and S.C. Blacklow. 2004. Notch subunit heterodimerization and prevention of ligand-independent proteolytic activation depend, respectively, on a novel domain and the LNR repeats. *Mol Cell Biol*. 24:9265-9273.

Selkoe, D., and R. Kopan. 2003. Notch and Presenilin: regulated intramembrane proteolysis links development and degeneration. *Annu Rev Neurosci*. 26:565-597.

Seugnet, L., P. Simpson, and M. Haenlin. 1997. Requirement for dynamin during Notch signaling in Drosophila neurogenesis. *Dev Biol*. 192:585-598.

Struhl, G., and A. Adachi. 1998. Nuclear access and action of notch in vivo. *Cell*. 93:649-660.

Struhl, G., and A. Adachi. 2000. Requirements for presenilin-dependent cleavage of notch and other transmembrane proteins. *Mol Cell*. 6:625-636.

Sun, X., and S. Artavanis-Tsakonas. 1996. The intracellular deletions of Delta and Serrate define dominant negative forms of the Drosophila Notch ligands. *Development*. 122:2465-2474.

Sun, X., and S. Artavanis-Tsakonas. 1997. Secreted forms of DELTA and SERRATE define antagonists of Notch signaling in Drosophila. *Development*. 124:3439-3448.

Tagami, S., M. Okochi, K. Yanagida, A. Ikuta, A. Fukumori, N. Matsumoto, Y. Ishizuka-Katsura, T. Nakayama, N. Itoh, J. Jiang, K. Nishitomi, K. Kamino, T. Morihara, R. Hashimoto, T. Tanaka, T. Kudo, S. Chiba, and M. Takeda. 2008. Regulation of Notch signaling by dynamic changes in the precision of S3 cleavage of Notch-1. *Mol Cell Biol*. 28:165-176.

Tien, A.C., A. Rajan, and H.J. Bellen. 2009. A Notch updated. *The Journal of cell biology*. 184:621-629.

Vaccari, T., H. Lu, R. Kanwar, M.E. Fortini, and D. Bilder. 2008. Endosomal entry regulates Notch receptor activation in Drosophila melanogaster. *J Cell Biol*. 180:755-762.

Varnum-Finney, B., L.E. Purton, M. Yu, C. Brashem-Stein, D. Flowers, S. Staats, K.A. Moore, I. Le Roux, R. Mann, G. Gray, S. Artavanis-Tsakonas, and I.D. Bernstein. 1998. The Notch ligand, Jagged-1, influences the development of primitive hematopoietic precursor cells. *Blood*. 91:4084-4091.

Wang, W., and G. Struhl. 2004. Drosophila Epsin mediates a select endocytic pathway that DSL ligands must enter to activate Notch. *Development*. 131:5367-5380.

Wang, W., and G. Struhl. 2005. Distinct roles for Mind bomb, Neuralized and Epsin in mediating DSL endocytosis and signaling in Drosophila. *Development*. 132:2883-2894.

Weinmaster, G. 1997. The ins and outs of notch signaling. *Mol Cell Neurosci*. 9:91-102.

Weng, A.P., A.A. Ferrando, W. Lee, J.P.t. Morris, L.B. Silverman, C. Sanchez-Irizarry, S.C. Blacklow, A.T. Look, and J.C. Aster. 2004. Activating mutations of NOTCH1 in human T cell acute lymphoblastic leukemia. *Science*. 306:269-271.

Wilkin, M.B., A.M. Carbery, M. Fostier, H. Aslam, S.L. Mazaleyrat, J. Higgs, A. Myat, D.A. Evans, M. Cornell, and M. Baron. 2004. Regulation of notch endosomal sorting and signaling by Drosophila Nedd4 family proteins. *Curr Biol*. 14:2237-2244.